Catecholaminergic Modulation of Sensory Processing in functionally distinct Primary Sensory and Association Cortex

Dissertation

zur Erlangung des Grades eines
Doktors der Naturwissenschaften

der Mathematisch-Naturwissenschaftlichen Fakultät
und
der Medizinischen Fakultät
der Eberhard-Karls-Universität Tübingen

vorgelegt
von

Silvia van Keulen
aus Horb am Neckar, Deutschland

Dezember - 2016

Tag der mündlichen Prüfung: 3. Mai 2017

Dekan der Math.-Nat. Fakultät:	Prof. Dr. W. Rosenstiel
Dekan der Medizinischen Fakultät:	Prof. Dr. I. B. Autenrieth

1. Berichterstatter:	Prof. Dr. Nikos K. Logothetis
2. Berichterstatter:	Prof. Dr. Uwe Ilg
Prüfungskommission:	Prof. Dr./PD Dr. Peter Pilz
	Prof. Dr./PD Dr. Cornelius Schwarz

Erklärung / Declaration:

Ich erkläre, dass ich die zur Promotion eingereichte Arbeit mit dem Titel:

„Catecholaminergic Modulation of Sensory Processing in functionally distinct Primary Sensory and Association Cortex“

selbständig verfasst, nur die angegebenen Quellen und Hilfsmittel benutzt und wörtlich oder inhaltlich übernommene Stellen als solche gekennzeichnet habe. Ich versichere an Eides statt, dass diese Angaben wahr sind und dass ich nichts verschwiegen habe. Mir ist bekannt, dass die falsche Abgabe einer Versicherung an Eides statt mit Freiheitsstrafe bis zu drei Jahren oder mit Geldstrafe bestraft wird.

I hereby declare that I have produced the work entitled:

„Catecholaminergic Modulation of Sensory Processing in functionally distinct Primary Sensory and Association Cortex“,

submitted for the award of a doctorate, on my own (without external help), have used only the sources and aids indicated and have marked passages included from other works, whether verbatim or in content, as such. I swear upon oath that these statements are true and that I have not concealed anything. I am aware that making a false declaration under oath is punishable by a term of imprisonment of up to three years or by a fine.

Tübingen, den 16.5.2017

Datum / Date

Unterschrift /Signature

Contents

Abstract I

Abbreviations II

1. Introduction 1

1.1. Noradrenergic modulation of sensory processing in two functionally distinct cortical regions 1

1.1.1. Transmission of innocuous and noxious tactile somatosensory information 1

1.1.2. Two pain pathways for the physiological and the psychological aspects of pain 2

1.1.3. The cortical activity state and its behavioral correlates 3

1.1.4. SEPs and single unit responses to noxious stimulation in the primary somatosensory cortex versus the medial prefrontal cortex 5

1.1.5. Neuromodulation as a source of flexible information processing 7

1.1.6. The locus coeruleus noradrenergic system 7

1.1.7. Noradrenergic modulation of the cortical activity state 9

1.1.8. Heterogeneous neuromodulation of neuronal activity in functionally distinct cortical regions by the LC noradrenergic system 10

1.1.9. Noradrenergic modulation of sensory evoked neuronal responses in functionally distinct cortical regions 12

1.1.10. Research question study 1 14

1.2. Noradrenergic modulation of the midbrain dopaminergic system 14

1.2.1. The ventral midbrain dopaminergic system 14

1.2.2. Stimulus-related activation of the midbrain dopaminergic system 15

1.2.3. Dopaminergic modulation of neuronal activity in ventral midbrain target regions 16

1.2.4. Noradrenergic modulation of the midbrain dopaminergic system 19
1.2.5. Research question study 2 20
1.3. Dopaminergic modulation of sensory gating 21
1.3.1. Catecholaminergic interactions in prefrontal cortex 21
1.3.2. Sensory gating deficits in schizophrenia 22
1.3.3. Mediation and modulation of sensory gating in rats 23
1.3.4. Dopaminergic modulation of sensory gating deficits in rats 25
1.3.5. Research question study 3 27
1.3.6. Brief summary of the research aims in this thesis 29
2. Material and Methods 30
2.1. Noradrenergic modulation of sensory processing in two functionally distinct cortical regions 30
2.1.1. Surgery and electrophysiological recording 30
2.1.2. Somatosensory stimulation 32
2.1.3. Drug administration 32
2.1.4. Data analysis 34
2.1.5. Perfusion and histology. 36
2.1.6. Statistical analysis 37
2.2. Noradrenergic modulation of the midbrain dopaminergic system 37
2.3. Dopaminergic modulation of sensory gating 38
2.3.1. Surgical procedures 38
2.3.2. Drug design 39
2.3.3. Drugs 40
2.3.4. Drug infusion 41

2.3.5. Behavioral testing 41
2.3.6. Perfusion and histology. 42
2.3.7. Data analysis 43
2.3.8. Statistical analysis 43
3. Results 43
3.1. Noradrenergic modulation of sensory processing in two functionally distinct cortical regions 44
3.1.1. Direct comparison of ongoing neuronal activity in S1HL and mPFC 48
3.1.2. Noradrenergic modulation of spontaneous neuronal activity in S1HL and mPFC 49
3.1.3. Comparison of sensory-evoked neuronal responses in S1HL and mPFC 55
3.1.3.1. Examination of effective stimulation parameters 55
3.1.3.2. Characterization of cortical state activation in response to somatosensory stimulation in S1HL and mPFC 58
3.1.3.3. Understanding the difference between effective and non-effective sensory stimulation in mPFC 62
3.1.3.4. Influence of stimulus-related cortical activity state in mPFC on spectral composition of TCA in S1HL 64
3.1.3.5. Relationships between stimulus-related TCA and underlying voltage fluctuations 65
3.1.3.6. Characterization of single unit responses to somatosensory stimulation in S1HL and mPFC 69
3.1.4. Noradrenergic modulation of sensory-evoked neuronal responses in S1HL and mPFC 71
3.1.4.1. Effect of pharmacological manipulation on LC neuronal activity 72

3.1.4.2. Noradrenergic modulation of stimulus-induced changes of spectral composition in S1HL and mPFC 73
3.1.4.3. Noradrenergic modulation of SEPs and single unit responses to sensory stimulation in S1HL and mPFC 76
3.2. Noradrenergic modulation of the midbrain dopaminergic system 85
3.2.1. Noradrenergic modulation of spontaneous activity in the ventral midbrain .. 85
3.2.2. Validation of parameters for effective stimulation in the VTA 87
3.2.3. Noradrenergic modulation of multi unit responses to sensory stimulation in the ventral midbrain 87
3.3. Dopaminergic modulation of sensory gating 89
3.3.1. Characterization of PPI and ASG under baseline condition 91
3.3.2. Dopaminergic modulation of sensory gating in mPFC 92
3.3.2.1. Modulation of sensory gating under general decrease of dopaminergic transmission 93
3.3.2.2. Modulation of sensory gating under decrease of dopaminergic transmission selectively to mPFC 95
3.3.2.3. Modulation of sensory gating under decrease of dopaminergic transmission in ventral midbrain target regions other than mPFC 96
4. Discussion 98
4.1. Noradrenergic modulation of sensory processing in two functionally distinct cortical regions 98
4.1.1. Somatosensory stimulation addressed dermal nociceptors 98
4.1.2. Comparable effects between local and systemic clonidine administration suggests that reduced NE release mainly affected sensory processing in both cortical regions 99

4.1.3. Cortical NE deprivation activated ongoing cortical state in higher association cortex while deactivation was observed in primary sensory cortex 100

4.1.4. Systemic injection of clonidine induced cortical activation in mPFC in favor of internal long-range cortico-cortical interaction 101

4.1.5. Power in Theta and Alpha frequency range in S1HL is modulated by cortical activity state in mPFC 102

4.1.6. Sensitivity differences to sensory stimulation between S1HL and mPFC might functionally result from differences in neuronal excitability during ongoing cortical state 103

4.1.7. Reduction of cortical NE release induced responsiveness to sensory stimulation in initial mPFC TCA- cases while power in Sigma and Beta frequency bands was differentially modulated in S1HL and mPFC TCA+ cases 104

4.1.8. Depletion of cortical NE release reduced SNR in S1HL while local network properties in mPFC were reorganized by redistribution of neuronal activity 106

4.1.9. Neuronal responses to noxious stimulation are sustained by phasic NE release in cortical regions 108

4.2. Noradrenergic modulation of the midbrain dopaminergic system 109

4.2.1. Noradrenergic modulation of ventral midbrain spontaneous activity is dependent on localization of the recorded population within VTA 109

4.2.2. Phasic release of NE in VTA enhances sensory processing 110

4.3. Dopaminergic modulation of sensory gating 111

4.3.1. DA in mPFC is essential for adequate sensory gating 111

4.3.2. PPI and ASG might share neuronal mechanisms under certain conditions . 112

4.3.3. Inhibition of mPFC dopaminergic transmission affects only neuronal signals but not behavioral ASR 113

4.4. Further methodological considerations 114
4.5. Outlook and future studies 115
5. Summary 116
6. References 118
7. Supplemental Material 167
Acknowledgements 178

Abstract

The vertebrate sensory system is enabled to differentiate between a vast variety of sensory information under different behavioral and environmental conditions. The required flexibility is provided by complex brain functions including neuromodulation. Specific structures contributing in neuromodulation of sensory processing are the noradrenergic nucleus locus coeruleus and the dopaminergic ventral tegmental area (VTA), combined referred to as catecholaminergic system. However, how catecholaminergic neuromodulation affects sensory processing in functionally different brain regions is not well discovered. To approach this question, experiments in anesthetized rats were conducted in order to examine qualitative differences of noradrenergic modulation of sensory processing between the functionally distinct primary somatosensory cortex (S1) and the associative medial prefrontal cortex (mPFC). These experiments confirmed the already reported function of noradrenaline (NE) in activation of the cortical state and increase of the signal-to-noise ratio (SNR) of sensory-evoked responses, however only for S1. In mPFC, reorganization of neuronal activity, orchestrated by NE, is suggested in order to adequately evaluate the biological relevance of the stimulus and integrate sensory and non-sensory information. Further results show that NE improves noxious somatosensory processing within the VTA to induce the observed reorganization of local networks in mPFC in synergy with dopamine (DA). A possible outcome includes enhanced sensory gating by suppression of irrelevant and accentuation of relevant network information. This prefrontal cortical function was finally specifically explored in awake rats. Target specific manipulation of DA release revealed that prefrontal DA is essential to ensure adequate prefronto-accumbal interactions which, in turn, are necessary for sensory gating. Together, this work demonstrated that catecholamines are needed to improve sensory processing in functionally distinct cortical and subcortical brain regions. Thereby, classical improvement of SNR is not the only mechanism but also the catecholaminergic modulation of complex local network dynamics contributes to processing of relevant or irrelevant sensory information.

Abbreviations

%PPI – percentage of Prepulse Inhibition

%ASG – percentage of Auditory Sensory Gating

AHP – afterhyperpolarization

ANOVA – Analysis of Variance

AP – antero-posterior

ASG – Auditory Sensory Gating

ASR – Acoustic Startle Response

Base – Baseline

BLP – Band-Limited Power

cAMP – cyclic adenosine monophosphate

clo – Clonidine

DA – Dopamine

DAT – Dopamine transporter

dB – decibel

DV – dorso-ventral

EEG – Electroencephalogram

FIR – Finite Impulse Response digital filter

FS(s) – Foot-Shock(s)

GABA – gamma-Aminobutyric acid

HCN – hyperpolarization-activated cyclic nucleotide-gated cation

HPC – Hippocampus

Hz – Hertz

IASP – The International Association for the Study of Pain

ID – inner diameter

kHz – Kilohertz

LC – Locus Coeruleus

LFP – Local Field Potential

mA – milliampere

max – maximum

ML – medio-lateral

mPFC – medial Prefrontal Cortex

MUA – Multi Unit Activity

n.s. – not significant

NAc – Nucleus Accumbens

NE – Noradrenaline, Norepinephrine

NERI – Noradrenaline Reuptake Inhibitor

NET – Noradrenaline transporter

NMDA – N-methyl-D-aspartate

PB – phosphate buffer

PFC – Prefrontal Cortex

PGi – Nucleus Paragigantocellularis

PnC – Nucleus reticularis pontis caudalis

PPI – Prepulse Inhibition

PPS – Paired-Pulse Suppression

PPTg – Pedunculopontine Tegmental Nucleus

pre – prestimulus interval

PrL – prelimbic subregion of medial Prefrontal Cortex

PSD – power source density

PSTH – poststimulus time histogram

REM – Rapid eye movement

S1 – primary Somatosensory Cortex

S1HL – hind limb area of the primary Somatosensory Cortex

SE – standard error of mean

SD – standard deviation

sec – second

SEP(s) – sensory evoked Potential(s)

SNc – Substantia Nigra pars compacta

SNR – Signal-to-noise ratio

SP – Single Pulse stimulation

SUA – Single Unit Activity

TCA – Transient Cortical Activation

TR – Train Stimulation

VTA – Ventral Tegmental Area

1. Introduction

A vast variety of sensory stimuli under different behavioral and environmental conditions requires highly flexible neuronal information processing for adequate orientation. In the vertebrate central nervous system, this is achieved by a complex synergy between different sensory systems, each optimized for its own modality: auditory, visual, olfactory, gustatory and somatosensory. The somatosensory system is specifically complex because it processes information of four different modalities: discriminative touch, pain (nociception), body position and movement (proprioception) and temperature (thermoreception). The work presented in this thesis is primarily focused on sensory processing of strong salient tactile stimuli while proprioception and thermoreception is not relevant.

1.1. Noradrenergic modulation of sensory processing in two functionally distinct cortical regions

1.1.1. Transmission of innocuous and noxious tactile somatosensory information

Information about tactile stimuli is conveyed by primary sensory afferents differing in axon diameter and degree of myelination, which determine the velocity of information transfer. So-called mechanoreceptors transmit sensory information of discriminative touch via myelinated A β-fibers with a conduction velocity of ~45 m/sec. Painful stimuli, perceived by nociceptors, are conveyed either via A δ-fibers, which are myelinated but exhibit a slower conduction velocity of ~9 m/sec, or non-myelinated C-fibers with a very slow conduction velocity of < 1m/sec[1]. Once entering the dorsal horn of the spinal cord, primary afferents of mechanoreceptors project ipsilaterally dorsal to the medulla and make their first synapse onto cells, referred to as the second order neurons. Second order neuronal axons then cross to the contralateral side of the brainstem and project via the medial lemniscal tract to the somatosensory thalamus in the midbrain and from there to sensory cortical regions. Primary afferents of nociceptive modality enter the dorsal horn and synapse almost

immediately onto second order neurons, which then cross the midline and project dorsally to the brain via the spinothalamic tract.
Despite differentiated sensory pathways, the transmission of mechanoreceptive and nociceptive sensory information is not exclusive. It has been shown that noxious stimulation of the exposed sural nerve evoked neuronal responses in the primary somatosensory cortex (S1) which were transferred by mechanoreceptive A β-fibers in addition to nociceptive A δ- and C-fibers[2] indicating that a tactile component is contributing to the neuronal response evoked by nociceptive electrical stimulation.
Thus, the transfer of sensory information of painful stimuli is slower than of discriminative touch and the neural pathways within the central nervous system are different.
Nevertheless, painful stimuli simultaneously activate the innocuous mechanoreceptive system.

1.1.2. Two pain pathways for the physiological and the psychological aspects of pain

In contrast to discriminative touch, pain is not primarily represented in somatosensory structures. The International Association for the Study of Pain (IASP) defines pain as "an unpleasant sensory and emotional experience associated with actual or potential tissue damage, or described in terms of such damage". This interpretation implements the physical perception of noxious stimuli in addition to a subjective experience associated with attention[3-5], anxiety[6], anticipation[7-9] or empathy[10]. In this sense, the physiological as well as the psychological aspects of pain perception are centrally processed within the so-called "pain-matrix"[11]. Subcortical and cortical structures, which contribute to the pain matrix, are divided into a lateral and a medial pain pathway dependent on the networks related to the lateral or medial thalamic structures[12-18]. The lateral pathway projects via the ventroposterior lateral and the ventroposterior inferior nucleus of the thalamus to somatosensory areas and mediates the localization and intensity of nociceptive stimuli. The medial pathway projects via intralaminar and ventromedial thalamic nuclei to limbic structures like the frontal cortices mediating the emotional, cognitive and affective component of noxious stimulation[19-24]. Thereby, the insula is believed to build a bridge

between the lateral and the medial system in order to promote integration of information from both[12,13].

1.1.3. The cortical activity state and its behavioral correlates

The neuronal response to sensory stimulation can be detected on different levels of cortical neuronal activity including cortical activity state, sensory evoked potentials (SEPs) and unit activity. The cortical activity state, which was initially explored as oscillation patterns in the electroencephalogram (EEG), is also reflected in the low frequency component (< 300 Hz) of the extracellular electrophysiological signal recorded within the brain and referred to as the Local Field Potential (LFP). Electric currents from all active cellular processes within a volume of brain tissue in addition to "volume conducted" potentials from distant sites are averaged at a given location in the extracellular medium determining the LFP[25]. The characteristics of the LFP waveform depend on the spontaneous oscillatory behavior of neurons in accordance to shifts in behavioral states of vigilance[26,27]. During awake state and rapid-eye-movement (REM) sleep, the cortical activity is operating in an activated state defined by low amplitude-high frequency oscillations. During so-called quiet awake state, when the animal is awake but drowsy, and during non-REM sleep also known as slow wave sleep, the cortical state activity operates in a deactivated state defined by high amplitude-low frequency oscillations. Under this condition, neuronal ensembles in thalamocortical networks synchronize their firing resulting in rhythmic shifting between high (Up-states) and low (Down-states) excitability states[28].

The different frequency components which characterize the cortical activity states are superimposed in the LFP signal. They can be separated and quantified as band-limited power (BLP) in different predefined frequency bands in order to analyze the cortical state in detail. Segmentation of the frequency bands varies nowadays between publications but classically, the frequency ranges are defined as Delta (< 3.5 Hz), Theta (4-7.5 Hz), Alpha (8-13 Hz), Beta (14-30 Hz) and Gamma (> 30 Hz)[29]. In addition, two frequency bands have been introduced as specifically related to sleep states: a frequency band below 1 Hz called slow oscillations (SLO)[30-32] and a frequency band from 12-15 Hz which was determined as sleep spindles[33,34] and later referred to as Sigma frequency band[35].

Each of these denoted frequency bands has been associated with behavioral correlates under different cortical activity states. SLO and Delta frequency band are associated with deep sleep while power in Sigma frequency band is enhanced during slow wave sleep[36,37]. Compelling evidence suggests that sleep contributes to long-term memory consolidation[38,39]. Power in Theta frequency range is believed to result from long-range interaction between hippocampus (HPC) and cortex during learning and memory processes[40-42]. Enhanced power in Alpha frequency range is assumed to be related to internally directed cognitive processes during awake resting state in absence of sensory input[43-45]. Power in Beta frequency band is considerably high in primary motor cortex[46,47] and is classically linked to motor functions[48,49]. However, interestingly, it has additionally been shown to be related to sensory processing in S1[50]. Finally, generation of Gamma band activity is associated with an activated cortical network related to different cognitive processes like attention, multisensory integration or sensory stimulus detection[27,37,51]. Accordingly, activation of cortical neuronal activity during spontaneous state changes or by sensory stimulation enhances Gamma band activity which is, in turn, frequently associated with suppression of power in low frequency range in human and animals[52-56]. Increased Gamma band activity is, however, also detected during REM sleep[57-59] which is highly associated with dreaming[58,60].

The cortical state activity under anesthesia, induced by commonly used general anesthetics (ketamine, propofol, pentobarbital, isofluran, etc.) is considered as artificial sleep-like state although without REM occurrence[61-63]. Concomitantly, the power in the frequency spectrum shifts to lower frequencies[64,65]. Cortical state under urethane anesthesia is however particularly interesting, since it has been shown in rats to be characterized by spontaneous shifts between activated and deactivated state resembling state shifts observed during natural sleep[66,67]. In addition to spontaneous transition, noxious sensory stimulation is also able to induce a shift from high amplitude slow waves to an activated state under urethane anesthesia in rats. Such an activated state is usually associated with increased neuronal firing activity[68-70].

1.1.4. SEPs and single unit responses to noxious stimulation in the primary somatosensory cortex versus the medial prefrontal cortex

Beyond cortical state activation, stimulus-related neuronal activation is reflected in SEPs which basically represent evoked changes in the electric potential revealed by averaging the low pass filtered signal. It has been shown that SEP characteristics are closely related to the ongoing cortical state before stimulus presentation because magnitude and dynamics change with variation in cortical activity state in awake human[71] and also urethane anesthetized rats[72,73]. However, laminar recordings show that SEP profiles also change depending on cortical layer exhibiting positive deflections in superficial layers which reverse with increasing cortical depth[74-78]. Reversal of SEP polarity is associated with increased responsiveness of unit activity in deep cortical layers[77] which is, in turn, positively related to magnitude of cortical state activation[68-70].

In the lateral pain pathway, the response profiles of the SEPs as well as the stimulus-related unit responses represent the transfer of sensory information via aforementioned primary somatosensory afferents. For example, the mechanoreceptive A β-fibers are enabled to convey discriminative information about the stimulus intensity which is reflected in the incrementally increased amplitude of the SEP. As soon as the stimulation is strong enough to additionally activate A δ- or C-fibers, the response amplitude reaches a plateau and only reports the presence of the stimulus[79]. Moreover, the latencies of the response components are dependent on peripheral conduction velocities. Non-specific innocuous electrical or mechanical stimulation commonly evokes a phasic response in S1 with a very short latency of 10 – 20 ms mediated by A β-fibers[2,80-84]. Nociceptive mechanical stimulation or electrical median or sural nerve stimulation evoked neuronal responses with longer latencies related to transmission via A δ- (50 – 60 ms peak latency) and C-fibers (~300 ms peak latency)[2,80,82,83,85].

The latencies closely resemble those measured in response to specific electrical stimulation of individual isolated afferent somatosensory fibers in pentobarbital anesthetized cats[79,86]. Furthermore, stimulation with noxious CO2-laser radiation, which has been shown to specifically activate nociceptors without activating low-threshold mechanoreceptors in

rats[87] and human[88,89], confirmed latencies of 50 – 60 ms and ~300 ms for Aδ- and C-fiber mediated cortical neuronal responses, respectively[82-84,90-92]. Somatosensory stimulation in most of the aforementioned studies conducted in rats was applied to the middle part of the tail or the contralateral hind paw and thus with comparable distance to the recording site. Additionally, peak latencies of response components assigned to A β-, A δ- and C-fiber transmission were comparable between evoked potentials and unit responses[82,92] as well as between anesthetized and awake preparations[82,83].

Sensory processing of nociceptive stimuli in the medial pain pathway has been very well documented in the anterior cingulate cortex in rodents[24,93-95] and human[96-100]. In addition, the medial prefrontal cortex (mPFC) has been shown to be similarly involved[19,94,101-103]. Studies combining recordings from prelimbic (PrL) and cingulate subdivision of rat mPFC[68,69,94,104] indicate similar electrophysiological properties of the nociception-related neuronal activity in these structures. Types of noxious peripheral stimuli which activate neuronal activity in mPFC in awake and anesthetized rats include mechanical pressure stimulation[68-70,102,104,105], electrical stimulation of exposed sciatic nerve[95], noxious heat stimulation[102] and CO_2 laser heat stimulation[94,106]. Albeit the stimulation is of a noxious nature, the sensitivity of prefrontal neuronal activation is lower than in S1 as only 6 – 50 % of recorded single units in mPFC respond to nociceptive stimuli[70,94,102] compared to ~90 % in primary sensorimotor cortex[94]. The response profiles of unit activity were both tonic and phasic with various response latencies ranging between 80 – 600 ms[68,70,94,107] resulting in a merged single voltage deflection on the population level. Converse decomposition of SEPs in prefrontal cortex by independent component analysis confirmed complex processing of sensory information reflected in different response patterns with variable latencies[106]. Accordingly, it was suggested that the population evoked field potential is a mixture of integrated sensory information in cognitive processes transferred from different brain structures with overlapping time courses[108,109]. Therefore, sensory processing in prefrontal cortex was mostly studied related to cognitive functions like sensory discrimination, association or attention[110] rather than the representation of a sensory stimulus per se[111].

In summary, SEPs in the somatosensory cortex, a terminal region of the lateral pain pathway, differ dependent on ongoing cortical state and cortical depth. Differentiable

response components with different peak latencies inform about type of afferents, and thus type of modality, which convey the information to the cortex. In contrast, the SEP profile in the medial prefrontal cortex, a terminal region of the medial pain pathway, is monophasic merged from various incoming information from different structures with different latencies. Additionally, the neuronal excitability in response to noxious somatosensory stimulation in medial prefrontal cortex is lower than in primary somatosensory cortex.

1.1.5. Neuromodulation as a source of flexible information processing

The necessary flexibility to process complex and variable somatosensory information in contributing brain structures is promoted by neuromodulation, one of two different mechanisms providing the chemical transfer of information in the brain. In contrast to fast synaptic transmission, which is enabled by ligand-gated ion channels and affects the target cell within a few milliseconds, neuromodulation is achieved by slow metabotropic receptors involving sequences of biochemical processes including different enzymes and second messenger systems. It may take hundreds of milliseconds to even minutes until synaptic transmission is completed. In addition, neuromodulatory effects are longer-lasting and more spatially diffuse than fast synaptic transmission[112]. These properties enable neuromodulators to rather regulate than mediate neuronal activity by changing the electrical properties of target neurons in many different ways[113] which provides highly flexible information processing. Catecholamines, a group of neuromodulators including dopamine and its derivate noradrenaline, also known as norepinephrine (NE), have been shown to play a very important role in modulation of sensory processing. The sources for catecholamines are the brain nuclei A1 – A14, mapped and named by Annica Dahlström and Kjell Fuxe who implemented the “aminergic” property in the name as an “A”[114].

1.1.6. The locus coeruleus noradrenergic system

The pontine A6 group, Nucleus Locus Coeruleus (LC), is a very small nucleus comprised of only ~15.000 cells per hemisphere in humans[115] and ~1.500 in the rat[116]. LC has been found to be the major source of NE[117] to the entire central nervous system except the basal ganglia[118-123]. Spontaneously, single neurons of LC exhibit regular tonic discharge rates of

1 – 5 Hz[124,125] and phasic firing occurs in addition to this spontaneous activity in response to top-down input resulting from cognitive processes or bottom-up input like incoming sensory information[126,127]. Under anesthetized condition, LC neurons respond only to direct electrical stimulation of peripheral nerves or noxious somatosensory stimuli[125,128-130]. The activity state of LC noradrenergic neurons is directly related to rates of NE release in terminal regions. Local pharmacological activation or inhibition of LC noradrenergic neurons results respectively in enhanced or decreased turnover of NE in mPFC[131,132] and S1[133]. Electrical microstimulation of LC neuronal activity induces a frequency dependent increase of NE efflux in the cortex[134,135] up to a fourfold higher release of NE in response to a phasic stimulation pattern when compared to tonic stimulation at 1 Hz[134]. Similarly, the extracellular concentration of NE is elevated in response to electrical foot-shock (FS) stimulation in awake rats[136,137].

Ascending LC afferents arise from only two nuclei located in the rostral medulla: the nucleus prepositus hypoglossi and the nucleus paragigantocellularis (PGi)[138]. The former has been shown to be involved in gaze control[139,140] and the latter in the integration of autonomic and environmental stimuli arising from other sensory nuclei or directly from the spinal cord[141,142]. This includes nociceptive somatosensory information[143-145] which is then transferred from PGi to LC[146] where noradrenergic neurons respond with a biphasic neuronal activation. The response components exhibit latencies reflecting the transfer of somatosensory information via peripheral afferents just as it was demonstrated for S1 sensory-evoked responses described earlier[147].

From LC, the neuronal information is transferred via thin (< 1 µm) and non-myelinated[124,130,148] axons to LC terminal regions with a low conduction velocity of < 0.6 m/sec[124,130,149,150]. After activation of LC terminals, NE is released by axonal varicosities via volume transmission[151-153] acting on two families of G-protein coupled receptors: alpha and beta-adrenoceptors. Based on their pharmacological properties, the alpha-adrenoceptors have been subdivided into alpha 1- and alpha 2-adrenoceptors[154-156]. Binding of NE to alpha 1-adrenoceptors activates a signal cascade which results in the release of Ca^{2+} from intracellular stores and thus in enhanced excitatory processes. Actions on alpha 2- and beta-adrenoceptors both modulate the intracellular concentration of cyclic

adenosine monophosphate (cAMP), albeit in opposite directions: activation of alpha 2-adrenoceptors decreases cAMP and leads to hyperpolarization of the affected neuron while activation of beta-adrenoceptors increases cAMP thus resulting in excitation[157].

1.1.7. Noradrenergic modulation of the cortical activity state

In spite of its tiny size, LC exerts global impact on brain functions like attention[158,159], perception[160-163], memory[164-166] or the behavioral state of vigilance[160,167-169]. The latter is represented in the cortical activity state which has been shown to be directly related to the activity state of LC noradrenergic neurons. Their discharge rate successively decreases from awake state over the course of quiet awake state to slow wave sleep until it ceases during REM sleep in rats[170-173], cats[174] and monkeys[175]. A causal role of LC activity in the regulation of behavioral vigilance can be suggested by the fact that changes in the firing activity of LC neurons precede changes in cortical activity state[170,172,174-177]. Supporting experiments showed that manipulation of LC neuronal activity in anesthetized and non-anesthetized rats modulates cortical state activity. Specifically, pharmacological or optogenetic activation of LC induced cortical activation in frontal[178-181] as well as sensory cortical areas[182]. Conversely, decrease of noradrenergic transmission by bilateral pharmacological inhibition of LC activity resulted in deactivated cortical state[183] as has been also described for systemic injection of alpha 2-noradrenergic agonists[184-186]. A specific example shows that systemic injection of clonidine increases power between 1 - 30 Hz with maximum power increase between 14 – 24 Hz and systemic blockade of alpha 2-adrenoceptors showed the opposite effect in PFC cortical surface EEG[186]. Behaviorally, cortical deactivation induces a sleep-like behavioral state of sedation in humans[187-192] and animals[193-196], a property which has been medically exploited for the use in clinics[197-199].

Nevertheless, rather than fulfilling these functions alone, LC exerts a modulatory influence on neurons in other structures contributing to the regulation of sleep-wake states including regions of the so-called brainstem arousal system (reticular formation, cholinergic laterodorsal tegmentum and pedunculopontine tegmental nucleus), serotonergic raphe

nuclei, midbrain dopaminergic neurons, non-specific thalamocortical activation system, hypothalamic activation systems and cholinergic neurons in the basal forebrain[160,200-202]. In summary, LC neuronal activity and related release of NE affects the behavioral state of vigilance. Increase of LC activity leads to cortical and behavioral activation while decrease of the noradrenergic tone results in cortical deactivation and behavioral sedation.

1.1.8. Heterogeneous neuromodulation of neuronal activity in functionally distinct cortical regions by the LC noradrenergic system

Activation and deactivation of cortical state are global phenomena and, indeed, the classical belief about noradrenergic modulation was a homogeneous action in all cortical regions because of the densely packed population of purely noradrenergic cells[114,123], synchronous firing pattern[170,203] and simultaneous activation in response to electrical or sensory stimulation[204]. Additionally, LC sends extensive projections throughout the brain and the spinal cord[118-122,205] including vast axonal collateralization of single noradrenergic neurons in LC to cytoarchitectonically and functionally distinct brain regions[206-210]. Finally, NE is released via volume transmission[121,135,148,211] by LC terminals originally defined to be uniformly distributed in the cortex[212]. Yet, how does a small and homogeneous structure, like LC, impressively provide the flexibility which is needed to integrate intrinsic and environmentally driven neuronal information during the processing of aforementioned cognitive functions? The answer developed with the innovation of methodology providing increased accuracy and resolution during functional and anatomical studies. Increasing evidence suggests that the LC noradrenergic system is actually a heterogeneous structure exhibiting properties which provide high flexibility in modulation of neuronal activity. Specific anatomical work revealed, for example, that subpopulations of LC neurons can be differentiated by cell morphology and localization within LC[116,118,213]. Furthermore, LC neurons can be differentiated based on their molecular composition[214] and the intra-LC receptor composition[215]. Finally, anatomical projection studies have revealed topographic organization of neurons in the LC depending upon their target regions in the brain[210,216-222]. A heterogeneity in noradrenergic activity has been observed not only at the level of LC but also in its target regions. For example, the highest density of noradrenergic fibers are

observed in frontal areas[208,223,224] which provides the PFC with a higher concentration of extracellular NE in comparison to sensory cortical areas[223,225,226]. A greater demand for NE in higher order cognitive brain regions has been confirmed by a study showing that segregated LC populations innervating functionally different cortical regions (PFC and motor cortex) are phenotypically, biochemically and electrophysiologically distinct from each other[223]. Laminar inspection demonstrated localization of noradrenergic terminals in PFC superficial layers[148,212] while in sensory cortical areas the terminals were additionally located in deeper layers[212]. As a consequence, PFC cells in superficial layers were more sensitive to local administration of NE[227] while in S1 cells in all cortical layers could be modulated[228,229].

Distribution of noradrenergic receptors has been found to be similarly specific between cortical regions and layers. However, this applies only to alpha-adrenoceptors while beta-adrenoceptors are homogeneously distributed over cortical regions[225]. The highest concentration of alpha 1-adrenoceptors was detected in the PFC while the lowest concentration was found in sensory cortical areas[225]. Alpha 2-adrenoceptors were most prominent in temporal and parietal cortical regions[225,230,231] distributed to all cortical layers in comparison to frontal regions where alpha 2-adrenoceptors are rather localized in deep layers[231]. Interestingly, activation of alpha 2-adrenoceptors in PFC does not necessarily result in hyperpolarization of target cells but also in enhanced excitability dependent on postsynaptic receptor composition. If so-called hyperpolarization-activated cyclic nucleotide-gated cation (HCN) channels are co-localized with alpha 2-adrenoceptors on dendritic spines of pyramidal neurons in PFC, activation of alpha 2-adrenoceptors results in depolarization[232]. Originally, activation of alpha 2-adrenoceptors inhibits intracellular cAMP production which is needed to open HCN channels in response to membrane potential fluctuations. Inhibition of HCN currents hyperpolarizes the resting membrane potential but significantly enhances the temporal integration of synaptic input by increasing the input resistance. The net effect is an increase in the overall gain of the response of PFC pyramidal neurons to excitatory synaptic input[233].

Finally, a specific activation pattern is, however not only dependent on the presence and distribution of the receptors in a given brain structure but also on their affinity to NE which is alpha 2 >> alpha 1 > beta[234].
In summary, a huge diversity among anatomical targets and physiological effects of noradrenergic actions demonstrates that noradrenergic modulation of cortical functions is inhomogeneous, highly flexible and complex.

1.1.9. Noradrenergic modulation of sensory evoked neuronal responses in functionally distinct cortical regions

Despite a vast divergence of noradrenergic properties in hierarchically distinct brain regions like S1 and PFC, activation of cortical state and related noradrenergic modulation is consistent over cortical regions[160,169]. Therefore, a finer scale is necessary in order to characterize region-specific functional differences in sensory processing. At the level of single unit activity, it has been shown that NE classically optimizes information processing in primary sensory cortical regions. Increase of noradrenergic concentration in sensory cortical areas by local infusion of NE or electrical stimulation of LC leads to alpha 2-adrenoceptor related inhibition of spontaneous neuronal activity[228,229,235-239] and concurrent alpha 1-adrenoceptor mediated enhancement of sensory evoked neural responses[229,236,238,240-244]. These effects confirm the major view about improvement of stimulus-coding by increase of the signal-to-noise ratio in sensory cortical areas. Similarly to S1, spontaneous activity in mPFC was commonly found to be decreased after electrical microstimulation of LC or local infusion of NE[227,245-248] which was also mediated by alpha 2-adrenoceptors[249-253]. However in contrast to S1, the suppressant effect of alpha 2-adrenoceptor activation was shown to be dose-dependent in mPFC since iontophoretic clonidine injection resulted in enhanced spontaneous activity with increased ejection current[251]. This effect was also demonstrated for neuronal activation in response to either glutamate infusion or electrical microstimulation of synaptic afferents[246,254,255]. When clonidine was iontophoretically infused into PFC with low ejection currents, excitatory synaptic currents were decreased[251,252,256] but turned to enhancement with increasing concentration of clonidine[251,252]. In vitro studies demonstrated a contribution of alpha 2-

adrenoceptor-releated inhibition of HCN channels to increased excitatory postsynaptic currents[233,246]. However, studies reporting enhancement of excitatory drive in PFC by noradrenergic modulation were only performed in vitro. Less artificial in vivo neuronal responses to noxious somatosensory stimulation in mPFC were either inhibited[245] or preserved[247,248] after priming electrical microstimulation of LC. The latter effect resulted in increased signal-to-noise ratio (SNR) comparable to the role of NE in sensory regions.
The modulation of cortical neuronal activity by beta-adrenoceptors is not very well studied and discrepant actions have been reported. Mostly studied in vitro, infusion of beta-adrenoceptor agonists into the bath led to enhanced, suppressed or unaffected neuronal responses to depolarizing current pulse or iontophoretic glutamate pulse to PFC or S1 cells[235,240,257,258]. The suppressant effect, however, was only shown under high concentration of NE. Initially, excitatory discharges evoked by iontophoretic glutamate pulse in single units of S1 were enhanced after NE infusion into the bath. With an increase in concentration of NE, the neuronal discharges showed a so-called 'inverted U' dose-response relationship and turned to suppressed neuronal activity. More specific pharmacological experiments showed that initial facilitation was mediated by postsynaptic alpha 1-noradrenergic actions and the suppression under high NE concentration was mediated by postsynaptic low affine beta-adrenoceptors[240].
Suppression of spontaneous activity as well as neuronal activation in response to iontophoretic acetylcholine pulses was confirmed in vivo after local infusion of beta-adrenoceptor agonist isoproterenol into S1[238]. It is believed that beta-receptor mediated suppression of neuronal activity in pyramidal neurons is induced indirectly by postsynaptic activation of GABAergic interneurons[160,259-261].
In summary, NE in S1 classically increases SNR by decrease of spontaneous neuronal activity and increase of evoked activity mediated by alpha 2- and alpha 1-adrenoceptors, respectively. Decrease of spontaneous activity has been also reported for PFC neuronal activity, however only for low doses of NE in the cortical tissue. Increased concentration of NE results in faster neuronal firing. Evoked activity in PFC was either inhibited or preserved dependent on the receptor composition of the postsynaptic membrane. Thus,

noradrenergic modulation of neuronal activity in PFC is, in contrast to S1, not homogeneous but differs between neuronal subpopulations.

1.1.10. Research question study 1

Target specific populations of noradrenergic neurons within LC and region specific noradrenergic innervation and receptor composition give rise to the idea of differential noradrenergic modulation of sensory processing in functionally distinct cortical regions. Previous work supports the notion (see section 1.1.8). However, because of the independent examination of the effects under different experimental conditions, it is uncertain whether these results reflect mechanisms of noradrenergic modulation of neural activity or methodological differences. The first study of the present work was designed to directly compare how anatomical and physiological differences of the noradrenergic system in functionally distinct cortical regions affect neuromodulation of spontaneous and sensory-evoked responses to intradermal electrical FSs. The LFP and unit activity was simultaneously recorded in LC, S1 hindlimb representation (S1HL) and mPFC in the anesthetized rat. The noradrenergic system was manipulated by 1) systemic injection of clonidine which acts globally on alpha 2-adrenoceptors, suppresses LC spontaneous activity[205,262] and decreases NE turnover in the brain by presynaptic inhibition of NE release[263-265] and 2) local infusion of clonidine into LC, which suppresses LC spontaneous activity[205,266-268] and decreases release of NE in the cortex[132,266,269-271].

1.2. Noradrenergic modulation of the midbrain dopaminergic system

1.2.1. The ventral midbrain dopaminergic system

Especially for neuromodulation of sensory and cognitive processes in mPFC it is known that NE acts in synergy with its direct precursor Dopamine (DA)[136,272-275]. They even share the norepinephrine transporter (NET)[276,277], which, surprisingly, has a higher affinity for DA than the dopamine transporter (DAT) itself[278-280]. Since NET is exclusively localized in the membrane of NE neurons[281], DA is transported from the extracellular space into noradrenergic terminals and, after endocytosis into vesicles and activation of the

presynaptic terminal, co-released with NE[282-287], for example upon electrical microstimulation of LC[288,289].

The sources for DA are the midbrain nuclei A8 – A14[114] besides two more nuclei which were identified in diencephalon and olfactory bulb[290]. Major sources are A 9, the substantia nigra pars compacta (SNc) and A 10, the ventral tegmental area (VTA) both located in the ventral midbrain. The efferent pathways of this midbrain DA complex are subdivided into three major divisions. The nigrostriatal pathway projects from the SNc to the dorsal striatum and basal ganglia[291-294] and is greatly involved in execution of voluntary motor actions[291,295-297]. The mesolimbic pathway projects from the paranigral subdivision of the VTA to Nucleus Accumbens (NAc)[298-301] and regulates reward and motivation[302-305]. Lastly, the mesocortical pathway, which projects from the parabrachial subdivision of the VTA to mPFC, HPC and amygdala[299,300] contributes to goal-directed behavior as well as aversive behavior[302,306]. Classical electrophysiological properties of dopaminergic neurons are based on studies performed in the SNc in which > 90% of the neurons are dopaminergic[307,308]. In contrast, the VTA is a heterogeneous structure composed of 60 - 70 % dopaminergic, ~30 % GABAergic and ~ 5 % glutamatergic neurons[309-320]. VTA dopaminergic neurons receive input from a vast variety of sources including striatum, pallidum, hypothalamus, amygdala, cortex, thalamus, hindbrain and other midbrain regions meaning that GABAergic, glutamatergic, serotonergic, noradrenergic and cholinergic projections converge in the VTA[321-325]. In addition, DA neurons receive input from local GABAergic, glutamatergic and other dopaminergic neurons[321-323,325].

1.2.2. Stimulus-related activation of the midbrain dopaminergic system

Midbrain dopaminergic neurons display phasic excitation in response to sensory events of alerting (unexpected sensory cues which generally trigger immediate reactions) or aversive (unpleasant sensations like air puffs, bitter tastes, electrical shocks, pinch) character[326-328]. This implies that basically every salient sensory stimulus of any intensity or modality as well as every novel stimulus is able to activate VTA dopaminergic neurons resulting in phasic release of DA into VTA target regions[329-339]. Accordingly, VTA dopaminergic neurons are also excited in response to noxious somatosensory stimulation[340-342]. Related

cortical activation and release of DA has been shown to be restricted to mPFC and cingulate cortex which is why it was suggested that noxious stimuli are specifically processed in the mesocortical dopaminergic pathway[300,332,343-345]. Functionally, the denoted target structures of the mesocortical dopaminergic system (PFC, HPC and amygdala) might contribute to cognitive processes after the initial reflexive behavior which terminates noxious stimulation. This implies the association between the unpleasant experience and preceding actions, learning the association and attributing the cause adequately for future prevention.

1.2.3. Dopaminergic modulation of neuronal activity in ventral midbrain target regions

Ventral midbrain dopaminergic neurons show 3 main types of activation pattern:
1) inactive, hyperpolarized[346,347] by a strong GABAergic inhibition from ventral pallidum[348,349], 2) regular tonic, induced by either intrinsic pacemaker potential[346,350,351] or glutamatergic afferents[352-354] and 3) phasic or burst activity in response to short-term glutamatergic afferents[308,348,352,355-357]. While regular tonic firing of dopaminergic neurons provides a baseline tone of DA release in VTA terminals, which is dependent on the size of active dopaminergic population[348,353,358], burst activity produces a larger synaptic release of DA albeit only transiently[348,359-366].
DA exerts its actions on at least 5 distinct subtypes of G-protein coupled DA receptors which are divided into D_1-like (D_1 and D_5) and D_2-like (D_2, D_3 and D_4) receptor subtypes according to their intracellular signaling events. D_1-like receptors are positively coupled to signaling molecules and thus enhance the intracellular concentration of cAMP which results in depolarization of the membrane while on the contrary, D_2-like receptors exert negative coupling and hyperpolarize the membrane[367].
In NAc and the dorsal striatum, the phasic release of DA is restricted by presynaptic actions on inhibitory D_2-receptors[368-370] and released DA is rapidly removed from the synapse by DAT reuptake[371]. However, properties like axon collateralization of single dopaminergic neurons, topographic overlapping, synchronous firing of dopaminergic neurons and the use of gap junctions contribute to massive increase of DA concentrations which compensate for

rapid removal[353]. In contrast, dopaminergic neurons of the mesocortical system do not express D_2-receptors and therefore the release of DA is prolonged which enables the neuromodulator to accumulate and diffuse in the target tissue[299,361,372-374]. Furthermore, DA provision is much faster in PFC in comparison to other target areas of the VTA[375,376]. Lastly, mesocortical dopaminergic neurons display a higher firing rate than mesolimbic or mesostriatal dopaminergic neurons[374,377]. In combination, this suggests a greater demand of dopamine in PFC compared to other VTA target structures. This might be related to a high functional significance of D_1-receptors which is illustrated by a higher abundancy (10 - 20 times higher expression than D_2-receptors) in the PFC of human[378], monkey[379] and rodent[380]. Activation of D_1-receptors requires more DA since the affinity in binding DA is naturally lower than of D_2-receptors[381]. This implies a preferential activation of D_2-receptors when dopaminergic neurons are tonically activated and additional activation of D_1-receptors occurs with increased release of DA, such as during phasic firing in response to cognitive engagement or salient stimuli[382-384]. Given this background, it must be assumed that phasic release of DA in mPFC increases the SNR of sensory-evoked responses. However, experimental manipulation of the PFC DA concentration by intra-PFC infusion of DA, pharmacological and electrical stimulation of VTA DA neuron activity or neurotoxic lesion of VTA DA neurons in anesthetized rats revealed that DA in PFC has an inhibitory effect on both spontaneous firing activity[227,247,248,385-396] as well as neuronal response to MD-thalamus stimulation or peripheral noxious stimulation[247,386]. Since both D_1- and D_2-receptors are expressed in the membrane of deep-layer pyramidal as well as non-pyramidal neurons in PFC[380,397-400], DA exerts both direct and indirect effects on pyramidal cell activity[401-403]. Further, it has been shown that DA and GABA mutually contribute to the inhibitory actions of VTA DA input to PFC[393,402,404-406].

Complex modulation of mPFC neuronal activity might additionally result from DA-glutamate coactivation. The importance of glutamate was repeatedly emphasized for several PFC functions[407-409] and glutamate is even co-released from mesocortical dopaminergic neurons[410-413]. Anatomical studies revealed a close proximity between mesocortical dopaminergic neurons and glutamatergic terminals arising from cortical and subcortical afferents[414-422] which converge onto the same postsynaptic pyramidal cell in

mPFC[423-427] creating so-called "synaptic triads"[424,428,429] (Figure 1.1). Thus, a simultaneous presynaptic and postsynaptic dopaminergic modulation of excitatory synaptic transmission by glutamate is possible. At the postsynaptic site, DA generally increases the amplitudes of N-methyl-D-aspartate (NMDA)-mediated currents by acting on D_1-receptors[430-436]. Reports about the actions on the presynaptic site are discrepant. Certain studies have demonstrated that the presynaptic activation of D_1-receptors results in elevated release of glutamate[406,429,436,437] while other studies have reported a reduction of glutamate release[438,439]. In this context, it has been shown that both D_1-receptor hypoactivation[440-442] as well as hyperactivation[443-445] in PFC disrupts performance in certain prefrontal-related cognitive tasks implying that an optimal level of D_1-receptor activation, in the sense of an inverted U-shaped function, is required for adequate performance in rodents, monkeys and human[443,446-453].

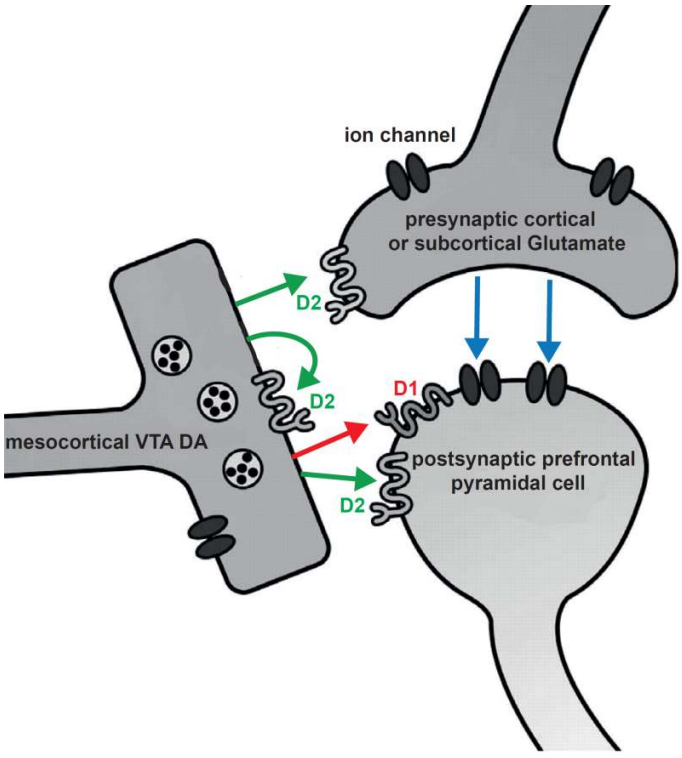

Figure 1.1: Schematic illustration of a so-called 'synaptic triad' in PFC. Mesocortical dopaminergic neurons from the ventral midbrain terminate in close proximity to glutamatergic afferents from cortical or subcortical structures. Both afferents converge mutually onto the postsynaptic pyramidal neuron. This configuration enables a simultaneous dopaminergic modulation of presynaptic glutamate release and postsynaptic response in addition to presynaptic dopamine release by auto-inhibition mechanisms. Modified from Rhodes et al. 2005.

In summary, DA exerts a variety of modulatory effects on prefrontal neuronal activity in order to regulate functions like memory[110,455,456] including working memory[452,457-459], behavioral flexibility[110,460-462], attention[110,458], motivation[463-466] and other cognitive

operations[455,459,462,467]. Functional impairment of the dopaminergic modulation of prefrontal activity results in neurological and psychiatric impairments, for example schizophrenia[468-472] or attention-deficit-hyperactivity-disorder[473-476].

1.2.4. Noradrenergic modulation of the midbrain dopaminergic system

The activity of dopaminergic neurons and related engagement in sensory processing or cognitive functions is modulated by the activity state of LC noradrenergic neurons. Anatomical studies reveal a dense projection of noradrenergic neurons from LC to the VTA[119,477-482] where alpha 1-[483] and alpha 2-adrenoceptors[484-487] are expressed on dopaminergic neurons and activation results in a complex local modulation pattern. Presynaptic blockade of alpha 2-adrenoceptors within the VTA, which blocks auto-inhibition processes and thereby increases NE release[488-491], resulted in either decreased[492] or increased[493] dopaminergic firing activity. Also, neurotoxic lesion of LC noradrenergic neurons revealed contrasting results. While increased dopaminergic discharge rate was shown after bilateral lesion of LC noradrenergic neurons by infusion of 6-Hydroxydopamine[494], another study reported decreased release of DA in VTA terminal regions[495] indicating decreased dopaminergic discharge. Nevertheless, direct enhancement of NA concentration by infusion of NE into VTA or systemic injection of a selective NE reuptake inhibitor (NERI) resulted consistently in suppression of the discharge rate of VTA DA neurons[496,497] which, accordingly, reduced the release of DA in NAc[498].
Alpha 2-adrenoceptors are the most abundant noradrenergic receptors[499] with the highest affinity[234] in the VTA. Therefore, a low concentration of NE activates alpha 2-adrenoceptors leading to inhibition of dopaminergic cell activity in contrast to high NE concentration in response to phasic NE release or experimentally induced hypernoradrenergic state. However, receptor-specific pharmacological experiments suggest a mutual contribution of alpha 2-adrenoceptors in addition to D_2-receptors in suppression of dopaminergic activity[377,496,500-503], the latter presumably by presynaptic inhibition of glutamate transmission[504]. On the contrary, enhancement of dopaminergic activity is enabled by actions on alpha 1-adrenoceptors[493,505]. Correspondingly, phasic release of NE in response to electrical microstimulation of LC evoked transient burst activity in putative

VTA and SNc DA neurons[506,507] in accordance with the idea that NE in high concentration affects alpha 1-adrenoceptors in addition to alpha 2-adrenoceptors.
Furthermore, noradrenergic modulation of the firing pattern but not the firing rate of midbrain DA neurons has been reported. A reduced burst firing and regularized firing pattern in VTA and SNc putative dopaminergic neurons was observed after systemic injection of alpha 2-noradrenergic agonist and alpha 1-noradrenergic antagonist[493,508,509] indicating that NE induces burst firing in ventral midbrain dopaminergic neurons and thus, leads to increased release of DA in related target regions[359,361-366,510].
Finally, a presynaptic location of noradrenergic alpha 1-receptors[511,512] and alpha 2-adrenoceptors[504] on glutamatergic and GABAergic terminals within the VTA have been reported indicating a noradrenergic modulation of glutamate and GABA release, which indirectly modulates VTA dopaminergic activity[311,513-516].
In summary, noradrenergic modulation of the activity of VTA dopaminergic neurons is dependent on receptor composition, local network connectivity and firing pattern of LC noradrenergic neurons. Low concentration of NE by tonic activity of LC neurons primarily activates alpha 2-adrenoceptors and D_2-receptors which results in suppression of dopaminergic, GABAergic and glutamatergic activity within the VTA. When LC neurons are phasically activated, alpha 1-adrenoceptors are additionally activated, leading to increased firing of VTA neurons. Additionally, NE shifts the firing pattern of VTA dopaminergic neurons to burst activity, which results in increased release of DA in VTA target structures.

1.2.5. Research question study 2

Phasic excitation of dopaminergic neurons in the VTA in response to salient stimulation[326-328] including noxious somatosensory stimulation[332,336,337,340,516-520] is well documented. However, noradrenergic modulation of sensory evoked neuronal responses in VTA DA neurons has not been explored in detail. The response latency of noradrenergic neurons in LC is 20 – 50 ms[129,147,521] and thus shorter than the reported response latency of VTA dopaminergic neurons (40 – 100 ms)[341,516-519,522]. This implicates that both tonic and stimulus-related phasic release of NE is able to modulate sensory processing in the VTA.

Therefore, in the second part of this work, LC activity was unilaterally inactivated by local infusion of alpha 2-noradrenergic agonist. Next, modulation of population sensory-evoked responses to electrical FSs in ipsilateral VTA was examined in the anesthetized rat.

1.3. Dopaminergic modulation of sensory gating

1.3.1. Catecholaminergic interactions in prefrontal cortex

Interestingly, the interactions of NE and DA in the VTA seem to specifically affect the mesocortical dopaminergic system. It has been demonstrated that systemic injection of a selective NERI increased DA release in PFC but not in the striatum[283,523], an effect which was abolished by neurotoxic lesion of LC[523]. Furthermore, systemic injection of a selective DA reuptake inhibitor increased DA concentration in PFC only in rats with neurotoxically lesioned LC while DA release in NAc was independent from neuronal activity in LC[523]. Finally, neurotoxic lesion of the LC – VTA noradrenergic pathway decreased DA utilization in PFC while the level in NAc remained unchanged[524]. Accordingly, stimulation of LC increases extracellular levels of DA in PFC[525].

The mPFC receives convergent projections of LC noradrenergic and VTA dopaminergic neurons[209,224,421,526,527] and it has been demonstrated that NE regulates extracellular DA and vice versa within mPFC[528]. For example, local infusion of NE or a selective NERI into PFC has been shown to increase extracellular NE as well as DA in anesthetized rats[272,283,528]. The DA release seems to be primarily mediated by alpha 1-adrenoceptors[272]. However, systemic or intra-mPFC infusion of alpha 2-adrenoceptor antagonist without prior manipulation of the noradrenergic tone also enhances extracellular levels of DA and NE in mPFC[528-531] suggesting co-release of catecholamines by presynaptic blockade of auto-inhibition mechanisms on LC terminals[284-287]. Concomitantly, a decrease has been observed after local infusion of alpha 2-noradrenergic agonist[528]. On the other hand, NE and DA exert pronounced compensatory mechanisms on each other. Loss of noradrenergic input by local neurotoxic lesion of LC terminals or lesion of ascending NE pathways, for example, increased DA release in PFC up to 70%[532,533] presumably by missing noradrenergic suppression of dopaminergic firing activity in VTA[496-498].

Vice versa, the noradrenergic tone in mPFC is modulated by dopaminergic actions. So was the extracellular NE release increased by local infusion of DA into mPFC of anesthetized rats. This effect was reversed by blockade of D_1- but not D_2-receptors[272]. Comparable to modulation of extracellular DA release in mPFC by noradrenergic alpha 2-receptors, it was shown that pharmacological manipulation of D_2-receptors without prior increase of DA concentration actually increased NE release after D_2-receptor blockade and decreased it after D_2-receptor activation[534]. Nonetheless, a co-release of catecholamines from dopaminergic terminals is not reported.
In summary, DA and NE interact with each other on the somatodendritic level in the VTA as well as in the mutual terminal projection area mPFC. Presentation of noxious tail shocks increase both NE and DA in PFC[528] suggesting synergistic modulation of higher order processing of nociceptive stimuli. Optimal processing of sensory information is a prerequisite for optimal cognitive performance. This is because only well perceived environmental stimuli of all modalities during a variety of conditions may be adequately integrated and processed to determine an appropriate behavioral outcome[535]. Thereby, NE and DA play a complementary and critical role in PFC function and small perturbations of the neurochemical environment may contribute substantially to cognitive deficits[275,446,451,536]. Such a deficit might be as severe as surgical ablation of the cortical region[440].

1.3.2. Sensory gating deficits in schizophrenia

A chronic and severe mental disorder induced by catecholamine imbalance is schizophrenia. The complex and heterogeneous symptoms are divided into cognitive symptoms (attention deficits, working memory deficits, poor executive functions), negative symptoms (reduced expression of emotions, inactivity, social withdrawal, anhedonia) and positive symptoms (hallucinations, delusions, thought disorders, movement disorders)[471,537]. Specific positive symptoms in schizophrenia are so-called sensory gating deficits which refer to the basic inability of the brain to extract biologically relevant sensory information from “noise” in the environment[538-540]. The consequence is a sensory overload or sensory “flooding” by uncontrollable, overwhelming sensory stimulation[541]. In 1985, a

mother describes the sensory gating deficits of her schizophrenic son very illustrative: “If he isn’t hallucinating, his hearing is different when he’s ill. One of the first things we notice when he’s deteriorating is his heightened sense of hearing. He cannot filter out anything. He hears each and every sound around him with equal intensity. He hears the sounds from the street, in the yard and in the house, and they are all much louder than normal.”[542]. Experimentally, the ability of sensory gating is tested by using two different standard sensory-gating paradigms in animals and humans: Prepulse Inhibition (PPI) and Auditory Sensory Gating (ASG). In the PPI paradigm, the acoustic startle response (ASR), a substantial reflexive behavioral response to sudden loud stimuli, is reduced in healthy subjects when a mild stimulus, the prepulse, is presented 30 – 500 ms prior to the startle stimulus[543-545]. The prepulse might be of any modality although experimentally, an acoustic prepulse is commonly used[545-547]. The face, predictive and construct validity for the rat model of PPI has been demonstrated[548]. In ASG, paired auditory stimuli consisting of two tones usually 500 ms apart, are presented. In a healthy subject, the neuronal response to the second stimulus (test stimulus) is reduced due to sensory gating mechanisms evoked by the first stimulus (condition stimulus). A behavioral response is not expected in ASG[549,550]. Convergent or divergent underlying mechanisms between these two paradigms are still a matter of debate[551-554]. The general assumption for the mediation and modulation of ASG is a polysynaptic co-activation of non-specific inhibitory afferents along the sensory neuraxis, possibly from areas like the reticular formation or thalamus[555-557]. Additionally, cortical inhibitory mechanisms by simple contribution of GABAergic neurons, acting on metabotropic $GABA_B$ receptors have been proposed[550,553]. While the exploration of the contributing circuits for ASG attracted less attention, the underlying mechanisms of PPI are very well explored and will be discussed in the next section.

1.3.3. Mediation and modulation of sensory gating in rats

The ASR is mediated by an oligosynaptic pathway located in the pontomedullary brainstem with a latency of only 10 ms[558-561]. The acoustic startle stimulus is transferred from the auditory nerve via the cochlear nuclei to the nuclei of the lateral lemniscus and from there to the nucleus reticularis pontis caudalis (PnC) down the reticulo-spinal tract to the lower

motor neurons which transfer the information for muscle contraction[562-564] (Figure 1.2 white boxes).

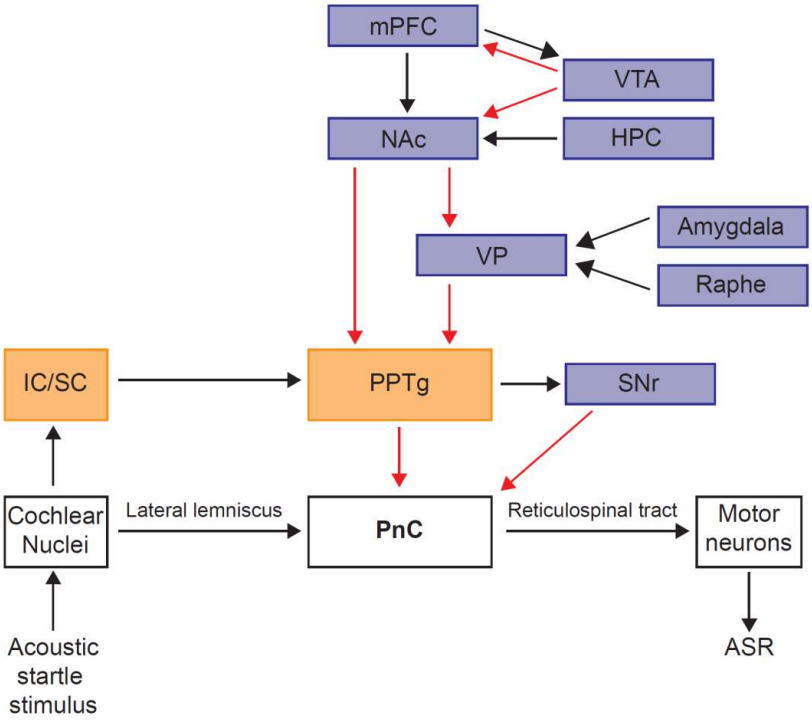

Figure 1.2: Schematic illustration of the pathway mediating the acoustic startle response (white) in addition to the pathway mediating (orange) and modulating (blue) auditory prepulse inhibition. Red arrows illustrate inhibitory connections. mPFC = medial prefrontal cortex, VTA = ventral tegmental area, HPC = Hippocampus, NAc = Nucleus Accumbens, VP = Ventral Pallidum, IC/SC = Colliculus inferior/superior, PPTg = Pedunculopontine tegmental nucleus, SNr = Substantia nigra pars reticulata, PnC = Nucleus reticularis pontis caudalis, ASR = acoustic startle response.

Within this pathway, the giant reticulospinal neurons in PnC are critical for attenuation of the ASR by presentation of a prepulse[565-567]. The mediating primary auditory PPI circuit projects from the auditory nerve to the cochlear nuclei and from there via colliculus inferior and colliculus superior to the pedunculopontine tegmental nucleus (PPTg) (Figure 1.2 orange boxes). This nucleus exerts cholinergic inhibition on the PnC[568-572] and, thus, directly intervenes in the pathway of the ASR. In addition, an excitation of the GABAergic substantia nigra pars reticulata by PPTg has been suggested, which in turn inhibits PnC activity[573]. Higher order brain structures including mPFC, NAc, HPC, amygdala, midbrain dopaminergic and serotonergic systems and the ventral pallidum contribute to a circuitry which modulates PPI[571,574,575] (Figure 1.2 blue boxes).

1.3.4. Dopaminergic modulation of sensory gating deficits in rats

The contribution of DA to sensory gating was subject of a number of studies which generally showed an impairment of PPI or ASG in rats after systemic increase of extracellular DA levels in DAT-KO mice[576] or by injection of amphetamine or apomorphine[554,577-584]. Other studies reported impaired PPI after systemic injection of a D_2-receptor antagonist in humans[585-587] and rodents[588,589]. The latter might be able to induce a hyperdopaminergic state by actions on presynaptic autoreceptors of dopaminergic terminals[369,377,590]. It is worth mentioning that PPI deficits induced by hyperdopaminergic state are reversed by increasing extracellular NE by NET inhibitors[576,582,591] confirming the previously mentioned complementary and compensating synergy between the catecholamines.

Originally, PPI deficits were consistently found to be related to hyperactivity in the mesolimbic DA system leading to a hyperdopaminergic state in ventral striatum, specifically NAc[570,592-594]. In support, it has been shown that PPI impairment induced by systemic amphetamine was reversed by neurotoxic lesion of dopaminergic terminals in NAc[592]. However, further region-specific exploration also provided strong evidence for the contribution of mPFC in modulation of PPI and also ASG[595-598]. Such mPFC-related modulation of PPI has been explored in much more detail. Both hyperactivation of mPFC by local infusion of a GABA-receptor antagonist[599] and hypoactivation by cytotoxic lesion of mPFC[600,601] impair PPI. In contrast to the hyperdopaminergic state in NAc, a hypodopaminergic state in mPFC has been reported to be related to PPI deficits. This was revealed by detailed pharmacological experiments involving local neurotoxic lesion of dopaminergic terminals in mPFC[602,603] or infusion of D_1- or D_2-receptor antagonist[580,604,605]. However, since the mPFC controls the tonic release of DA in the limbic striatum, these two mechanisms are not independent from each other. It has been demonstrated that electrical and pharmacological stimulation of mPFC neuronal activity increases the release of DA in NAc[606-608] and pharmacological inhibition by GABA-receptor agonists accordingly decreased it[607-609]. Furthermore, local infusion of DA-receptor agonists into mPFC reduced[609-611] while opposing depletion of DA by neurotoxic lesion in mPFC increased DA

metabolism in NAc[612,613]. It was suggested that the extracellular DA concentration in NAc is modulated by the activity state of prefrontal glutamatergic efferents. Since DA in mPFC inhibits neuronal activity of pyramidal neurons[386,392,395], depletion of prefrontal DA disinhibits glutamatergic projections to NAc and VTA[614-616]. The cortico-accumbal glutamatergic input naturally maintains a tonic release of DA into NAc by presynaptic activation of mesolimbic dopaminergic terminals[614,617-620] (

Figure 1.3). Thus, mPFC can control the extracellular level of DA either directly in NAc or indirectly by excitation of mesolimbic dopaminergic projections in the VTA[607,614,621,622].

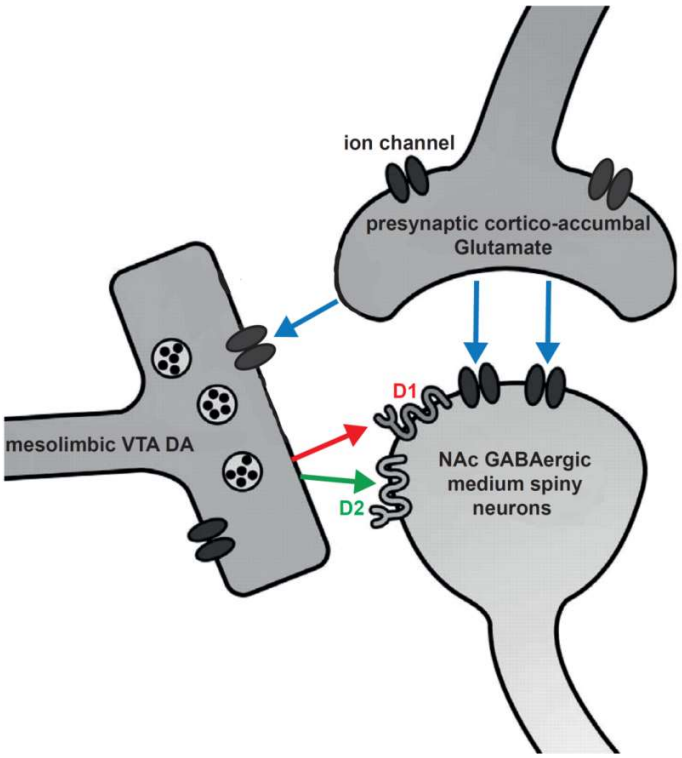

Figure 1.3: Schematic illustration of a 'synaptic triad' in NAc. Under physiological condition the glutamate release from prefronto-accumbal terminals activates postsynaptic GABAergic medium spiny neurons in NAc and simultaneously ensures a tonic release of DA by activation of presynaptic mesolimbic dopaminergic terminals. Thus, glutamate from mPFC directly mediates and indirectly modulates postsynaptic release of GABA from NAc neurons. Modified from Rhodes et al. 2005.

A resulting hyperdopaminergic state in NAc might impair PPI by suppression of the NAc spontaneous activity, as has been demonstrated in response to electrical stimulation of VTA[623-627], and related decreased release of accumbal GABA into the ventral pallidum. The ventral pallidum is hereafter disinhibited releasing more GABA into PPTg. As a

consequence the inhibitory impact of PPTg on PnC giant neurons is removed and the ASR is mediated unfiltered.

Nevertheless, PPI was similarly disrupted after increasing the extracellular DA concentration in mPFC by local infusion of apomorphine[628,629] indicating that a hyperdopaminergic state in NAc is not the only reason for sensory gating deficits. An alternative hypothesis suggests a dopaminergic hyper-responsivity in the ventral striatum due to decreased excitatory input from mPFC[353,630]. More specific, the tonic release of DA into NAc recedes with pathological decrease of the glutamatergic drive from mPFC. In consequence, DA system activity is upregulated by compensatory processes (e.g. decreased autoreceptor-mediated inhibition of DA synthesis and release, increase in the number of postsynaptic receptors, DA axon sprouting, increased receptor sensitivity) to ensure sufficient tonic DA receptor stimulation. Under this pathological condition, normally irrelevant and thus gated environmental stimuli produce phasic DA responses. In addition, strong salient sensory stimulation of aversive or alerting character[326-328] cause extraordinarily strong phasic activation of dopaminergic receptors in NAc which, in combination, results in sensory flooding[353].

In summary, it was suggested that sensory gating deficits are induced by neural circuit dysfunction in the prefrontal-striatal network[612,613,631]. In support, a comparable extent of PPI impairment was reported after depletion of DA in mPFC and local infusion of DA in NAc[593,603].

1.3.5. Research question study 3

Two alternative hypotheses have been proposed regarding how DA modulates sensory gating deficits in patients suffering from schizophrenia. The main question is whether the symptoms result from a hyperdopaminergic or a hypodopaminergic state in mPFC and, in consequence in NAc. It was suggested that a chronic hypodopaminergic state in NAc impairs sensory gating after compensatory mechanisms which enhance the sensitivity to phasically released DA. However, acute enhancement of DA concentration impairs sensory gating[554,576-584] and hence, it would be interesting whether acute reduction of DA concentration in NAc also modulates PPI. If this would be true, then an inverted U-shaped

dose-response function could be assumed. Supportive studies have shown that local infusion of dopaminergic D_2-agonists into NAc impair PPI[632,633] and that presynaptic dopaminergic autoreceptors are involved[634]. This implicates a presynaptic inhibition of DA release and, thus, a reduced DA transmission into NAc which disrupts sensory gating.
In the third study of this work, a VTA-target specific pharmacological approach was performed in order to clarify the importance of the contribution of DA release in mPFC or NAc to impairments in PPI as well as ASG. Therefore, target-specific receptor composition of VTA dopaminergic neurons was exploited for pharmacological inhibition of DA release in different VTA target structures. Dopaminergic neurons in the ventral midbrain express alpha 2-adrenoceptors on the presynaptic as well as alpha 1- and alpha 2-adrenoceptors on the postsynaptic membrane[493,494,496,505]. Commonly, tonic NE in the VTA has an inhibitory effect by actions on more abundant[499] and affine[234] alpha 2-adrenoceptors[494,496,505,635]. Local infusion of the alpha 2-noradrenergic agonist clonidine into the ventral midbrain additionally decreases potentially excitatory noradrenergic transmission by presynaptic actions[493,496,636]. Furthermore, activation of alpha 2-adrenoceptors by systemic or local infusion of clonidine into the VTA decreases burst activity and regularizes DA cell firing[508,509]. Accordingly, blockade of alpha 2-adrenoceptors increased burst activity in VTA DA neurons[493,509]. In summary, activation of alpha 2-adrenoceptors in VTA results in decreased dopaminergic turnover in VTA target regions like mPFC and NAc.
Besides alpha 2-adrenoceptors, dopaminergic neurons in the VTA also carry κ-opioid receptors; yet, it has been shown that the expression is selective for dopaminergic neurons projecting to mPFC[315,373]. On the other hand, these neurons lack the expression of dopaminergic D_2-receptors[299,361,372-374], which are in turn carried by dopaminergic neurons in the VTA projecting to other targets than mPFC[299,343,373].
Based on these target-specific properties of VTA dopaminergic neurons, three drugs were separately infused into the ventral midbrain of awake rats previous to simultaneous tests on PPI and ASG:

- alpha 2-adrenoceptor agonist clonidine in order to generally decrease dopaminergic transmission from VTA.
- κ-opioid receptor agonist U69593 to decrease DA release specifically in mPFC.

- D_2-receptor agonist quinpirole, which decreases DA release in structures besides mPFC.

1.3.6. Brief summary of the research aims in this thesis

The general question of this work is how the catecholaminergic neuromodulators NE and DA affect sensory processing in primary sensory and higher association cortex. To approach this question, a series of experiments were performed to first examine qualitative differences in sensory processing between these functionally distinct cortical regions and then explore the role of the LC noradrenergic system in modulation of cortical sensory processing in anesthetized rats. Since the catecholaminergic systems exert synergistic effects on cortical functions, next, the noradrenergic modulation of the ventral midbrain dopaminergic system was explored in an attempt to distinguish between noradrenergic and dopaminergic actions on cortical activity. Finally, the modulation of sensory gating and related neuronal activity in prefrontal association cortex was examined with an emphasis on the midbrain dopaminergic system in awake rats.

2. Material and Methods

All rats used in this study were housed on a 12 h light/dark illumination cycle with constant access to food and water. All experimental procedures were approved by the local authorities (*Regierungspräsidium*) and were in full compliance with the European Parliament and Council Directive 2010/63/EU on the protection of animals used for experimental and other scientific purposes.

2.1. Noradrenergic modulation of sensory processing in two functionally distinct cortical regions

Two sets of experiments were performed in order to explore the catecholaminergic modulation of sensory processing in urethane-anesthetized rats. In one set, the neuronal activity was simultaneously recorded in LC, S1HL and PFC. In a second set of experiments, neuronal activity was recorded from LC and VTA.

2.1.1. Surgery and electrophysiological recording

Twenty-two male Sprague-Dawley rats (250 - 350 g) were used as part of the study. All procedures were conducted under deep anesthesia with urethane (1.5 g/kg, i.p. with drug supplements given if needed). Rectal temperature, heart rate and SpO_2 levels were monitored and kept constant throughout the experiment. Once deeply anesthetized, each rat was mounted in a standard stereotaxic frame (David Kopf Instruments, Tujunga, CA, USA) with the head angle adjusted at zero degrees in the horizontal plane. The skull was surgically exposed and local anesthetic (1 % Lidocaine-hydrochloride; AstraZeneca, Wedel, Germany) was applied on the skin and bone. After approximately 3-5 min, small burr holes were drilled over the target brain regions. The following stereotaxic coordinates were used for the locus coeruleus (LC): AP= -4.1 mm from lambda, ML = 1.2 mm, medial prefrontal cortex (mPFC): AP = +3.5 to +4.5 mm, ML = 0.5 mm and primary somatosensory cortex (S1HL): AP= -0.5 to -2.5 mm from bregma, ML = 2 to 3.5 mm[637]. The final S1HL coordinates in the denoted window were determined according to the receptive field of the stimulation site in the contralateral hindlimb. Specifically, the S1HL

region was mapped by recording the epidural EEG responses to sensory stimulation (single FSs: 0.5 ms, 5 mA) and the site showing the maximal response amplitude was used for experiments. The recording depth was adjusted within a range of 3 – 4 mm for mPFC and 1 – 1.5 mm for S1HL to obtain best possible extracellular activity on all electrodes.
For extracellular recording in mPFC and S1HL, silicone-based multi-electrode arrays with tetrode configuration (Neuronexus Technologies, Ann Arbor, MI, USA) were used. Each electrode array consisted of four shanks, each equipped with one tetrode. In mPFC, the spacing between the shanks was 0.4 mm and covered ~ 1.2 mm in the antero-posterior direction. In S1HL, shank spacing was 0.15 mm, which covered ~ 0.45 mm in total. In LC, a three-barrel glass recording/iontophoresis microelectrode (Carbostar-3, Kation Scientific, MN, USA) enabled combined extracellular recording and drug injections. One barrel was incorporated with a carbon fiber electrode (6-7 μm) and a second barrel was filled with drug. The tip of the pipette, including the distal orifices of the barrels and the electrode did not exceed 10 μm. The electrode was fixed at 15 degrees in postero-anterior plane in order to avoid transverse sinus damage during the electrode penetration. The final position of the electrode in LC was electrophysiologically guided by the distinctive activity pattern of noradrenergic neurons. Specifically, the following criteria were applied for identification of LC neurons: 1) resumption of neuronal firing activity after absent electrophysiological activity due to passage of the IV ventricle; 2) broad spike width (~ 0.6 ms) and 3) a brief excitation followed by prolonged inhibition of neuronal activity in response to paw pinch[125,262,638]. The neurochemical nature of the recorded LC cells was further verified by inhibition of their firing due to systemic and/or intra-LC clonidine injection[205,267,639].
Signals were recorded by using a broad-band filter (0.1 Hz – 8 kHz) in at least one channel per cortical structure while the rest of the channels were recorded by application of a high-pass filter (300 Hz – 8 kHz). After preamplification (x 25) using a custom-made 32-channel preamplifier, the signals were again amplified (x 2k and x 5k for broad band signal and unit activity, respectively) using an Alfa Omega multi-channel processor (MPC Plus, Alpha Omega Co., Alpharetta, GA, USA). The signals were digitized at 24 kHz using CED Power1401mkII converter and Spike2 data acquisition software (Cambridge Electronic Design, Cambridge, UK).

2.1.2. Somatosensory stimulation

For somatosensory stimulation, electrical FSs were applied via two stainless steel needles which were placed subcutaneously ~ 1 cm apart in the paw of the hind limb contralateral to the recording sites. Electrical current was delivered using a biphasic stimulus isolator (BSI - 1, Bak Electronics, Inc., Mount Airy, MD). The stimulation parameters were digitally controlled by Spike2 software and transmitted to the current source via digital-to-analogue converter built-in to the data acquisition unit CED Power 1401mkII (Cambridge Electronic Design, Cambridge, UK). Actually applied current was monitored on the oscilloscope via a custom-built voltage output unit and compared with the digital input. Examination of effective stimulation parameters was performed by using different stimulation protocols. In one protocol, amplitudes of neuronal responses to electrical FS-stimulation were compared between single pulse (0.5 ms pulse duration, 5 mA) and train stimulation (0.5 ms pulse duration, 100 ms at 50 Hz) with a respective interstimulus interval of 10 sec. In another protocol, trains of pulses were applied using different stimulation currents: 1, 2, 3, 4 and 5 mA. Final stimulation protocol consisted of trains of rectangular pulses (0.5 ms pulse duration, 100 ms at 50 Hz) with a current intensity of 5 mA. The stimulus was repeated 25 times every 10 sec for each experimental condition.

2.1.3. Drug administration

Clonidine chloride (Tocris Bioscience, Bristol, UK) was dissolved in 0.9 % saline to a concentration of 50 µg/ml and either injected systemically (50 mg/kg, i.p.) or iontophoretically into LC via the glass pipette attached to the recording electrode placed in LC using a custom-made current source. In order to prevent unwanted leakage of clonidine during LC targeting and baseline recording, a holding current of -40 nA was applied. To ensure extensive drug diffusion in the LC nucleus, a continuous current of +50 to +90 nA was applied for at least 20 minutes between onset of infusion and presentation of sensory stimuli. The activity of LC neurons was simultaneously monitored. The injection current was applied for the entire duration of the stimulation series and no spontaneous LC activity was observed during the drug injection period (30 - 45 min). In order to estimate the radius

of drug diffusion in LC, three-barrel recording/iontophoresis microelectrodes were glued to single tungsten electrodes (FHC Inc., Bowdoin, ME, USA). Three experiments were performed using different tip distances between the tungsten electrodes and the infusion barrels: 238 µm, 251 µm and 354 µm (Figure 2.1). The electrode-pair was implanted by targeting LC at least with the tip of the tungsten electrode. After successful placement, clonidine was iontophoretically injected with parameters described above and the firing frequency of LC neurons was recorded via the distant tungsten electrode in order to assess inhibition.

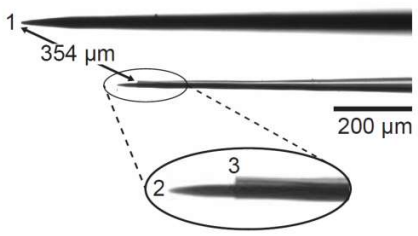

Figure 2.1: Electrode configuration for electrophysiological monitoring of diffusion radius of iontophoretically infused clonidine into LC. A standard tungsten microelectrode (1) was glued to a carbon-fiber microelectrode (2) attached to a barrel used for recording under simultaneous drug injection in LC. In this example, the tip of the tungsten electrode was 354 µm apart from the infusion site (3).

In the majority of experiments (n = 14), the data was collected according to the following experimental design: 1) FS series before the drug manipulation (referred in text below as baseline condition); 2) FS series on the background of local clonidine injection (local clonidine); 3) FS series after termination of the iontophoretic drug injection and recovery of the LC spiking activity to the baseline level (recovery); 4) another FS series under baseline condition; 5) systemic clonidine injection followed by the FS series repeated 4.2 ± 0.4 min, 20.2 ± 0.5 min, 33.9 ± 0.6 min and 55.5 ± 0.7 min after injection (systemic clonidine). The start of the first FS series was dependent on the first period of complete inhibition of LC neuronal activity after systemic injection of clonidine. In the remaining 8 experiments the effects of either local (5 experiments) or systemic (3 experiments) clonidine injection were tested.

2.1.4. Data analysis

All data analysis was performed using custom MATLAB functions (The MathWorks, Natick, MA, USA) unless otherwise stated.

For extraction of SEP, the raw broad-band extracellular signal was resampled and low-pass filtered to < 300 Hz (Finite Impulse Response (FIR) digital filter) using Spike2 software. SEP was obtained by across trial averaging of the signal in the time-domain.

For extraction of band-limited power (BLP), the broad-band extracellular signal was resampled at 300 Hz and band-pass filtered (butterworth Infinite Impulse Response digital filter) in seven non-overlapping frequency bands. The frequency distribution across the bands was adapted from what is classically used in human EEG[29-34]: SLO (0.1 – 1 Hz), Delta (1 – 4 Hz), Theta (5 – 8 Hz), Alpha (9 – 11 Hz), Sigma (12 – 15 Hz), Beta (16 – 20 Hz) and Gamma (60 – 90 Hz). Rectification of the respective absolute values for each frequency band provided the BLP. The filtering method is described in detail elsewhere[640]. Composition of spectral power in response to electrical stimulation to FSs was analyzed by computing the change of BLP during 1 sec poststimulus period (postBLP) relative to BLP in 4 sec prestimulus period (preBLP) using the following formula:

((postBLP - preBLP)/preBLP) x 100.

For cortical single unit isolation, the signal was first high-pass filtered above 300 Hz and spike shapes, exceeding at least 2-fold the background activity were extracted. Next, the template matching algorithm complemented by manual cluster analysis based on principal components and on specific waveform measurements (amplitude, spike width, maximum slope, etc.) were applied using Spike2 software. The recording was classified as a single-unit if a refractory period of at least 1 ms was present between two consecutive spikes. In cases when the recording quality and spike sorting method did not allow unambiguous single unit isolation, the recording was conservatively classified as multiunit activity (MUA). The cortical MUA data was excluded from further analysis. In LC, MUA was extracted from high-pass filtered signal (> 300 Hz) for exploration of neuronal activity. In case of systemic clonidine administration, the effects of clonidine on spontaneous neuronal discharge in LC was evaluated by extracting the firing rate over 60 sec before each FS

series and comparing it with the preinjection (baseline) activity level. Thereafter, the cortical effects were assessed by extraction of the firing rate over 60 sec before the FS series within the interval of maximum LC-inhibition (20.2 ± 0.5 min). The direction of firing rate modulation of each cortical neuron was determined by paired t-test between baseline and clonidine condition (average rate of 60 s spontaneous activity with 1 sec bin width).

Based on previous studies, the population of single units in each cortical region was divided into putative interneurons and pyramidal neurons according to the duration of the afterhyperpolarization (AHP), spike width and peak-to-trough amplitude ratio. In nearly all cases, the waveform was initially negative-going. This negative voltage deflection was the maximum component of the waveform and it was assumed to be the inward sodium current of the action potential. After inversion of this waveform, the spike width was defined by the width between the peak and the following trough of the high-pass filtered signal[641,642]. The peak-to-trough ratio was computed out of the maximum amplitudes of the peak and the AHP[643-645] and the duration of the AHP was defined by onset and end of AHP at resting potential. The distribution of all three parameters revealed two populations with a partition at duration of AHP of 0.87 ms, spike width of 0.56 ms and at peak-to-trough ratio of 3.95, respectively (Supplementary Figure 7.1). Neurons with spike width and AHP-duration exceeding the values at partition and neurons with peak-to-trough ratio below 4 were considered as putative pyramidal neurons and contributed to analysis.

To characterize neuronal responses of S1HL and mPFC single units to FS, for each experimental condition the peristimulus time histograms (PSTH) of spike density converted into Z-Scores were plotted from -0.5 sec to +1.5 sec around stimulation onset with 10 ms bins smoothed by a Gaussian Filter with a filter width of 3 bins using NeuroExplorer software (Nex Technologies, Madison, AL, USA). A single unit was classified as responsive, if at least one bin during post-stimulus interval was below or above 95 % confidence interval. The response peak latency was calculated from the stimulus onset to the maximum amplitude of the PSTH during poststimulus interval. The bin size was still 10 ms with exception of the latency for the early transient burst of the S1HL neurons which were extracted using 1 ms bin size. The duration of the response was defined between the

first and the last bin that exceeded threshold providing that the last bin was followed by at least 10 consecutive bins within the mean ± 2 SD boundary. The cortical neuronal responses were clustered according to the shape of the response profile using K-Means clustering algorithm.

Due to complete absence of the LC spikes during pre-stimulus period in some experimental conditions, the LC firing rate was plotted in PSTH normalized by dividing each 10 ms-bin by the average baseline spontaneous activity in 0.5 sec pre-stimulus interval for each individual recording. For illustration all PSTH-series have been smoothed again using a moving average filter with a span of 3 bins.

Magnitudes of SEPs or PSTHs of single unit responses to sensory stimulation were estimated as the integral of the area under or above the curve. Unless otherwise stated, the period for integration was generally defined as between response onset to offset, determined by exceeding 2 SD of baseline activity.

2.1.5. Perfusion and histology.

At the end of an experiment, the rat was euthanized with a lethal dose of sodium pentobarbital (100 mg/kg i.p.; Narcoren®, Merial GmbH, Germany) and perfused transcardially with 0.9 % saline followed by 4 % paraformaldehyde in 0.1 M phosphate buffer (PB, pH 7.4). The brain was removed and stored in the same fixative. Before sectioning, the whole brain was placed in 0.1 M PB containing 30 % sucrose until sinking. Serial 60 µm-thick coronal sections were then cut on a horizontal freezing microtome (Microm HM 440E, Walldorf, Germany) and collected in 0.1 M PB saline. After mounting and drying on glass microscope slides (Thermo Scientific Adhesion Slides SuperFrost® Plus), Nissl staining was performed on every other section following a standard procedure. Briefly, sections were defatted, stained with cresyl violet, rinsed with acetic acid, dehydrated and coverslipped (Depex Mounting Media, VWR International GmbH, Darmstadt, Germany). The sections in between were just coverslipped using polyvinylalcohol (Mowiol 4-88, Hoechst, Frankfurt, Germany) without previous staining. On these sections, the placement of silicone-based electrode arrays was visualized by preliminary coating of the back side of the shanks with fluorescent substance (DiI or DiO,

Life Technologies GmbH, Darmstadt, Germany) before tissue penetration. All cortical sections were examined using an AxioPhot or AxioImager microscope (Carl Zeiss, Goettingen, Germany). Nissl sections were examined under brightfield. Fluorescent sections were examined under epifluorescent illumination using custom-made sets of filters for Alexa Fluor® 546 (AHF, Tuebingen, Germany).

2.1.6. Statistical analysis

A significance level of 0.05 was applied for all statistical tests in this study which were computed in MATLAB.
One-sample t-test against 0 was used when effects of drug condition on the population activity change within a cortical region was tested. Furthermore, this test was used to examine effective cortical state activation in response to sensory stimulation.
Non-parametric Chi-square-test was performed to compare absolute numbers between conditions. If not otherwise stated, between-group comparison was performed using one- or n-way analysis of variance (ANOVA) followed by Bonferroni post-hoc multiple comparison.
In order to evaluate which component of the single unit response profile was affected by drug manipulation, a pairwise comparison of each bin was applied in the post-stimulus period between 0 and 1.5 sec. The first and the last significantly modulated bin within this period provided the affected interval, which was then analyzed by two-way repeated measures ANOVA (condition x bins) followed by Bonferroni corrected multiple comparison analysis.

2.2. Noradrenergic modulation of the midbrain dopaminergic system

Fifteen male Sprague-Dawley rats (250 - 350 g) were used in this part of the study in which data was simultaneously recorded in LC and VTA. Stereotaxic coordinates for VTA recordings were AP = -5.3 mm from bregma, ML = 0.8 to 1 mm, DV = adjusted between 8.0 to 9.0 dependent on signal quality[637].
Material and methods were used as described in section 2.1 except for the following changes: for extracellular MUA recording in VTA, a single-channel iridium microelectrode

(Neuronexus Technologies, Ann Arbor, Michigan) was used. Somatosensory stimulation was presented with parameters described in 2.1.2, except for the interstimulus interval which was randomized between 8 and 12 sec. Furthermore, the systemic injection of clonidine was spared and clonidine was only infused locally into LC with the parameters described above.

2.3. Dopaminergic modulation of sensory gating

2.3.1. Surgical procedures

Thirteen male Sprague-Dawley rats (250 – 300 g at time of the surgery) were used in this study. Implantation of electrodes and cannulae was conducted under aseptic conditions and deep anesthesia with isoflurane. Anesthesia was initiated with isoflurane (4 %) in oxygen enriched air accumulating in an anesthesia box. Following loss of righting reflex, anesthesia was applied by using a nose cone and concentration was reduced to 1.5 to 2 %. Sufficient anesthesia was ensured throughout the experiment by monitoring withdrawal reflex in response to paw pinch. Rectal temperature, heart rate and SpO_2 levels were monitored and kept constant throughout the experiment. Before placing the rat into a stereotactic frame (David Kopf Instruments, Tujunga, CA, USA), a xylocaine-gel (2 % Lidocaine-hydrochloride; AstraZeneca, Wedel, Germany) was applied into the ear canal for analgesia. Three to five minutes later, each rat was fixed with the head angle adjusted at zero degrees in the horizontal plane. Before skin incision, anesthetic solution (1 % Lidocaine-hydrochloride; AstraZeneca, Wedel, Germany) was injected at 4-5 different sites (0.01 to 0.02 ml each) beneath the scalp. Three to five minutes later, the skull was surgically exposed and, after covering with lidocaine for further 3-5 min, small burr holes were drilled over the target brain regions. Great care was taken to avoid bleeding from cerebral arteries and veins throughout the surgical procedure. First, 3 anchor screws were fixed into the skull in addition to a grounding screw, which was placed into the parietal bone near lambda. For extracellular recordings in mPFC, a single tungsten electrode for chronic use (FHC Inc., Bowdoin, ME, USA) was aimed at the following stereotaxic coordinates: AP = +3.5 to +4.5 mm from bregma, ML = 0.5 mm, DV = 3.0 mm[637]. For drug infusion into the ventral

midbrain, bilateral stainless steel guide cannulae (PlasticsOne Inc., Minneapolis, MN) with diameter of 22 gauge were used. First, stylets were placed into the guides to prevent occlusion. After cutting small incisions into the dura, the bilateral cannulae were slowly placed at the stereotaxic coordinates AP = -5.3 mm from bregma, ML = 0.75 or 1.0 mm, DV 6.5 mm. The gaps between implants and skull were filled with grease and the implants were fixed to the skull with dental acrylic cement (PalaXpress ultra, Heraeus Kulzer GmbH, Hanau, Germany). The recording channel and the grounding screw were then soldered to a connector, which was in turn fixed to the rest of the implant by use of dental acrylic cement. Approximately 30 min before the end of the surgery, a cocktail containing analgesics (12.5 mg/kg Flunixine-Meglumin, MSD Tiergesundheit, Unterschleißheim, Germany) and antibiotics (5 mg/kg Baytril; Bayer AG, Leverkusen, Germany) was subcutaneously injected. This treatment was repeated on a daily basis for 5 days after surgery.

2.3.2. Drug design

The properties of receptor composition in VTA (Figure 2.2A) were exploited to achieve a target-specific pharmacological manipulation in the ventral midbrain. Specifically, in order to decrease general dopaminergic transmission, alpha 2-noradrenergic receptors were activated by local infusion of clonidine. Furthermore, infusion of κ-opioid agonist U69593 and dopaminergic D_2-receptor agonist quinpirole was used to selectively inhibit dopaminergic transmission to mPFC or non-PFC target structures, respectively. An overview of the individual effects is illustrated in Figure 2.2B.

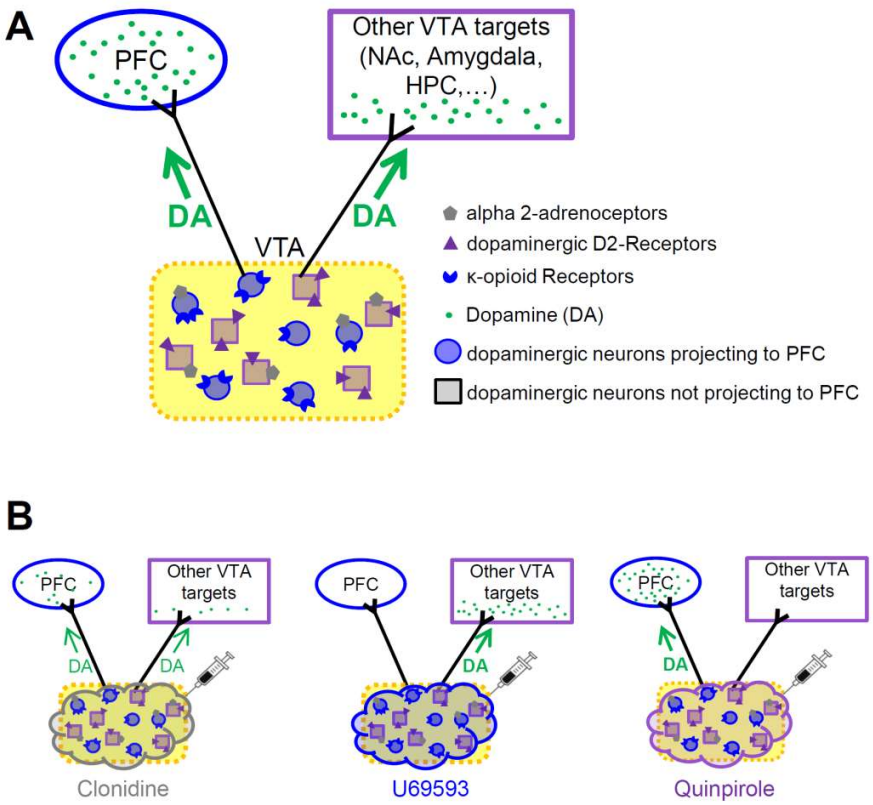

Figure 2.2: Schematic illustration of receptor composition in dopaminergic neurons in the VTA exploited for target-specific dopaminergic manipulation. A) Two populations of dopamine (DA) releasing neurons in the VTA express different inhibitory receptors dependent on specific target regions. Additionally, both populations carry alpha 2-noradrenergic receptors. B) Drug effects induced by activation of specific inhibitory receptors in VTA: Infusion of alpha 2-noradrenergic agonist clonidine reduces dopaminergic transmission to all VTA target regions, infusion of κ-opioid receptor Agonist U69593 inhibits dopaminergic transmission specifically to prefrontal cortex (PFC) and infusion of dopaminergic D_2-receptor agonist inhibits release of DA in target areas other than PFC. NAc = Nucleus Accumbens, HPC = Hippocampus.

2.3.3. Drugs

All drugs were purchased from Sigma Aldrich Chemie GmbH, Taufkirchen, Germany. Clonidine chloride was dissolved in 0.9 % saline to a concentration of 50 µg/ml It was shown to reliably inhibit neuronal activity of noradrenergic neurons in LC (see section 3.1.2). Concentrations of U69593 and quinpirole were chosen according to reported behavioral modulation after local infusion into the VTA. U69593 was dissolved in 12 % aqueous propylene glycol to a concentration of 0.3 mg/ml[646] and Quinpirole hydrochloride

was dissolved in 0.9 % saline to a concentration of 2 mg/ml[647,648]. Drug solutions were prepared weekly under aseptic conditions and stored at +7 °C.

2.3.4. Drug infusion

Three sessions were recorded under each drug condition. Distribution of the drugs over the 9 sessions was randomly determined. Control sessions after saline infusion were performed in between, so that each session under drug condition has a corresponding saline control session. By this design, each rat underwent 18 sessions (9 x saline, 3 x clonidine, 3 x U69593 and 3 x quinpirole).
For drug infusion, stylets were replaced by sterile stainless steel infusion cannulae (28 gauge), which were 2 mm longer than the guide cannulae, reaching a final depth of 8.5 mm. The infusion cannulae were connected to two 2 – 5 µl Hamilton syringes by polyethylene tubing (ID 0.58 mm). By aid of a microdrive infusion pump (UMP3 Ultra micro pump, World Precision Instruments, Sarasota, FL, USA) 0.5 µl of the drug was infused into each hemisphere at a rate of 200 nl per minute. Rate and volume were computed such that tissue damage was prevented[649-651] and a final drug diffusion of approximately 1 – 1.5 mm diameter was reached[652]. During the infusion the freely moving rat was placed in a small box (25 x 15 x 15 cm). After end of the infusion the cannulae were left in place for 60 sec to allow diffusion of the drug into the tissue. Thereafter, the cannulae were replaced with the stylets and the rat was placed into the behavioral box for testing.

2.3.5. Behavioral testing

One week after surgery the rats were tested simultaneously on two standard sensory gating paradigms in the same session: PPI and ASG. Feasibility of simultaneous assessment of both paradigms was confirmed before[653]. Rats were placed non-restricted in a box made of transparent plastic (25 x 15 x 15 cm) inside a custom-made chamber (30 cm x 20 cm x 40 cm) consisting of three non-transparent walls and a front one made of plexiglas. The plastic box had two mesh-covered holes directed to the sides of the chamber where, in a distance of 3 cm, a speaker was mounted on each side. In addition, a custom-built

piezoelectric accelerometer was located under the floor for movement detection of the animal.

Speakers and piezoelectric sensors were connected to a computer which automatically presented the stimuli and recorded the outcome by use of custom-written functions in Spike2 data acquisition software (Cambridge Electronic Design, Cambridge, UK). During the entire session a continuous white background noise of 50 dB was presented. After a short acclimatization period of 60 sec, sensory stimulation started on top of the background noise. Four different types of acoustic stimuli were randomly presented with variable inter-stimulus interval of 15 – 20 sec. Three of them, namely acoustic startle stimulus (broad band noise, 20 ms, 100 dB), acoustic prepulse stimulus (10 kHz, 20 ms, 75 dB) and acoustic prepulse stimulus presented 100 ms prior to the startle stimulus, belong to the PPI-paradigm (n = 50 each). The magnitude of the ASR was detected by the piezoelectric sensors in the floor and digitized at 1 kHz. The last stimulus type, 2 clicks presented 500 ms apart from each other (parameters identical to acoustic prepulse stimulus, n = 100), belongs to the ASG paradigm in which no behavioral outcome is expected.

During the sessions, the local field potential in mPFC was continuously monitored. After preamplification (x 25) using a custom-made preamplifier, the band-passed signal (1 Hz – 1 kHz) was amplified (x 1k) using an Alfa Omega multi-channel processor (MPC Plus, Alpha Omega Co., Alpharetta, GA, USA). The signal was digitized at 1 kHz using CED Power1401mkII converter and Spike2 data acquisition software.

To familiarize the animal with experimental conditions, each rat underwent the first session without any drug infusion.

2.3.6. Perfusion and histology.

At the end of experiment, the rat was euthanized, transcardially perfused and histology was performed as described in section 2.1.5, except that Nissl staining was performed on every section. The placement of the tungsten microelectrode and cannulae were examined under brightfield by using an AxioPhot or AxioImager microscope (Carl Zeiss, Goettingen, Germany).

2.3.7. Data analysis

After data acquisition, both the converted signal of the movement and local field potential recorded in mPFC were down-sampled and filtered to < 100 Hz (FIR digital filter) by using custom Spike2-functions. Obvious artifacts created by excessive movements of the animal were removed from recording (Supplementary Figure 7.2).
All further data analysis was performed using custom MATLAB functions (The MathWorks, Natick, MA). Due to variable delays between trigger and sensory stimulation, created by switching between recording and stimulus presentation in the Spike2 software, the minimum amplitudes of the voltage deflection of negative-going SEP and ASR during 500 ms after trigger position were aligned to zero before averaging the signal across trials in the time domain.

2.3.8. Statistical analysis

A significance level of 0.05 was applied for all statistical tests in this study. All statistics was computed in MATLAB.
Degree of sensory gating was analyzed as percentage of PPI or ASG by using the following formula: %PPI/ASG = 100 – ((response amplitude to prepulse followed by startle stimulus/response amplitude to startle stimuli alone) x 100). Grand average of %PPI and %ASG as well as grand average of maximum amplitudes of SEP and ASR over all sessions was compared between different stimuli and between conditions by using one-way ANOVA followed by Bonferroni post-hoc multiple comparison analysis. Data of the first session without any saline or drug infusion was discarded.

3. Results

The basic question of this study is how the catecholaminergic neuromodulators NE and DA affect sensory processing in the cortex. To answer this question, first, the differences between sensory processing in two functionally distinct cortical regions were examined. Afterwards, the role of NE in neuromodulation of the cortical neuronal activity during sensory processing was explored by pharmacological manipulation of the noradrenergic

system. Furthermore, by exploration of the noradrenergic modulation of the VTA-DA system, the synergistic effects of catecholaminergic neuromodulation of neuronal activity in the medial prefrontal cortex was examined. Finally, the role of DA in the modulation of neuronal and behavioral sensory gating effects was studied by target-specific dopaminergic manipulation of the midbrain dopaminergic system. While the first two studies were performed in urethane anesthetized rats, the last study was conducted in awake animals.

3.1. Noradrenergic modulation of sensory processing in two functionally distinct cortical regions

Neuronal activities during sensory processing in different brain regions have been extensively studied (see Introduction for detail), however, direct comparison to the literature is difficult because of the use of different methods related to specific rationales. Therefore, functional differences in neuronal processing of sensory-evoked responses were first characterized and compared between two functionally different brain regions. The S1HL and the PrL subdivision of the mPFC were chosen as representatives for a primary sensory and a higher association cortical area. Direct comparison requires identical experimental conditions, which was achieved by simultaneous recordings in S1HL and mPFC during experiments in 30 urethane anesthetized rats. Additionally, neuronal activity in LC was recorded to monitor the activity state of the noradrenergic system.
Histological examination confirmed that the neuronal activity of all three target structures was simultaneously recorded in 8 rats. In additional 20 rats the simultaneous recordings were obtained from two out of three structures and in another two cases only data from LC recordings contributed to analysis (Table 3.1).

Table 3.1: Number of simultaneous recorded structure combinations out of 30 anesthetized rats.

Structure combinations	LC S1HL mPFC	LC mPFC	LC S1HL	S1HL mPFC	LC
Number of recordings	8	13	4	3	2

Most of the recordings in S1HL were performed in deeper cortical layers (> 1 mm depth,

Figure 3.1A) while in mPFC the electrode positions were distributed over all layers in the PrL subregion (

Figure 3.1B).

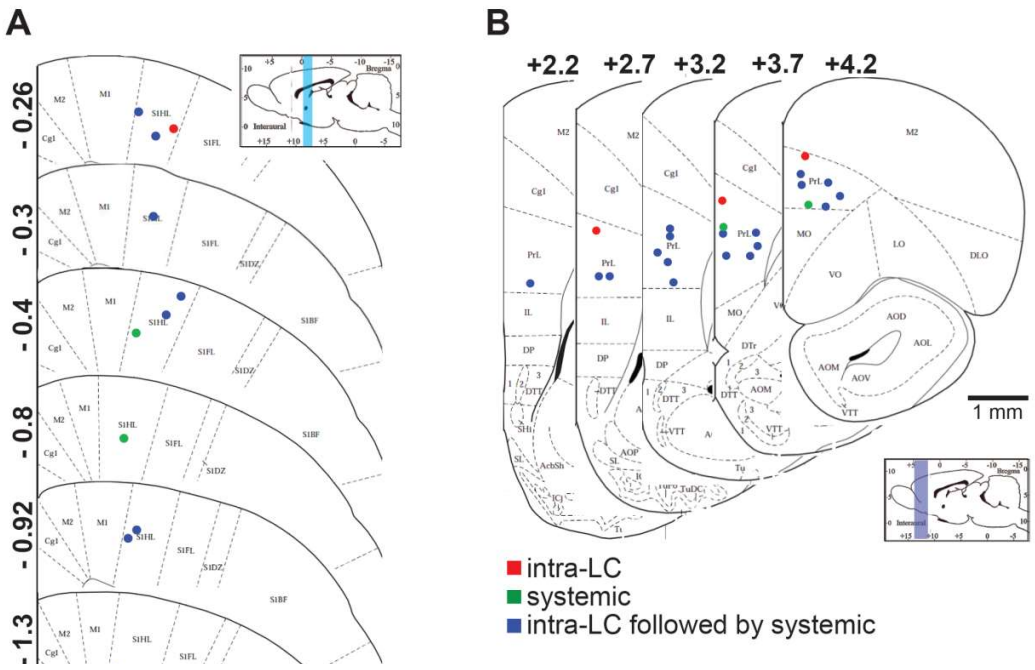

Figure 3.1: Coronal schematic views showing the electrode positions under local infusion into LC (red), systemic injection (green) or local followed by systemic injection of clonidine (blue) in A) S1HL and B) prelimbic subregion of PFC (PrL) in urethane anesthetized rats. Numbers illustrate distance from bregma in mm for each section. Respective insets illustrate the antero-posterior extent of recording sites by aid of color coded bars in a sagittal plane of the brain. Top numbers indicate distance from bregma, bottom numbers distance from interaural line and vertical numbers depth in mm, respectively.

From these locations in the cortex, neuronal activity was recorded by using a Low Pass Filter with a cut off frequency set to 8 kHz, which enabled acquisition of both LFP and underlying SUA. Inspection of the extracellular voltage-traces, after repeated off-line low-pass filtering (0.1 – 300 Hz), confirmed spontaneous alternations of the LFP between activated and deactivated state under urethane anesthesia (Figure 3.2) as has been already reported before[66,654-657].

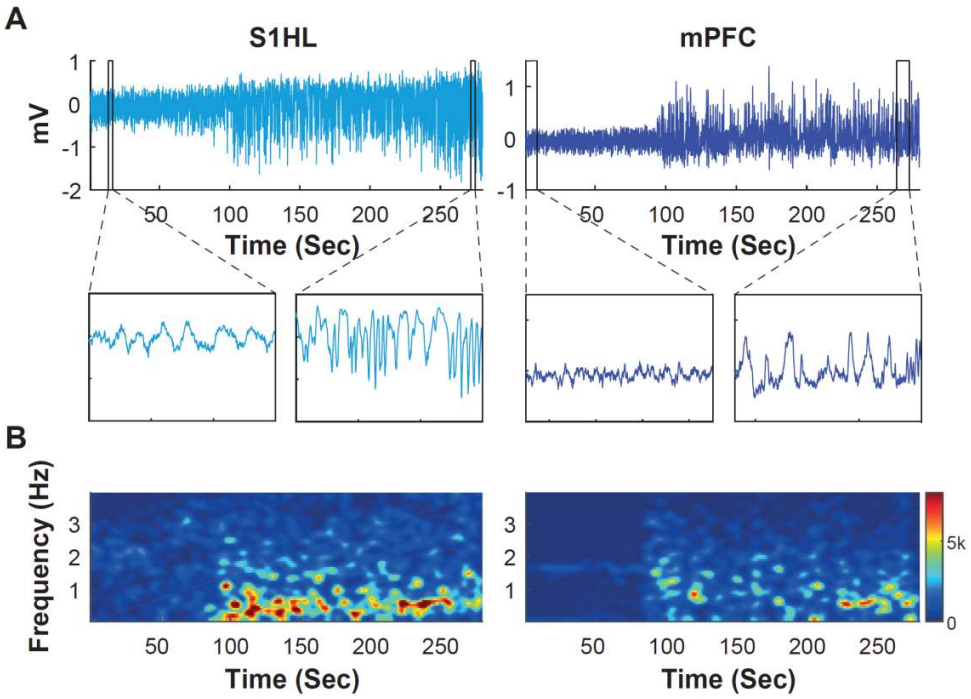

Figure 3.2: Spontaneous alternation of cortical oscillatory activity between different brain states under urethane anesthesia. A) Representative examples of extracellular voltage traces (0.1 - 300 Hz) continuously recorded in S1HL (left) and mPFC (right). Approximately at 100 sec, the brain state switches from activated state to lower frequency oscillations with higher amplitude. Figures below illustrate magnifications during 3 sec in S1HL and 9 sec in mPFC showing different brain states out of the continuously recorded voltage trace above. B) Corresponding spectrograms of the low-frequency (0.1 - 4 Hz) range. Note the power increase in the low-frequencies of LFPs at approximately 100 sec in both cortical areas.

In order to gain statistical power for further LFP analyses under this condition of variable cortical state activity, each period of baseline condition before local and systemic injection of clonidine was treated as individual case, regardless of whether these recordings were obtained from the same rat. By this, out of 30 rats, 23 recordings of ongoing brain activity were obtained from S1HL and 41 from mPFC (Table 3.2). A detailed description about the structural distribution of simultaneous recordings over all rats, analogous to Table 3.1 is provided in section 3.1.2.

Table 3.2: Number of recordings of ongoing cortical state activity during the period before local and systemic injection of clonidine in both cortical structures

	mPFC	S1HL
Systemic clonidine	20	12

Local clonidine	21	11
Total	41	23

3.1.1. Direct comparison of ongoing neuronal activity in S1HL and mPFC

For a detailed comparison of the oscillation properties between S1HL and mPFC, the LFP was decomposed into 7 classically defined non-overlapping frequency bands[29,31,35]: SLO (0.1 – 1 Hz), Delta (1 – 4 Hz), Theta (5 – 8 Hz), Alpha (9 – 11 Hz), Sigma (12 – 15 Hz), Beta (16 – 20 Hz) and Gamma (60 – 90 Hz). As expected, BLP analysis of these frequency bands revealed the highest power in low frequency bands in both cortical regions (Figure 3.3, Supplementary Table 7.1). Following one-way ANOVA with the 7 different frequency bands as factors, multiple comparison revealed significantly higher power in SLO and Delta frequency bands compared to higher frequency bands from Alpha upwards (S1HL: $F(6, 154) = 69.21$, $p < 0.001$; mPFC: $F(6, 280) = 68.95$, $p < 0.001$).

Between group comparison of individual BLP in cortical structures showed that BLP in medial frequency bands from Theta to Beta range was higher in S1HL compared to mPFC (SLO: $F(1, 62) = 0.23$, p = n.s., Delta: $F(1, 62) = 0.00$, p = n.s., Theta: $F(1, 62) = 8.96$, $p < 0.01$, Alpha: $F(1, 62) = 7.9$, $p < 0.01$, Sigma: $F(1, 62) = 5.09$, $p < 0.05$, Beta: $F(1, 62) = 4.2$, $p < 0.05$, Gamma: $F(1, 62) = 2.74$, p = n.s.). This increased synchrony in medial frequency bands in S1HL was accompanied by higher underlying single unit spontaneous activity ($F(1, 202) = 9.84$, $p < 0.01$) of 3.15 ± 0.31 spikes/sec compared to 1.99 ± 0.22 spikes/sec in mPFC.

Despite of the differences between neuronal activities in the cortical regions, correlation analysis of simultaneous recorded cases only, revealed that the BLP in each frequency band correlated positively between the two cortical regions with maximum correlation coefficients in Theta and Alpha frequency bands (Table 3.3).

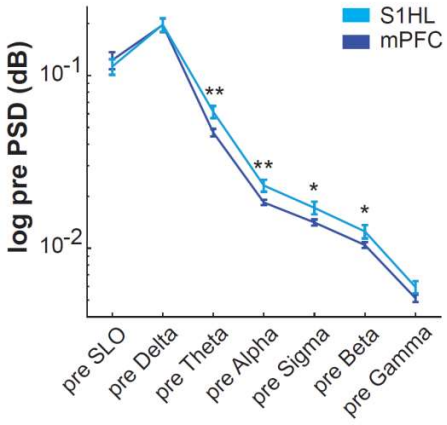

Figure 3.3: Average power source density (PSD) in the analyzed frequency bands during the 4 sec before stimulus-presentation (pre) in S1HL and mPFC. Mean ± SE, * p < 0.05; ** p < 0.01.

Table 3.3: Summary of correlation analysis of prestimulus BLP between simultaneously recorded S1HL and mPFC in each analyzed frequency band. Note the maximum correlation coefficient in Theta and Alpha frequency bands.

	Pearsons's Correlation
pre SLO	r = 0.62, n = 16, p < 0.05
pre Delta	r = 0.51, n = 16, p < 0.05
pre Theta	r = 0.74, n = 16, p < 0.01
pre Alpha	r = 0.73, n = 16, p < 0.01
pre Sigma	r = 0.62, n = 16, p < 0.05
pre Beta	r = 0.53, n = 16, p < 0.05
pre Gamma	r = 0.55, n = 16, p < 0.05

In brief, although the LFP spontaneously alternates between activated and deactivated state under urethane anesthesia, power in low frequency bands dominates the spectrum as commonly reported for brain state under anesthesia[658-660]. Synchrony in medial frequency range as well as associated single unit firing activity was higher in S1HL compared to mPFC, indicating a higher activity state. Nevertheless, it still appeared that mPFC and S1HL interact with each other especially in the Theta and Alpha frequency band.

3.1.2. Noradrenergic modulation of spontaneous neuronal activity in S1HL and mPFC

The role of the LC NE system in modulation of neuronal activity in two functionally distinct cortical regions was studied by using two pharmacological manipulation techniques: 1) global activation of alpha 2-adrenoceptors by systemic bolus injection of alpha 2-adrenergic agonist, clonidine (50 µg/kg, i.p.) or 2) constant local infusion of clonidine (50µg/ml, current +50nA to 90nA, for 20 min) into LC. The radius of clonidine diffusion was tested by pairing the infusion pipette with a tungsten electrode using different distances between the tips. Infusion of clonidine resulted in complete cessation of LC-firing (

Figure 3.4A) 238 µm, 251 µm and 354 µm apart from the infusion site. The duration between infusion onset and inhibition of LC neurons increased linearly with the distance between the tips (

Figure 3.4B; r = 0.94).

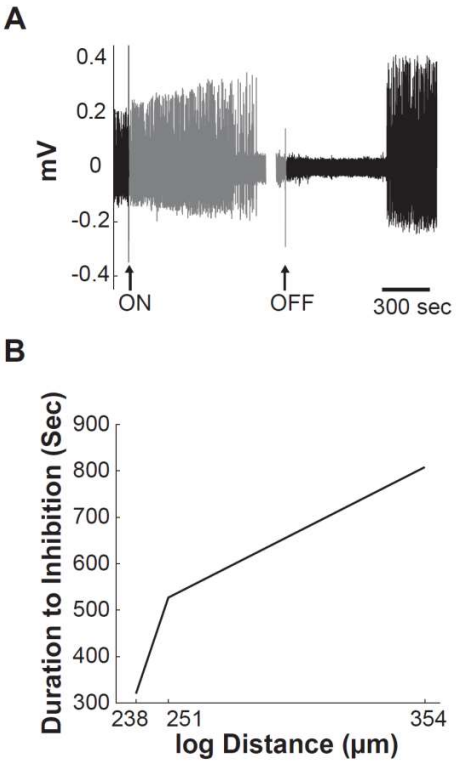

Figure 3.4: Electrophysiological monitoring of diffusion radius of iontophoretically infused clonidine into LC. A) Raw high-passed (300Hz – 8kHz) extracellular signal recorded in LC with the tungsten electrode 354 µm apart from the infusion site. Gray area indicates the period of iontophoretic infusion of clonidine into LC (50 µg/ml, +40 nA to +60 nA, for 20 min), which induced complete cessation of neuronal activity. Note the artefacts created by the switch to start (ON) and stop (OFF) of the infusion. For illustration purpose, the period of maximum inhibition of neuronal activity in LC was shortened (gap). B) Duration between start of the infusion of clonidine and maximum inhibition of LC-activity recorded by distant tungsten electrodes paired to recording/iontophoresis microelectrodes. Note the increased duration to inhibition dependent on the distance between the recording tip and the infusion site.

MUA-recording in LC was achieved in 27 out of 30 experiments, out of which monitoring of LC activity under pharmacological manipulation was performed in 25 and 15 recordings after intra-LC and systemic administration of clonidine, respectively. Previous studies show that either method of clonidine administration is expected to inhibit activity of noradrenergic neurons in LC[205,262,266,267]. Therefore, cases were excluded if the simultaneously monitored neuronal spontaneous activity in LC was not inhibited. Table 3.4 provides a detailed overview about the simultaneously recorded structure combinations for each experimental manipulation.

Table 3.4: Number of simultaneous recorded structure combinations under each experimental manipulation.

Structure combinations	LC S1HL mPFC	LC mPFC	LC S1HL	S1HL mPFC	LC
Systemic	7	3	3	2	2

Local	8	13	3	1	1

While both manipulations deplete the brain from NE[132,263-266,269-271] by acting on the presynaptic noradrenergic autoreceptors in LC terminals or on somatodendritic autoreceptors in LC itself, the systemic injection of clonidine affects additionally noradrenergic heteroceptors on postsynaptic cells in LC terminal regions.

Analysis of the recorded temporal dynamics of LC activity after clonidine administration showed that, in agreement with previous reports, systemic clonidine injection resulted in a sustained decrease of LC activity (Figure 3.5A). The onset of LC inhibition was typically observed after 283.8 ± 30.8 sec. The LC firing reached minimum (71.5 ± 5.4 % change) at 16.43 ± 0.78 min post-injection (n = 15). One-way ANOVA with repeated measures on time confirmed that the clonidine-induced decrease of LC firing was significant compared to pre-injection LC activity ($F(2.46, 46.74) = 8.545$, $p < 0.001$). Injection of clonidine locally into LC resulted in complete cessation of the LC firing that was observed 376.6 ± 22.8 sec (n = 25) after onset of injection current (Figure 3.5B). The LC inhibition lasted as long as the current was passing through the pipette. The firing rate recovered to the baseline level 428.9 ± 21.3 sec after termination of clonidine injection.

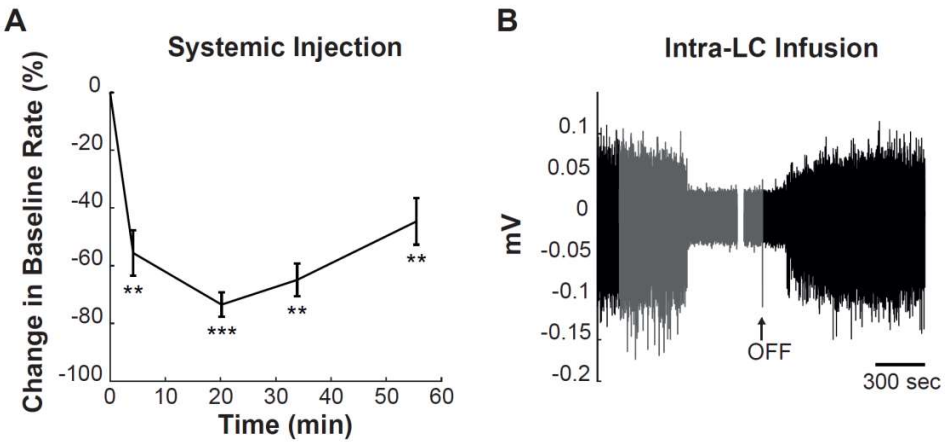

Figure 3.5: The effect of clonidine administration on spontaneous neural activity in LC. A) Prolonged decrease of LC firing rate following systemic clonidine administration (0.05 mg/kg, i.p.). Average baseline change is plotted for different post-injection times (n = 15 LC MUA recordings). Mean ± SE, *** p < 0.001, ** p < 0.01 (one-sample t-test). B) Representative example of a raw extracellular signal recorded in LC illustrating complete cessation of LC discharge after local infusion of clonidine into the nucleus. Conventions are the same shown in

Figure 3.4A.

Commonly, NE activates the cortical activity state[178-182] and, accordingly, inhibition of LC-activity or systemic treatment using noradrenergic alpha 2-receptor agonists resulted in deactivation[183-186]. However, how the noradrenergic system modulates power in specific frequency bands in primary sensory or medial prefrontal cortical regions is rarely studied. Comparison of modulation after systemic and intra-LC clonidine injection between the denoted frequency bands revealed different effects on resting state brain activity dependent on cortical region and type of manipulation. In S1HL, systemic clonidine injection increased BLP in medial frequency bands (Figure 3.6; Theta: $t(11) = 3.09$, $p = 0.01$, Alpha: $t(11) = 5.45$, $p < 0.001$, Sigma: $t(11) = 5.59$, $p < 0.01$, Beta: $t(11) = 5.70$, $p < 0.01$) while local inhibition of LC activity increased BLP in high frequency bands (Sigma: $t(10) = 2.91$, $p < 0.05$, Beta: $t(10) = 3.11$, $p < 0.05$, Gamma: $t(10) = 3.44$, $p < 0.01$). Both drug conditions induced the strongest effect in Sigma frequency band but did not affect frequency range below 4 Hz.

In mPFC, local inhibition of LC activity did not modulate power in any frequency band. However, global activation of alpha 2-adrenoceptors increased BLP in Theta ($t(19) = 2.97$, $p < 0.01$) and Alpha ($t(19) = 2.96$, $p < 0.05$) frequency band and, unexpectedly, decreased BLP in SLO frequency band ($t(19) = -2.47$, $p < 0.05$), the latter indicating activation of the cortical activity state while power change in S1HL indicates deactivation of the cortical state. Respective percentages of average change are provided in Supplementary Table 7.2.

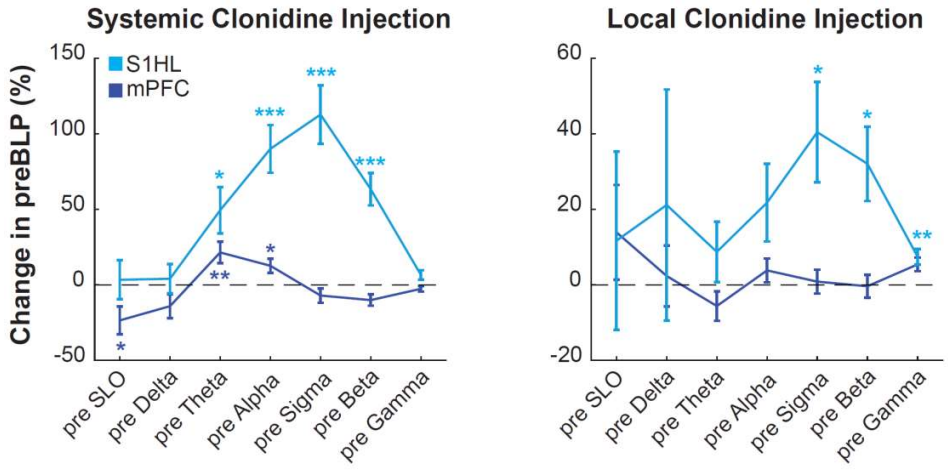

Figure 3.6: Noradrenergic modulation of ongoing cortical state in S1HL (cyan) and mPFC (blue) after systemic (left) and intra-LC (right) injection of clonidine. Illustrated is the average baseline change of the band-limited power (BLP) in the analyzed frequency bands during 4 sec before stimulus-presentation. Mean ± SE, one-sample t-test: *** p < 0.001, ** p < 0.01, * p < 0.05.

Cortical unit activity is classically reported to be under inhibitory control by NE in S1HL[228,229,240,661-663] and PFC[227,245,247,252]. However, increased spontaneous activity was also reported in a minority of neurons in PFC[252]. Inhibitory control by NE is believed to be exerted by activation of alpha 2-adrenoceptors[249,253,664] but systemic administration of alpha 2-noradrenergic agonists is also able to increase firing rate of PFC neurons[233]. Nevertheless, since only a minority of PFC neurons was reported to increase neuronal activity in response to alpha 2-adrenoceptor activation, on the population level both local inhibition of LC activity as well as systemic injection of clonidine are expected to disinhibit single unit spontaneous activity in mPFC and S1HL.

Unit isolation by using electrodes with tetrode configuration provided, in total, 70 and 134 regular spiking units in S1HL and mPFC, respectively, which satisfied the criteria for a single unit (see section 2.1.4 for detail). Remaining recordings were excluded from further analysis because either SNR was not sufficient for isolating single units and therefore these recordings were treated as MUA (178 in S1HL and 170 in mPFC) or extracted single units were classified as putative interneurons (27 units in S1HL an 17 units in mPFC).

Comparison of the activity of regular spiking single units under condition of noradrenergic manipulation revealed differential effects on the firing activity of cortical single units

dependent on cortical structure. Table 3.5 summarizes the number and proportion of single unit subpopulations differentially modulated during the period of maximal LC inhibition. The majority of cortical neurons did not significantly change their spontaneous firing rate following clonidine administration, while the firing rate in different proportions of neurons in each cortical region was bidirectionally modulated.

Table 3.5: Number and percentage of populations of cortical neurons dependent on the direction of spontaneous activity modulation following local and systemic clonidine administration.

	S1HL		mPFC	
	systemic	local	systemic	local
Direction of modulation	n (%)	n (%)	n (%)	n (%)
increase	17 (42.5)	15 (31.9)	10 (15.9)	9 (14.1)
decrease	4 (10)	12 (25.5)	19 (30.2)	9 (14.1)
unchanged	19 (47.5)	20 (42.6)	34 (54.0)	46 (71.9)

In S1HL, units which increased their firing rate dominated those which decreased activity, leading to increased population activity of 94.42 ± 35.83 % and 90.48 ± 36.41 % change after systemic ($t(39) = 2.64$, $p < 0.05$) and local ($t(47) = 2.49$, $p < 0.05$) injection, respectively (Figure 3.7). The magnitude of this activation was independent from pharmacological method ($t(86) = -0.08$, n.s.). In mPFC, neither manipulation method significantly affected the population SUA (Local: + 13.13 ± 7.88 spikes/sec, $t(63) = 1.67$, n.s.; Systemic: - 14.38 ± 11.21 spikes/sec, $t(62) = -1.28$, n.s.). This was the case, because, compared to S1HL, substantially fewer neurons were affected showing a comparable modulation of spontaneous firing rate in both directions. Average baseline change in firing rate under drug condition for each population individually is summarized in Supplementary Table 7.3.

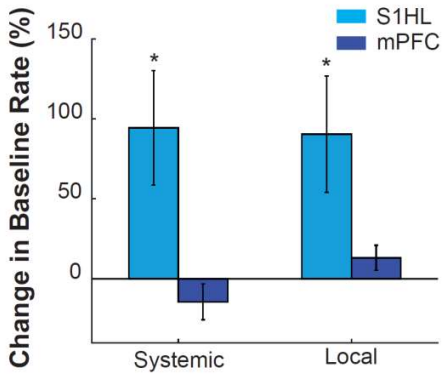

Figure 3.7: The effect of clonidine administration on spontaneous neural activity in S1HL (cyan) and mPFC (blue). Bars represent the average SUA firing rate change after systemic (left panel) and iontophoretic (right panel) clonidine administration. Mean ± SE, one-sample t-test: * $p < 0.05$.

To summarize the effect of NE on cortical spontaneous activity, first, either pharmacological treatment increased BLP in medial to high frequency range with maximum effect in Sigma frequency band in S1HL. Ongoing BLP in mPFC was only modulated after systemic activation of alpha 2-adrenoceptors showing an increase in Theta and Alpha frequency band while BLP in SLO frequency band was surprisingly decreased demonstrating activation of cortical activity state.

The underlying population single unit activity in S1HL was expectedly disinhibited after either manipulation. A similar effect was also assumed for population SUA in mPFC. However, a majority of units were not modulated at all and remaining neurons exhibited disinhibition as well as inhibition resulting in a non-modulated population unit activity.

3.1.3. Comparison of sensory-evoked neuronal responses in S1HL and mPFC

3.1.3.1. Examination of effective stimulation parameters

Following the examination of the noradrenergic modulation of region-specific spontaneous neuronal activity, the next question to solve was how sensory processing in both cortical regions was modulated by the LC noradrenergic system. In order to answer this question, the neuronal response to sensory stimulation was first characterized and compared between S1HL and mPFC without any pharmacological manipulation.

In the beginning, different stimulation protocols were tested in order to ensure reliable sensory-evoked modulation of neuronal activity in all three recorded brain regions. Frequency coding was tested by using different stimulation frequencies at the same

amplitude of 5 mA: single pulse (SP) and train of pulses (TR). Intensity coding was tested by using TR with different amplitudes (1, 2, 3, 4 or 5 mA).
Frequency coding stimulation protocol was performed in 16 rats. While MUA was analyzed in LC (n = 14), single units were extracted from S1HL (n = 39) and mPFC (n = 46). Amplitude coding stimulation protocol was performed in another set of experiments designed for a project focused on prefrontal neuronal activity and less specific to primary sensory areas. Therefore, only 4 rats with recordings in S1HL (n = 13 SUA) but 16 rats with recordings in mPFC (n = 67 SUA) were subjected to this stimulation protocol. Out of these experiments, 14 MUA recordings from LC contributed to analysis. Table 3.6 summarizes the number of simultaneous recorded structure combinations for each stimulation protocol analogous to Table 3.1.

Table 3.6: Number of simultaneous recorded structure combinations using frequency and amplitude coding stimulation protocols.

Structure combinations	LC S1HL mPFC	LC mPFC	LC S1HL	S1HL mPFC	LC
Frequency coding	6	6	0	2	2
Amplitude coding	2	12	0	2	0

Comparison of maximum amplitudes of sensory-evoked responses (Supplementary Table 7.4) showed that sensory stimulation with high stimulation amplitude of 5 mA evoked reliable excitation in LC-MUA and S1HL-SUA independent from stimulation using SP or TR (LC-MUA: $F(1, 27) = 0.82$, p = n.s.; S1HL-SUA: $F(1, 27) = 0.82$, p = n.s.). Single units in mPFC were less sensitive showing significantly higher firing amplitudes in response to FSs using TR stimulation compared to SP (Figure 3.8, $F(1, 91) = 8.61$, $p < 0.01$).

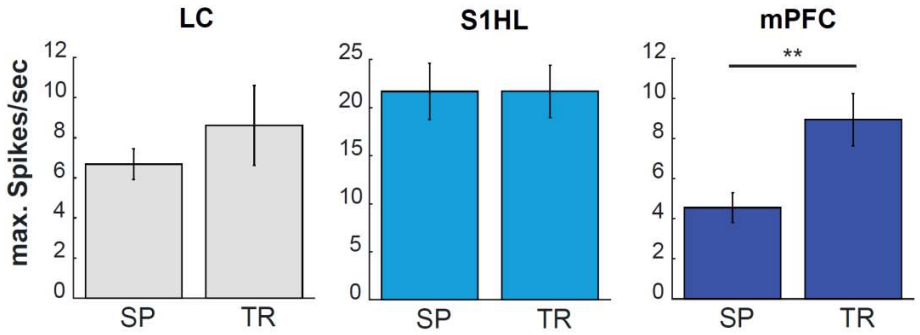

Figure 3.8: The effect of increasing stimulus frequency under constant stimulus strength (5 mA) on average maximum neuronal response amplitudes to sensory stimulation in LC (MUA), S1HL and mPFC (both SUA). Mean ± SE, *** p < 0.001, * p < 0.05.

Reduced sensitivity of mPFC neurons was confirmed when maximum response amplitudes were compared after stimulation with different magnitudes. Repeated measures ANOVA with increasing stimulation current as factors indicated that neurons in all three recorded structures were modulated dependent on stimulation magnitude (Figure 3.9; LC: $F(4, 52) = 3.53$, $p < 0.05$, S1HL: $F(4, 48) = 12.28$, $p < 0.001$ and mPFC: $F(4, 264) = 5.14$, $p < 0.001$).

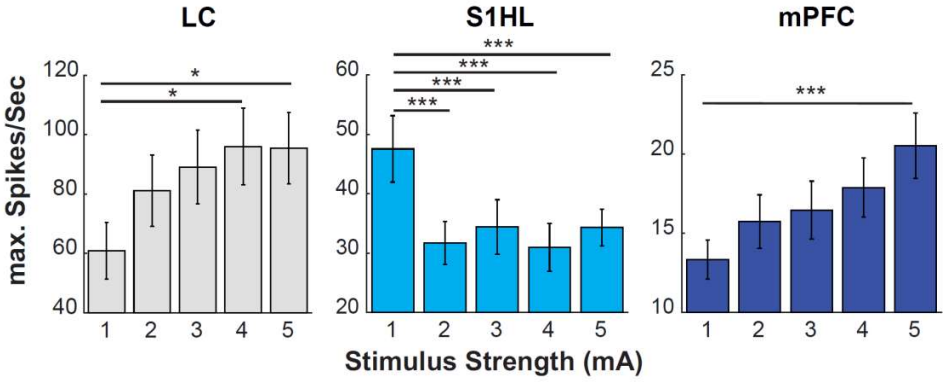

Figure 3.9: The effect of increasing stimulus strength on average amplitudes of neuronal responses to sensory stimulation in LC (MUA), S1HL and mPFC (both SUA). Note the sequentially increasing response amplitudes in LC and mPFC in contrast to neuronal activity in S1HL. Mean ± SE, *** p < 0.001, * p < 0.05.

After post-hoc multiple comparison analysis, it became apparent that maximum response amplitudes in S1HL did not comply with increasing stimulation magnitude but the response amplitude to stimulation using a current of 1 mA was significantly higher than to other stimulation currents. In contrast, neuronal activity in LC and mPFC showed incrementally higher response amplitudes with increasing stimulation currents. The average response amplitudes to each stimulation parameter are listed in Supplementary Table 7.5.
In conclusion, reliable sensory-evoked responses in LC neurons of rats under urethane anesthesia were only evoked with very strong, potentially noxious sensory stimulation, which is in accordance with the literature[125,129,262,665,666]. This turned out to be true also for mPFC sensory-evoked neuronal activity while neurons in S1HL were reliably activated in response to electrical FS stimulation of all parameters tested here. In order to compare, how the LC NE system affects sensory processing in distinct brain structures, reliable sensory-evoked responses had to be ensured and, thus, further experiments were conducted using TR stimulation with stimulation currents of 5 mA.

3.1.3.2. Characterization of cortical state activation in response to somatosensory stimulation in S1HL and mPFC

Inspection of the low-passed (0.1 – 300 Hz) extracellular voltage-traces revealed, already described transient cortical activation (TCA) in response to effective somatosensory stimulation[53,667-672]. TCA was characterized by a shift from high amplitude-low frequency to low amplitude-high frequency oscillations in both S1HL and mPFC (Figure 3.10A). Analysis of the LFP power spectrum confirmed a decrease of power in low frequency range (Figure 3.10B top) and an increase of power in high frequency range (Figure 3.10B bottom) immediately following the stimulus presentation.

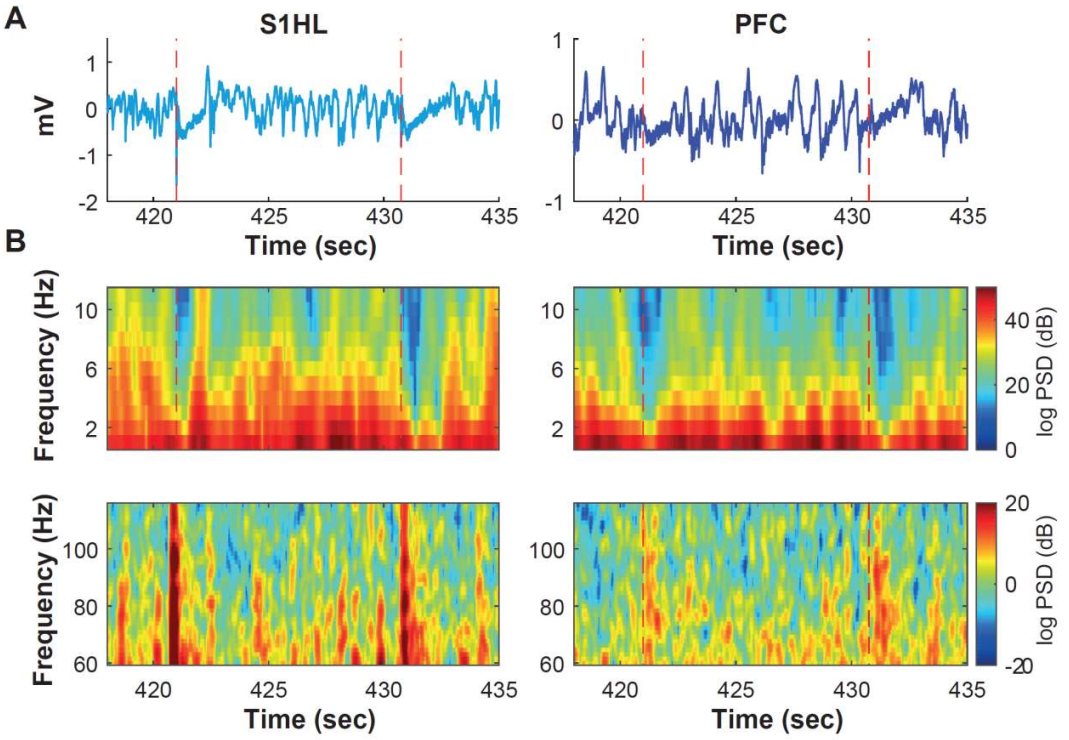

Figure 3.10: Somatosensory stimulation induces transient cortical activation (TCA) under urethane anesthesia. A) Representative examples of the extracellular voltage traces (0.1 - 300 Hz) recorded in S1HL (left) and mPFC (right). Red dashed lines illustrate stimulus-onset. B) Corresponding spectrograms of the low-frequency (0.5 - 11.5 Hz, top row) and high-frequency (60 - 120 Hz, bottom row) ranges. Note, the foot-shocks (FSs) produced a power decrease in the low-frequencies and power increase in the high-frequencies of LFPs in both cortical areas.

Changes in the power spectrum during 1 second after stimulus-presentation were analyzed in greater detail by decomposition of the LFP in the aforementioned frequency bands. However, since one cycle in SLO frequency band is longer than the analyzed one second, this frequency band was excluded from post-stimulus BLP analysis. Representative examples of post-stimulus BLP changes in S1HL and mPFC (Figure 3.11) confirmed a decrease of BLP in low frequency range along with increased power in Gamma frequency band which were most prominent during 1 sec after stimulus onset.

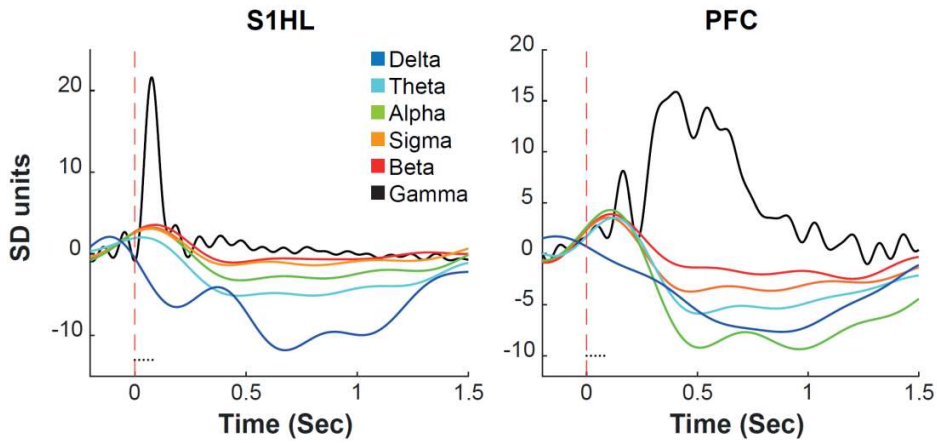

Figure 3.11: Representative examples of the stimulus-induced power modulation over time in different frequency bands. Stimulus-onset is illustrated by red dashed lines. Dots illustrate each individual FS in a train of five pulses (0.5 ms, 5 mA). Bin size = 4 ms.

Because of the variable ongoing cortical activity state under urethane anesthesia, the stimulus-induced BLP change was further analyzed relative to the prestimulus period. Effective stimulus-related TCA was only considered when one-sample t-test of post-stimulus BLP change over FSs (n = 25) confirmed a significant decrease in Delta frequency band accompanied by a significant increase in Gamma frequency band. Overall, 91.3 % of the S1HL recordings (21/23) and 46.3 % of the mPFC recordings (19/41) were classified as effectively activated which is henceforth referred to as "TCA+". Accordingly, the contrary group of non-significant cases will be referred to as "TCA-". Figure 3.12 shows group averages of the stimulus-induced BLP change for all TCA+ and TCA- cases in S1HL and mPFC. One-sample t-test over cases in the TCA+ group confirmed that the post-stimulus BLP change in the Delta and Gamma power was statistically significant in both cortical regions (Delta: $t(20) = -4.9$, $p < 0.001$ and $t(18) = -12.4$, $p < 0.001$; Gamma: $t(20) = 8.3$, $p < 0.001$ and $t(18) = 7.5$, $p < 0.001$ for S1HL and mPFC, respectively).

TCA- cases in S1HL were assigned as such because decrease in Delta frequency band was not significantly different from zero. However, since significant increase in Gamma frequency band still indicated cortical activation and the number of TCA- cases was negligible in S1HL, all cases in S1HL were pooled and considered as TCA+.

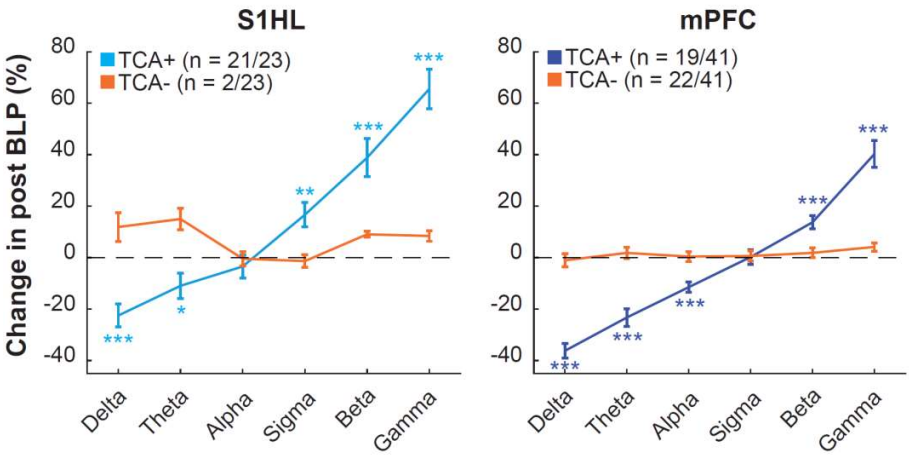

Figure 3.12: The TCA in S1HL and mPFC illustrated in BLP change during 1 sec post-stimulus interval averaged over 25 repetitions. The vast majority of S1HL cases were classified as effectively activated in response to FSs (TCA+) while in mPFC the number of TCA+ cases was comparable to non-effective cases (TCA-). Mean ± SE, * $p < 0.05$, ** $p < 0.01$, *** $p < 0.001$.

To assess functional differences in stimulus-induced cortical state activation between S1HL and mPFC, a two-way ANOVA (frequency bands × structure) between TCA+ cases was subsequently performed. It revealed a significant difference in spectral composition ($F(5,190) = 105.65$, $p < 0.001$) between the two cortical regions ($F(1,190) = 14.05$, $p < 0.001$). Multiple-comparison analysis showed a weaker decrease of BLP in Delta frequency band and stronger increase of power in high frequency range in S1HL compared to mPFC (Figure 3.13, Supplementary Table 7.6) indicating a stronger activation of neuronal activity in S1HL.

In addition, the frequency band which did not change the BLP in response to stimulation and, thus, built the intersection between decreasing and increasing frequency bands, was different between the two cortical regions: in S1HL, the intersection was located in the Alpha frequency band (one-sample t-test: $t(20) = -0.75$, p = n.s.) while in mPFC, it was located in the Sigma frequency band ($t(18) = 0.09$, p = n.s.). Thus, the frequency range of increasing BLP was extended to more medial frequency range in S1HL.

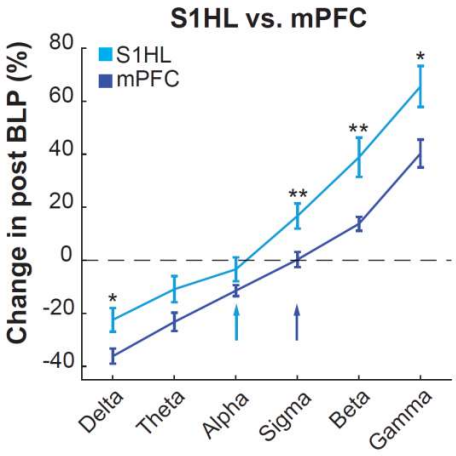

Figure 3.13: Comparison of stimulus-induced BLP change between TCA+ cases recorded in S1HL and mPFC illustrates a generally higher activation level in S1HL as opposed to mPFC. Color coded arrows indicate region specific shift of interceptions. Mean ± SE. * p < 0.05, ** p < 0.01.

In summary, electrical FS stimulation evoked TCA in both cortical regions which was characterized by a region-specific change in the power spectrum in response to sensory stimulation of the same intensity. Specifically, in S1HL, a cortical target of the feed-forward somatosensory pathway, the stimulus-induced activation was very robust and present in nearly all recordings. In the associative mPFC, a cortical target of multiple pathways related to different operations, the change of cortical activity state was detected only in about half of the cases showing a weaker extent compared to S1HL. In brief, sensory stimulation evoked a higher cortical activity state in S1HL in agreement with its function in processing of somatosensory stimulation.

3.1.3.3. Understanding the difference between effective and non-effective sensory stimulation in mPFC

While nearly all recorded cases in S1HL were successfully activated in response to FSs, the responsiveness in mPFC was reduced to about half of the cases. Previous literature suggests that modulation of neuronal activity by sensory stimulation is dependent on cortical layer[673] or dynamics of ongoing activity[73,673-679] in the neocortex.

Therefore, it was first explored, whether the potential to induce a TCA in mPFC was dependent on the cortical layer. Consequently, the number of TCA+ versus TCA- groups was compared between the depths of the recording sites divided into tertiles. Table 3.7 summarizes that most of the cases were recorded in the medial layers of mPFC and that TCA+ as well as TCA- cases were present independent of recording depth.

Table 3.7: Number of recordings in different cortical depths is comparable between effective and non-effective cortical state activation.

	TCA+	TCA-	Chi - square
Superficial (< 400 µm)	5	2	$\chi 2(1, N = 7) = 1.29$, p = n.s.
Medial (400 – 800 µm)	11	17	$\chi 2(1, N = 28) = 1.29$, p = n.s.
Deep (> 800 µm)	2	2	$\chi 2(1, N = 4) = 0.00$, p = n.s.

In support, the absolute cortical recording depth, without subdivision into tertiles, was not significantly different between TCA+ and TCA- cases ($F(1,37) = 1.36$, p = n.s.). Thus, the effectiveness of sensory stimulation was independent from cortical layer.

Alternatively, the dependency of FS effectiveness on the cortical activity state preceding the sensory stimulation was tested. This was especially reasonable on the background of observed spontaneous alternation of cortical activity state under urethane anesthesia. Comparison of BLP during 4 seconds immediately before sensory stimulation between TCA+ and TCA- groups revealed that BLP in low frequency bands was significantly lower in TCA+ cases (Figure 3.14; SLO: $F(1,39) = 6.7$, $p < 0.05$, Delta: $F(1,39) = 4.09$, $p = 0.05$). This implies that the power of ongoing slow oscillatory activity determines sensory processing in mPFC. A higher cognitive evaluation and processing of sensory stimulation happens only when the system is active while S1HL, as a structure specifically related to sensory operations, detects and processes salient sensory input independent of the ongoing cortical activity state.

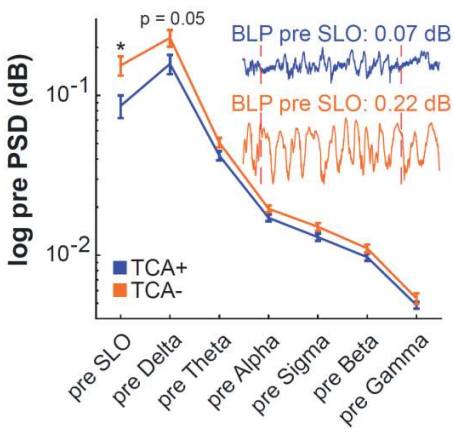

Figure 3.14: BLP in mPFC during 4 sec before stimulus presentation divided in TCA+ and TCA- cases suggests a dependency of stimulus-induced BLP profile on power in low frequency range during prestimulus interval. Inset shows representative examples of extracellular voltage traces (0.1 - 300 Hz) recorded in mPFC during a TCA+ (top) and TCA- case (bottom). A robust, transient desynchronization followed the FS presentation when pre-stimulus cortical activity was characterized by relatively low amplitude (blue trace), while there was essentially no detectable change in the LFP signal during periods with predominant high-amplitude slow wave activity (orange trace). Text indicates the absolute PSD in SLO frequency range (0.1-1Hz) during prestimulus interval. Red bars mark stimulus-presentation onset. Mean ± SE. * p < 0.05.

3.1.3.4. Influence of stimulus-related cortical activity state in mPFC on spectral composition of TCA in S1HL

Previous comparison of ongoing oscillatory activity between the two cortical structures revealed that the BLP, especially in Theta and Alpha frequency band, between S1HL and mPFC was related to each other (see Section 0). To explore whether stimulus induced modulation of BLP is also related between the two cortical regions, all cases from S1HL, which were simultaneously recorded with mPFC (n = 16), were divided according to effectiveness of sensory stimulation in mPFC. When cortical state in mPFC was effectively activated by FS stimulation (n = 7), stimulus-induced BLP in low frequency range was significantly decreased in S1HL (Figure 3.15). In contrast, when cortical state in mPFC was unaffected (n = 9), low-frequency BLP in S1HL was likewise unaffected. However, BLP in high frequency range was still increased in response to sensory stimulation. A summary of statistical results for each frequency band is given in Supplementary Table 7.7.

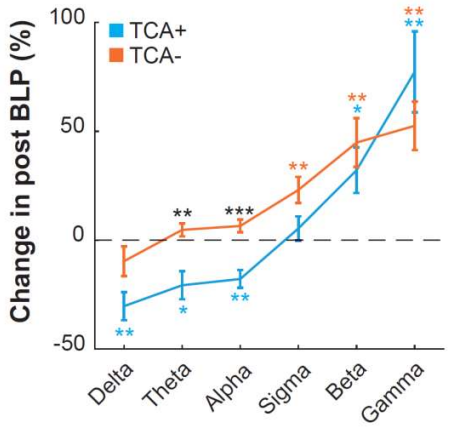

Figure 3.15: Stimulus-induced BLP change during 1 sec post-stimulus interval in S1HL separated according to TCA+ (n = 7) and TCA- (n = 9) cases in simultaneously recorded mPFC. Between group comparison was performed using one-way ANOVA between TCA+ and TCA- cases (black asterisks) and within group comparison against 0 by using one-sample t-test (cyan and orange asterisks). Mean ± SE, * $p < 0.05$; ** $p < 0.01$; *** $p < 0.001$.

Interestingly, stimulus-induced BLP change in Theta and Alpha frequency bands, which showed the strongest correlation between the two structures during spontaneous oscillatory activity, were significantly different from each other (Theta: $F(1, 14) = 13.03$, $p < 0.01$; Alpha: $F(1, 14) = 21.48$, $p < 0.001$). Subsequent correlation analysis confirmed a positive relationship between poststimulus BLP in S1HL and mPFC, however, this was the case only in Theta and not in Alpha frequency band ($r = 0.61$, $n = 16$, $p < 0.05$).

Hence, the BLP in Theta frequency band in both cortical regions is related to each other during ongoing as well as stimulus-induced state activity. Additionally, the magnitude of stimulus-related BLP change in Delta, Theta and Alpha frequency band in S1HL is modulated by cortical activation state in mPFC. In combination, this could indicate a top-down modulation of low frequency spectral composition in S1HL by mPFC while stimulus-related increase of BLP in high frequency range in S1HL is reliably evoked and independent from activity state in mPFC.

3.1.3.5. Relationships between stimulus-related TCA and underlying voltage fluctuations

The spectral composition of the LFP is dependent on underlying neuronal voltage fluctuations. Previous literature suggests that low frequency power reflects subthreshold currents, like synaptic activity and other non-spike related transmembrane currents, and high frequency power is largely associated with spiking frequency of neurons[26,680,681]. In the following, this study investigates the underlying stimulus-induced voltage fluctuations in S1HL and mPFC by examination of SEPs as well as SUA. In mPFC, SEPs and SUA were further compared between TCA+ and TCA- recordings.

SEPs in both cortical regions showed exclusively negative voltage deflections of LFP, which confirmed recordings mostly in medial to deep layers[74-78]. Cases with SEP amplitude exceeding twice the standard deviation of baseline voltage were considered as responsive and referred to as SEP+. Analogous, cases with SEP amplitude smaller than the threshold are referred to as SEP-.

In both cortical regions, SEP was effectively evoked in all but one TCA+ cases (n = 22 and n = 18 for S1HL and mPFC, respectively). Interestingly, threshold-exceeding SEP+ was also present in 59.1 % (n = 13) of TCA- recordings in mPFC and, actually, the proportions of SEP+ was comparable between TCA+ (n = 18) and TCA- (n = 13) cases ($Chi^2(1, 31) = 0.81$, p = n.s.). Additionally, in TCA- cases, the proportions of SEP+ (n = 13) and SEP- (n = 9) were neither significantly different ($Chi^2(1, 22) = 0.73$, p = n.s.) suggesting that SEP is evoked independent from cortical activity state.

The profile of SEPs vastly differed between cortical regions (Figure 3.16). In S1HL, the average SEP+ profile exhibited 3 response components with latencies similar to what was reported for afferent-specific information transfer: the first transient component exhibited a short peak latency of 20.8 ± 1.0 ms typical for transfer of mechanoreceptive information by A β-fibers. The second response component was detected after 82.0 ± 2.5 ms followed by a third sustained and long latency (309.9 ± 19.8 ms) component characteristic for transferred nociceptive information via A δ- and C-fibers, respectively. In contrast, SEP+ profile in mPFC consisted of only one single voltage deflection showing average peak latency after 253.82 ± 17.66 ms.

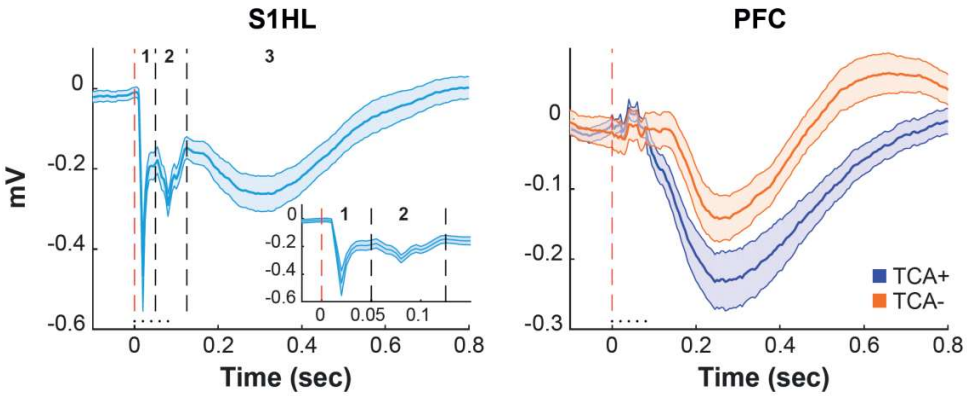

Figure 3.16: Somatosensory stimulation induces SEP under urethane anesthesia. Illustrated are the average waveforms of the extracellular voltage trace (0.1 - 300 Hz) during 800ms after stimulus-presentation (red dashed line at 0 sec) in S1HL and mPFC. In S1HL, SEP consisted of 3 response components (1, 2, 3) separated by dashed lines. Inset shows a magnification of the first two short latency response components. In mPFC, the average single voltage deflections are separated according to TCA+ (blue) and TCA- (orange) cases. Dots illustrate each individual FS in a train of five pulses (0.5 ms, 5 mA). Bin size = 5 ms, Mean ± SE.

Next, the SEPs in mPFC were specifically examined depending upon the effectiveness of stimulus-related cortical state activation. Therefore, peak latency, amplitude and integral of the SEP+ profiles were compared between TCA+ and TCA- cases (Table 3.8). There was no significant difference between peak latency ($F(1, 29) = 0.12$, p = n.s.) or maximum amplitude ($F(1, 29) = 0.32$, p = n.s.) of SEPs between the two groups, however, the

integral, as a measurement of the magnitude of SEPs, was significantly larger in TCA+ cases compared to TCA- cases (Figure 3.16 right; $F(1, 29) = 6.92$, $p < 0.05$).

Table 3.8: Summary of SEP characteristics in mPFC dependent on effectiveness of cortical state activation. Mean ± SE.

	TCA+	TCA-
Peak latency (ms)	262.05 ± 13.06	245.58 ± 22.26
Maximum amplitude (mV)	-0.26 ± 0.04	-0.18 ± 0.04
Integral (µV*sec)	-89.07 ± 15.80	-19.72 ± 18.44

In short, the response in S1HL was partitioned into three different response components reflecting temporally integrated input from afferent pathways conveying somatosensory information of different qualities. In mPFC, only one response component was apparent which might reflect a mixture of incoming information from different structural signal generators at different time courses, so that the individual signals merge to one voltage deflection with maximum activity at the time of most incoming information.

In both cortical regions stimulus-related activation of cortical state was nearly always accompanied by an underlying SEP. In mPFC, where neuronal activity was less sensitive to sensory stimulation, threshold-exceeding SEPs were still present when the cortical state remained unchanged after the stimulus presentation albeit with a weaker magnitude. This suggests that, SEPs might be a prerequisite for an activation of the cortical state only if it is strong enough.

SEPs reflect mass neuronal voltage deflections in response to sensory input in a volume of brain tissue. Like the LFP, SEPs include subthreshold transmembrane currents as well as spiking activity. In contrast, SUA provides information on the level of single action potentials and excludes subthreshold membrane currents[112]. In response to sensory stimulation, a strong relation between LFP power in the Gamma frequency band and spiking activity is suggested[26,680,681]. Therefore, in the current study, the spiking activity in response to sensory stimulation is assumed to be increased when cortical state is reliably activated. This is examined in the following section.

Isolated SUA exceeding a threshold of 95 % confidence interval during 1.5 sec after stimulus-presentation were classified as “FS-responsive”. The FSs evoked exclusively excitatory responses in both cortical regions, which is in accordance to the proposed relation to increased BLP in Gamma frequency band during TCA. Because of the somatosensory nature of the stimulation, a larger proportion of FS-responsive neurons was recorded in S1HL (67.2%), compared to mPFC (35.9%).

Prior to a detailed description of the single unit response profiles in each cortical structure, sensory-evoked population SUA in mPFC was compared between TCA+ and TCA- cases. In contrast to SEPs, whose occurrence was independent from effectiveness of stimulus-induced cortical state activation, the proportion of FS-responsive single units was significantly higher in the TCA+ cases compared to TCA- cases (n = 34 vs. 13, $Chi^2(1, 47) = 9.38$, $p < 0.01$). Within the latter, the number of FS-responsive single units was significantly lower than unaffected single units (n = 13 vs. 40; $Chi^2(1, 53) = 13.76$, $p < 0.001$).

Comparable to SEPs, neither peak latency ($F(1, 45) = 0.77$, p = n.s.) nor maximum amplitude ($F(1, 45) = 1.91$, p = n.s.) differed between TCA+ and TCA- but the magnitude of the population single unit response, reflected in the integral of the PSTH, was significantly higher in TCA+ (0.73 ± 0.09 Z-Scores*sec) compared to TCA- cases (0.33 ± 0.15 Z-Scores*sec, $F(1, 29) = 5.28$, $p < 0.05$).

Hence, a large proportion of responsive units in S1HL and increased stimulus-induced single unit activation in mPFC TCA+ cases supports the presumed relationship between stimulus-induced cortical activation and single unit firing activity. In S1HL, majority of recorded single units were activated in response to sensory stimulation under reliable increase of BLP in high frequency range (see section 3.1.3.4). The comparative approach in mPFC showed that, when the cortical state was significantly activated, the response probability of individual neurons was higher and the magnitude of the population single unit response to FSs was larger compared to unaffected cortical activity state. SEPs likewise showed a larger magnitude in TCA+ cases but, in contrast to single unit sensory-evoked responses, the response probability did not differ between TCA+ and TCA- cases

(see section 3.1.3.5). This leads to the suggestion that single unit firing activity in response to sensory stimulation enhances SEP magnitude which, in turn, activates cortical state.

3.1.3.6. Characterization of single unit responses to somatosensory stimulation in S1HL and mPFC

The results described above indicated already a higher complexity in neuronal activity recorded in the association cortex in contrast to primary sensory areas. This was reflected in a decreased, state-dependent sensitivity of stimulus-evoked activation in mPFC compared to S1HL, where stimulus-induced activation on all explored levels was very reliable. On the other hand, the SEPs were composed out of three distinguishable response components in S1HL and only one single voltage deflection in mPFC. Population single unit responses averaged from all responsive single units for each cortical region exhibit similar profiles (Supplementary Figure 7.3): the population of 47 out of 70 FS-responsive S1HL SUA showed a biphasic stimulus-evoked response profile with an average peak latency of 19.92 ± 0.91 ms and 288.54 ± 9.73 ms, for early and late response components respectively. The amplitude of early response was higher (3.33 ± 0.39 Z-Scores) than the amplitude of the late response component (1.15 ± 0.18 Z-Scores, $t(78) = 2.5$; $p < 0.05$). The single voltage deflection of population SUA in mPFC (47 out of 134) exhibited a peak latency of 200.31 ± 0.27 ms and maximum amplitude of 1.69 ± 0.25 Z-Scores.
Intuitively, this looks like a simpler response profile in mPFC, however the complexity of different brain networks is dependent on the computational demand of the processes which has been described to increase from so-called unimodal areas (including primary sensory areas) to multimodal networks (including limbic cortices like mPFC)[468,682]. The bottom-up sensory input to S1HL is well explored and the origin of the different response components can be related to modality specific information transfer based on their response latency. However, mPFC integrates information from multiple cortical and subcortical networks and one can imagine that the single voltage deflection on the population level is merged from fluctuations created by incoming information which varies vastly, beyond others, in spatial and temporal coding as has been indicated before[108,109].

To provide an insight into underlying voltage fluctuations of individual responsive neurons, the stimulus-induced population single unit response in each cortical structure was categorized into subgroups depending on response profiles. Specifically, the PSTH profiles of individual neurons were subdivided by using K-Means Cluster analysis. Figure 3.17 illustrates the individual sensory response profiles of each recorded unit (Figure 3.17A) and the average response profiles of each group within a cortical structure (Figure 3.17B).

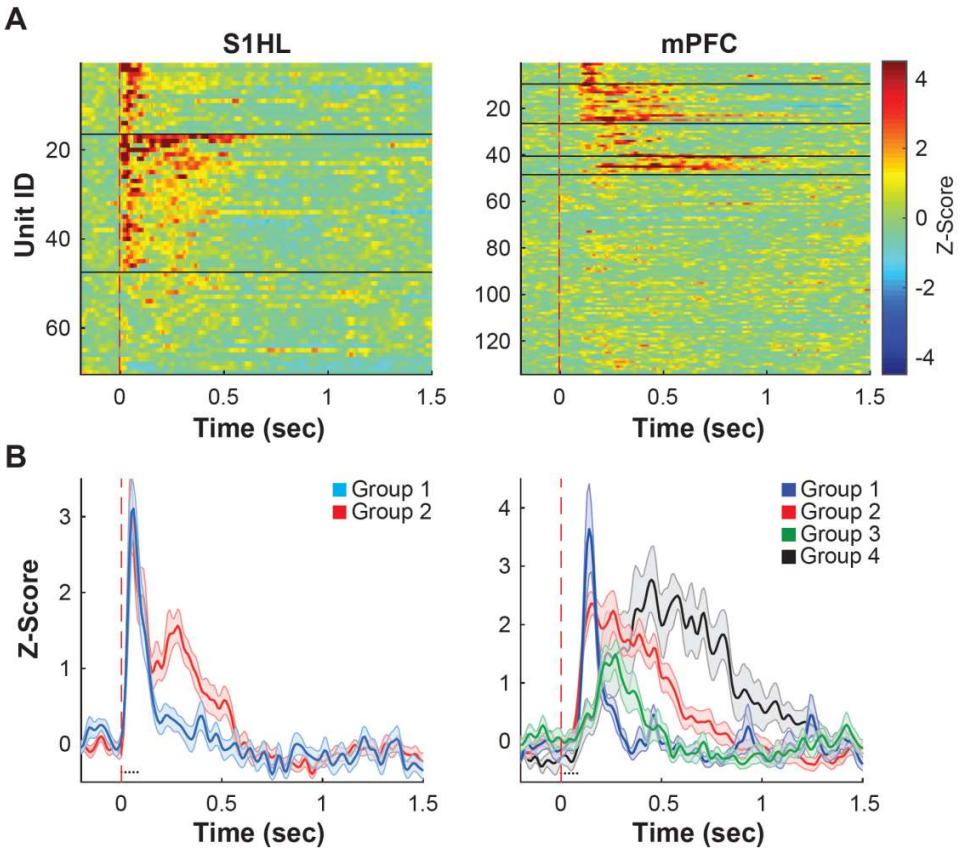

Figure 3.17: Somatosensory-evoked single unit responses in S1HL and mPFC. A) The stimulus-induced modulation of the firing rate of all isolated single units in S1HL and mPFC sorted according to response profile. For each single unit, the firing rate was normalized to Z-Score and averaged over 25 trials. B) Smoothed average peri-stimulus-time histograms (PSTHs) for each group of single units (mean ± SE) in S1HL (left) and mPFC (right). The averages for non-responsive units are not shown. Stimulation was applied at time 0 (red dashed line). Dots illustrate each individual FS in a train of five pulses (0.5 ms, 5 mA). Bin size = 10ms.

Similar to the response profile of the population single unit response to FSs, the S1HL neurons displayed a short latency burst which was followed by a second phase of sustained excitation in 66.0% of responsive neurons (group 2). The mPFC response profiles were, indeed, more complex. Out of the population of responsive neurons, cluster analysis provided four groups of response profiles: 1) short latency transient excitation (group 1, 18.8 %), 2) short latency sustained excitation (group 2, 35.4 %), 3) transient excitation with variable latency (group 3, 29.2 %) and 4) long latency sustained excitation (group 4, 16.6 %). The peak latencies of group 1 to group 4 are 122.0 ± 4.2 ms, 242.1 ± 30.0 ms, 289.2 ± 24.9 ms and 408.3 ± 25.0 ms and significantly different from each other ($F(3, 38) = 15.9$, $p < 0.001$) with exception of group 2, which is not significantly different from group 3.

Thus, neurons in S1HL display two populations with response profiles matching the processing via different bottom-up sensory afferents. Higher complexity in mPFC was supported by the number of populations with different response profiles in addition to a vast number of neurons, which are not activated by sensory stimulation. This suggests the presence of multiple networks in the mPFC circuitry, wherein incoming activity is merged into a monophasic cortical population response.

3.1.4. Noradrenergic modulation of sensory-evoked neuronal responses in S1HL and mPFC

One functional role classically attributed to NE in sensory processing, is to increase SNR in primary sensory regions via inhibition of spontaneous neuronal activity[228,229,235,236,264] and concurrent enhancement of sensory-evoked responses[229,236,238,244]. Noradrenergic modulation of neuronal activity in prefrontal cortex, however, is reported to be more complex. Spontaneous activity was found to be decreased[227,245,247,249,252] or increased[245,252] and bidirectional modulation was also reported for stimulus-induced responses[245,247,251,256]. The reported role of NE on cortical activity state, however, seems to be consistent over cortical regions. Both excitation of LC neuronal discharge and intracortical or systemic infusion of NE have been shown to activate the cortical state in order to promote wakefulness and arousal[160,179,683-685].

In the following, an attempt shall be made to clarify how sensory-evoked neuronal activity is modulated by NE on different neuronal levels in functionally distinct cortical regions. However, first, the modulation of sensory-evoked activity by pharmacological manipulation was explored in LC itself in order to estimate the change of stimulus-induced phasic NE release in terminal regions.

3.1.4.1. Effect of pharmacological manipulation on LC neuronal activity

Neuronal activity in LC was monitored simultaneously along with recordings of neuronal activity in the cortex. Under baseline condition, the LC NE neurons typically responded to FSs with a brief excitation (peak latency: 67.08 ± 3.19 ms) followed by prolonged inhibition[129,147,521,666,686,687] (Figure 3.18). The response amplitude of average LC activity recorded during baseline condition before local and systemic injection of clonidine was comparable ($F(1, 32) = 1.25$, p = n.s.).

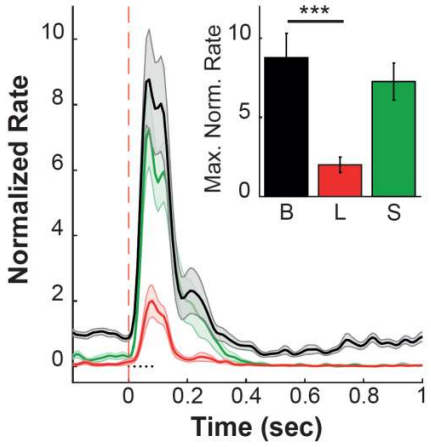

Figure 3.18: The effect of clonidine on sensory-evoked responses of noradrenergic neurons in LC. The smoothed PSTHs of the normalized firing rate of LC multiunit activity (MUA) are plotted during baseline (black), iontophoretic application of clonidine in LC (red) and after systemic clonidine injection (green). The data averaged over 25 trials for each drug condition are shown. For illustrative purpose, sensory-evoked response during baseline condition was averaged over cases which were recorded before local and systemic injection of clonidine, respectively. Bin size 10 ms. Inset shows the maximum amplitudes of the responses to FS stimulation. Note a clonidine-induced decrease of spontaneous LC activity, while substantial decrease of evoked responses was observed only in case of local LC inhibition. Mean ± SE. *** $p < 0.001$.

As described before, both pharmacological conditions decrease the spontaneous LC activity (see section 3.1.2) and, concomitantly, tonic release of NE. Sensory-evoked activity in LC was also massively inhibited by local injection of clonidine into the nucleus (Figure 3.18, $F(1, 37) = 26.39$, $p < 0.001$), similar as reported in a previous study addressing peri-LC drug infusion with simultaneous recording of FS-evoked LC activation[266]. In contrast,

systemic administration of clonidine did not significantly affect the amplitude of the evoked responses of the LC NE neurons ($F(1, 28) = 0.15$, p = n.s.).
Thus, while local drug infusion prevents tonic as well as phasic NE release in LC terminals, systemic drug injection leaves the phasic release intact. In consequence, a phasic increase of NE release in response to FSs can be expected in LC terminal regions under condition of systemic clonidine in addition to global activation of alpha 2-adrenoceptors. The latter, in turn, reduces release of NE from LC terminals by presynaptic actions on noradrenergic autoreceptors[488-491,688] while postsynaptic actions typically lead to hyperpolarization of target neurons[157].

3.1.4.2. Noradrenergic modulation of stimulus-induced changes of spectral composition in S1HL and mPFC

NE is consistently reported to activate the ongoing cortical state and, accordingly, systemic injection of alpha 2-adrenoceptor agonists is reported to result in cortical deactivation in frontal, parietal and temporal cortical regions[186,195,689-693]. Unilateral manipulation of LC activity seems to be insufficient[180,183] and, therefore, only systemic injection of clonidine is expected to modulate the spectral composition of TCA towards higher power in low frequency range.
Surprisingly, to anticipate this part of the result, it was generally found that both manipulations evoked similar effects on cortical state activation as well as single unit responses to sensory stimulation save that the effects after systemic injection of clonidine were much stronger compared to intra-LC injection.
Individual comparison of stimulus-related BLP change after either noradrenergic manipulation revealed opposing effects on cortical state activity in S1HL and mPFC (Figure 3.19). Specifically, global activation of alpha 2-adrenoceptors significantly decreased stimulus-induced BLP change in Sigma ($F(1, 23) = 17.55$, $p < 0.001$) and Beta ($F(1, 23) = 8.88$, $p < 0.01$) frequency bands in S1HL while BLP change in the same frequency bands were increased in mPFC (Sigma: $F(1, 39) = 10.34$, $p < 0.01$, Beta: $F(1, 39) = 4.88$, $p < 0.05$). The increase in Sigma frequency band in mPFC could also be

observed after inhibition of LC activity by local infusion of clonidine ($F(1, 41) = 5.63$, $p < 0.05$) while in S1HL, none of the bands were affected by the latter treatment.

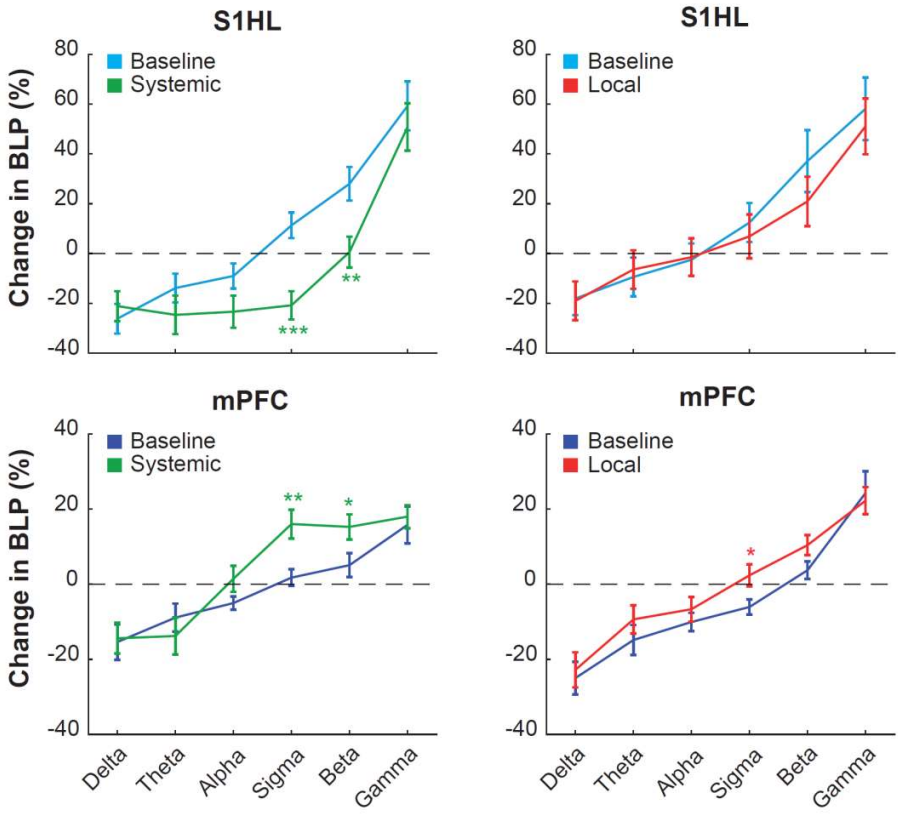

Figure 3.19: Noradrenergic modulation of stimulus-related BLP change in S1HL (top row) and mPFC TCA+ cases (bottom row) after systemic clonidine injection (green) and under local inhibition of LC activity (red). Note the contrary modulation of the same frequency bands in the cortical regions. Mean ± SE, * $p < 0.05$, ** $p < 0.01$, ***$p < 0.001$.

It was shown before that stimulus-induced cortical state activation in mPFC is inversely dependent on power during ongoing slow oscillations between 0.1 and 1 Hz (SLO, see section 3.1.3.3). Systemic clonidine administration unexpectedly decreased power in this frequency band (see section 3.1.2). In combination with increased stimulus-induced BLP change in Beta frequency band, which is associated with enhanced cortical activity[48,49], this raises the question whether the number of TCA+ cases, in which cortical state could be effectively activated by sensory stimulation, increased after clonidine administration.

Accordingly, TCA- cases, in which FS-stimulation initially could not activate the cortical state in mPFC, were again tested for responsiveness to FSs under drug condition (Local: n = 10; Systemic: n = 12). One-way ANOVA followed by multiple comparison analysis for each frequency band individually, revealed indeed significant increase of BLP in Sigma (Local: $F(1, 19) = 4.76$, $p < 0.05$, Systemic: $F(1, 23) = 7.37$, $p < 0.05$), Beta (Local: $F(1, 19) = 8.64$, $p < 0.01$, Systemic: $F(1, 23) = 7.13$, $p < 0.05$) and Gamma (Local: $F(1, 19) = 4.36$, $p = 0.05$, Systemic: $F(1, 23) = 6.33$, $p < 0.05$) frequency band after either drug injection method (Figure 3.20). Detailed results are summarized in Supplementary Table 7.8. One-sample t-test of stimulus-induced BLP change against zero did not show significances in any frequency band during drug-free condition. However, after local clonidine infusion into LC, BLP in Beta ($t(9) = 3.60$, $p < 0.01$) and Gamma ($t(9) = 2.91$, $p < 0.05$) frequency band was significantly increased in response to FS stimulation. This modulated frequency range was extended to Sigma frequency band after systemic clonidine injection (Sigma: $t(11) = 3.64$, $p < 0.01$, Beta: $t(11) = 4.39$, $p < 0.01$, Gamma: $t(11) = 4.72$, $p < 0.01$). BLP in low frequency range was not affected by any pharmacological manipulation (Supplementary Table 7.9).

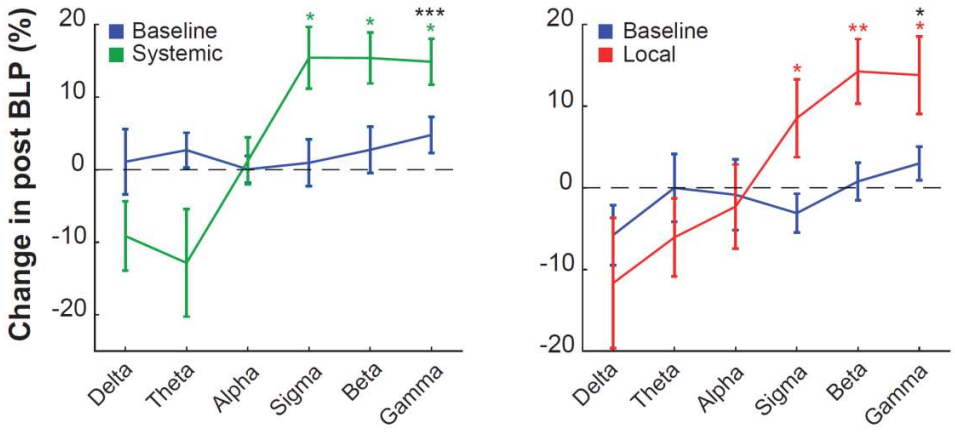

Figure 3.20: Noradrenergic modulation of stimulus-related BLP change in mPFC TCA- cases after systemic clonidine injection (left) and under local inhibition of LC activity (right). Between group comparison was performed using one-way ANOVA between baseline and drug condition (green and red asterisks) and within group comparison against 0 with one-sample t-test (black asterisks). Mean ± SE, * p < 0.05, ** p < 0.01, ***p < 0.001.

In conclusion, both reduction of noradrenergic tone by inhibition of LC activity as well as global activation of alpha 2-receptors induced activation of cortical activity state in mPFC even though the activity of noradrenergic neurons in LC was inhibited. This effect was presumably enabled by decreased power of slow oscillations during prestimulus interval. In cases, in which sensory stimulation activated the cortical state already under baseline condition, poststimulus BLP in Sigma and Beta frequency bands were increased in mPFC and decreased in S1HL.

Given that cortical power in Sigma frequency range is associated with sleep processes[36,37] and power in Beta frequency band with cortical activation[48-50], unidirectional modulation of both frequency bands under clonidine condition indicate a simultaneous inhibition of sleep-promoting and wake-promoting activity in S1HL and simultaneous activation of both in mPFC.

3.1.4.3. Noradrenergic modulation of SEPs and single unit responses to sensory stimulation in S1HL and mPFC

Referring to the reported role of NE in sensory regions, to increase SNR by decrease of spontaneous neuronal activity, depletion of cortical NE expectedly disinhibited spontaneous activity in S1HL (see section 3.1.2). A corresponding inhibition of the sensory-evoked responses in S1HL might be only expected after intra-LC infusion of clonidine and associated inhibition of phasic activation of LC neurons in contrast to systemic injection. Nevertheless, a reduction of cortical sensory-evoked responses to FSs can still be assumed after systemic treatment because of the global activation of pre- and postsynaptic inhibitory alpha 2-adrenoceptors. Accordingly, the population activity represented by SEPs is expected to be reduced in S1HL.

In mPFC, NE was reported to bidirectionally modulate single unit responses to sensory stimulation which might be dependent on neuronal population[245-248,251,252,254-256]. Therefore, a differential modulation of the four mPFC neuronal groups is expected which should, however, not affect the SEPs as population response.

To explore the underlying voltage fluctuations of the spectral composition of the LFP, first, SEPs were compared between baseline and drug conditions whereby data for baseline

condition was combined from baseline before local and baseline before systemic administration of clonidine. In S1HL, the maximum amplitude of the early (first short latency transient component) and late response component as well as the integral of the entire voltage deflection or late response component only, were analyzed separately. It was found in S1HL that local inhibition of LC activity decreased the amplitude of the late response component ($F(1, 32) = 4.02$, $p = 0.05$, Figure 3.21A right). However, neither manipulation method affected any of the other parameters (Supplementary Table 7.10).
In mPFC, analysis of maximum amplitude and integral of the single voltage deflection was subdivided into TCA+ and TCA- cases (Table 3.9).

Table 3.9: Number and percentage of recorded SEPs in mPFC subdivided into effectiveness of sensory stimulation for each pharmacological condition.

	TCA+	TCA-
Systemic Clonidine	7 (38.89 %)	8 (61.54 %)
Local Clonidine	11 (61.11 %)	5 (38.46 %)

In contrast to SEPs in S1HL, local injection of clonidine did not have any significant effect on any parameter; however, systemic injection of clonidine decreased the integral of the voltage deflection in TCA+ cases only (Figure 3.21, $F(1, 24) = 5.92$, $p < 0.05$). In TCA- cases, neither the amplitude nor the integral were significantly affected. SEP amplitudes and integrals including statistical comparison are summarized in Supplementary Table 7.11 and Supplementary Table 7.12 for TCA+ and TCA- cases, respectively.
In summary, pharmacological manipulation differentially modulated SEPs in the cortical structures. While systemic activation of alpha 2-adrenoceptors decreased SEP only in mPFC TCA+ cases, this treatment did not affect any response parameters in S1HL. Local inhibition of LC activity, on the other hand, reduced the amplitude of only the late response component in S1HL. In addition, in mPFC, a reduction of SEP amplitude as well as integral was indicated for TCA- cases, however, this modulation was not significant.

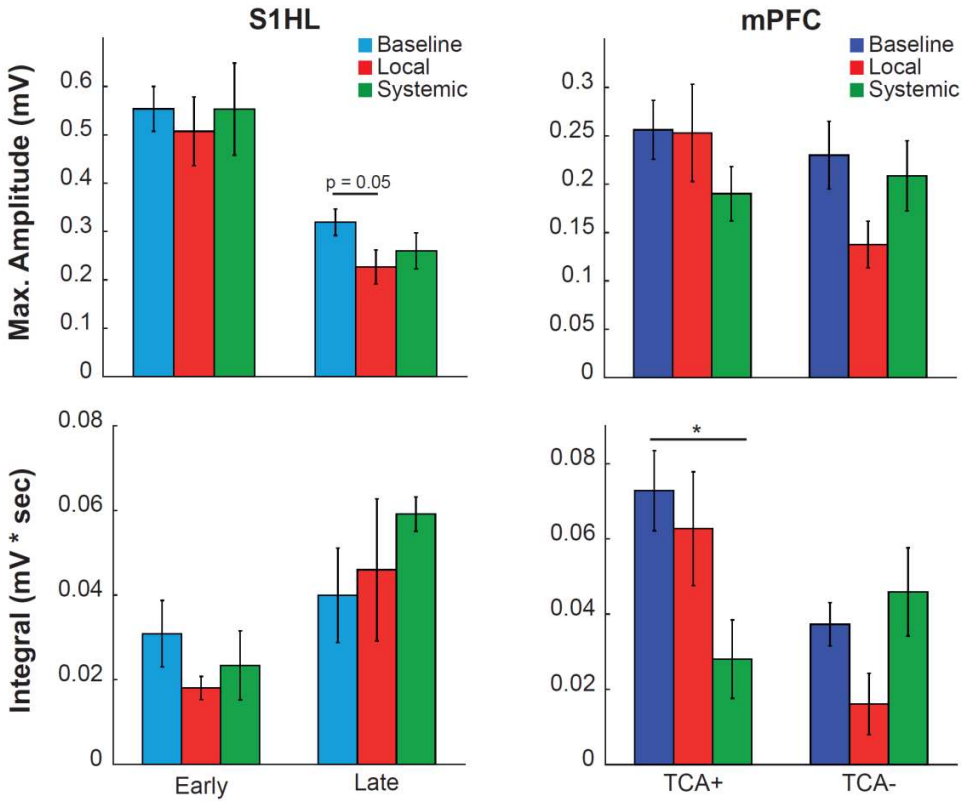

Figure 3.21: The effect of clonidine administration on maximum amplitude (top row) and integral (bottom row) of SEP in S1HL (left column) and mPFC (right column). In S1HL, combined two short-latency response components (Early) and the late response component (Late) were analyzed individually. Recordings in mPFC were separated in TCA+ and TCA- cases. Mean ± SE, * $p < 0.05$.

Finally, noradrenergic modulation of sensory-evoked single unit responses was compared between S1HL and mPFC. First, the effects of clonidine on the population of cortical neurons that showed significant responses to FS during baseline ('initially responsive' neurons) were analyzed independent from cortical state activation. To recall briefly, different populations of neurons were found in S1HL as well as mPFC dependent on their profile in response to electrical FSs. In S1HL, two populations were characterized which differed on the presence of a late response component. In mPFC, four populations with different latencies and response durations were found (see section 3.1.3.6).

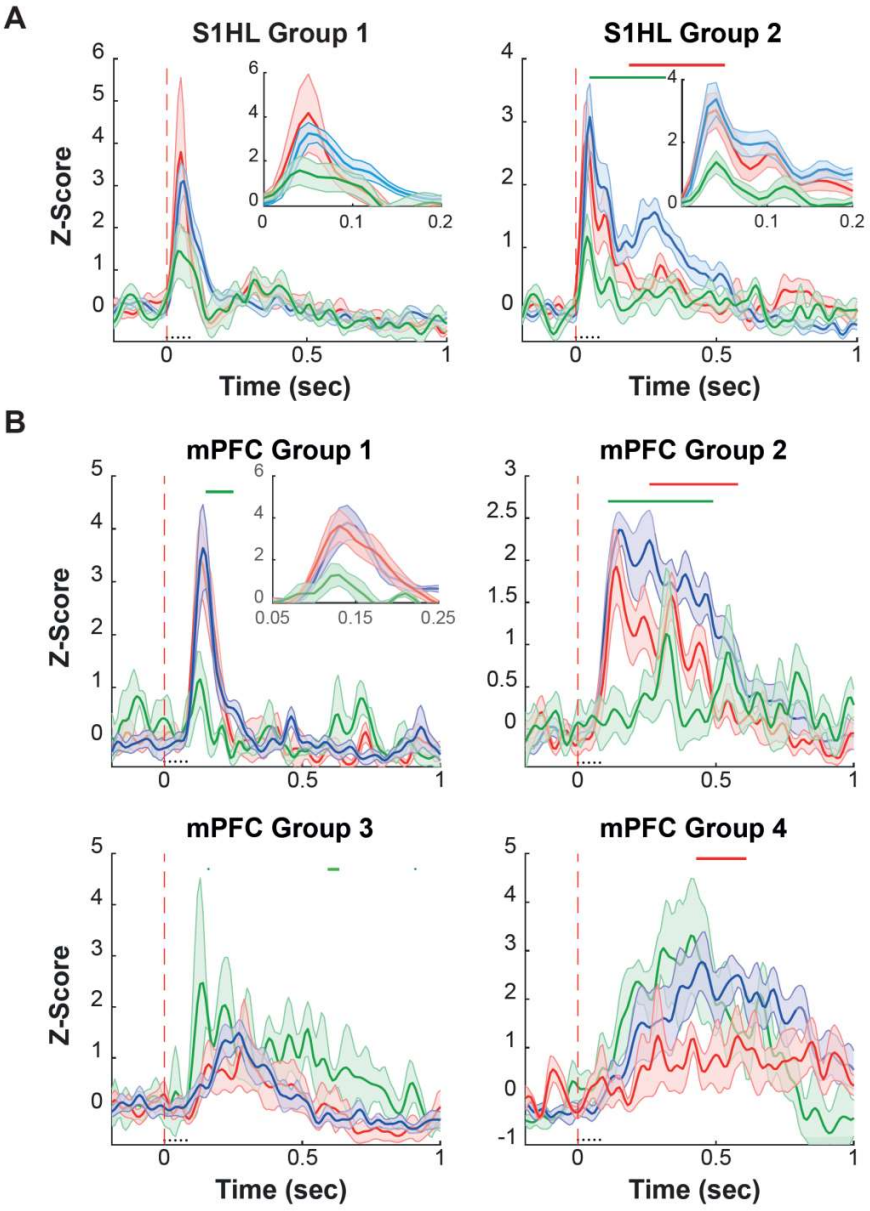

Figure 3.22: The modulation of individual groups of single unit responses to somatosensory stimulation in A) S1HL and B) mPFC after clonidine administration. Smoothed average PSTHs of the responses to FS during baseline (S1HL: cyan, mPFC: blue), iontophoretic injection of clondine into LC (red) and systemic clonidine injection (green) are plotted. Insets show magnifications of transient response components. Color coded bars above the response profiles illustrate significantly different bins between baseline and drug condition. The group classification is the same as shown on Figure 3.17. Stimulation was applied at time 0. Bin size = 10ms.

Exploration of response characteristics of individual groups of neurons under drug conditions in both cortical regions revealed that S1HL group 2 and mPFC group 1, 2 and 4 neurons were mostly affected. S1HL group 1 did not show any modulation in response to clonidine administration and mPFC group 3 neurons showed only minor effects. Specifically, systemic clonidine administration resulted in substantial decrease of the average Z-Scores of the response in S1HL group 2 neurons and in mPFC group 1 and 2 neurons (as revealed by two-way repeated measures ANOVA with 10 ms-bins as repeated measures) (Figure 3.22). In S1HL, the group 2 neurons showed a significant decrease of the response amplitude between 0.05 to 0.32 sec (Figure 3.22A, $F(1, 20) = 11.14$, $p < 0.01$). In mPFC, the affected interval was 0.15 to 0.25 sec ($F(1, 4) = 35.37$, $p < 0.01$) in group 1 neurons and 0.11 to 0.49 sec ($F(1, 10) = 15.31$, $p < 0.01$) in 6 out of 8 group 2 neurons (Figure 3.22B). The two remaining group 2 neurons drastically increased average Z-Scores (Supplementary Figure 7.4, $F(1, 2) = 26.54$, $p < 0.05$). Increase of the average Z-Scores was also occasionally revealed by pairwise comparison of each bin in mPFC group 3 neurons, however, the overall response magnitude did not significantly change ($F(1, 6) = 3.23$, n.s.). On the background that this group represents a merged population of mPFC neurons with different properties, a modulation was not expected because potential modulation effects would cancel each other out. The inhibition of noradrenergic transmission by local injection of clonidine into LC decreased only the late response component of the neurons in group 2 of S1HL between 0.19 to 0.53 sec ($F(1, 38) = 15.71$, $p < 0.001$) while the short latency component was preserved. Note, that SEP in S1HL was likewise modulated under this condition. Similarly, in mPFC, neurons of group 1, which showed a transient response profile, were not affected while the later response components of neurons which showed a sustained excitation were decreased. Group 2 neurons were decreased in the interval between 0.28 - 0.65 sec ($F(1, 18) = 12.51$, $p < 0.01$) and group 4 neurons showed a reduction between 0.43 to 0.61 sec ($F(1, 8) = 7.18$, $p < 0.05$).

In brief, systemic clonidine injection led to a reduction of activity during the entire response duration in affected neuronal groups while local inhibition of LC activity shortened the response duration. Overall, these effects led to a decreased number of initially responsive units after either clonidine condition in both cortical areas (Table 3.10). Neurons

in S1HL showed the strongest effects after systemic injection of clonidine by significantly decreasing the number of initially responsive neurons about ~ 60 % ($Chi^2(1, 25) = 4.84$, $p < 0.05$). In mPFC, the proportion decreased about ~ 40 %. Local inhibition of LC activity decreased the proportion to a similar amount in both cortical regions.

Table 3.10: Number of responsive single units in each group within a cortical structure after systemic and local clonidine injection (clo) in comparison to the number of responsive units under baseline condition (base). Percentage indicates the proportion of neurons which kept responsiveness after clonidine injection.

Groups	S1HL		mPFC	
	systemic	local	systemic	local
	$n_{(clo)}/n_{(base)}$	$n_{(clo)}/n_{(base)}$	$n_{(clo)}/n_{(base)}$	$n_{(clo)}/n_{(base)}$
Group 1	4/7	6/9	0/3	4/6
Group 2	3/11	11/20	3/8	6/9
Group 3	-	-	4/4	5/10
Group 4	-	-	3/3	3/5
Total	7/18 (39%)	17/29 (59%)	10/18 (56%)	18/30 (60%)

Next, we expanded our analysis on the initially non-responsive neurons in each brain region and observed so-called 'gating' effect, which was present only in mPFC after either pharmacological manipulation. About 30 % of initially non-responsive neurons became responsive after systemic application of clonidine and approximately a quarter after local LC inhibition (Figure 3.23A). The post-stimulus interval of significant increase of response amplitude was 0.11 to 0.88 sec after systemic ($F(1, 28) = 22.64$, $p < 0.001$) and 0.17 to 0.61 sec after local clonidine injection (Figure 3.23B; $F(1, 16) = 27.74$, $p < 0.001$).

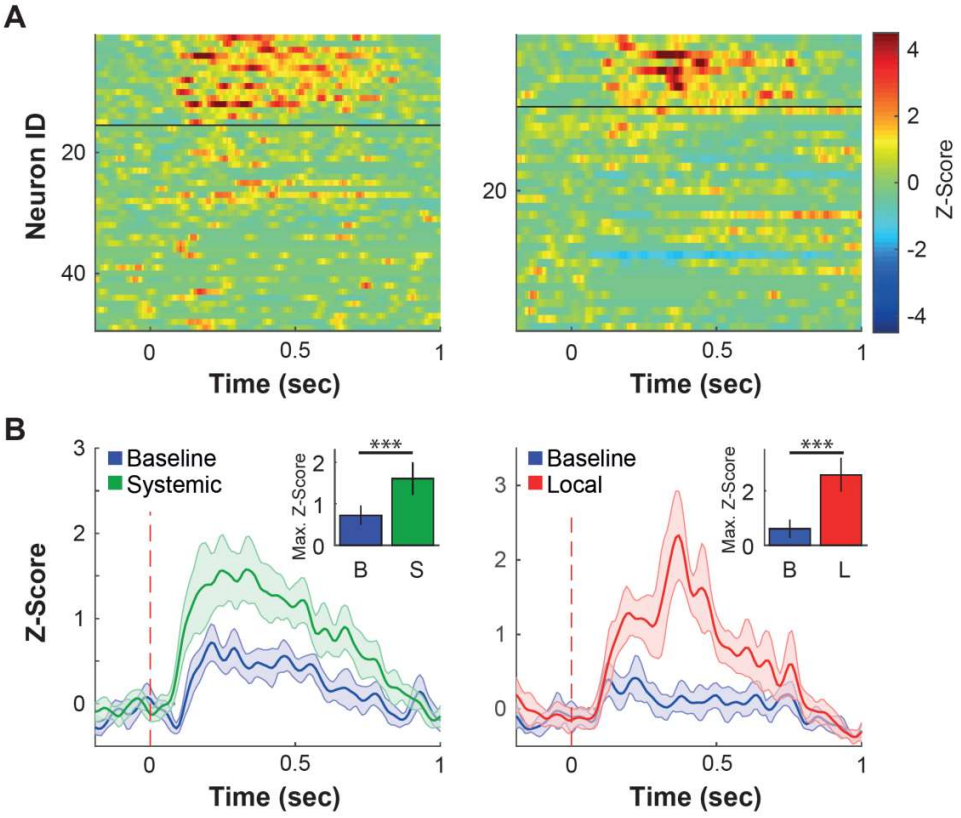

Figure 3.23: The sensory-gating effect in mPFC after systemic (left) and local (right) administration of clonidine. A) The normalized firing rate of all initially non-responsive single units is plotted after either clonidine injection. B) Smoothed average PSTHs of the gated neurons under baseline and drug condition. Stimulation was applied at time 0. Bin size = 10ms. Insets illustrate the difference between the maximum amplitude in baseline (B) and after local (L) or systemic (S) clonidine injection.

In combination with the decreased number of initially responsive neurons under clonidine condition, a redistribution of active cortical pyramidal neurons was observed in mPFC, maintaining the overall number of responsive neurons comparable to baseline condition after either clonidine application (Figure 3.24; Systemic: $Chi^2(1, 43) = 1.14$, n.s.; Local: $Chi^2(1, 59) = 0.42$, n.s.).

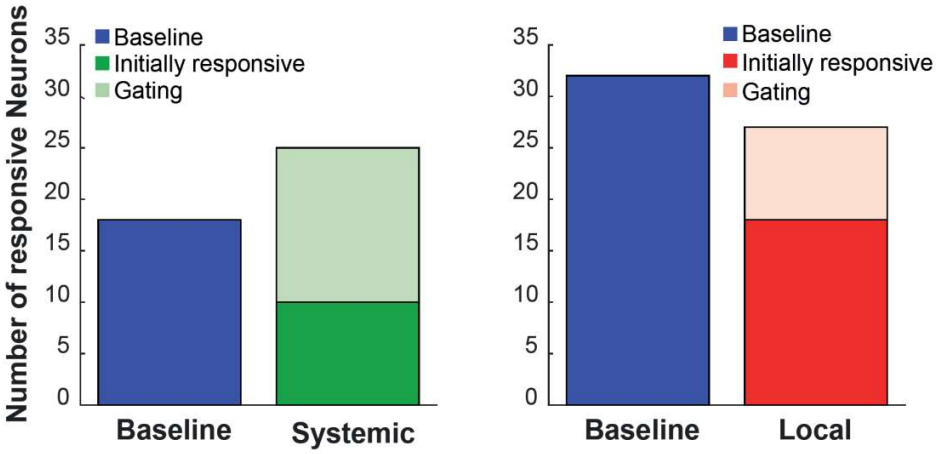

Figure 3.24: The effect of clonidine administration on the number of responsive single units in mPFC. The number of initially responsive neurons (blue) was reduced under condition of systemic clonidine (green) and local inhibition of LC activity (red). This effect was accompanied by simultaneous gating effects of initially non-responsive single units (shaded green and red after systemic and local injection of clonidine, respectively) which resulted in a drug induced redistribution of activated neurons without changing the population size.

In the current study, noradrenergic modulation of sensory-evoked responses was studied independent from drug-induced effects on spontaneous activity by analyzing firing rates normalized to Z-Scores. Therefore, it would be interesting whether a decrease of spontaneous activity uncovered the sensory evoked response and induced the gating effects. Interestingly, spontaneous activity of the affected population of neurons was not reduced under either drug condition in comparison to the baseline spontaneous activity (Systemic: $F(1, 26) = 0.50$, p = n.s.; Local: $F(1, 16) = 0.17$, p = n.s.). In contrast, although only after systemic clonidine application, the population of gated neurons exhibited a higher spontaneous activity under clonidine condition compared to the neurons which preserved unresponsiveness (2.15 ± 0.42 spikes/s vs. 1.14 ± 0.23 spikes/s; $F(1, 43) = 6.47$, $p < 0.05$). These results suggest that the gated neurons belong to a population with specific electrophysiological properties.

A further question to ask resulted from the belief that the firing rate of SUA is positively related to power in high frequency range (see section 3.1.3.5). An increase of high frequency power was observed in mPFC TCA- cases after local and systemic injection of clonidine, which were unaffected by sensory stimulation under baseline condition. To test

whether this effect is related to the drug-induced gating effects of mPFC single units, the magnitude of sensory-evoked responses in gated neurons was compared between TCA+ and TCA- cases under each drug condition. Therefore, the integral over 1 sec immediately after stimulus presentation was compared between baseline and clonidine condition. The number of gated neurons subdivided into cortical activity groups for each pharmacological manipulation is summarized in Table 3.11.

Table 3.11: Number of gated neurons out of the population of initially non-responsive (non-resp.) single units in mPFC after either pharmacological manipulation for TCA+ and TCA- cases, respectively.

	Systemic ($n_{(gated)}/n_{(non\text{-}resp.)}$)	Local ($n_{(gated)}/n_{(non\text{-}resp.)}$)
TCA+	9/23	2/22
TCA-	5/22	7/18

When recorded in TCA- cases, the population of gated neurons vastly increased the response magnitude after local ($F(1, 12) = 49.17$, $p < 0.001$) and systemic ($F(1, 8) = 7.17$, $p < 0.05$) injection of clonidine (Figure 3.25). This effect was also observed in TCA+ cases but only under condition of systemic clonidine injection ($F(1, 16) = 11.44$, $p < 0.01$), while local inhibition of LC activity did not have an effect ($F(1, 2) = 0.03$, p = n.s.).

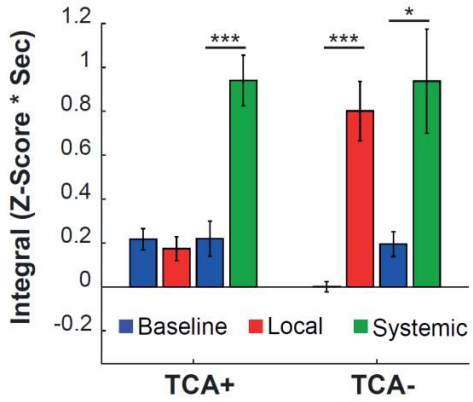

Figure 3.25: The effect of clonidine on gated single units in mPFC dependent on stimulus-evoked cortical state activation. Bars illustrate the average integral over 1 sec after stimulus onset of the PSTH in response to FSs separated in TCA+ and TCA- cases. Mean ± SE, * $p < 0.05$, *** $p < 0.001$.

In conclusion, cortical NE deprivation results in gating of single unit responses to sensory stimulation which seems to mediate the drug-induced increase of power in high frequency range in initial TCA- cases.

3.2. Noradrenergic modulation of the midbrain dopaminergic system

All sensory information, which is integrated by mPFC, is a result of multiple bottom-up processes from many different brain regions. The LC is known to globally project to every brain structure, with the exception of basal ganglia. Thus, NE is able to modulate incoming sensory information already at early processing stages including the modulation of neuronal activity in other neuromodulatory systems than the noradrenergic LC. Out of these, especially the dopaminergic system has been described to play a major role in processing of salient sensory information[329-339] and the dopaminergic VTA in the midbrain is strongly modulated by NE[119,377,477-482,492,493,495-497,500-503,506-509]. Hence, the question of how the noradrenergic system modulates the neuronal activity in the dopaminergic ventral midbrain, which synergistically contributes to the effects in the cortex described in the previous section, was explored in a separate set of experiments. Here, simultaneous recordings in LC, VTA and mPFC were performed in 15 rats, albeit data from mPFC contributed to the previous study. Although the VTA consists of different neuronal types, including dopaminergic, glutamatergic and GABAergic neurons[309-320], MUA was analyzed in order to study the net outcome of sensory processing of the VTA. Furthermore, the population of dopaminergic neurons represents more than 70 % of all neurons in the VTA[318] and, presumably, dominates potential effects. In order to explore the noradrenergic modulation of MUA in the dopaminergic VTA specifically related to LC-activity, local infusion of clonidine into the LC was used only while global activation of alpha 2-adrenoceptors by systemic clonidine injection was spared in the experimental protocol. Sensory stimulation was performed according to the stimulation protocol used before.

3.2.1. Noradrenergic modulation of spontaneous activity in the ventral midbrain

Most of the recordings in the ventral midbrain were performed in the VTA (Figure 3.26A) while two out of 15 recordings were performed in the lateral dopaminergic SNc.

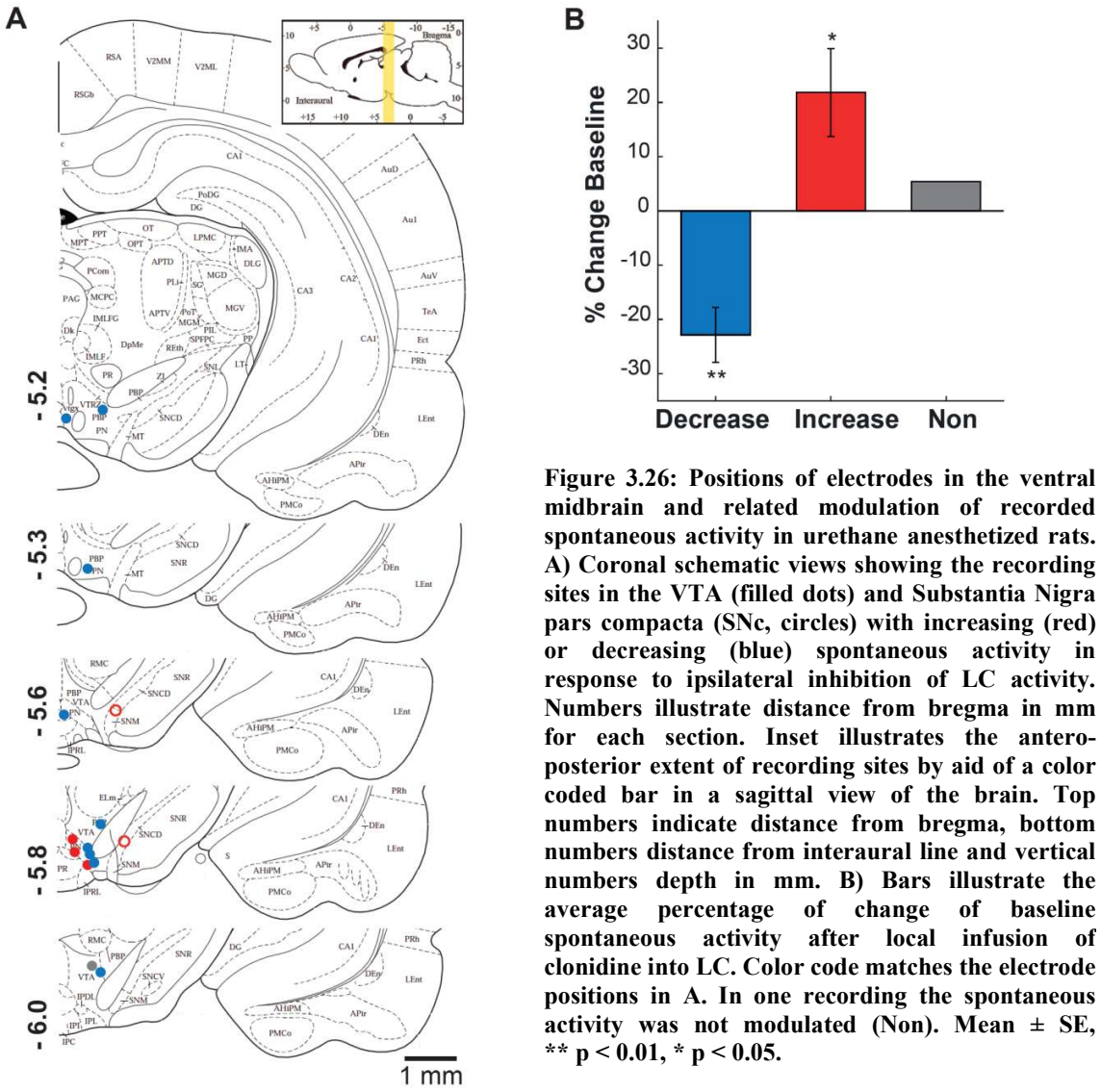

Figure 3.26: Positions of electrodes in the ventral midbrain and related modulation of recorded spontaneous activity in urethane anesthetized rats. A) Coronal schematic views showing the recording sites in the VTA (filled dots) and Substantia Nigra pars compacta (SNc, circles) with increasing (red) or decreasing (blue) spontaneous activity in response to ipsilateral inhibition of LC activity. Numbers illustrate distance from bregma in mm for each section. Inset illustrates the antero-posterior extent of recording sites by aid of a color coded bar in a sagittal view of the brain. Top numbers indicate distance from bregma, bottom numbers distance from interaural line and vertical numbers depth in mm. B) Bars illustrate the average percentage of change of baseline spontaneous activity after local infusion of clonidine into LC. Color code matches the electrode positions in A. In one recording the spontaneous activity was not modulated (Non). Mean ± SE, ** $p < 0.01$, * $p < 0.05$.

First, the modulation of spontaneous MUA by local inhibition of LC activity was explored for each recording. Therefore, a paired-sample t-test over 50 bins during 0.5 sec prestimulus interval (bin size = 10 ms) between baseline and drug condition was performed. This analysis revealed a bidirectional modulation of spontaneous MUA dependent on recording site in the ventral midbrain (Figure 3.26B). Sites with a decrease in MUA firing rate ($t(8) = -4.48$, $p < 0.01$) were recorded in the anterior and lateral VTA (n = 9) illustrated

as blue dots in Panel A. Sites with an increase in MUA firing rate (n = 5, t(4) = 2.69, p = 0.05) were recorded in the medial VTA (red dots, n = 3) or SNc (red circles, n = 2). Only one recording site did not show any significant modulation in spontaneous MUA (gray).

3.2.2. Validation of parameters for effective stimulation in the VTA

Comparable to recordings in LC, S1HL and mPFC (see section 3.1.3.1), different stimulation protocols were tested in order to ensure reliable sensory-evoked modulation of neuronal activity in the VTA whereby this time, only amplitude coding was tested. Similar to neuronal responses to sensory stimulation observed in LC and mPFC, neuronal responses in the VTA were exclusively excitatory and showed incrementally higher response amplitudes with increased stimulation current from 1 mA to 5 mA (Figure 3.27; $F(4, 70) = 4.51$, $p < 0.01$). The corresponding average maximum firing amplitudes are provided in Supplementary Table 7.13.

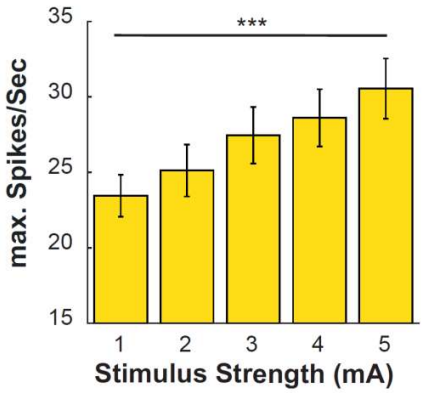

Figure 3.27: The effect of FS using TR stimulation with increasing stimulus strength on average amplitudes of population single unit responses in the ventral midbrain. Note sequentially increased response amplitude with increased stimulus strength. Mean ± SE, *** p < 0.001.

Therefore, further experiments were conducted using TR stimulation with stimulation current of 5 mA to explore reliable sensory evoked responses in the VTA comparable to neuronal responses in LC and mPFC.

3.2.3. Noradrenergic modulation of multi unit responses to sensory stimulation in the ventral midbrain

Next, the magnitude of neuronal MUA responses to sensory stimulation was compared between baseline condition and under inhibition of LC neuronal activity.

Theoretically, the two different dopaminergic structures in the ventral midbrain, VTA and SNc, have very different functions. While the dopaminergic neurons in VTA are known to play a role in sensory processing among other functions[340-342], neuronal activity in SNc are mostly discussed in relation to motoric processes[694]. Therefore, sensory-evoked responses recorded in SNc were analyzed separately from responses recorded in VTA. Comparison of the integral of sensory-evoked responses during 0.5 sec poststimulus interval between baseline and drug condition revealed an overall decreased response magnitude in the average VTA population (Figure 3.28 left; $F(1, 25) = 5.41$, $p < 0.05$), independent from direction of spontaneous activity modulation. MUA recorded in two sites in the SNc did not show any effect (Figure 3.28 right; $F(1, 3) = 0.06$, p = n.s.).

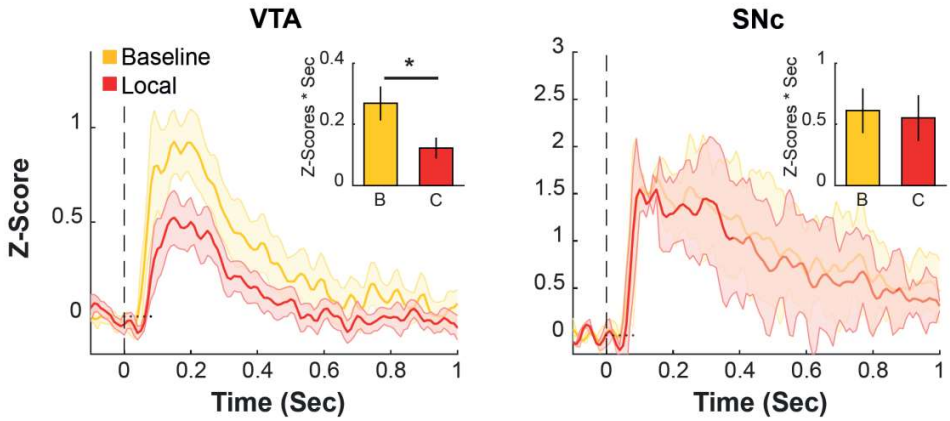

Figure 3.28: Single unit responses to FSs in the VTA and SNc. Smoothed average PSTHs during baseline condition (yellow) and under local inhibition of LC activity (red) are shown. Stimulation was applied at time 0 (black dashed line). Bin size = 10 ms. Insets illustrate the difference between the integral over 0.5 sec during baseline (B) and clonidine (C) condition. Mean ± SE, * $p < 0.05$.

In conclusion, removal of stimulus-related phasic release of NE into the VTA generally diminished ventral tegmental sensory signaling. In contrast, the sensory-evoked responses in the SNc are not modulated by NE. Since phasic activity generally leads to higher release of neurotransmitters in target regions[134,348,359-366], a reduction of sensory-evoked phasic responses in VTA dopaminergic neurons, results in a decrease of available DA in mPFC during sensory processing.

3.3. Dopaminergic modulation of sensory gating

In the previous experiment, a decrease of stimulus-induced excitation of neurons in the dopaminergic VTA was observed when the tonic and phasic activity of the noradrenergic system was inhibited by local infusion of clonidine into LC. Under this condition, the release of NE as well as DA is reduced in mPFC which resulted in the complex effects described in section 3.1.

Next, sensory processing in mPFC was explored under specific manipulation of the dopaminergic system while leaving the noradrenergic system intact. A new set of experiments was designed in order to explore both the modulation of neuronal activity in mPFC and the behavioral outcome after processing of sensory stimulation. Therefore, non-anesthetized rats were tested on sensory gating by using two different standard sensory-gating paradigms: PPI and ASG. Thirteen rats were simultaneously tested on both sensory gating paradigms. Concurrently, SEPs were recorded in PrL, confirmed by histological examination of the recording sites (Figure 3.29). In two out of 13 rats, the recording was not successful and only the magnitude of the behavioral acoustic startle response detected by the piezoelectric sensor under the floor was analyzed. Before testing, the midbrain dopaminergic system was pharmacologically manipulated by drug infusion via bilaterally implanted cannulae targeting the ventral midbrain (Figure 3.30).

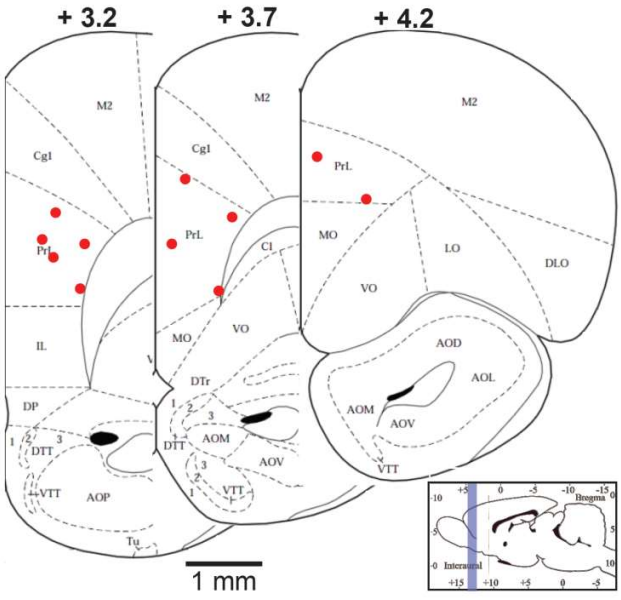

Figure 3.29: Coronal schematic views showing the electrode positions in the PrL in awake rats tested on sensory gating. Numbers illustrate distance from bregma in mm for each section. Inset illustrates the antero-posterior extent of recording sites by aid of a colored bar in a sagittal plane of the brain. Top numbers indicate distance from bregma, bottom numbers distance from interaural line and vertical numbers depth in mm, respectively.

The pharmacological manipulation was specifically designed to explore the role of dopaminergic modulation of sensory gating in mPFC. To recap briefly, alpha 2-adrenoceptors were activated by local infusion of clonidine into the ventral midbrain in order to generally decrease dopaminergic transmission to VTA target structures. Furthermore, infusion of κ-opioid agonist U69593 and dopaminergic D_2-receptor agonist quinpirole was used to selectively inhibit dopaminergic transmission to mPFC or non-PFC target structures, respectively. Saline infusion was used as control condition.

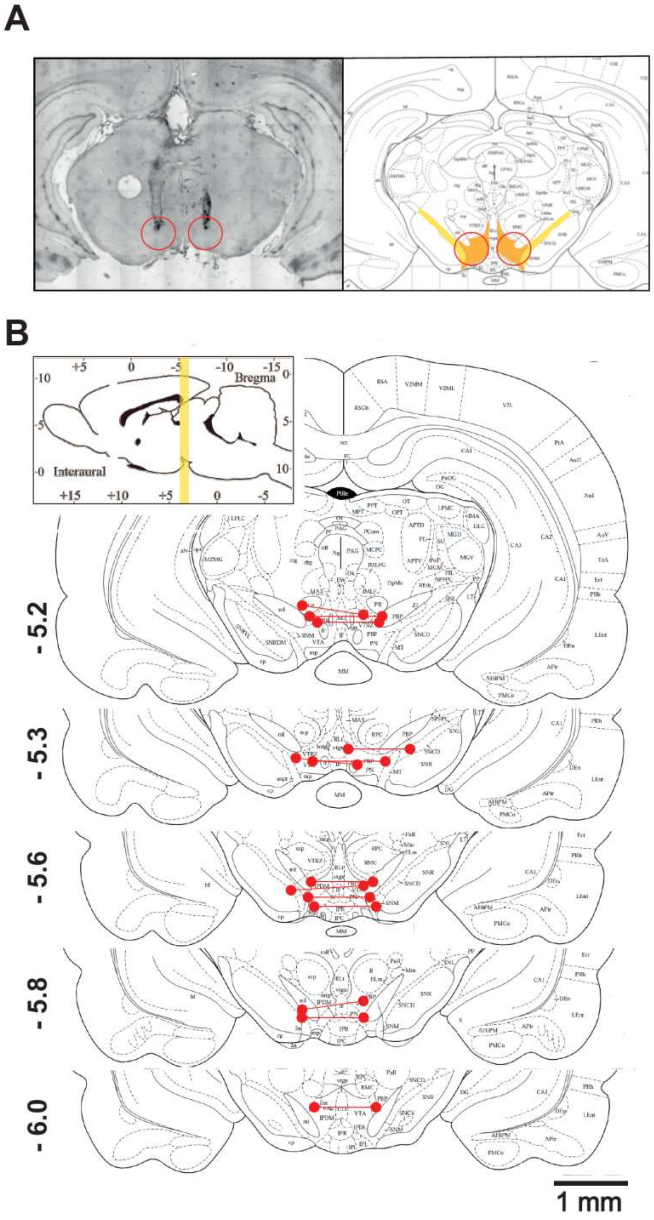

Figure 3.30: Coronal views showing the tips of chronically implanted bilateral cannulas used for drug infusion into the ventral midbrain. A) Representative histological section showing lesions created by implanted cannulas into the ventral midbrain (left). Red circles indicate estimation of drug diffusion in the tissue. Coronal schematic view of corresponding section (right) shows estimated drug diffusion in VTA (orange) as well as partly in SNc (yellow). B) Schematic views illustrate tips of implanted infusion cannulas for all rats tested on sensory gating. Corresponding tips of bilateral cannulas are connected by a red line. Numbers illustrate distance from bregma in mm for each section. Inset illustrates the antero-posterior extent of infusion sites by aid of a colored bar in a sagittal plane of the brain. Top numbers indicate distance from bregma, bottom numbers distance from interaural line and vertical numbers depth in mm, respectively.

3.3.1. Characterization of PPI and ASG under baseline condition

First, the behavioral and neuronal effects of sensory stimulation are described under saline condition only. For the PPI paradigm, 65 sessions were recorded out of which 52 sessions included SEP recordings from mPFC. Effective PPI was confirmed by decrease of the ASR from -0.66 ± 0.09 mV to -0.19 ± 0.02 mV when prepulse was presented 100 ms prior to startle pulse (Figure 3.31A, $F(1,129) = 23.65$, $p < 0.001$). Simultaneous recording in mPFC revealed that PPI was also present on the neuronal level (Figure 3.31B) as the amplitude of the SEP was significantly decreased from -0.12 ± 0.01 mV to -0.06 ± 0.01 mV when prepulse was paired with a startle pulse (Figure 3.31B; $F(1,103) = 18.37$, $p < 0.001$).

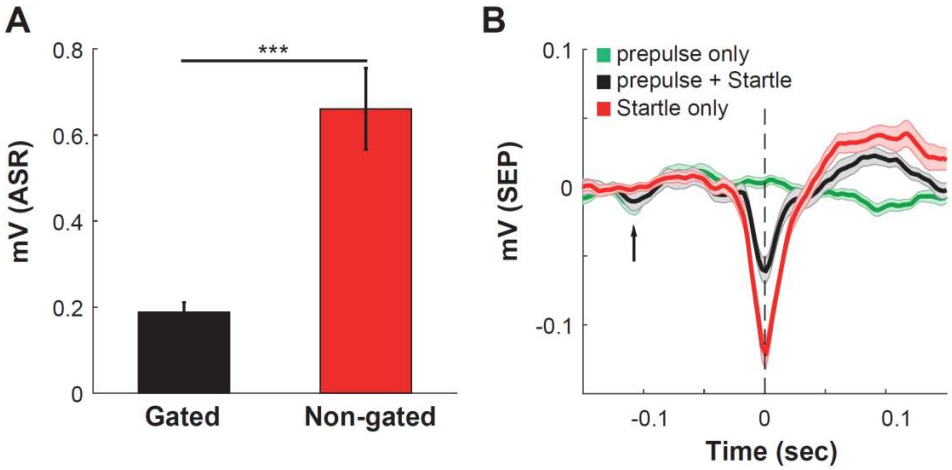

Figure 3.31: Prepulse Inhibition of the acoustic startle response (ASR) and corresponding prefrontal SEPs after infusion of saline into the ventral midbrain. A) The amplitude of the ASR in response to startle stimulus (broad band noise, 20ms, 100dB) only (Non-gated) was reduced when a prepulse (10kHz, 20ms, 75dB) was presented 100 ms prior to the startle stimulus (Gated). Bars illustrate average magnitude of the ASR. B) PPI was also evoked at the neuronal level. Comparable to the ASR in A, presentation of a prepulse prior to a startle stimulus (prepulse + Startle) reduced the amplitude of the SEP in response to startle stimulus only (Startle only). Arrow illustrates neuronal response to presentation of prepulse. Mean ± SE, *** $p < 0.001$.

The ASG paradigm was tested simultaneously with PPI. The parameters used for this stimulation were identical to the parameters used for the prepulse in the PPI paradigm. Since this stimulation was not as salient as the startle pulse used for PPI, the SNR of the neuronal signal was much lower. The average amplitude of the SEP in response to

condition stimulus was -0.05 ± 0.00 mV compared to -0.12 ± 0.01 mV in response to startle pulse only. According to the literature, the amplitude of the neuronal response to condition stimuli is supposed to be larger than the amplitude of the response to test stimuli in healthy animals. Therefore, sessions were excluded when, due to low SNR, this condition was not fulfilled for average amplitude of SEPs. In total, data out of 40 sessions represent the sensory gating effect in mPFC neuronal activity (Figure 3.32) in which the average amplitude of the neuronal response to test stimuli was confirmed to be significantly smaller than to condition stimuli (0.05 ± 0.00 mV vs. 0.02 ± 0.00 mV; $F(1,79) = 49.11$, $p < 0.001$).

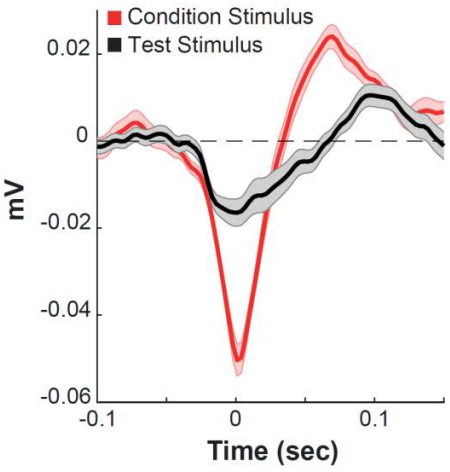

Figure 3.32: Auditory Sensory Gating of SEP in mPFC after infusion of saline into the ventral midbrain. A superposition of average SEPs in response to two identical auditory stimuli (10kHz, 20ms, 75dB), presented 500 ms apart from each other, is illustrated. Naturally, the SEP in response to the second stimulus (Test stimulus) is reduced in comparison with the SEP in response to the first stimulus (Condition stimulus). Mean ± SE.

3.3.2. Dopaminergic modulation of sensory gating in mPFC

ASR and SEPs, which were reduced due to sensory gating mechanisms, induced by either prior presentation of the prepulse or condition stimulus, are henceforth referred to as "gated" responses. Accordingly, responses to only startle stimulus or to condition stimulus are referred to as "non-gated" responses.

The magnitude of sensory gating is illustrated as percentage of inhibition relative to the non-gated response. However, modulation of sensory gating might have different underlying mechanisms. An impairment of PPI, for example, is illustrated by a decrease of percentage of PPI (%PPI), which might result from either an increase of the gated response or a decrease of the non-gated response. Therefore, the absolute response amplitudes are

additionally illustrated in order to compare the underlying mechanisms between the drug effects and between the paradigms.

3.3.2.1. Modulation of sensory gating under general decrease of dopaminergic transmission

Activation of alpha 2-adrenoceptors by infusion of clonidine into the ventral midbrain was performed in 22 sessions which were compared to corresponding sessions under saline condition. PPI of the ASR was not affected by this treatment (Figure 3.33A; $F(1, 43) = 0.02$, p = n.s.): neither the amplitude of the non-gated ASR ($F(1, 43) = 0.02$, p = n.s.) nor the gated ASR ($F(1, 43) = 0.00$, p = n.s.) was modulated. However, the PPI of the SEP (n = 18) was significantly reduced from 67.98 ± 10.24 % to 39.66 ± 10.00 % (Figure 3.33B left; $F(1, 35) = 3.91$, $p = 0.05$). This reduction resulted from a significant increase of the amplitude of gated SEP ($F(1, 35) = 5.21$, $p < 0.05$) from -0.04 ± 0.01 mV to -0.09 ± 0.01 mV (Figure 3.33B right). Nevertheless, ASG (n = 13) was not affected by this treatment ($F(1, 27) = 0.35$, p = n.s.) indicating a different sensory gating mechanism than for PPI (Figure 3.33C). Neither the amplitude of SEP in response to condition stimulus (-0.05 ± 0.00 mV and -0.04 ± 0.00 mV for saline and drug condition, respectively) nor the amplitude of SEP to test stimulus (-0.03 ± 0.00 mV and -0.02 ± 0.00 mV for saline and drug condition, respectively) differed between saline and drug condition (condition stimulus: $F(1, 27) = 0.29$, p = n.s.; test stimulus: $F(1, 27) = 0.03$, p = n.s.).

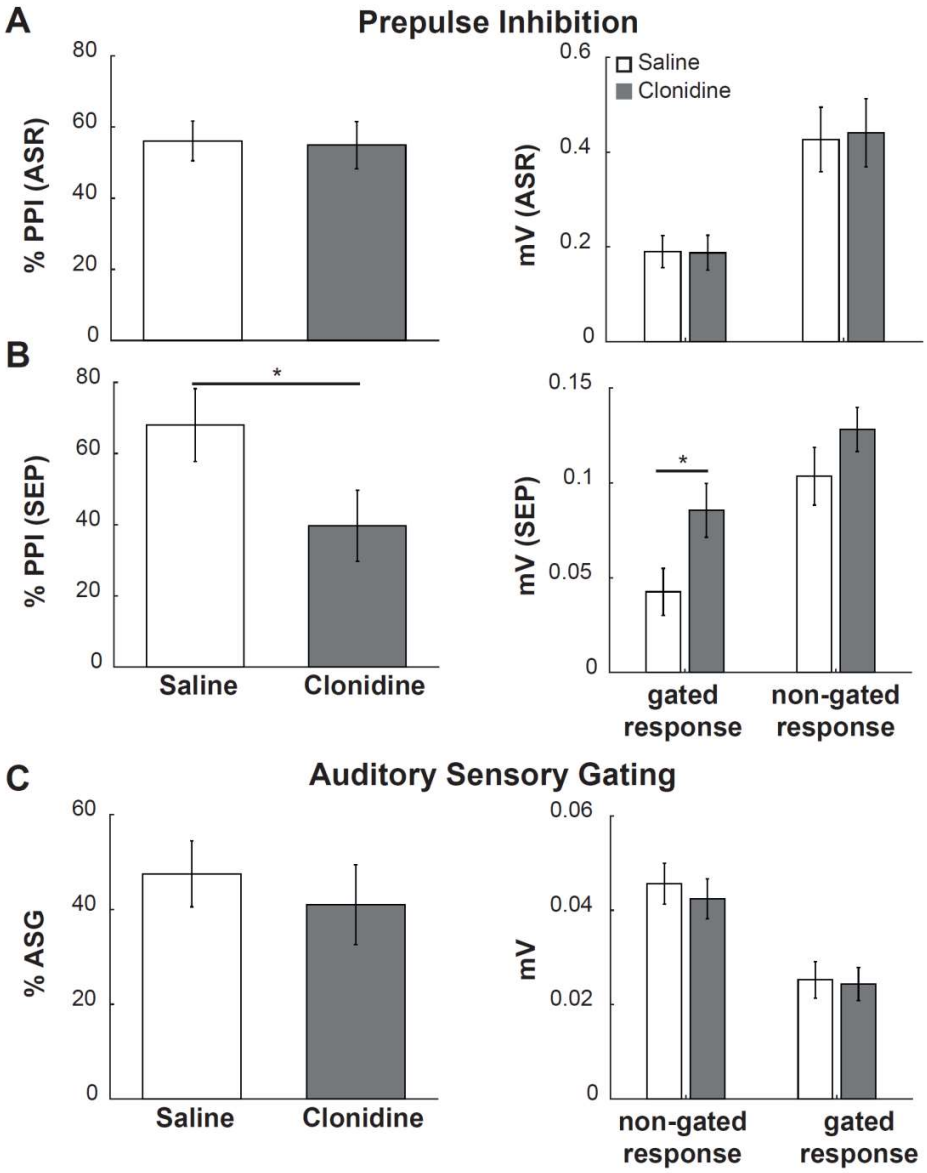

Figure 3.33: Modulation of sensory gating after infusion of clonidine into the ventral midbrain. Degree of sensory gating is illustrated as percentage of inhibition relative to the non-gated response (left column). Absolute response amplitudes are additionally illustrated (right column). A) Average percentage of Prepulse Inhibition of the ASR (PPI, left) and average amplitudes of gated and non-gated ASR (right) are compared between saline and drug condition. B) The prefrontal SEPs are compared between saline and drug injection analogous to A. C) Average percentage of Auditory Sensory Gating (ASG, left) and average amplitudes of non-gated and gated SEPs in response to Condition and Test stimuli (right) are compared between saline and drug condition. Mean ± SE, * $p < 0.05$.

3.3.2.2. Modulation of sensory gating under decrease of dopaminergic transmission selectively to mPFC

Infusion of the the κ-opioid agonist U69593 was performed in 23 sessions to selectively inhibit the dopaminergic transmission to mPFC.

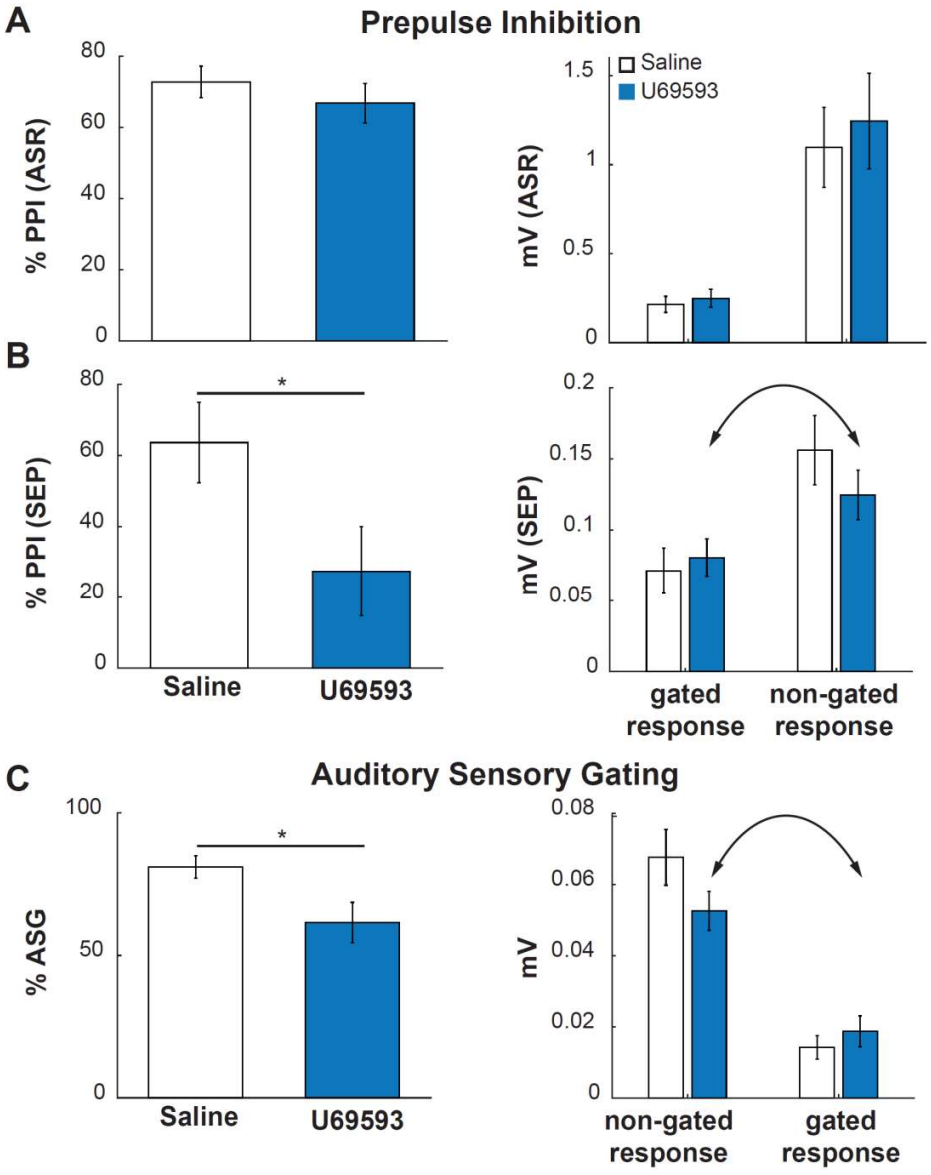

Figure 3.34: Modulation of sensory gating after infusion of U69593 into the ventral midbrain. Conventions are the same shown in Figure 3.33. Arrows indicate shift of the amplitude balance between

gated and non-gated responses resulting in modulation of percentage of sensory gating (left). Mean ± SE, * p < 0.05.

Comparable to the condition after infusion of clonidine into the ventral midbrain, this treatment left the PPI of the ASR unaffected (Figure 3.34A; $F(1, 45) = 0.7$, p = n.s.) but reduced the PPI of SEP (Figure 3.34B left; n = 15; $F(1, 29) = 4.6$, $p < 0.05$) from 63.60 ± 11.32 % to 27.36 ± 12.55 %. However, in contrast to the effect under clonidine condition, reduced PPI resulted from a non-significant increase of the amplitude of gated SEP amplitude from -0.07 ± 0.02 % to -0.08 ± 0.01 % when startle stimulus was preceded by prepulse ($F(1, 29) = 0.2$, p = n.s.), in combination with a non-significant decrease of non-gated SEP amplitude from -0.16 ± 0.02 % to -0.12 ± 0.02 % when startle stimulus was presented only (Figure 3.34B right; $F(1, 29) = 1.1$, p = n.s.). Likewise, but in contrast to effects under clonidine condition, percentage of ASG was significantly decreased ($F(1, 27) = 5.83$, $p < 0.05$) from 81.06 ± 3.89 % to 61.54 ± 7.09 %. This happened because of a slight increase of the amplitude of gated SEP ($F(1, 27) = 2.48$, p = n.s.) from -0.01 ± 0.00 mV to -0.02 ± 0.00 mV combined with a slight decrease of non-gated SEP (Figure 3.34C; $F(1, 27) = 0.7$, p = n.s.) from -0.07 ± 0.01 mV to -0.05 ± 0.01 mV. Hence, when dopaminergic transmission was selectively decreased in mPFC, PPI and ASG seemed to share underlying gating mechanisms.

3.3.2.3. Modulation of sensory gating under decrease of dopaminergic transmission in ventral midbrain target regions other than mPFC

Finally, the dopaminergic D2-receptor agonist quinpirole was infused into the ventral midbrain of 22 rats (21 rats including recordings of SEPs in mPFC) with the aim to inhibit dopaminergic transmission to all target regions except mPFC. This pharmacological manipulation, however, did not have any effect on the tested parameters (Figure 3.35, Supplementary Table 7.14).

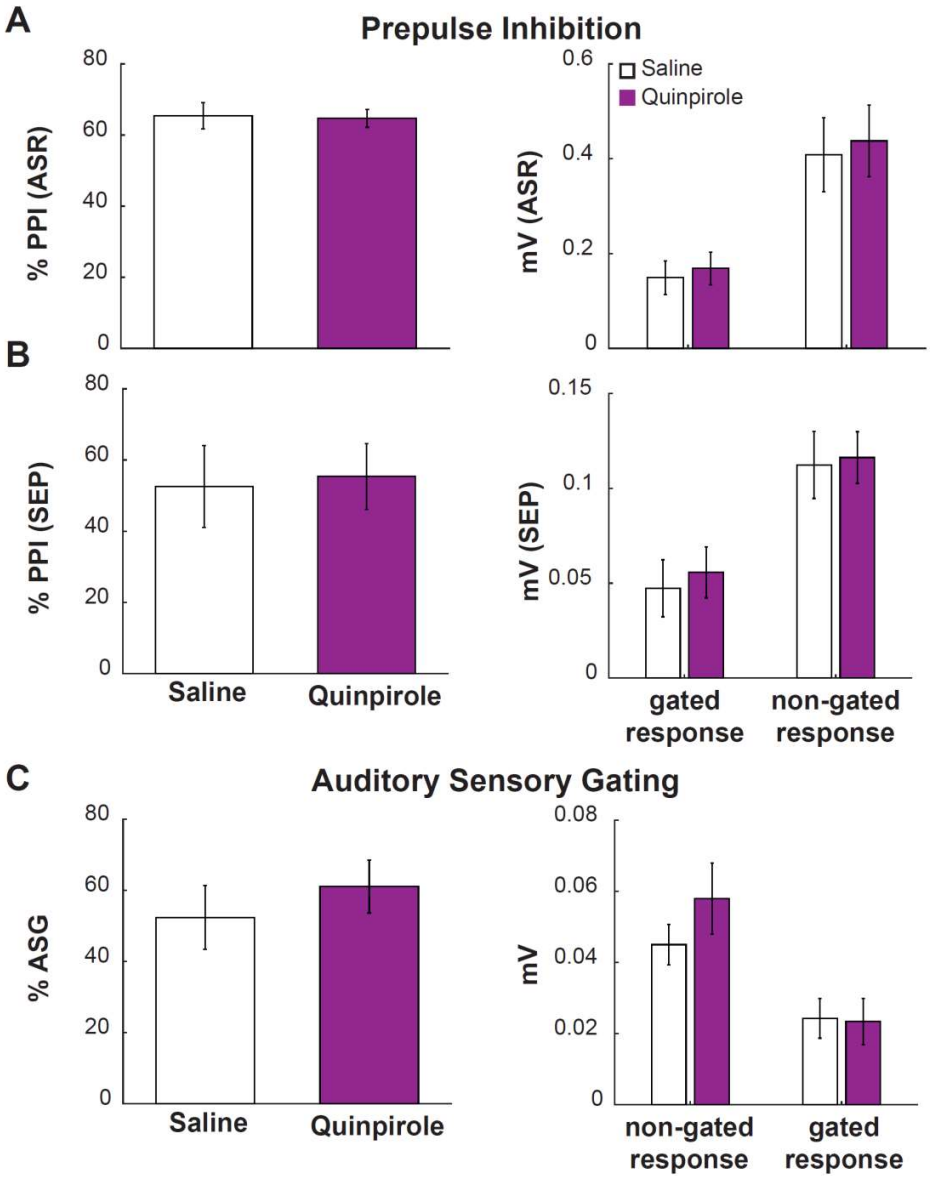

Figure 3.35: Sensory gating was not modulated after infusion of quinpirole into the ventral midbrain. Conventions are the same shown in Figure 3.33.

Together, pharmacological manipulation of the ventral midbrain only affected sensory gating when dopaminergic transmission to mPFC was reduced. Infusion of both clonidine and U69593 resulted in sensory gating deficits only at the neuronal level, while the ASR was not affected by any of the drugs. Observed sensory gating deficits appeared to have

different mechanisms: after infusion of clonidine, the gating effect of the prepulse was eliminated while after infusion of U69593, a shift in the balance of the amplitude of gated and non-gated SEP resulted in a decreased percentage of PPI as well as ASG. The latter, however, was not affected under clonidine condition. In conclusion, mPFC is essential in order to adequately extract biologically relevant sensory information but only when DA release in this brain structure is provided.

4. Discussion

4.1. Noradrenergic modulation of sensory processing in two functionally distinct cortical regions

The first part of this thesis aimed to resolve the question about how neuronal activity during functionally different sensory processing in primary sensory and higher association cortical areas is modulated by the catecholaminergic neuromodulator NE. Simultaneous recording of LFP and SUA in S1HL and mPFC under constant monitoring of LC neuronal activity enabled a direct comparison of spontaneous and sensory-evoked neuronal activity under identical experimental conditions.

4.1.1. Somatosensory stimulation addressed dermal nociceptors

Electrical transcutaneous stimulation into the hind paw with different stimulation parameters revealed several indicators suggesting that stimulation was of a nociceptive nature: 1) Unlike neuronal activity in LC and mPFC, response amplitude in S1HL was not dependent on stimulus intensity. Previous literature shows that amplitude modulation of neuronal activity in S1 was observed in response to innocuous somatosensory stimulation but as soon as peripheral A δ- or C-fibers were addressed by noxious somatosensory stimulation, neuronal activity responded with constant amplitude reporting the presence of the stimulation only[79]. 2) According to previous studies, LC noradrenergic neurons in rats under urethane anesthesia, like in the present study, only respond to noxious somatosensory stimulation[125,128-130]. 3) Cortical sensory-evoked responses emerged to be only excitatory. However, previous studies, examining the response profiles of neurons in the S1 and the

PFC to different strengths of stimulation, showed that the neurons are excited or inhibited to natural sensory stimulation[81,695,696]. Interestingly, particular strong or noxious sensory stimulation evoked exclusively excitatory response profiles[70,105,695]. 4) Finally, reported biphasic response profile in S1HL[84,92] as well as tonic sustained response in mPFC[70], resembling recorded profiles in response to electrical FS stimulation in the current study, has been observed to be characteristic for peripheral nociceptive stimulation. In conclusion, the somatosensory stimulation with the parameters used here was of noxious nature and, thus, sensory information was processed in brain structures belonging to the pain matrix[11-18].

4.1.2. Comparable effects between local and systemic clonidine administration suggests that reduced NE release mainly affected sensory processing in both cortical regions

Manipulation of the noradrenergic system was performed by local infusion of clonidine into LC and by systemic injection of clonidine. In response to either pharmacological manipulation, the spontaneous activity of LC noradrenergic neurons was decreased, as already demonstrated in previous studies[205,262,266,270,271,697]. The phasic excitation of LC neurons to peripheral FS stimulation, however, was differentially affected. Specifically, local injection of clonidine into LC expectedly decreased the phasic sensory-evoked response as demonstrated before[266] but, surprisingly, the response after systemic injection of clonidine was preserved. This effect might result from a selective action of clonidine on excitatory imidazoline-receptors on neurons in the PGi[698] which mediates the somatosensory response in LC[146,699]. Activation of imidazoline-receptors exerts additional excitatory drive on LC noradrenergic neurons[268,700] supposedly overwhelming the inhibitory action of clonidine on alpha 2-adrenoceptors within LC. Consequently, local somatodendritic LC inactivation suppressed tonic and phasic release of NE in LC terminal regions[132,266,269-271,701,702] but systemic injection of clonidine is expected to leave the phasic release intact. On the other hand, since clonidine is ubiquitously present after systemic injection, activation of inhibitory alpha 2-noradrenergic autoreceptors in the presynaptic membrane of LC afferents might inhibit terminal release of NE[488-491,688] despite phasic

activation of LC neurons. In the current study, the overall effects were mostly comparable between the two drug conditions albeit the global effects after systemic injection were regularly stronger than after local unilateral inhibition of LC activity. Therefore, a general deprivation of NE from the CNS by predominant actions on somatodendritic and terminal presynaptic alpha 2-noradrenergic autoreceptors is assumed.

4.1.3. Cortical NE deprivation activated ongoing cortical state in higher association cortex while deactivation was observed in primary sensory cortex

The main and most surprising result was an activation of the ongoing cortical activity state in mPFC after systemic injection of clonidine while ongoing cortical state in S1HL was expectedly deactivated after either pharmacological manipulation method. Naturally, the neuronal firing activity in LC is strongly related to behavioral state of vigilance in rats[170-173], cats[174] and monkeys[175]. Accordingly, noradrenergic neurons in LC are active during awake state and associated release of NE activates cortical state. Over the course of slow wave sleep, LC neuronal activity is decreased until it ceases during REM sleep. Consequently, artificial reduction of NE release by local LC inactivation or systemic activation of presynaptic alpha 2-autoreceptors is expected to induce cortical deactivation. Previous studies show that systemic injection of alpha 2-adrenoceptor agonists increases power in low frequency range[186], creates a slow wave sleep-like cortical state and induces resting behavior in animals[193-196] and humans[187-192]. Correspondingly, systemic treatment with alpha 2-adrenoceptor agonists is used in clinics as sedative and thus, to induce resting state[197-199]. In contrast to the present study, these effects were shown in non-anesthetized rats and humans. General anesthesia, however, is also known to induce a sleep-like state characterized by high amplitude-low frequency oscillation pattern[63-65] although urethane anesthesia is special by demonstrating spontaneous alternations of cortical activity between activated and deactivated state[66,67]. Therefore, urethane anesthesia resembles natural sleep via integration of REM-like cortical state activity. This was confirmed in the current study and, under this condition, systemic and intra-LC injection of clonidine induced expected

increase of power in medial frequency range with maximum effect in sleep-related Sigma frequency band, but only in S1HL.

4.1.4. Systemic injection of clonidine induced cortical activation in mPFC in favor of internal long-range cortico-cortical interaction

Prefrontal cortical state was activated after systemic clonidine administration, which was reflected in decreased power in SLO frequency band accompanied with an increase in power in Theta and Alpha frequency range. Power in SLO frequency band is usually associated with synchronized oscillation in Sigma frequency band and thus with a transition from awake to sleep state in animals[30,32] and humans[703]. Transition from slow wave sleep to REM sleep is characterized by activation of cortical state resembling awake state, however including muscle atonia, regular eye movements and dreaming[704,705]. In both sleep states, a deafferentation of the cortex is discussed in favor of an intrinsic thalamo-cortical, cortico-cortical and cortico-hippocampal information processing[27,37,706-710]. Increased power in Theta and Alpha frequency band might be beneficial for such interactions. Indeed, a close relationship between power in Theta and Alpha frequency band was reported in PFC[706], not only during Theta-related memory processes[711-713] but also during Alpha-related internal mental activities, for example meditation[714]. More specific, in non-awake condition, it was shown that power in Theta frequency band increases during REM sleep in humans[715,716] and rats[717]. During awake state, increased power in Theta frequency band was observed during performance of memory-related tasks in humans[711,718-721] and rats[722-725] or during experience of emotional memory in humans[726] and rodents[717,727]. Power in Alpha frequency band is commonly associated with internally directed cortical operations during the resting state in absence of sensory input[43-45] but it was also related to memory-related cognitive processes[711,728-731]. In summary, power in Theta and Alpha frequency range is increased during conditions requiring cortical state activation for internal cognitive processes related to memory functions in mPFC. Global actions on pre- and postsynaptic alpha 2-adrenoceptors by systemic clonidine injection, might promote these processes by uncoupling of the cortex from the outside world and enhancement of long-range

communication in Theta and Alpha frequency range with related structures outside of mPFC.

4.1.5. Power in Theta and Alpha frequency range in S1HL is modulated by cortical activity state in mPFC

Such a long-range interaction in Theta and Alpha frequency range was also indicated between mPFC and S1HL in the current study. This was observed during baseline condition after comparison of TCA in S1HL distinguished by effectiveness of cortical state activation in mPFC (TCA+ vs. TCA-). The analysis revealed, interestingly, that only power increase in high frequency range in S1HL was highly sensitive to sensory stimulation while modulation of spectral composition in low frequency range was dependent on effectiveness of FS stimulation in mPFC. In particular, a decrease of power in low frequency range was only significant when cortical state in mPFC was effectively activated in response to sensory stimulation. Thereby, BLP changes in Theta and Alpha frequency range differed significantly between conditions. Interestingly, a strong relationship of power in these two frequency bands between S1HL and mPFC was also observed during ongoing cortical state activity. Previous literature demonstrated long-range fronto-parietal or fronto-temporal interactions in Theta and Alpha frequency range during internal mental processing, i.e. top-down processing, in humans[712,726,728,732] while power in high frequency range is rather locally generated[26,712]. Alternatively, correlated power especially in low frequency range between mPFC and S1HL does not necessarily reflect functional coupling between the two brain regions but might result from so-called volume conduction. Accordingly, it is believed that low frequencies travel further through the neuronal tissue than high frequencies[26,733,734]. This is related to the commonly observed "1/f" power distribution of LFP, implying an inverse relation of the magnitude of LFP power to its temporal frequency[658-660] which was also observed in the present study. If, however, effects like volume conduction would lead to the cortico-cortical interactions in Theta and Alpha frequency bands observed here, then BLP in the lowest Delta frequency band would also be related between the two cortical regions.

Another possibility might be that a third structure modulates power in low frequency range in mPFC and S1HL in a similar manner. However, top-down modulation of S1 by higher brain areas in favor of accurate sensory perception has already been demonstrated before[735]. In conclusion, a top-down functional modulation of power in Theta and Alpha frequency range in S1HL by cortical activity state in mPFC can be assumed, while increase of power in high frequency range in response to sensory stimulation is regulated by local neuronal activation within the primary sensory region.

4.1.6. Sensitivity differences to sensory stimulation between S1HL and mPFC might functionally result from differences in neuronal excitability during ongoing cortical state

Activation of the cortical state in mPFC by systemic clonidine injection was additionally indicated by increased probability of TCA in response to electrical FS stimulation. Under drug-free baseline condition, significant neuronal activation in mPFC was only selectively evoked (as estimated on different neuronal levels such as TCA, SEP and SUA) even though the peripheral somatosensory stimulation was of noxious nature. In contrast, neuronal activity in S1HL was highly sensitive to somatosensory stimulation. In general, the decreased response sensitivity in mPFC in comparison to S1HL pyramidal neurons might result from lower power in medial frequency bands accompanied by lower single unit spontaneous firing rate. This indicates decreased baseline excitability in mPFC pyramidal neurons during ongoing cortical state under urethane anesthesia. A similar difference in neuronal excitability state between mPFC and primary visual cortex was reported in awake mice[65]. Anesthesia, however, induced a cortical state with contrasting oscillation pattern in comparison to the current study. Under isoflurane anesthesia, power in the frequency spectrum < 40 Hz in mPFC was higher compared to primary visual cortex[65]. Ketamine anesthesia induced a state in which BLP in prefrontal Beta and Gamma frequency bands was higher than in S1[64]. Nevertheless, spectral composition between primary sensory and prefrontal regions was never compared under urethane anesthesia which, as demonstrated, exhibits an incomparable physiological state to other commonly used anesthetics.

4.1.7. Reduction of cortical NE release induced responsiveness to sensory stimulation in initial mPFC TCA- cases while power in Sigma and Beta frequency bands was differentially modulated in S1HL and mPFC TCA+ cases

Sensory-related activation of mPFC was inversely related to cortical state activity during prestimulus interval under baseline condition. Consequently, TCA was evoked in about half of the cases when BLP in SLO frequency band was low, while cortical state in residual cases remained unaffected (TCA-) during high power in SLO frequency band. Hence, S1HL, which was reliably activated in response to noxious stimulation, detects and processes sensory input, irrespective of whether the system is active or not, however, for higher cognitive processing, the system has to active.

When the cortex was deprived from NE by either experimental manipulation, initial TCA- cases, unexpectedly, became activated in response to sensory stimulation albeit the spectral composition was different from the initial definition of TCA. Instead of significant decrease of power in Delta frequency band accompanied by a significant increase of power in Gamma frequency band, stimulus-induced cortical state activation under clonidine condition was represented by increased power in high frequency range only, while power in low frequency range was unaffected. In accordance with the general notion that power in Gamma frequency band is related to unit firing activity[26,680,681], initially non-responsive single units showed gating effects which were directly related to the stimulus-evoked increase in high frequency band.

Prefrontal TCA+ cases kept their responsiveness to sensory stimulation but their spectral composition was modulated. Specifically, stimulus-induced BLP change in Sigma and Beta frequency band was increased in mPFC under condition of systemic clonidine, which, interestingly, was just contrary to decreased BLP change in the same frequency bands in S1HL. Decrease of power in Sigma frequency range is associated with increased cortical state activation and, thus, indicates enhanced probability to process incoming noxious information although the ongoing cortical state is highly deactivated in S1HL. Accordingly, simultaneous increase of stimulus-related BLP change in Sigma frequency band in mPFC

suggested resting state processing and, thus, a lower priority in higher order processing of sensory stimuli. Together these results postulate that under anesthetized condition and along with using systemic alpha 2-adrenoceptor agonists, information about noxious sensory stimulation might still be able to access the system. However, this occurs without an interpretation of the biological meaning by processes in cognitive regions like mPFC. In short, the stimulation might be sensed but not perceived. On the other hand, cortical state activation of initially non-affected TCA- cases indicates enabled higher order cognitive processing of sensory stimulation in mPFC. Nonetheless, about modulation of sensory perception can be only speculated as experiments here were performed in anesthetized condition. Therefore, more research in non-anesthetized subjects is needed in order to explore whether noxious sensory stimulation is perceived under sedated condition. Noradrenergic modulation of stimulus-related BLP change in Beta frequency band was homologous to BLP change in Sigma frequency band in both cortical regions. Classically, power in Beta frequency band is related to sensorimotor functions and activation of the cortical state[48,49]. Synchronization in Beta frequency band was observed in response to voluntary, passive or imagined movements[736-740] as well as to movements which were induced by electrical muscle stimulation[737]. A muscle twitch of the foot was indeed observed in response to intradermal electrical FS stimulation which might have induced transient increase of power in Beta frequency band. However, homologous modulation of stimulus-related power change in sleep-related Sigma and activity-related Beta frequency band under condition of systemic clonidine is hard to interpret, especially on the background that the modulation in S1HL and mPFC is quite contrary to each other. On the other hand, homologous modulation of BLP in different frequency bands is not necessarily functionally related to each other. It is not uncommon that certain cortical regions engage in different neuronal interactions exhibiting distinct spectral profiles for local encoding and remote integrative functions[26,741-744].

4.1.8. Depletion of cortical NE release reduced SNR in S1HL while local network properties in mPFC were reorganized by redistribution of neuronal activity

Modulation of cortical activity state reflects only the net outcome of underlying voltage fluctuations during different experimental conditions. Further exploration of SEPs and SUA revealed that neuronal activity in mPFC was not generally activated by a decreased NE tone in LC target regions. Instead, affected neurons in mPFC showed a complex modulation pattern suggesting a drug-induced reorganization of activated neurons in the local network, thus resulting in a generally activated cortical state. Specifically, in addition to aforementioned gating effects in initially non-responsive single units, amplitude of sensory evoked responses in initially responsive single units was decreased after either pharmacological manipulation. Moreover, spontaneous activity was similarly bidirectionally modulated as already reported in previous work[227,245,247,252]. In contrast, NE in sensory regions is known to promote SNR by inhibition of spontaneous activity[228,229,240,661-663] and enhancement of synaptic excitation[228,229,236-239]. Accordingly, deprivation of NE in the brain resulted in decreased SNR and hence decreased neuronal responsiveness under condition of deactivated cortical state in S1HL.

The differential modulation of neuronal activity between S1HL and mPFC probably results from divergent receptor composition in the two cortical regions. Alpha 1-adrenoceptors are most prominent in PFC[225] while alpha 2-adrenoceptors are predominant in parietal and temporal cortical regions where sensory cortices are located [225,230,231]. Functionally, the latter was reflected in the stronger reduction of responsiveness in S1HL compared to mPFC after systemic injection of clonidine which acts on postsynaptic alpha 2-adrenoceptors. It therefore leads to a decrease in the excitability of the pyramidal neurons[256] in addition to presynaptic inhibition of NE release[488-491,688,701,745-748]. In mPFC, adequate activation of alpha 1-adrenoceptors is essential for cognitive functions in rodents, monkeys and humans[443,446-453]. It was shown that mPFC has a higher demand for NE[223,749], presumably because alpha 1-adrenoceptors exhibit a lower affinity than alpha 2-adrenoceptors[234]. During baseline conditions, this demand is covered by heterogeneously organized LC

projections and activity state of LC noradrenergic neurons[223], e.g. phasic NE release in response to salient stimuli or cognitive engagement[126,127,134]. Alpha 2-adrenoceptors are additionally expressed in PFC[225,230,231] which suggests that the bidirectional noradrenergic modulation of neuronal activity in mPFC results from different neuronal populations with distinct receptor properties. Consequently, postsynaptic activation of alpha 2-adrenoceptors reduces neuronal activity in one population, while actions on alpha 1-adrenoceptors enhance synaptic drive in another population. Accordingly, removal of NE from mPFC reorganized the local neuronal network activities by disinhibition due to missing actions on alpha 2-adrenoceptors and deactivation by missing actions on alpha 1-adrenoceptors in respective populations.

Beyond an apparent population-dependent noradrenergic modulation of single units, complex composition of functionally divergent networks in mPFC is reflected in the number of neuronal subpopulations, defined by different PSTH profiles in response to sensory stimulation. In contrast to S1HL, where two groups could be distinguished by whether or not a late response component was present, four groups were extracted in mPFC of which one was even merged out of intermixed profiles (group 3). Additionally, the SEP in S1HL was composed of clearly distinguishable response components which have been previously reported[2,80-85]. In comparison, a single merged voltage deflection was observed in mPFC, most likely integrated from incoming sensory information arising from multiple afferent structures[108,109]. Certainly, sensory-evoked responses in mPFC do not consist of a pure somatosensory component but a composition resulting from integrating information incoming from various structures of the limbic system. This is further suggested by the observed longer response latency of > 120 ms. Information flows from the medial part of the thalamus either directly to the mPFC[750] or indirectly via the Amygdala[68,751], the HPC[752], the Insula[750] or other structures of the limbic system[109,750] integrating the sensory aspect of the stimulus to higher cognitive components[109]. Processing of information between these different contributing networks might result in the different groups of prefrontal response profiles, which are merged into one single voltage deflection at the population level. This complex cortical population responsiveness to salient sensory stimulation in mPFC depends therefore on the afferent input and local organization of the cortical microcircuitry and NE

apparently orchestrates the network properties by suppression of irrelevant and accentuation of relevant information within the network. The aim would be to adequately evaluate the biological relevance of the stimulus and integrate complex properties of sensory information along with matching input from other, non-sensory brain structures in order to coordinate an appropriate behavioral outcome.

4.1.9. Neuronal responses to noxious stimulation are sustained by phasic NE release in cortical regions

A detailed observation of suppressive effects of noradrenergic manipulation on single unit responses to noxious stimulation noticeably revealed that systemic injection of clonidine reduced the entire response profile in the cortical regions under study. In contrast, local LC inactivation suppressed only the late response components in the two cortical structures. This might be attributed to, firstly the long response latency of LC noradrenergic neurons (~ 70 ms) in relation to the short latency phasic response component in S1HL (~ 20 ms). Secondly, this could be explained by the general delayed time course of LC mediated effects due to slow conduction velocity of thin, non-myelinated axons of catecholaminergic neurons and slow dynamics of NE release[753,754]. Accordingly, it was demonstrated that NE release in S1 in response to strong salient events occurs within a range of 100 – 350 ms[755]. Furthermore, priming phasic activation of LC neurons increased excitatory cortical neuronal responses to forepaw stimulation in S1 only with a long interstimulus interval of 200 – 300 ms[243]. These time windows are comparable to the modulation periods of the delayed response components in S1HL and mPFC single units after local injection of clonidine in the current study. Modulation of the late response components only, instead of entire response profiles, indicates dependency from phasic release of NE which results in a fourfold higher concentration of neuromodulator in cortical tissue compared to tonic release[134]. This concentration is effective to act on depolarizing, low-affinity alpha 1-noradrenergic receptors[234] in order to sustain sensory-evoked single unit activity in LC cortical target regions which has been previously demonstrated[246]. Amplification of stimulus-related neuronal activation by NE was additionally demonstrated by reduction of SEPs in mPFC TCA+ cases under condition of NE deprivation by systemic clonidine

injection. SEPs in TCA- cases were already of smaller magnitude during baseline condition. Given the background that the neuronal activity of LC noradrenergic neurons is directly related to the cortical activity state[170-173], this might be related to a decreased NE release when cortical state is more deactivated. Nevertheless, a further decrease of amplitude and magnitude was indicated in mPFC TCA- cases after local LC inactivation albeit not significantly. Confirmation of this effect together with examination of a functional relationship would be a potential subject to future studies.

4.2. Noradrenergic modulation of the midbrain dopaminergic system

4.2.1. Noradrenergic modulation of ventral midbrain spontaneous activity is dependent on localization of the recorded population within VTA

In addition to the LC noradrenergic system, neuronal activity in the midbrain dopaminergic VTA modulates neuronal activity in mPFC via the mesocortical DA system. Furthermore, it was shown that the VTA is engaged in salient sensory processing including nociceptive input[326-328,332,336,337,340,516-520]. When neuronal activity in LC was unilaterally inhibited in the current study, population spontaneous activity in ipsilateral VTA was bidirectionally modulated. Interestingly, this modulation was dependent on the localization of the recorded population within the VTA: MUA recordings which were performed in the anterior and lateral VTA demonstrated decreased spontaneous firing activity while in the posterior-medial VTA increased spontaneous firing was observed. Previous observations showed that dopaminergic neurons within the VTA reduced their firing activity and associated DA release in VTA target regions when the concentration of NE was enhanced by intra-VTA infusion of NE or systemic injection of selective NERI[496-498]. Accordingly, VTA dopaminergic neurons enhanced firing activity after lesion of LC[494,496], which was also demonstrated here in the population activity recorded from posterior-medial VTA after local LC inactivation. Nevertheless, this does not indicate that dopaminergic neurons are exclusively located in the posterior-medial VTA. In recent years, it was demonstrated that dopaminergic neurons in the VTA show less uniform properties than dopaminergic neurons in the SNc[307,756,757]. In fact, dopaminergic neurons in the VTA are very diverse in their

electrophysiological properties and molecular characteristics including receptor composition[758-762]. Additionally, the functional identity of VTA dopaminergic neurons depends on their afferent and efferent connectivity[761-764] which is related to dopaminergic modulation of behavioral functions[765]. It was specifically shown that reward and aversion are modulated by dopaminergic populations in the VTA with diverging electrophysiological and molecular properties[299,300,345,373,766]. Neurons from the laterodorsal tegmentum preferentially synapse on dopaminergic neurons within the VTA which project to the NAc and code for rewarding events. On the other hand, aversive events are processed in a pathway originating in neurons of the lateral Habenula which synapse on VTA dopaminergic neurons projecting to the mPFC. These meso-prefrontal dopaminergic neurons are located in the medio-posterior VTA[299,300,345,762] just like the neuronal populations which increased the spontaneous firing when LC neuronal activity was inhibited in the present study.

4.2.2. Phasic release of NE in VTA enhances sensory processing

Independent from localization within the VTA, the magnitude of the sensory-evoked multi unit response to noxious stimulation was suppressed when the noradrenergic transmission from LC was inhibited. This implies that NE in VTA is needed to reinforce sensory processing of VTA net outcome. Consequently, phasic release of both NE from LC[134,135,767] and DA from VTA[329-339] in response to noxious stimulation was reduced in the mutual target structure mPFC. Hence, the observed effects in the previous section most likely reflect synergistic modulation of prefrontal neuronal activity by catecholaminergic systems. Reduction of noradrenergic tone induced a reorganization of the neuronal activity in mPFC local networks which was reflected in bidirectional modulation of cortical activity state and SUA. A possible outcome of this modulation pattern might be the suppression of irrelevant and accentuation of relevant information, a brain function called Sensory Gating. Very early studies from the 1980s demonstrated that neurotoxic lesion of the dorsal noradrenergic bundle by local 6-OHDA infusion, which deprives the forebrain from NE but not DA, impairs the ability to ignore irrelevant stimuli in rats[158,768-770]. Sensory Gating deficits are, however, not only induced by suppression of NE release in frontal brain

regions but also by changes in neuronal activity of the mesocortical dopaminergic system. This is discussed in the next section.

4.3. Dopaminergic modulation of sensory gating

4.3.1. DA in mPFC is essential for adequate sensory gating

The importance of prefrontal DA release in modulation of PPI and ASG was explored by selective inhibition of DA release 1) in mPFC, 2) in VTA target structures besides mPFC or 3) all VTA target structures. This approach revealed that DA in mPFC is essential for adequate sensory gating. However, PPI was only modulated at the neuronal level while behavioral ASR remained unaffected. When DA release from VTA was generally suppressed in all VTA target structures, including mPFC, only PPI was impaired by decreased effectiveness of the prepulse. Selective reduction of DA release in mPFC impaired PPI as well as ASG by both a decreased effectiveness of the prepulse and decreased sensitivity to startle pulse alone. However, when DA release in mPFC was not manipulated, sensory gating was unaffected although several other limbic target structures (e.g. NAc, HPC, amygdala, …) were deprived from DA. Impaired PPI based on a hypodopaminergic state in mPFC has been reported before[580,602-605]. However, the effect was associated with a related top-down disinhibition of neuronal activity of prefrontal glutamatergic afferents to NAc or VTA[614-616]. This, consequently, increases extracellular DA release in NAc[607,614,621,622] and leads to sensory gating deficits[570,592-594]. According to previous literature, neuronal activity in mPFC is strongly associated with dopaminergic transmission in NAc[606-613] . This is why it can be assumed that a reduction of DA in NAc similarly impairs sensory gating, resulting in an inverted-U shaped dose-response function which is not uncommon in regards to mPFC functions[447,453,461,771]. In support, disruption of PPI after local infusion of dopaminergic D2-agonists into NAc[632,633] in addition to a contribution of dopaminergic autoreceptors[634], which reduce release of DA upon activation[369,377,590], was reported. Nevertheless, in the present study, reduction of accumbal DA did not affect sensory gating, neither PPI nor ASG.

In conclusion, under conditions of decreased dopaminergic transmission, top-down interactions from mPFC are critically involved in sensory gating deficits. Common neurophysiological disorders, which are associated with sensory gating deficits, are Parkinson's disease[772-775] or depression[776-778] and since both are related to hypodopaminergic states, the mPFC might be an adequate target for symptom-related therapy.

4.3.2. PPI and ASG might share neuronal mechanisms under certain conditions

Another interesting question, which was repeatedly discussed in previous literature, was whether PPI and ASG share similar neuronal mechanisms[551-554]. Brain functions related to both paradigms are disturbed in schizophrenic patients and share some pharmacological, methodological and neurobiological aspects[779-781].

It was shown earlier that inhibition of noradrenergic transmission reduces VTA sensory-evoked responses. Clonidine infusion into ventral midbrain might have similar effects by inhibition of NE release via actions on presynaptic α2-noradrenergic receptors[488-491,688,701,745-748]. Additionally, clonidine reduces spontaneous activity of neurons by post-synaptic effects[507,636]. Thus, the spontaneous and sensory-evoked activity in VTA is decreased which reduces the release of DA in all VTA target regions including mPFC. Consequently, prefrontal spontaneous and sensory-evoked activity is increased[247,782]. The increased spontaneous activity might mask the neuronal response to non-salient stimuli like the prepulse and, hence, reduces its effectiveness.

Infusion of κ-opioid agonist into the ventral midbrain additionally affected ASG in contrast to infusion of clonidine, after which only PPI was reduced. Thus, DA in mPFC seems to be critically important for ASG. Furthermore, the underlying mechanisms of PPI and ASG are slightly different. While presentation of the prepulse became ineffective when dopaminergic transmission to VTA target regions was generally reduced after clonidine infusion into the ventral midbrain, infusion of κ-opioid agonist changed the balance between prepulse effectiveness and sensitivity to startle stimulus only. Consequently, the ASR to the former was increased while the ASR to the latter was decreased, which,

together resulted in decreased PPI. Modulation of ASG was comparable suggesting common neuronal mechanisms for PPI and ASG when mPFC was selectively depleted of DA.

In conclusion, a general statement whether PPI and ASG share common mechanisms is difficult. However, it might be possible that under certain conditions, like selective reduction of dopaminergic transmission in mPFC, sensory gating mechanisms are comparable. In contrast, when dopaminergic transmission is generally reduced, mechanisms are different. At least in healthy human subjects and rats as well as after systemic injection of D_2-receptor agonists in humans and rats, differential mechanisms for PPI and ASG had been demonstrated[552,585,783]. Nevertheless, common mechanisms under specific conditions cannot be ruled out.

4.3.3. Inhibition of mPFC dopaminergic transmission affects only neuronal signals but not behavioral ASR

Observed sensory gating deficits after inhibition of DA release in mPFC affected only the neuronal PPI and ASG but not the behavioral ASR in case of PPI. Nevertheless, impaired PPI of the ASR was reported after local neurotoxic lesion of dopaminergic terminals in mPFC[602,603] or local infusion of D_1- or D_2-receptor antagonist into mPFC[580,604,605]. In the present study, the release of DA was manipulated at the somatodendritic level within the VTA. Nevertheless, there is no reason why the decrease of DA release in mPFC should notably differ between those methods. However, in the present study, the infusion of the drugs into the ventral midbrain was not performed continuously over the course of the sessions but > 2 minutes before presentation of the first sensory stimulation. Therefore, the observed effects might be weakened by washout of the drug which began already before the sessions started. A repetition of the experiments is therefore suggested under continuous infusion of the drugs over the entire duration of the sessions in order to ensure a constant drug concentration within the ventral midbrain.

4.4. Further methodological considerations

Major methodological consideration in the current work concerns the pharmacological manipulations of catecholaminergic systems by local drug infusions.

Local infusion of clonidine into LC, which was used in the first two studies of this work in order to explore the noradrenergic modulation of neuronal activity in S1HL, mPFC and VTA, was based on classical electrophysiological guidance by the distinctive activity pattern of noradrenergic neurons. This approach, however, does not provide any information about the detailed localization of the electrode within LC. In addition, the diffusion width of clonidine within the tissue can hardly be estimated. Therefore, neither an incomplete inhibition of the LC nucleus nor activation of alpha 2-adrenoceptors in structures outside of LC can be excluded. Based on previous literature, the closest structure expressing clonidine binding sites is the subcoeruleus nucleus adjacent to LC and the medial vestibular nucleus 200 µm apart from LC[231,784,785].

In preceding pilot experiments, the diffusion of clonidine in LC was visualized by chemical attachment of the fluorescent marker rhodamine to apraclonidine. Diffusion of this chemical compound in LC was confined to ~100 – 150 µm (Supplementary Figure 7.5). However, because of the much bigger molecule size, diffusion was not comparable to diffusion of clonidine alone[786-788]. In addition, iontophoretic injection of this chemical compound did not reliably inhibit neuronal activity in LC, presumably because iontophoretic transport becomes more difficult with larger molecules[789-791]. Therefore, unmarked clonidine was used for pharmacological manipulation during the experiments and the radius of drug diffusion was > 354 µm estimated by distant recordings from the infusion site. Therefore, it can be assumed that observed effects are induced by at least partial inhibition of LC neuronal activity.

Dopaminergic modulation of sensory Gating was explored by local drug infusion into the ventral midbrain. Restricted drug infusion within the VTA is very difficult because of other dopaminergic structures (e.g. SNc or retrorubral field) in direct vicinity. Therefore, pharmacological manipulation of indirect pathways in addition to direct mesocortical, mesoaccumbal and mesostriatal pathways cannot be excluded.

Furthermore, the manipulation of DA release was based on reported receptor composition on dopaminergic neurons within the VTA. However, this does not exclude that other types of neurons, e.g. glutamatergic or GABAergic neurons, in the heterogeneous VTA are affected by infused agonists. In conclusion, observed effects represent the net outcome of pharmacological manipulation in the ventral midbrain. On the other hand, dopaminergic neurons represent ~70 % of the VTA[310,312,315,318] and SNc is not majorly involved in sensory gating but in motor functions[291,295-297]. Thus, observed results might reflect a good approximation of ventral tegmental dopaminergic modulation of sensory gating.

4.5. Outlook and future studies

A direct comparison of sensory processing in S1HL and mPFC required utilizing stimulation parameters which reasonably activated neuronal populations in all recorded structures. However, under urethane anesthesia, neurons in LC, VTA and mPFC could only be reliably activated with high amplitude sensory stimulation which primarily activated the somatosensory pain system. The LC noradrenergic system is critically involved in modulation of pain-related sensory processing[15,792,793] and impairment of noradrenergic modulation of nociceptive stimuli lead to pathological pain experiences like hyperesthesia or neuropathic pain[794-798]. Nevertheless, it would be interesting to repeat the first two studies with presentation of innocuous physiological sensory stimulation in awake or naturally sleeping rats instead of noxious stimulation in urethane anesthetized animals. Furthermore, in the present work, the noradrenergic modulation of the VTA net sensory processing was explored. However, it would be especially interesting to disentangle observed net effects according to neuronal specificity. Detailed information about individual noradrenergic modulation of dopaminergic, GABAergic and glutamatergic neurons within the VTA might help to develop specific treatment of, for example, schizophrenia or depression.

Finally, an interesting observation in the current study was a convergence of sensory-evoked BLP change in Sigma and Beta frequency bands under condition of systemic clonidine injection. Specifically, BLP change in Sigma and Beta frequency bands increased in mPFC and decreased in S1HL (see section 3.1.4.2, Figure 3.19). However, during

baseline condition BLP change in the same frequency bands differed between the two cortical regions (see section 0 Figure 3.3). An interesting idea behind this observation would be whether systemic injection of clonidine increases Sigma and Beta frequency coherence between prefrontal and primary sensory regions and, if yes, whether and how this affects sensory processing during sedation.

5. Summary

In urethane anesthetized rats, when the cortex spontaneously alternates between an activated and a deactivated state, neuronal activity in S1HL and mPFC is responsive to noxious somatosensory stimulation, although the sensitivity differs between the two cortical regions. While sensory-evoked responses in mPFC are only evoked when LFP power in low frequency range is reduced and the cortical state is more activated, neuronal activity in S1HL is highly sensitive, apparently independent from cortical state activity. However, only stimulus-related increase of power in high frequency range is highly reliable in S1HL but decreased power in low frequency range, especially power in Theta and Alpha frequency bands, is dependent on the cortical activity state in mPFC. This dependency might reflect top-down interactions between these two cortical regions presumably in favor of memory-related processes not only during processing of noxious stimuli but also spontaneous activity.

Decreased sensitivity of prefrontal neuronal responsiveness in comparison with S1HL was also reflected in SEPs and SUA. In addition, single units in S1HL responded to FSs with maximum activation while responses in mPFC were tuned to stimulus strength implicating the functions of the respective cortical regions: Neurons in S1HL code for presence and maybe localization of noxious stimuli while neurons in mPFC reflect higher cognitive processing presumably with the aim to prevent the origin of noxious stimulation in the future.

NE in cortical regions is known to activate cortical state during arousal and increase the SNR of underlying single unit responses to sensory stimulation which was repeatedly demonstrated in primary sensory regions of the brain. Removal of NE from LC terminal regions therefore expectedly deactivated ongoing cortical activity state in S1HL resembling

sleep-like oscillation pattern while SNR of single unit responses to FSs was decreased. Ongoing cortical activity state in mPFC, however, was more activated. Spectral composition under noradrenergic deprivation suggested redistribution of spectral power in favor of internally directed long-range cognitive processing. Bidirectional modulation of spontaneous as well as sensory-evoked activity of underlying single unit activity in mPFC suggested a reorganization of active local networks. This reorganization is orchestrated by NE, presumably, in order to adequately evaluate the biological relevance of the stimulus and integrate sensory and non-sensory information.

Within the VTA, NE is required to improve noxious somatosensory processing. Hence, decreased sensory-evoked response after LC inactivation reduced phasic release of DA in addition to NE. Therefore, observed reorganization of local networks in mPFC results from synergistic actions of both catecholaminergic systems. A discussed possible outcome of catecholaminergic modulation of noxious somatosensory processing in mPFC includes enhanced sensory gating by suppression of irrelevant and accentuation of relevant network information. This prefrontal cortical function was specifically explored in the last study of this work, albeit restricted to modulation by the ventral midbrain dopaminergic system in awake rats. Specific manipulation of DA release in ventral midbrain target regions revealed that DA in mPFC is essential for both sensory gating paradigms: PPI and ASG although modulation appeared only on the neuronal level while the ASR was not affected. Previous reports discuss PPI deficits after manipulation of prefrontal neuronal activity as purely related to modulation of neuronal activity in NAc. In combination with present results, it is suggested that prefrontal DA is essential to ensure adequate prefronto-accumbal interactions which, in turn, are necessary for sensory gating.

Together, this work demonstrated that catecholamines are needed to improve sensory processing in functionally distinct cortical and subcortical brain regions. Thereby, classical improvement of SNR is not the only mechanism but also the catecholaminergic modulation of complex local network dynamics contributes to processing of relevant or irrelevant sensory information.

6. References

1. Georgopoulos, A.P. (1976). Functional properties of primary afferent units probably related to pain mechanisms in primate glabrous skin. *Journal of Neurophysiology*. **39**(1): p. 71-83.
2. Schouenborg, J., et al. (1986). Field potentials evoked in rat primary somatosensory cortex (SI) by impulses in cutaneous A beta- and C-fibres. *Brain Res*. **397**(1): p. 86-92.
3. Eccleston, C. (1995). The attentional control of pain: methodological and theoretical concerns. *Pain*. **63**(1): p. 3-10.
4. Eccleston, C. and G. Crombez (1999). Pain demands attention: a cognitive-affective model of the interruptive function of pain. *Psychol Bull*. **125**(3): p. 356-66.
5. Eccleston, C., et al. (1997). Attention and somatic awareness in chronic pain. *Pain*. **72**(1-2): p. 209-15.
6. Bowers, K.S. (1968). Pain, anxiety, and perceived control. *J Consult Clin Psychol*. **32**(5): p. 596-602.
7. Koyama, T., Y.Z. Tanaka, and A. Mikami (1998). Nociceptive neurons in the macaque anterior cingulate activate during anticipation of pain. *NeuroReport*. **9**(11): p. 2663-2667.
8. Porro, C.A., et al. (2002). Does anticipation of pain affect cortical nociceptive systems? *J Neurosci*. **22**(8): p. 3206-14.
9. Seifert, F., et al. (2013). Brain activity during sympathetic response in anticipation and experience of pain. *Human Brain Mapping*. **34**(8): p. 1768-1782.
10. Jackson, P.L., P. Rainville, and J. Decety (2006). To what extent do we share the pain of others? Insight from the neural bases of pain empathy. *Pain*. **125**(1-2): p. 5-9.
11. Ingvar, M. (1999). Pain and functional imaging. *Philosophical Transactions of the Royal Society of London. Series B: Biological Sciences*. **354**(1387): p. 1347-1358.
12. Almeida, T.F., S. Roizenblatt, and S. Tufik (2004). Afferent pain pathways: a neuroanatomical review. *Brain Res*. **1000**(1-2): p. 40-56.
13. Brooks, J. and I. Tracey (2005). From nociception to pain perception: imaging the spinal and supraspinal pathways. *J Anat*. **207**(1): p. 19-33.
14. Gauriau, C. and J.F. Bernard (2002). Pain pathways and parabrachial circuits in the rat. *Exp Physiol*. **87**(2): p. 251-8.
15. Pertovaara, A. (2006). Noradrenergic pain modulation. *Prog Neurobiol*. **80**(2): p. 53-83.
16. Sewards, T.V. and M.A. Sewards (2002). The medial pain system: Neural representations of the motivational aspect of pain. *Brain Research Bulletin*. **59**(3): p. 163-180.
17. Wang, J.Y., et al. (2004). Differential modulation of nociceptive neural responses in medial and lateral pain pathways by peripheral electrical stimulation: a multichannel recording study. *Brain Res*. **1014**(1-2): p. 197-208.
18. Willis, W.D. and K.N. Westlund (1997). Neuroanatomy of the pain system and of the pathways that modulate pain. *J Clin Neurophysiol*. **14**(1): p. 2-31.

19. Coghill, R.C., et al. (1994). Distributed processing of pain and vibration by the human brain. *J Neurosci*. **14**(7): p. 4095-108.
20. Kenshalo Jr, D.R. and W.D. Willis Jr (1991). The role of the cerebral cortex in pain sensation, in *Normal and altered states of function*. Springer. p. 153-212.
21. Melzack, R. and K.L. Casey (1968). Sensory, motivational and central control determinants of pain: a new conceptual model. *The skin senses*. **1**.
22. Price, D.D. and R. Dubner (1977). Neurons that subserve the sensory-discriminative aspects of pain. *Pain*. **3**(4): p. 307-38.
23. Treede, R.D., et al. (1999). The cortical representation of pain. *Pain*. **79**(2-3): p. 105-11.
24. Wang, J.Y., et al. (2003). Parallel pain processing in freely moving rats revealed by distributed neuron recording. *Brain Res*. **992**(2): p. 263-71.
25. Kajikawa, Y. and C.E. Schroeder (2011). How Local Is the Local Field Potential? *Neuron*. **72**(5): p. 847-858.
26. Buzsaki, G., C.A. Anastassiou, and C. Koch (2012). The origin of extracellular fields and currents--EEG, ECoG, LFP and spikes. *Nat Rev Neurosci*. **13**(6): p. 407-20.
27. Steriade, M. (1997). Synchronized activities of coupled oscillators in the cerebral cortex and thalamus at different levels of vigilance. *Cereb Cortex*. **7**(6): p. 583-604.
28. Schroeder, C.E. and P. Lakatos (2009). Low-frequency neuronal oscillations as instruments of sensory selection. *Trends in Neurosciences*. **32**(1): p. 9-18.
29. Niedermeyer, E. and F.H. Lopes da Silva (2005). Electroencephalography : basic principles, clinical applications, and related fields (5th ed.). Philadelphia: Lippincott Williams & Wilkins.
30. Steriade, M., et al. (1993). The slow (< 1 Hz) oscillation in reticular thalamic and thalamocortical neurons: scenario of sleep rhythm generation in interacting thalamic and neocortical networks. *J Neurosci*. **13**(8): p. 3284-99.
31. Steriade, M., A. Nunez, and F. Amzica (1993). A novel slow (< 1 Hz) oscillation of neocortical neurons in vivo: depolarizing and hyperpolarizing components. *J Neurosci*. **13**(8): p. 3252-65.
32. Steriade, M., A. Nunez, and F. Amzica (1993). Intracellular analysis of relations between the slow (< 1 Hz) neocortical oscillation and other sleep rhythms of the electroencephalogram. *J Neurosci*. **13**(8): p. 3266-83.
33. Gibbs, F.A. and E.L. Gibbs (1950). Atlas of electroencephalography (2d ed.). Cambridge, Mass.,: Addison-Wesley Press.
34. Loomis, A.L., E.N. Harvey, and G.A. Hobart (1938). Distribution of disturbance-patterns in the human electroencephalogram with special reference to sleep. *Journal of Neurophysiology*.
35. Kugler, J. (1981). Elektroenzephalographie in Klinik und Praxis: eine Einführung: Thieme.
36. Steriade, M., D. Contreras, and F. Amzica (1994). Synchronized sleep oscillations and their paroxysmal developments. *Trends Neurosci*. **17**(5): p. 199-208.
37. Steriade, M., D.A. McCormick, and T.J. Sejnowski (1993). Thalamocortical oscillations in the sleeping and aroused brain. *Science*. **262**(5134): p. 679-85.

38. Marshall, L., et al. (2006). Boosting slow oscillations during sleep potentiates memory. *Nature*. **444**(7119): p. 610-613.
39. Stickgold, R. (2005). Sleep-dependent memory consolidation. *Nature*. **437**(7063): p. 1272-1278.
40. Buzsaki, G. (2005). Theta rhythm of navigation: link between path integration and landmark navigation, episodic and semantic memory. *Hippocampus*. **15**(7): p. 827-40.
41. Siapas, A.G., E.V. Lubenov, and M.A. Wilson (2005). Prefrontal phase locking to hippocampal theta oscillations. *Neuron*. **46**(1): p. 141-51.
42. Sirota, A., et al. (2008). Entrainment of neocortical neurons and gamma oscillations by the hippocampal theta rhythm. *Neuron*. **60**(4): p. 683-97.
43. Berger, H. (1930). Über das Elektrenkephalogramm des Menschen. Zweite Mitteilung. *J Psychol Neurol*. **40**: p. 160-179.
44. Klimesch, W. (2012). alpha-band oscillations, attention, and controlled access to stored information. *Trends Cogn Sci*. **16**(12): p. 606-17.
45. Palva, S. and J.M. Palva (2007). New vistas for alpha-frequency band oscillations. *Trends Neurosci*. **30**(4): p. 150-8.
46. Pfurtscheller, G., et al. (2002). Contrasting behavior of beta event-related synchronization and somatosensory evoked potential after median nerve stimulation during finger manipulation in man. *Neurosci Lett*. **323**(2): p. 113-6.
47. Jurkiewicz, M.T., et al. (2006). Post-movement beta rebound is generated in motor cortex: Evidence from neuromagnetic recordings. *NeuroImage*. **32**(3): p. 1281-1289.
48. Engel, A.K. and P. Fries (2010). Beta-band oscillations - signalling the status quo? *Current Opinion in Neurobiology*. **20**(2): p. 156-165.
49. Pfurtscheller, G., A. Stancak, and C. Neuper (1996). Post-movement beta synchronization. A correlate of an idling motor area? *Electroencephalography and clinical neurophysiology*. **98**(4): p. 281-293.
50. Lalo, E., et al. (2007). Phasic increases in cortical beta activity are associated with alterations in sensory processing in the human. *Experimental brain research*. **177**(1): p. 137-145.
51. Basar-Eroglu, C., et al. (1996). Gamma-band responses in the brain: a short review of psychophysiological correlates and functional significance. *Int J Psychophysiol*. **24**(1-2): p. 101-12.
52. Ball, T., et al. (2008). Movement related activity in the high gamma range of the human EEG. *Neuroimage*. **41**(2): p. 302-10.
53. Gray, C.M. and W. Singer (1989). Stimulus-Specific Neuronal Oscillations in Orientation Columns of Cat Visual-Cortex. *Proceedings of the National Academy of Sciences of the United States of America*. **86**(5): p. 1698-1702.
54. Jia, X. and A. Kohn (2011). Gamma rhythms in the brain. *PLoS Biol*. **9**(4): p. e1001045.
55. Liu, J. and W.T. Newsome (2006). Local field potential in cortical area MT: stimulus tuning and behavioral correlations. *J Neurosci*. **26**(30): p. 7779-90.
56. Siegel, M., et al. (2007). High-frequency activity in human visual cortex is modulated by visual motion strength. *Cereb Cortex*. **17**(3): p. 732-41.

57. Jouny, C., F. Chapotot, and H. Merica (2000). EEG spectral activity during paradoxical sleep: further evidence for cognitive processing. *Neuroreport*. **11**(17): p. 3667-71.
58. Llinas, R. and U. Ribary (1993). Coherent 40-Hz oscillation characterizes dream state in humans. *Proc Natl Acad Sci U S A*. **90**(5): p. 2078-81.
59. Maloney, K.J., et al. (1997). High-frequency gamma electroencephalogram activity in association with sleep-wake states and spontaneous behaviors in the rat. *Neuroscience*. **76**(2): p. 541-55.
60. Llinas, R.R. and D. Pare (1991). Of dreaming and wakefulness. *Neuroscience*. **44**(3): p. 521-35.
61. Tung, A., et al. (2004). Recovery from sleep deprivation occurs during propofol anesthesia. *Anesthesiology*. **100**(6): p. 1419-26.
62. Alkire, M.T., et al. (1999). Functional brain imaging during anesthesia in humans: effects of halothane on global and regional cerebral glucose metabolism. *Anesthesiology*. **90**(3): p. 701-9.
63. Nelson, L.E., N.P. Franks, and M. Maze (2004). Rested and refreshed after anesthesia? Overlapping neurobiologic mechanisms of sleep and anesthesia. *Anesthesiology*. **100**(6): p. 1341-2.
64. Ruiz-Mejias, M., et al. (2011). Slow and fast rhythms generated in the cerebral cortex of the anesthetized mouse. *J Neurophysiol*. **106**(6): p. 2910-21.
65. Sellers, K.K., et al. (2013). Anesthesia differentially modulates spontaneous network dynamics by cortical area and layer. *J Neurophysiol*. **110**(12): p. 2739-51.
66. Clement, E.A., et al. (2008). Cyclic and Sleep-Like Spontaneous Alternations of Brain State Under Urethane Anaesthesia. *Plos One*. **3**(4).
67. Pagliardini, S., G.D. Funk, and C.T. Dickson (2013). Breathing and brain state: Urethane anesthesia as a model for natural sleep. *Respiratory Physiology & Neurobiology*. **188**(3): p. 324-332.
68. Onozawa, K., et al. (2011). Amygdala-prefrontal pathways and the dopamine system affect nociceptive responses in the prefrontal cortex. *BMC Neurosci*. **12**: p. 115.
69. Sogabe, S., et al. (2013). Mesocortical dopamine system modulates mechanical nociceptive responses recorded in the rat prefrontal cortex. *BMC Neurosci*. **14**: p. 65.
70. Zhang, R., et al. (2004). Response durations encode nociceptive stimulus intensity in the rat medial prefrontal cortex. *Neuroscience*. **125**(3): p. 777-85.
71. Brandt, M.E., B.H. Jansen, and J.P. Carbonari (1991). Pre-stimulus spectral EEG patterns and the visual evoked response. *Electroencephalogr Clin Neurophysiol*. **80**(1): p. 16-20.
72. Castro-Alamancos, M.A. (2004). Absence of rapid sensory adaptation in neocortex during information processing states. *Neuron*. **41**(3): p. 455-64.
73. Curto, C., et al. (2009). A simple model of cortical dynamics explains variability and state dependence of sensory responses in urethane-anesthetized auditory cortex. *J Neurosci*. **29**(34): p. 10600-12.
74. Barth, D.S. and S. Di (1990). Three-dimensional analysis of auditory-evoked potentials in rat neocortex. *J Neurophysiol*. **64**(5): p. 1527-36.

75. Di, S., C. Baumgartner, and D.S. Barth (1990). Laminar analysis of extracellular field potentials in rat vibrissa/barrel cortex. *J Neurophysiol*. **63**(4): p. 832-40.
76. Harris, K.D., et al. (2011). How do neurons work together? Lessons from auditory cortex. *Hear Res*. **271**(1-2): p. 37-53.
77. Sakata, S. and K.D. Harris (2009). Laminar structure of spontaneous and sensory-evoked population activity in auditory cortex. *Neuron*. **64**(3): p. 404-18.
78. Sukov, W. and D.S. Barth (1998). Three-dimensional analysis of spontaneous and thalamically evoked gamma oscillations in auditory cortex. *J Neurophysiol*. **79**(6): p. 2875-84.
79. Mark, R.F. and J. Steiner (1958). Cortical projection of impulses in myelinated cutaneous afferent nerve fibres of the cat. *J Physiol*. **142**(3): p. 544-62.
80. Chapin, J.K., S.M. Sorensen, and D.J. Woodward (1986). Acute ethanol effects on sensory responses of single units in the somatosensory cortex of rats during different behavioral states. *Pharmacology Biochemistry and Behavior*. **25**(3): p. 607-614.
81. Chapin, J.K., B.D. Waterhouse, and D.J. Woodward (1981). Differences in cutaneous sensory response properties of single somatosensory cortical neurons in awake and halothane anesthetized rats. *Brain Res Bull*. **6**(1): p. 63-70.
82. Shaw, F.Z., et al. (1999). Comparison of touch- and laser heat-evoked cortical field potentials in conscious rats. *Brain Res*. **824**(2): p. 183-96.
83. Shaw, F.Z., R.F. Chen, and C.T. Yen (2001). Dynamic changes of touch- and laser heat-evoked field potentials of primary somatosensory cortex in awake and pentobarbital-anesthetized rats. *Brain Res*. **911**(2): p. 105-15.
84. Sun, J.J., J.W. Yang, and B.C. Shyu (2006). Current source density analysis of laser heat-evoked intra-cortical field potentials in the primary somatosensory cortex of rats. *Neuroscience*. **140**(4): p. 1321-36.
85. Handwerker, H.O. and M. Zimmermann (1972). Cortical evoked responses upon selective stimulations of cutaneous group 3 fibers and the mediating spinal pathways. *Brain Res*. **36**(2): p. 437-40.
86. Alpsan, D. (1981). The effect of the selective activation of different peripheral nerve fiber groups on the somatosensory evoked potentials in the cat. *Electroencephalogr Clin Neurophysiol*. **51**(6): p. 589-98.
87. Devor, M., A. Carmon, and R. Frostig (1982). Primary afferent and spinal sensory neurons that respond to brief pulses of intense infrared laser radiation: a preliminary survey in rats. *Exp Neurol*. **76**(3): p. 483-94.
88. Bromm, B., M.T. Jahnke, and R.D. Treede (1984). Responses of human cutaneous afferents to CO2 laser stimuli causing pain. *Exp Brain Res*. **55**(1): p. 158-66.
89. Bromm, B. and R.D. Treede (1983). CO2 laser radiant heat pulses activate C nociceptors in man. *Pflugers Arch*. **399**(2): p. 155-6.
90. Jaw, F.S., et al. (2009). Cerebral columnar organization of the first nociceptive component induced by CO2 laser on the tail of the rat. *Neuroscience*. **158**(2): p. 945-50.
91. Kalliomaki, J., et al. (1993). Nociceptive C fibre input to the primary somatosensory cortex (SI). A field potential study in the rat. *Brain Res*. **622**(1-2): p. 262-70.

92. Tsai, M.L., et al. (2004). Differential morphine effects on short- and long-latency laser-evoked cortical responses in the rat. *Pain*. **110**(3): p. 665-74.
93. Johansen, J.P., H.L. Fields, and B.H. Manning (2001). The affective component of pain in rodents: direct evidence for a contribution of the anterior cingulate cortex. *Proc Natl Acad Sci U S A*. **98**(14): p. 8077-82.
94. Kuo, C.C. and C.T. Yen (2005). Comparison of anterior cingulate and primary somatosensory neuronal responses to noxious laser-heat stimuli in conscious, behaving rats. *J Neurophysiol*. **94**(3): p. 1825-36.
95. Yang, J.W., H.C. Shih, and B.C. Shyu (2006). Intracortical circuits in rat anterior cingulate cortex are activated by nociceptive inputs mediated by medial thalamus. *J Neurophysiol*. **96**(6): p. 3409-22.
96. Casey, K.L. (1999). Forebrain mechanisms of nociception and pain: analysis through imaging. *Proc Natl Acad Sci U S A*. **96**(14): p. 7668-74.
97. Casey, K.L., et al. (1994). Positron emission tomographic analysis of cerebral structures activated specifically by repetitive noxious heat stimuli. *J Neurophysiol*. **71**(2): p. 802-7.
98. Craig, A.D., et al. (1996). Functional imaging of an illusion of pain. *Nature*. **384**(6606): p. 258-60.
99. Davis, K.D., et al. (1995). fMRI of human somatosensory and cingulate cortex during painful electrical nerve stimulation. *Neuroreport*. **7**(1): p. 321-5.
100. Vogt, B.A., S. Derbyshire, and A.K. Jones (1996). Pain processing in four regions of human cingulate cortex localized with co-registered PET and MR imaging. *Eur J Neurosci*. **8**(7): p. 1461-73.
101. Derbyshire, S.W., et al. (1997). Pain processing during three levels of noxious stimulation produces differential patterns of central activity. *Pain*. **73**(3): p. 431-45.
102. Pereira, A.C.D. (2012). The role of the medial Prefrontal Cortex in nociception: functional characterization of Prelimbic and Infralimbic nuclei.
103. Talbot, J.D., et al. (1991). Multiple representations of pain in human cerebral cortex. *Science*. **251**(4999): p. 1355-8.
104. Yamamura, H., et al. (1996). Morphological and electrophysiological properties of ACCx nociceptive neurons in rats. *Brain Res*. **735**(1): p. 83-92.
105. Nogueira, L. and A. Lavin (2010). Strong somatic stimulation differentially regulates the firing properties of prefrontal cortex neurons. *Brain Res*. **1351**: p. 57-63.
106. Qiao, Z.M., et al. (2008). Dynamic processing of nociception in cortical network in conscious rats: a laser-evoked field potential study. *Cell Mol Neurobiol*. **28**(5): p. 671-87.
107. Tanaka, E., et al. (2008). A transition from unimodal to multimodal activations in four sensory modalities in humans: an electrophysiological study. *BMC Neurosci*. **9**: p. 116.
108. Groenewegen, H.J. and H.B. Uylings (2000). The prefrontal cortex and the integration of sensory, limbic and autonomic information. *Prog Brain Res*. **126**: p. 3-28.
109. Price, D.D. (2000). Psychological and neural mechanisms of the affective dimension of pain. *Science*. **288**(5472): p. 1769-72.

110. Dalley, J.W., R.N. Cardinal, and T.W. Robbins (2004). Prefrontal executive and cognitive functions in rodents: neural and neurochemical substrates. *Neurosci Biobehav Rev*. **28**(7): p. 771-84.
111. Heidbreder, C.A. and H.J. Groenewegen (2003). The medial prefrontal cortex in the rat: evidence for a dorso-ventral distinction based upon functional and anatomical characteristics. *Neurosci Biobehav Rev*. **27**(6): p. 555-79.
112. Kandel, E.R. and J.H. Schwartz (2000). Principles of neural science (4th ed.). Stamford, Conn.: Appleton & Lange.
113. Barchas, J.D., et al. (1978). Behavioral neurochemistry: neuroregulators and behavioral states. *Science*. **200**(4344): p. 964-73.
114. Dahlstroem, A. and K. Fuxe (1964). Evidence for the Existence of Monoamine-Containing Neurons in the Central Nervous System. I. Demonstration of Monoamines in the Cell Bodies of Brain Stem Neurons. *Acta Physiol Scand Suppl*. p. SUPPL 232:1-55.
115. Ohm, T.G., C. Busch, and J. Bohl (1997). Unbiased Estimation of Neuronal Numbers in the Human Nucleus Coeruleus during Aging. *Neurobiology of Aging*. **18**(4): p. 393-399.
116. Swanson, L.W. (1976). The locus coeruleus: a cytoarchitectonic, Golgi and immunohistochemical study in the albino rat. *Brain Res*. **110**(1): p. 39-56.
117. Moore, R.Y. and F.E. Bloom (1979). Central catecholamine neuron systems: anatomy and physiology of the norepinephrine and epinephrine systems. *Annu Rev Neurosci*. **2**: p. 113-68.
118. Grzanna, R. and M.E. Molliver (1980). The locus coeruleus in the rat: An immunohistochemical delineation. *Neuroscience*. **5**(1): p. 21-40.
119. Jones, B.E. and R.Y. Moore (1977). Ascending projections of the locus coeruleus in the rat. II. Autoradiographic study. *Brain Res*. **127**(1): p. 25-53.
120. Jones, B.E. and T. Yang (1985). The efferent projections from the reticular formation and the locus coeruleus studied by anterograde and retrograde axonal transport in the rat. *The Journal of Comparative Neurology*. **242**(1): p. 56-92.
121. Kobayashi, R.M., et al. (1974). Biochemical mapping of noradrenergic nerves arising from the rat locus coeruleus. *Brain Res*. **77**(2): p. 269-79.
122. Pickel, V.M., M. Segal, and F.E. Bloom (1974). A radioautographic study of the efferent pathways of the nucleus locus coeruleus. *J Comp Neurol*. **155**(1): p. 15-42.
123. Swanson, L.W. and B.K. Hartman (1975). The central adrenergic system. An immunofluorescence study of the location of cell bodies and their efferent connections in the rat utilizing dopamine-B-hydroxylase as a marker. *Journal of Comparative Neurology*. **163**(4): p. 467-505.
124. Faiers, A.A. and G.J. Mogenson (1976). Electrophysiological identification of neurons in locus coeruleus. *Exp Neurol*. **53**(1): p. 254-66.
125. Korf, J., B.S. Bunney, and G.K. Aghajanian (1974). Noradrenergic neurons: morphine inhibition of spontaneous activity. *Eur J Pharmacol*. **25**(2): p. 165-9.
126. Jodo, E., C. Chiang, and G. Aston-Jones (1998). Potent excitatory influence of prefrontal cortex activity on noradrenergic locus coeruleus neurons. *Neuroscience*. **83**(1): p. 63-79.

127. Aston-Jones, G., et al. (1991). Afferent regulation of locus coeruleus neurons: anatomy, physiology and pharmacology. *Prog Brain Res*. **88**: p. 47-75.
128. Aston-Jones, G., S.L. Foote, and F.E. Bloom (1982). Low doses of ethanol disrupt sensory responses of brain noradrenergic neurones.
129. Cedarbaum, J.M. and G.K. Aghajanian (1978). Activation of locus coeruleus neurons by peripheral stimuli: modulation by a collateral inhibitory mechanism. *Life Sci*. **23**(13): p. 1383-92.
130. Takigawa, M. and G.J. Mogenson (1977). A study of inputs to antidromically identified neurons of the locus coeruleus. *Brain Res*. **135**(2): p. 217-30.
131. Berridge, C.W. and E.D. Abercrombie (1999). Relationship between locus coeruleus discharge rates and rates of norepinephrine release within neocortex as assessed by in vivo microdialysis. *Neuroscience*. **93**(4): p. 1263-70.
132. Kawahara, Y., H. Kawahara, and B.H. Westerink (1999). Tonic regulation of the activity of noradrenergic neurons in the locus coeruleus of the conscious rat studied by dual-probe microdialysis. *Brain Res*. **823**(1-2): p. 42-8.
133. Devilbiss, D.M., M.E. Page, and B.D. Waterhouse (2006). Locus ceruleus regulates sensory encoding by neurons and networks in waking animals. *J Neurosci*. **26**(39): p. 9860-72.
134. Florin-Lechner, S.M., et al. (1996). Enhanced norepinephrine release in prefrontal cortex with burst stimulation of the locus coeruleus. *Brain Research*. **742**(1–2): p. 89-97.
135. Korf, J., G.K. Aghajanian, and R.H. Roth (1973). Stimulation and destruction of the locus coeruleus: Opposite effects on 3-methoxy-4-hydroxyphenylglycol sulfate levels in the rat cerebral cortex. *European Journal of Pharmacology*. **21**(3): p. 305-310.
136. Gresch, P.J., et al. (1994). Stress-induced sensitization of dopamine and norepinephrine efflux in medial prefrontal cortex of the rat. *J Neurochem*. **63**(2): p. 575-83.
137. Korf, J., G.K. Aghajanian, and R.H. Roth (1973). Increased turnover of norepinephrine in the rat cerebral cortex during stress: Role of the locus coeruleus. *Neuropharmacology*. **12**(10): p. 933-938.
138. Aston-Jones, G., et al. (1986). The brain nucleus locus coeruleus: restricted afferent control of a broad efferent network. *Science*. **234**(4777): p. 734-7.
139. Brodal, A. (1983). The perihypoglossal nuclei in the macaque monkey and thechimpanzee. *Journal of Comparative Neurology*. **218**(3): p. 257-269.
140. McCrea, R.A. and R. Baker (1985). Anatomical connections of the nucleus prepositus of the cat. *Journal of Comparative Neurology*. **237**(3): p. 377-407.
141. Andrezik, J.A., V. Chan-Palay, and S.L. Palay (1981). The nucleus paragigantocellularis lateralis in the rat. Demonstration of afferents by the retrograde transport of horseradish peroxidase. *Anat Embryol (Berl)*. **161**(4): p. 373-90.
142. Van Bockstaele, E.J., V.A. Pieribone, and G. Aston-Jones (1989). Diverse afferents converge on the nucleus paragigantocellularis in the rat ventrolateral medulla: retrograde and anterograde tracing studies. *J Comp Neurol*. **290**(4): p. 561-84.

143. Andrezik, J.A., V. Chan-Palay, and S.L. Palay (1981). The nucleus paragigantocellularis lateralis in the rat. *Anatomy and Embryology*. **161**(4): p. 373-390.
144. Van Bockstaele, E.J., H. Akaoka, and G. Aston-Jones (1993). Brainstem afferents to the rostral (juxtafacial) nucleus paragigantocellularis: integration of exteroceptive and interoceptive sensory inputs in the ventral tegmentum. *Brain Research*. **603**(1): p. 1-18.
145. Van Bockstaele, E.J. and G. Aston-Jones (1995). Integration in the Ventral Medulla and Coordination of Sympathetic, Pain and Arousal Functions. *Clinical and Experimental Hypertension*. **17**(1-2): p. 153-165.
146. Chiang, C. and G. Aston-Jones (1993). Response of locus coeruleus neurons to footshock stimulation is mediated by neurons in the rostral ventral medulla. *Neuroscience*. **53**(3): p. 705-15.
147. Hirata, H. and G. Aston-Jones (1994). A novel long-latency response of locus coeruleus neurons to noxious stimuli: mediation by peripheral C-fibers. *J Neurophysiol*. **71**(5): p. 1752-61.
148. Fuxe, K., B. Hamberger, and T. Hokfelt (1968). Distribution of noradrenaline nerve terminals in cortical areas of the rat. *Brain Res*. **8**(1): p. 125-31.
149. Aghajanian, G.K., J.M. Cedarbaum, and R.Y. Wang (1977). Evidence for norepinephrine-mediated collateral inhibition of locus coeruleus neurons. *Brain Res*. **136**(3): p. 570-7.
150. Guyenet, P.G. (1980). The coeruleospinal noradrenergic neurons: Anatomical and electrophysiological studies in the rat. *Brain Research*. **189**(1): p. 121-133.
151. Descarries, L., P. Séguéla, and K.C. Watkins (1991). Nonjunctional relationships of monoamine axon terminals in the cerebral cortex of adult rat, in *Volume transmission in the brain: novel mechanisms for neural transmission*. Raven Press New York. p. 53-62.
152. Descarries, L., K.C. Watkins, and Y. Lapierre (1977). Noradrenergic axon terminals in the cerebral cortex of rat. III. Topometric ultrastructural analysis. *Brain Res*. **133**(2): p. 197-222.
153. Molliver, M.E., et al. (1982). Monoamine systems in the cerebral cortex. *Cytochemical Methods in Neuroanatomy*. **1**: p. 255-277.
154. Berthelsen, S. and W.A. Pettinger (1977). A functional basis for classification of alpha-adrenergic receptors. *Life Sci*. **21**(5): p. 595-606.
155. Langer, S.Z. (1974). Presynaptic regulation of catecholamine release. *Biochem Pharmacol*. **23**(13): p. 1793-800.
156. U'Prichard, D.C. and S.H. Snyder (1979). Distinct α-noradrenergic receptors differentiated by binding and physiological relationships. *Life Sciences*. **24**(1): p. 79-88.
157. Duman, R.S. and E.J. Nestler (1995). Signal transduction pathways for catecholamine receptors (Vol. 303): Raven Press, New York.
158. Mason, S.T. (1980). Noradrenaline and selective attention: a review of the model and the evidence. *Life Sciences*. **27**(8): p. 617-631.
159. Robbins, T.W. (1984). Cortical noradrenaline, attention and arousal. *Psychol Med*. **14**(1): p. 13-21.

160. Berridge, C.W. and B.D. Waterhouse (2003). The locus coeruleus-noradrenergic system: modulation of behavioral state and state-dependent cognitive processes. *Brain Res Brain Res Rev*. **42**(1): p. 33-84.
161. Foote, S.L., et al. (1991). Electrophysiological evidence for the involvement of the locus coeruleus in alerting, orienting, and attending. *Prog Brain Res*. **88**: p. 521-32.
162. Sara, S.J. and S. Bouret (2012). Orienting and reorienting: the locus coeruleus mediates cognition through arousal. *Neuron*. **76**(1): p. 130-41.
163. Valentino, R.J. and A.L. Curtis (1991). Pharmacology of locus coeruleus spontaneous and sensory-evoked activity. *Prog Brain Res*. **88**: p. 249-56.
164. Harley, C. (1991). Noradrenergic and locus coeruleus modulation of the perforant path-evoked potential in rat dentate gyrus supports a role for the locus coeruleus in attentional and memorial processes. *Prog Brain Res*. **88**: p. 307-21.
165. Sara, S.J. (2015). Locus Coeruleus in time with the making of memories. *Curr Opin Neurobiol*. **35**: p. 87-94.
166. Sara, S.J., A. Vankov, and A. Herve (1994). Locus coeruleus-evoked responses in behaving rats: a clue to the role of noradrenaline in memory. *Brain Res Bull*. **35**(5-6): p. 457-65.
167. Aston-Jones, G., C. Chiang, and T. Alexinsky (1991). Discharge of noradrenergic locus coeruleus neurons in behaving rats and monkeys suggests a role in vigilance. *Prog Brain Res*. **88**: p. 501-20.
168. Berridge, C.W. (2008). Noradrenergic modulation of arousal. *Brain Res Rev*. **58**(1): p. 1-17.
169. Berridge, C.W., B.E. Schmeichel, and R.A. Espana (2012). Noradrenergic modulation of wakefulness/arousal. *Sleep Med Rev*. **16**(2): p. 187-97.
170. Aston-Jones, G. and F.E. Bloom (1981). Activity of norepinephrine-containing locus coeruleus neurons in behaving rats anticipates fluctuations in the sleep-waking cycle. *The Journal of Neuroscience*. **1**(8): p. 876-886.
171. Chu, N.-s. and F.E. Bloom (1973). Norepinephrine-Containing Neurons: Changes in Spontaneous Discharge Patterns during Sleeping and Waking. *Science*. **179**(4076): p. 908-910.
172. Foote, S.L., G. Aston-Jones, and F.E. Bloom (1980). Impulse activity of locus coeruleus neurons in awake rats and monkeys is a function of sensory stimulation and arousal. *Proc Natl Acad Sci U S A*. **77**(5): p. 3033-7.
173. Jones, B.E., et al. (1973). The effect of lesions of catecholamine-containing neurons upon monoamine content of the brain and EEG and behavioral waking in the cat. *Brain Research*. **58**(1): p. 157-177.
174. Hobson, J.A., R.W. McCarley, and P.W. Wyzinski (1975). Sleep cycle oscillation: reciprocal discharge by two brainstem neuronal groups. *Science*. **189**(4196): p. 55-8.
175. Rajkowski, J., P. Kubiak, and G. Aston-Jones (1994). Locus coeruleus activity in monkey: Phasic and tonic changes are associated with altered vigilance. *Brain Research Bulletin*. **35**(5–6): p. 607-616.
176. Eschenko, O., et al. (2012). Noradrenergic Neurons of the Locus Coeruleus Are Phase Locked to Cortical Up-Down States during Sleep. *Cerebral Cortex*. **22**(2): p. 426-435.

177. Safaai, H., et al. (2015). Modeling the effect of locus coeruleus firing on cortical state dynamics and single-trial sensory processing. *Proc Natl Acad Sci U S A*. **112**(41): p. 12834-9.
178. Berridge, C.W. and R.A. Espana (2000). Synergistic sedative effects of noradrenergic alpha(1)- and beta-receptor blockade on forebrain electroencephalographic and behavioral indices. *Neuroscience*. **99**(3): p. 495-505.
179. Berridge, C.W. and S.L. Foote (1991). Effects of locus coeruleus activation on electroencephalographic activity in neocortex and hippocampus. *J Neurosci*. **11**(10): p. 3135-45.
180. Berridge, C.W. and S.L. Foote (1994). Locus coeruleus-induced modulation of forebrain electroencephalographic (EEG) state in halothane-anesthetized rat. *Brain Res Bull*. **35**(5-6): p. 597-605.
181. Carter, M.E., et al. (2010). Tuning arousal with optogenetic modulation of locus coeruleus neurons. *Nat Neurosci*. **13**(12): p. 1526-33.
182. Kim, J.H., et al. (2016). Selectivity of Neuromodulatory Projections from the Basal Forebrain and Locus Ceruleus to Primary Sensory Cortices. *J Neurosci*. **36**(19): p. 5314-27.
183. Berridge, C.W., et al. (1993). Effects of locus coeruleus inactivation on electroencephalographic activity in neocortex and hippocampus. *Neuroscience*. **55**(2): p. 381-93.
184. De Sarro, G.B., et al. (1987). Evidence that locus coeruleus is the site where clonidine and drugs acting at alpha 1- and alpha 2-adrenoceptors affect sleep and arousal mechanisms. *Br J Pharmacol*. **90**(4): p. 675-85.
185. de Sarro, G.B., et al. (1988). Microinfusion of clonidine and yohimbine into locus coeruleus alters EEG power spectrum: effects of aging and reversal by phosphatidylserine. *Br J Pharmacol*. **95**(4): p. 1278-86.
186. Sebban, C., et al. (1999). Changes in EEG spectral power in the prefrontal cortex of conscious rats elicited by drugs interacting with dopaminergic and noradrenergic transmission. *Br J Pharmacol*. **128**(5): p. 1045-54.
187. Aho, M., et al. (1993). Comparison of dexmedetomidine and midazolam sedation and antagonism of dexmedetomidine with atipamezole. *Journal of Clinical Anesthesia*. **5**(3): p. 194-203.
188. Belleville, J.P., et al. (1992). Effects of intravenous dexmedetomidine in humans. I. Sedation, ventilation, and metabolic rate. *Anesthesiology*. **77**(6): p. 1125-1133.
189. Gabriel, J.S. and V. Gordin (2001). Alpha 2 agonists in regional anesthesia and analgesia. *Current Opinion in Anesthesiology*. **14**(6): p. 751-753.
190. Khan, Z.P., C.N. Ferguson, and R.M. Jones (1999). Alpha-2 and imidazoline receptor agonistsTheir pharmacology and therapeutic role. *Anaesthesia*. **54**(2): p. 146-165.
191. Mantz, J. (2000). Alpha2-adrenoceptor agonists: analgesia, sedation, anxiolysis, haemodynamics, respiratory function and weaning. *Best Practice & Research Clinical Anaesthesiology*. **14**(2): p. 433-448.
192. Martin, E., et al. (2003). The Role of the α2-Adrenoceptor Agonist Dexmedetomidine in Postsurgical Sedation in the Intensive Care Unit. *Journal of Intensive Care Medicine*. **18**(1): p. 29-41.

193. Buerkle, H. and T.L. Yaksh (1998). Pharmacological evidence for different alpha 2-adrenergic receptor sites mediating analgesia and sedation in the rat. *British Journal of Anaesthesia*. **81**(2): p. 208-215.
194. Cullen, L.K. (1996). Medetomidine sedation in dogs and cats:A review of its pharmacology, antagonism and dose. *British Veterinary Journal*. **152**(5): p. 519-535.
195. Dowlatshahi, P. and T.L. Yaksh (1997). Differential effects of two intraventricularly injected alpha 2 agonists, ST-91 and dexmedetomidine, on electroencephalogram, feeding, and electromyogram. *Anesth Analg*. **84**(1): p. 133-8.
196. Virtanen, R. (1988). Pharmacological profiles of medetomidine and its antagonist, atipamezole. *Acta veterinaria Scandinavica. Supplementum*. **85**: p. 29-37.
197. Maze, M., C. Scarfini, and F. Cavaliere (2001). New agents for sedation in the intensive care unit. *Crit Care Clin*. **17**(4): p. 881-97.
198. Venn, R.M., et al. (1999). Preliminary UK experience of dexmedetomidine, a novel agent for postoperative sedation in the intensive care unit. *Anaesthesia*. **54**(12): p. 1136-1142.
199. Wanat, M., et al. (2014). Comparison of dexmedetomidine versus propofol for sedation in mechanically ventilated patients after cardiovascular surgery. *Methodist Debakey Cardiovasc J*. **10**(2): p. 111-7.
200. Jones, B.E. (2003). Arousal systems. *Front Biosci*. **8**: p. s438-51.
201. Lee, S. and Y. Dan (2012). Neuromodulation of Brain States. *Neuron*. **76**(1): p. 209-222.
202. Samuels, E.R. and E. Szabadi (2008). Functional neuroanatomy of the noradrenergic locus coeruleus: its roles in the regulation of arousal and autonomic function part II: physiological and pharmacological manipulations and pathological alterations of locus coeruleus activity in humans. *Curr Neuropharmacol*. **6**(3): p. 254-85.
203. Ishimatsu, M. and J.T. Williams (1996). Synchronous activity in locus coeruleus results from dendritic interactions in pericoerulear regions. *Journal of Neuroscience*. **16**(16): p. 5196-5204.
204. Crawley, J.N., J.W. Maas, and R.H. Roth (1980). Biochemical evidence for simultaneous activation of multiple locus coeruleus efferents. *Life Sci*. **26**(17): p. 1373-8.
205. Svensson, T.H., B.S. Bunney, and G.K. Aghajanian (1975). Inhibition of both noradrenergic and serotonergic neurons in brain by the alpha-adrenergic agonist clonidine. *Brain Res*. **92**(2): p. 291-306.
206. Fuxe, K., et al. (1978). Mapping out central catecholamine neurons: immunohistochemical studies on catecholamine-synthesizing enzymes, in *Psychopharmacology: A Generation of Progress*. Raven Press New York. p. 67-94.
207. Hokfelt, T., et al. (1977). Immunohistochemical studies on the localization and distribution of monoamine neuron systems in the rat brain II. Tyrosine hydroxylase in the telencephalon. *Med Biol*. **55**(1): p. 21-40.
208. Levitt, P. and R.Y. Moore (1978). Noradrenaline neuron innervation of the neocortex in the rat. *Brain Res*. **139**(2): p. 219-31.

209. Lindvall, O. and A. Bjorklund (1974). The organization of the ascending catecholamine neuron systems in the rat brain as revealed by the glyoxylic acid fluorescence method. *Acta Physiol Scand Suppl*. **412**: p. 1-48.
210. Loughlin, S.E., S.L. Foote, and J.H. Fallon (1982). Locus coeruleus projections to cortex: topography, morphology and collateralization. *Brain Res Bull*. **9**(1-6): p. 287-94.
211. Arbuthnott, G.W., et al. (1973). Lesions of the locus ceruleus and noradrenaline metabolism in cerebral cortex. *Exp Neurol*. **41**(2): p. 411-7.
212. Morrison, J.H., et al. (1978). The distribution and orientation of noradrenergic fibers in neocortex of the rat: an immunofluorescence study. *J Comp Neurol*. **181**(1): p. 17-39.
213. Grzanna, R. and M.E. Molliver (1980). Cytoarchitecture and dendritic morphology of central noradrenergic neurons, in *The Reticular Formation Revisited*. Raven Press New York. p. 83-97.
214. Holets, V., et al. (1988). Locus coeruleus neurons in the rat containing neuropeptide Y, tyrosine hydroxylase or galanin and their efferent projections to the spinal cord, cerebral cortex and hypothalamus. *Neuroscience*. **24**(3): p. 893-906.
215. Chamba, G., et al. (1991). Distribution of alpha-1 and alpha-2 binding sites in the rat locus coeruleus. *Brain Res Bull*. **26**(2): p. 185-93.
216. Fallon, J.H. and S.E. Loughlin (1982). Monoamine innervation of the forebrain: collateralization. *Brain Res Bull*. **9**(1-6): p. 295-307.
217. Loughlin, S.E., S.L. Foote, and F.E. Bloom (1986). Efferent projections of nucleus locus coeruleus: topographic organization of cells of origin demonstrated by three-dimensional reconstruction. *Neuroscience*. **18**(2): p. 291-306.
218. Mason, S.T. and H.C. Fibiger (1979). Regional topography within noradrenergic locus coeruleus as revealed by retrograde transport of horseradish peroxidase. *J Comp Neurol*. **187**(4): p. 703-24.
219. Schwarz, L.A., et al. (2015). Viral-genetic tracing of the input-output organization of a central noradrenaline circuit. *Nature*. **524**(7563): p. 88-92.
220. Simpson, K.L., et al. (1997). Lateralization and functional organization of the locus coeruleus projection to the trigeminal somatosensory pathway in rat. *J Comp Neurol*. **385**(1): p. 135-47.
221. Waterhouse, B.D., et al. (1993). Topographic organization of rat locus coeruleus and dorsal raphe nuclei: distribution of cells projecting to visual system structures. *J Comp Neurol*. **336**(3): p. 345-61.
222. Waterhouse, B.D., et al. (1983). The distribution of neocortical projection neurons in the locus coeruleus. *J Comp Neurol*. **217**(4): p. 418-31.
223. Chandler, D.J., W.J. Gao, and B.D. Waterhouse (2014). Heterogeneous organization of the locus coeruleus projections to prefrontal and motor cortices. *Proceedings of the National Academy of Sciences of the United States of America*. **111**(18): p. 6816-6821.
224. Lindvall, O., A. Bjorklund, and I. Divac (1978). Organization of catecholamine neurons projecting to the frontal cortex in the rat. *Brain Res*. **142**(1): p. 1-24.

225. Diop, L., et al. (1987). Adrenergic receptor and catecholamine distribution in rat cerebral cortex: binding studies with [3H]prazosin, [3H]idazoxan and [3H]dihydroalprenolol. *Brain Res*. **402**(2): p. 403-8.
226. Reader, T.A. and L. Grondin (1987). Distribution of catecholamines, serotonin, and their major metabolites in the rat cingulate, piriform-entorhinal, somatosensory, and visual cortex: a biochemical survey using high-performance liquid chromatography. *Neurochem Res*. **12**(12): p. 1087-97.
227. Bunney, B.S. and G.K. Aghajanian (1976). Dopamine and norepinephrine innervated cells in the rat prefrontal cortex: pharmacological differentiation using microiontophoretic techniques. *Life Sci*. **19**(11): p. 1783-9.
228. Armstrong-James, M. and K. Fox (1983). Effects of ionophoresed noradrenaline on the spontaneous activity of neurones in rat primary somatosensory cortex. *J Physiol*. **335**: p. 427-47.
229. Waterhouse, B.D., H.C. Moises, and D.J. Woodward (1980). Noradrenergic modulation of somatosensory cortical neuronal responses to iontophoretically applied putative neurotransmitters. *Exp Neurol*. **69**(1): p. 30-49.
230. Young, W.S., 3rd and M.J. Kuhar (1980). Noradrenergic alpha 1 and alpha 2 receptors: light microscopic autoradiographic localization. *Proc Natl Acad Sci U S A*. **77**(3): p. 1696-700.
231. Scheinin, M., et al. (1994). Distribution of alpha 2-adrenergic receptor subtype gene expression in rat brain. *Brain Res Mol Brain Res*. **21**(1-2): p. 133-49.
232. Wang, M., et al. (2007). Alpha2A-adrenoceptors strengthen working memory networks by inhibiting cAMP-HCN channel signaling in prefrontal cortex. *Cell*. **129**(2): p. 397-410.
233. Carr, D.B., et al. (2007). alpha2-Noradrenergic receptors activation enhances excitability and synaptic integration in rat prefrontal cortex pyramidal neurons via inhibition of HCN currents. *J Physiol*. **584**(Pt 2): p. 437-50.
234. Arnsten, A.F. (2000). Through the looking glass: differential noradenergic modulation of prefrontal cortical function. *Neural Plast*. **7**(1-2): p. 133-46.
235. Dodt, H., H. Pawelzik, and W. Zieglga¨nsberger (1991). Actions of noradrenaline on neocortical neurons in vitro. *Brain Research*. **545**(1–2): p. 307-311.
236. Snow, P.J., P. Andre, and O. Pompeiano (1999). Effects of locus coeruleus stimulation on the responses of SI neurons of the rat to controlled natural and electrical stimulation of the skin. *Arch Ital Biol*. **137**(1): p. 1-28.
237. Waterhouse, B.D., et al. (1990). Modulation of rat cortical area 17 neuronal responses to moving visual stimuli during norepinephrine and serotonin microiontophoresis. *Brain Res*. **514**(2): p. 276-92.
238. Waterhouse, B.D., H.C. Moises, and D.J. Woodward (1981). Alpha-receptor-mediated facilitation of somatosensory cortical neuronal responses to excitatory synaptic inputs and iontophoretically applied acetylcholine. *Neuropharmacology*. **20**(10): p. 907-20.
239. Waterhouse, B.D. and D.J. Woodward (1980). Interaction of norepinephrine with cerebrocortical activity evoked by stimulation of somatosensory afferent pathways in the rat. *Exp Neurol*. **67**(1): p. 11-34.

240. Devilbiss, D.M. and B.D. Waterhouse (2000). Norepinephrine exhibits two distinct profiles of action on sensory cortical neuron responses to excitatory synaptic stimuli. *Synapse*. **37**(4): p. 273-82.
241. Manunta, Y. and J.M. Edeline (1998). Effects of noradrenaline on rate-level function of auditory cortex neurons: is there a "gating" effect of noradrenaline? *Exp Brain Res*. **118**(3): p. 361-72.
242. Motaghi, S., et al. (2006). Electrical stimulation of locus coeruleus strengthens the surround inhibition in layer V barrel cortex in rat. *Neurosci Lett*. **401**(3): p. 280-4.
243. Waterhouse, B.D., H.C. Moises, and D.J. Woodward (1998). Phasic activation of the locus coeruleus enhances responses of primary sensory cortical neurons to peripheral receptive field stimulation. *Brain Res*. **790**(1-2): p. 33-44.
244. Waterhouse, B.D., et al. (1988). New evidence for a gating action of norepinephrine in central neuronal circuits of mammalian brain. *Brain Res Bull*. **21**(3): p. 425-32.
245. Condes-Lara, M. (1998). Different direct pathways of locus coeruleus to medial prefrontal cortex and centrolateral thalamic nucleus: electrical stimulation effects on the evoked responses to nociceptive peripheral stimulation. *Eur J Pain*. **2**(1): p. 15-23.
246. Zhang, Z., et al. (2013). Norepinephrine drives persistent activity in prefrontal cortex via synergistic alpha1 and alpha2 adrenoceptors. *PLoS One*. **8**(6): p. e66122.
247. Mantz, J., et al. (1988). Differential effects of ascending neurons containing dopamine and noradrenaline in the control of spontaneous activity and of evoked responses in the rat prefrontal cortex. *Neuroscience*. **27**(2): p. 517-26.
248. Thierry, A.M., J. Mantz, and J. Glowinski (1992). Influence of dopaminergic and noradrenergic afferents on their target cells in the rat medial prefrontal cortex. *Adv Neurol*. **57**: p. 545-54.
249. Kovacs, P. and I. Hernadi (2003). Alpha2 antagonist yohimbine suppresses maintained firing of rat prefrontal neurons in vivo. *Neuroreport*. **14**(6): p. 833-6.
250. Kovacs, P. and I. Hernadi (2006). Yohimbine acts as a putative in vivo alpha2A/D-antagonist in the rat prefrontal cortex. *Neurosci Lett*. **402**(3): p. 253-8.
251. Lukhanina, E.P. and N.A. Pil'kevich (2011). Modulating Action of an α2Adrenoreceptor Agonist, Clonidine, on Neuronal Activity and Synaptic Transmission in the Rat Prefrontal Cortex. *Neurophysiology*. **43**(4): p. 327-330.
252. Wang, Y., et al. (2011). alpha2-Adrenoceptor regulates the spontaneous and the GABA/glutamate modulated firing activity of the rat medial prefrontal cortex pyramidal neurons. *Neuroscience*. **182**: p. 193-202.
253. Wang, Y., et al. (2010). Noradrenergic lesion of the locus coeruleus increases the firing activity of the medial prefrontal cortex pyramidal neurons and the role of alpha2-adrenoceptors in normal and medial forebrain bundle lesioned rats. *Brain Res*. **1324**: p. 64-74.
254. Luo, F., et al. (2014). Activation of alpha(1)-adrenoceptors enhances excitatory synaptic transmission via a pre- and postsynaptic protein kinase C-dependent mechanism in the medial prefrontal cortex of rats. *Eur J Neurosci*. **39**(8): p. 1281-93.

255. Marek, G.J. and G.K. Aghajanian (1999). 5-HT2A receptor or alpha1-adrenoceptor activation induces excitatory postsynaptic currents in layer V pyramidal cells of the medial prefrontal cortex. *Eur J Pharmacol*. **367**(2-3): p. 197-206.
256. Ji, X.H., et al. (2008). Stimulation of alpha2-adrenoceptors suppresses excitatory synaptic transmission in the medial prefrontal cortex of rat. *Neuropsychopharmacology*. **33**(9): p. 2263-71.
257. Law-Tho, D., F. Crepel, and J.C. Hirsch (1993). Noradrenaline decreases transmission of NMDA- and non-NMDA-receptor mediated monosynaptic EPSPs in rat prefrontal neurons in vitro. *Eur J Neurosci*. **5**(11): p. 1494-500.
258. Mouradian, R.D., F.M. Sessler, and B.D. Waterhouse (1991). Noradrenergic potentiation of excitatory transmitter action in cerebrocortical slices: evidence for mediation by an alpha 1 receptor-linked second messenger pathway. *Brain Res*. **546**(1): p. 83-95.
259. Salgado, H., et al. (2012). Pre- and postsynaptic effects of norepinephrine on gamma-aminobutyric acid-mediated synaptic transmission in layer 2/3 of the rat auditory cortex. *Synapse*. **66**(1): p. 20-8.
260. Salgado, H., et al. (2011). Layer-specific noradrenergic modulation of inhibition in cortical layer II/III. *Cereb Cortex*. **21**(1): p. 212-21.
261. Salgado, H., M. Trevino, and M. Atzori (2016). Layer- and area-specific actions of norepinephrine on cortical synaptic transmission. *Brain Res*. **1641**(Pt B): p. 163-76.
262. Cedarbaum, J.M. and G.K. Aghajanian (1976). Noradrenergic neurons of the locus coeruleus: inhibition by epinephrine and activation by the alpha-antagonist piperoxane. *Brain Res*. **112**(2): p. 413-9.
263. Anden, N.E., et al. (1970). Evidence for a central noradrenaline receptor stimulation by clonidine. *Life Sci*. **9**(9): p. 513-23.
264. Anderson, C. and T.W. Stone (1974). On the mechanism of action of clonidine: effects on single central neurones. *Br J Pharmacol*. **51**(3): p. 359-65.
265. Dalley, J.W. and S.C. Stanford (1995). Contrasting effects of the imidazol(in)e α2-adrenoceptor agonists, medetomidine, clonidine and UK 14,304 on extraneuronal levels of noradrenaline in the rat frontalcortex: evaluation using in vivo microdialysis and synaptosomal uptake studies. *British Journal of Pharmacology*. **114**(8): p. 1717-1723.
266. Adams, L.M. and S.L. Foote (1988). Effects of locally infused pharmacological agents on spontaneous and sensory-evoked activity of locus coeruleus neurons. *Brain Res Bull*. **21**(3): p. 395-400.
267. Cedarbaum, J.M. and G.K. Aghajanian (1977). Catecholamine receptors on locus coeruleus neurons: pharmacological characterization. *Eur J Pharmacol*. **44**(4): p. 375-85.
268. Ruiz-Ortega, J.A. and L. Ugedo (1997). The stimulatory effect of clonidine on locus coeruleus neurons of rats with inactivated alpha 2-adrenoceptors: involvement of imidazoline receptors located in the nucleus paragigantocellularis. *Naunyn Schmiedebergs Arch Pharmacol*. **355**(2): p. 288-94.
269. Pudovkina, O.L., et al. (2001). The release of noradrenaline in the locus coeruleus and prefrontal cortex studied with dual-probe microdialysis. *Brain Res*. **906**(1-2): p. 38-45.

270. Starke, K. and K.P. Altmann (1973). Inhibition of adrenergic neurotransmission by clonidine: an action on prejunctional -receptors. *Neuropharmacology*. **12**(4): p. 339-47.
271. Starke, K. and H. Montel (1973). Involvement of alpha-receptors in clonidine-induced inhibition of transmitter release from central monoamine neurones. *Neuropharmacology*. **12**(11): p. 1073-80.
272. Pan, W.H., S.Y. Yang, and S.K. Lin (2004). Neurochemical interaction between dopaminergic and noradrenergic neurons in the medial prefrontal cortex. *Synapse*. **53**(1): p. 44-52.
273. Smith, C.C. and R.W. Greene (2012). CNS dopamine transmission mediated by noradrenergic innervation. *J Neurosci*. **32**(18): p. 6072-80.
274. Steketee, J.D. (2003). Neurotransmitter systems of the medial prefrontal cortex: potential role in sensitization to psychostimulants. *Brain Res Brain Res Rev*. **41**(2-3): p. 203-28.
275. Tassin, J.P. (1992). NE/DA interactions in prefrontal cortex and their possible roles as neuromodulators in schizophrenia. *J Neural Transm Suppl*. **36**: p. 135-62.
276. Moron, J.A., et al. (2002). Dopamine Uptake through the Norepinephrine Transporter in Brain Regions with Low Levels of the Dopamine Transporter: Evidence from Knock-Out Mouse Lines. *The Journal of Neuroscience*. **22**(2): p. 389-395.
277. Raiteri, M., et al. (1977). Effect of sympathomimetic amines on the synaptosomal transport of noradrenaline, dopamine and 5-hydroxytryptamine. *European journal of pharmacology*. **41**(2): p. 133-143.
278. Eshleman, A.J., et al. (1999). Characteristics of drug interactions with recombinant biogenic amine transporters expressed in the same cell type. *Journal of Pharmacology and Experimental Therapeutics*. **289**(2): p. 877-885.
279. Giros, B., et al. (1994). Delineation of discrete domains for substrate, cocaine, and tricyclic antidepressant interactions using chimeric dopamine-norepinephrine transporters. *Journal of Biological Chemistry*. **269**(23): p. 15985-15988.
280. Gu, H., S.C. Wall, and G. Rudnick (1994). Stable expression of biogenic amine transporters reveals differences in inhibitor sensitivity, kinetics, and ion dependence. *Journal of Biological Chemistry*. **269**(10): p. 7124-7130.
281. Lorang, D., S.G. Amara, and R.B. Simerly (1994). Cell-type-specific expression of catecholamine transporters in the rat brain. *J Neurosci*. **14**(8): p. 4903-14.
282. Carboni, E. and A. Silvagni (2004). Dopamine reuptake by norepinephrine neurons: exception or rule? *Crit Rev Neurobiol*. **16**(1-2): p. 121-8.
283. Carboni, E., et al. (1990). Blockade of the noradrenaline carrier increases extracellular dopamine concentrations in the prefrontal cortex: evidence that dopamine is taken up in vivo by noradrenergic terminals. *J Neurochem*. **55**(3): p. 1067-70.
284. Devoto, P. and G. Flore (2006). On the origin of cortical dopamine: is it a co-transmitter in noradrenergic neurons? *Curr Neuropharmacol*. **4**(2): p. 115-25.
285. Devoto, P., et al. (2003). Origin of extracellular dopamine from dopamine and noradrenaline neurons in the medial prefrontal and occipital cortex. *Synapse*. **50**(3): p. 200-5.

286. Devoto, P., et al. (2001). Evidence for co-release of noradrenaline and dopamine from noradrenergic neurons in the cerebral cortex. *Molecular psychiatry*. **6**(6): p. 657-664.
287. Devoto, P., et al. (2004). Alpha2-adrenoceptor mediated co-release of dopamine and noradrenaline from noradrenergic neurons in the cerebral cortex. *J Neurochem*. **88**(4): p. 1003-9.
288. Devoto, P., et al. (2005). Co-release of noradrenaline and dopamine in the cerebral cortex elicited by single train and repeated train stimulation of the locus coeruleus. *BMC Neurosci*. **6**: p. 31.
289. Devoto, P., et al. (2005). Stimulation of the locus coeruleus elicits noradrenaline and dopamine release in the medial prefrontal and parietal cortex. *Journal of neurochemistry*. **92**(2): p. 368-374.
290. Bjorklund, A. and S.B. Dunnett (2007). Dopamine neuron systems in the brain: an update. *Trends Neurosci*. **30**(5): p. 194-202.
291. Albin, R.L., A.B. Young, and J.B. Penney (1989). The functional anatomy of basal ganglia disorders. *Trends in Neurosciences*. **12**(10): p. 366-375.
292. Gerfen, C.R. (1992). The neostriatal mosaic: multiple levels of compartmental organization in the basal ganglia. *Annual review of neuroscience*. **15**(1): p. 285-320.
293. Gerfen, C.R. and D.J. Surmeier (2011). Modulation of striatal projection systems by dopamine. *Annual review of neuroscience*. **34**: p. 441.
294. Smith, Y., et al. (1998). Microcircuitry of the direct and indirect pathways of the basal ganglia. *NEUROSCIENCE-OXFORD-*. **86**: p. 353-388.
295. DeLong, M.R. and A.P. Georgopoulos (2011). Motor Functions of the Basal Ganglia, in *Comprehensive Physiology*. John Wiley & Sons, Inc.
296. Graybiel, A.M. (2005). The basal ganglia: learning new tricks and loving it. *Current Opinion in Neurobiology*. **15**(6): p. 638-644.
297. Redgrave, P., et al. (2010). Goal-directed and habitual control in the basal ganglia: implications for Parkinson's disease. *Nat Rev Neurosci*. **11**(11): p. 760-772.
298. Ikemoto, S. (2007). Dopamine reward circuitry: Two projection systems from the ventral midbrain to the nucleus accumbens–olfactory tubercle complex. *Brain Research Reviews*. **56**(1): p. 27-78.
299. Lammel, S., et al. (2008). Unique properties of mesoprefrontal neurons within a dual mesocorticolimbic dopamine system. *Neuron*. **57**(5): p. 760-73.
300. Lammel, S., et al. (2011). Projection-specific modulation of dopamine neuron synapses by aversive and rewarding stimuli. *Neuron*. **70**(5): p. 855-62.
301. Phillipson, O.T. and A.C. Griffiths (1985). The topographic order of inputs to nucleus accumbens in the rat. *Neuroscience*. **16**(2): p. 275-296.
302. Le Moal, M. and H. Simon (1991). Mesocorticolimbic dopaminergic network: functional and regulatory roles. *Physiol Rev*. **71**(1): p. 155-234.
303. Schultz, W. (1998). Predictive reward signal of dopamine neurons. *J Neurophysiol*. **80**(1): p. 1-27.
304. Schultz, W. (2016). Dopamine reward prediction-error signalling: a two-component response. *Nature Reviews Neuroscience*. **17**(3): p. 183-195.
305. Spanagel, R. and F. Weiss (1999). The dopamine hypothesis of reward: past and current status. *Trends Neurosci*. **22**(11): p. 521-7.

306. Glowinski, J., J.P. Tassin, and A.M. Thierry (1984). The mesocortico-prefrontal dopaminergic neurons. *Trends in Neurosciences*. **7**(11): p. 415-418.
307. Grace, A.A. and B.S. Bunney (1983). Intracellular and extracellular electrophysiology of nigral dopaminergic neurons--1. Identification and characterization. *Neuroscience*. **10**(2): p. 301-15.
308. Grace, A.A. and B.S. Bunney (1984). The control of firing pattern in nigral dopamine neurons: burst firing. *J Neurosci*. **4**(11): p. 2877-90.
309. Carr, D.B. and S.R. Sesack (2000). GABA-containing neurons in the rat ventral tegmental area project to the prefrontal cortex. *Synapse*. **38**(2): p. 114-23.
310. Swanson, L.W. (1982). The projections of the ventral tegmental area and adjacent regions: a combined fluorescent retrograde tracer and immunofluorescence study in the rat. *Brain Res Bull*. **9**(1-6): p. 321-53.
311. Dobi, A., et al. (2010). Glutamatergic and nonglutamatergic neurons of the ventral tegmental area establish local synaptic contacts with dopaminergic and nondopaminergic neurons. *J Neurosci*. **30**(1): p. 218-29.
312. Kawano, M., et al. (2006). Particular subpopulations of midbrain and hypothalamic dopamine neurons express vesicular glutamate transporter 2 in the rat brain. *Journal of Comparative Neurology*. **498**(5): p. 581-592.
313. Kosaka, T., et al. (1987). Catecholaminergic neurons containing GABA-like and/or glutamic acid decarboxylase-like immunoreactivities in various brain regions of the rat. *Experimental Brain Research*. **66**(1): p. 191-210.
314. Margolis, E.B., et al. (2012). Identification of rat ventral tegmental area GABAergic neurons. *PloS one*. **7**(7): p. e42365.
315. Margolis, E.B., et al. (2006). Kappa opioids selectively control dopaminergic neurons projecting to the prefrontal cortex. *Proc Natl Acad Sci U S A*. **103**(8): p. 2938-42.
316. Mugnaini, E. and W.H. Oertel (1985). An atlas of the distribution of GABAergic neurons and terminals in the rat CNS as revealed by GAD immunohistochemistry. *Handbook of chemical neuroanatomy*. **4**(Part I): p. 436-608.
317. Nagai, T., P.L. McGeer, and E.G. McGeer (1983). Distribution of GABA-T-Intensive neurons in the hat forebrain and midbrain. *Journal of Comparative Neurology*. **218**(2): p. 220-238.
318. Nair-Roberts, R.G., et al. (2008). Stereological estimates of dopaminergic, GABAergic and glutamatergic neurons in the ventral tegmental area, substantia nigra and retrorubral field in the rat. *Neuroscience*. **152**(4): p. 1024-31.
319. Steffensen, S.C., et al. (1998). Electrophysiological characterization of GABAergic neurons in the ventral tegmental area. *Journal of Neuroscience*. **18**(19): p. 8003-8015.
320. Yamaguchi, T., et al. (2011). Mesocorticolimbic Glutamatergic Pathway. *The Journal of Neuroscience*. **31**(23): p. 8476-8490.
321. Fields, H.L., M.M. Heinricher, and P. Mason (1991). Neurotransmitters in Nociceptive Modulatory Circuits. *Annual Review of Neuroscience*. **14**: p. 219-245.
322. Oades, R.D. and G.M. Halliday (1987). Ventral tegmental (A10) system: neurobiology. 1. Anatomy and connectivity. *Brain Res*. **434**(2): p. 117-65.

323. Simon, H., M. Le Moal, and A. Calas (1979). Efferents and afferents of the ventral tegmental-A10 region studied after local injection of [3H]leucine and horseradish peroxidase. *Brain Res*. **178**(1): p. 17-40.
324. Watabe-Uchida, M., et al. Whole-brain mapping of direct inputs to midbrain dopamine neurons. *Neuron*. **74**(5): p. 858-73.
325. Yetnikoff, L., et al. (2014). An Update on the Connections of the Ventral Mesencephalic Dopaminergic Complex. *Neuroscience*. **282**: p. 23-48.
326. Bromberg-Martin, E.S., M. Matsumoto, and O. Hikosaka (2010). Dopamine in motivational control: rewarding, aversive, and alerting. *Neuron*. **68**(5): p. 815-34.
327. Horvitz, J.C. (2000). Mesolimbocortical and nigrostriatal dopamine responses to salient non-reward events. *Neuroscience*. **96**(4): p. 651-6.
328. Ungless, M.A. (2004). Dopamine: the salient issue. *Trends Neurosci*. **27**(12): p. 702-6.
329. Feenstra, M.G.P. and M.H.A. Botterblom (1996). Rapid sampling of extracellular dopamine in the rat prefrontal cortex during food consumption, handling and exposure to novelty. *Brain research*. **742**(1): p. 17-24.
330. Guarraci, F.A. and B.S. Kapp (1999). An electrophysiological characterization of ventral tegmental area dopaminergic neurons during differential pavlovian fear conditioning in the awake rabbit. *Behavioural brain research*. **99**(2): p. 169-179.
331. Horvitz, J.C., T. Stewart, and B.L. Jacobs (1997). Burst activity of ventral tegmental dopamine neurons is elicited by sensory stimuli in the awake cat. *Brain Res*. **759**(2): p. 251-8.
332. Mantz, J., A.M. Thierry, and J. Glowinski (1989). Effect of noxious tail pinch on the discharge rate of mesocortical and mesolimbic dopamine neurons: selective activation of the mesocortical system. *Brain Research*. **476**(2): p. 377-381.
333. Redgrave, P., T.J. Prescott, and K. Gurney (1999). Is the short-latency dopamine response too short to signal reward error? *Trends Neurosci*. **22**(4): p. 146-51.
334. Happel, M.F., et al. (2014). Dopamine-modulated recurrent corticoefferent feedback in primary sensory cortex promotes detection of behaviorally relevant stimuli. *J Neurosci*. **34**(4): p. 1234-47.
335. Redgrave, P. and K. Gurney (2006). The short-latency dopamine signal: a role in discovering novel actions? *Nature Reviews Neuroscience*. **7**(12): p. 967-975.
336. Maeda, H. and G.J. Mogenson (1982). Effects of peripheral stimulation on the activity of neurons in the ventral tegmental area, substantia nigra and midbrain reticular formation of rats. *Brain Res Bull*. **8**(1): p. 7-14.
337. Valenti, O., D.J. Lodge, and A.A. Grace (2011). Aversive stimuli alter ventral tegmental area dopamine neuron activity via a common action in the ventral hippocampus. *J Neurosci*. **31**(11): p. 4280-9.
338. Yang, P.B., A.C. Swann, and N. Dafny (2006). Chronic methylphenidate modulates locomotor activity and sensory evoked responses in the VTA and NAc of freely behaving rats. *Neuropharmacology*. **51**(3): p. 546-56.
339. Yang, P.B., A.C. Swann, and N. Dafny (2006). Sensory-evoked potentials recordings from the ventral tegmental area, nucleus accumbens, prefrontal cortex, and caudate nucleus and locomotor activity are modulated in dose-response characteristics by methylphenidate. *Brain Res*. **1073-1074**: p. 164-74.

340. Brischoux, F., et al. (2009). Phasic excitation of dopamine neurons in ventral VTA by noxious stimuli. *Proc Natl Acad Sci U S A*. **106**(12): p. 4894-9.
341. Coizet, V., et al. (2010). The parabrachial nucleus is a critical link in the transmission of short latency nociceptive information to midbrain dopaminergic neurons. *Neuroscience*. **168**(1): p. 263-72.
342. Coizet, V., et al. (2006). Nociceptive responses of midbrain dopaminergic neurones are modulated by the superior colliculus in the rat. *Neuroscience*. **139**(4): p. 1479-93.
343. Bannon, M.J. and R.H. Roth (1983). Pharmacology of mesocortical dopamine neurons. *Pharmacological Reviews*. **35**(1): p. 53-68.
344. Fadda, F., et al. (1978). Stress-induced increase in 3,4-dihydroxyphenylacetic acid (DOPAC) levels in the cerebral cortex and in n. accumbens: Reversal by diazepam. *Life Sciences*. **23**(22): p. 2219-2224.
345. Lammel, S., et al. (2012). Input-specific control of reward and aversion in the ventral tegmental area. *Nature*. **491**(7423): p. 212-7.
346. Grace, A.A. and B.S. Bunney (1984). The control of firing pattern in nigral dopamine neurons: single spike firing. *J Neurosci*. **4**(11): p. 2866-76.
347. Bunney, B.S. and A.A. Grace (1978). Acute and chronic haloperidol treatment: comparison of effects on nigral dopaminergic cell activity. *Life Sci*. **23**(16): p. 1715-27.
348. Floresco, S.B., et al. (2003). Afferent modulation of dopamine neuron firing differentially regulates tonic and phasic dopamine transmission. *Nat Neurosci*. **6**(9): p. 968-73.
349. Lisman, J.E. and A.A. Grace (2005). The hippocampal-VTA loop: controlling the entry of information into long-term memory. *Neuron*. **46**(5): p. 703-13.
350. Grace, A.A. and S.P. Onn (1989). Morphology and electrophysiological properties of immunocytochemically identified rat dopamine neurons recorded in vitro. *J Neurosci*. **9**(10): p. 3463-81.
351. Sanghera, M.K., M.E. Trulson, and D.C. German (1984). Electrophysiological properties of mouse dopamine neurons: in vivo and in vitro studies. *Neuroscience*. **12**(3): p. 793-801.
352. Floresco, S.B., C.L. Todd, and A.A. Grace (2001). Glutamatergic afferents from the hippocampus to the nucleus accumbens regulate activity of ventral tegmental area dopamine neurons. *J Neurosci*. **21**(13): p. 4915-22.
353. Grace, A.A. (1991). Phasic versus tonic dopamine release and the modulation of dopamine system responsivity: a hypothesis for the etiology of schizophrenia. *Neuroscience*. **41**(1): p. 1-24.
354. Howland, J.G., P. Taepavarapruk, and A.G. Phillips (2002). Glutamate receptor-dependent modulation of dopamine efflux in the nucleus accumbens by basolateral, but not central, nucleus of the amygdala in rats. *J Neurosci*. **22**(3): p. 1137-45.
355. Chergui, K., et al. (1994). Subthalamic nucleus modulates burst firing of nigral dopamine neurones via NMDA receptors. *Neuroreport*. **5**(10): p. 1185-8.
356. Lodge, D.J. and A.A. Grace (2006). The hippocampus modulates dopamine neuron responsivity by regulating the intensity of phasic neuron activation. *Neuropsychopharmacology*. **31**(7): p. 1356-61.

357. Lokwan, S.J., et al. (1999). Stimulation of the pedunculopontine tegmental nucleus in the rat produces burst firing in A9 dopaminergic neurons. *Neuroscience*. **92**(1): p. 245-54.
358. Keefe, K.A., M.J. Zigmond, and E.D. Abercrombie (1993). In vivo regulation of extracellular dopamine in the neostriatum: influence of impulse activity and local excitatory amino acids. *J Neural Transm Gen Sect*. **91**(2-3): p. 223-40.
359. Chergui, K., M.F. Suaud-Chagny, and F. Gonon (1994). Nonlinear relationship between impulse flow, dopamine release and dopamine elimination in the rat brain in vivo. *Neuroscience*. **62**(3): p. 641-5.
360. Garris, P.A., et al. (1994). Efflux of dopamine from the synaptic cleft in the nucleus accumbens of the rat brain. *J Neurosci*. **14**(10): p. 6084-93.
361. Garris, P.A. and R.M. Wightman (1994). Different kinetics govern dopaminergic transmission in the amygdala, prefrontal cortex, and striatum: an in vivo voltammetric study. *The Journal of neuroscience*. **14**(1): p. 442-450.
362. Gonon, F.G. (1988). Nonlinear relationship between impulse flow and dopamine released by rat midbrain dopaminergic neurons as studied by in vivo electrochemistry. *Neuroscience*. **24**(1): p. 19-28.
363. Kawagoe, K.T., et al. (1992). Regulation of transient dopamine concentration gradients in the microenvironment surrounding nerve terminals in the rat striatum. *Neuroscience*. **51**(1): p. 55-64.
364. Manley, L.D., et al. (1992). Effects of frequency and pattern of medial forebrain bundle stimulation on caudate dialysate dopamine and serotonin. *J Neurochem*. **58**(4): p. 1491-8.
365. Nissbrandt, H., A. Elverfors, and G. Engberg (1994). Pharmacologically induced cessation of burst activity in nigral dopamine neurons: significance for the terminal dopamine efflux. *Synapse*. **17**(4): p. 217-24.
366. Venton, B.J., et al. (2003). Real-time decoding of dopamine concentration changes in the caudate–putamen during tonic and phasic firing. *Journal of neurochemistry*. **87**(5): p. 1284-1295.
367. Missale, C., et al. (1998). Dopamine receptors: from structure to function. *Physiol Rev*. **78**(1): p. 189-225.
368. Cragg, S.J. and S.A. Greenfield (1997). Differential autoreceptor control of somatodendritic and axon terminal dopamine release in substantia nigra, ventral tegmental area, and striatum. *The Journal of neuroscience*. **17**(15): p. 5738-5746.
369. Kalivas, P.W. and P. Duffy (1991). A comparison of axonal and somatodendritic dopamine release using in vivo dialysis. *Journal of neurochemistry*. **56**(3): p. 961-967.
370. Lacey, M.G., N.B. Mercuri, and R.A. North (1987). Dopamine acts on D2 receptors to increase potassium conductance in neurones of the rat substantia nigra zona compacta. *The Journal of physiology*. **392**: p. 397.
371. Horn, A.S. (1990). Dopamine uptake: a review of progress in the last decade. *Progress in neurobiology*. **34**(5): p. 387-400.
372. Bannon, M.J., R.L. Michaud, and R.H. Roth (1981). Mesocortical dopamine neurons. Lack of autoreceptors modulating dopamine synthesis. *Mol Pharmacol*. **19**(2): p. 270-5.

373. Margolis, E.B., et al. (2008). Midbrain dopamine neurons: projection target determines action potential duration and dopamine D(2) receptor inhibition. *J Neurosci*. **28**(36): p. 8908-13.
374. Chiodo, L.A., et al. (1984). Evidence for the absence of impulse-regulating somatodendritic and synthesis-modulating nerve terminal autoreceptors on subpopulations of mesocortical dopamine neurons. *Neuroscience*. **12**(1): p. 1-16.
375. Bannon, M.J., E.B. Bunney, and R.H. Roth (1981). Mesocortical dopamine neurons: rapid transmitter turnover compared to other brain catecholamine systems. *Brain Res*. **218**(1-2): p. 376-82.
376. Lavielle, S., et al. (1979). Blockade by benzodiazepines of the selective high increase in dopamine turnover induced by stress in mesocortical dopaminergic neurons of the rat. *Brain Research*. **168**(3): p. 585-594.
377. White, F.J. and R.Y. Wang (1984). A10 dopamine neurons: role of autoreceptors in determining firing rate and sensitivity to dopamine agonists. *Life sciences*. **34**(12): p. 1161-1170.
378. Farde, L., et al. (1987). PET analysis of human dopamine receptor subtypes using 11C-SCH 23390 and 11C-raclopride. *Psychopharmacology*. **92**(3): p. 278-284.
379. Lidow, M.S., et al. (1991). Distribution of dopaminergic receptors in the primate cerebral cortex: quantitative autoradiographic analysis using [3 H] raclopride,[3 H] spiperone and [3 H] SCH23390. *Neuroscience*. **40**(3): p. 657-671.
380. Gaspar, P., B. Bloch, and C. Moine (1995). D1 and D2 receptor gene expression in the rat frontal cortex: cellular localization in different classes of efferent neurons. *European Journal of neuroscience*. **7**(5): p. 1050-1063.
381. Richfield, E.K., J.B. Penney, and A.B. Young (1989). Anatomical and affinity state comparisons between dopamine D1 and D2 receptors in the rat central nervous system. *Neuroscience*. **30**(3): p. 767-77.
382. Dreyer, J.K., et al. (2010). Influence of phasic and tonic dopamine release on receptor activation. *J Neurosci*. **30**(42): p. 14273-83.
383. Gonon, F. (1997). Prolonged and extrasynaptic excitatory action of dopamine mediated by D1 receptors in the rat striatum in vivo. *J Neurosci*. **17**(15): p. 5972-8.
384. Schultz, W. (2007). Multiple dopamine functions at different time courses. *Annu Rev Neurosci*. **30**: p. 259-88.
385. Bernardi, G., et al. (1982). Responses of intracellularly recorded cortical neurons to the iontophoretic application of dopamine. *Brain Res*. **245**(2): p. 267-74.
386. Ferron, A., et al. (1984). Inhibitory influence of the mesocortical dopaminergic system on spontaneous activity or excitatory response induced from the thalamic mediodorsal nucleus in the rat medial prefrontal cortex. *Brain Res*. **302**(2): p. 257-65.
387. Gioanni, Y., et al. (1998). Alpha1-adrenergic, D1, and D2 receptors interactions in the prefrontal cortex: implications for the modality of action of different types of neuroleptics. *Synapse*. **30**(4): p. 362-70.
388. Godbout, R., et al. (1991). Inhibitory influence of the mesocortical dopaminergic neurons on their target cells: electrophysiological and pharmacological characterization. *Journal of Pharmacology and Experimental Therapeutics*. **258**(2): p. 728-738.

389. Jay, T.M., J. Glowinski, and A.M. Thierry (1995). Inhibition of hippocampoprefrontal cortex excitatory responses by the mesocortical DA system. *Neuroreport*. **6**(14): p. 1845-8.
390. Mantz, J., et al. (1992). Inhibitory effects of mesocortical dopaminergic neurons on their target cells: electrophysiological and pharmacological characterization. *Neurochem Int*. **20 Suppl**: p. 251S-254S.
391. Mora, F., et al. (1976). Spontaneous Firing Rate of Neurons in Prefrontal Cortex of Rat - Evidence for a Dopaminergic Inhibition. *Brain Research*. **116**(3): p. 516-522.
392. Peterson, S.L., J.S.S. Mary, and N.R. Harding (1987). Cis-flupentixol antagonism of the rat prefrontal cortex neuronal response to apomorphine and ventral tegmental area input. *Brain research bulletin*. **18**(6): p. 723-729.
393. Pirot, S., et al. (1992). Inhibitory effects of ventral tegmental area stimulation on the activity of prefrontal cortical neurons: evidence for the involvement of both dopaminergic and GABAergic components. *Neuroscience*. **49**(4): p. 857-65.
394. Sawaguchi, T. and M. Matsumura (1985). Laminar distributions of neurons sensitive to acetylcholine, noradrenaline and dopamine in the dorsolateral prefrontal cortex of the monkey. *Neurosci Res*. **2**(4): p. 255-73.
395. Sesack, S.R. and B.S. Bunney (1989). Pharmacological characterization of the receptor mediating electrophysiological responses to dopamine in the rat medial prefrontal cortex: a microiontophoretic study. *J Pharmacol Exp Ther*. **248**(3): p. 1323-33.
396. Yang, C.R. and G.J. Mogenson (1990). Dopaminergic modulation of cholinergic responses in rat medial prefrontal cortex: an electrophysiological study. *Brain Res*. **524**(2): p. 271-81.
397. Benes, F.M. and S. Berretta (2001). GABAergic interneurons: implications for understanding schizophrenia and bipolar disorder. *Neuropsychopharmacology*. **25**(1): p. 1-27.
398. Vincent, S.L., Y. Khan, and F.M. Benes (1993). Cellular distribution of dopamine D1 and D2 receptors in rat medial prefrontal cortex. *The Journal of neuroscience*. **13**(6): p. 2551-2564.
399. Vincent, S.L., Y. Khan, and F.M. Benes (1995). Cellular colocalization of dopamine D1 and D2 receptors in rat medial prefrontal cortex. *Synapse*. **19**(2): p. 112-120.
400. Weiner, D.M., et al. (1991). D1 and D2 dopamine receptor mRNA in rat brain. *Proceedings of the National Academy of Sciences*. **88**(5): p. 1859-1863.
401. Gao, W.J. and P.S. Goldman-Rakic (2003). Selective modulation of excitatory and inhibitory microcircuits by dopamine. *Proc Natl Acad Sci U S A*. **100**(5): p. 2836-41.
402. Gorelova, N., J.K. Seamans, and C.R. Yang (2002). Mechanisms of dopamine activation of fast-spiking interneurons that exert inhibition in rat prefrontal cortex. *J Neurophysiol*. **88**(6): p. 3150-66.
403. Yang, C.R. and J.K. Seamans (1996). Dopamine D1 receptor actions in layers V-VI rat prefrontal cortex neurons in vitro: modulation of dendritic-somatic signal integration. *J Neurosci*. **16**(5): p. 1922-35.
404. Kabanova, A., et al. (2015). Function and developmental origin of a mesocortical inhibitory circuit. *Nat Neurosci*. **18**(6): p. 872-82.

405. Tseng, K.Y. and P. O'Donnell (2007). D2 dopamine receptors recruit a GABA component for their attenuation of excitatory synaptic transmission in the adult rat prefrontal cortex. *Synapse*. **61**(10): p. 843-50.
406. Tseng, K.Y. and P. O'Donnell (2004). Dopamine-glutamate interactions controlling prefrontal cortical pyramidal cell excitability involve multiple signaling mechanisms. *J Neurosci*. **24**(22): p. 5131-9.
407. Baldwin, A.E., K. Sadeghian, and A.E. Kelley (2002). Appetitive instrumental learning requires coincident activation of NMDA and dopamine D1 receptors within the medial prefrontal cortex. *J Neurosci*. **22**(3): p. 1063-71.
408. Gurden, H., J.P. Tassin, and T.M. Jay (1999). Integrity of the mesocortical dopaminergic system is necessary for complete expression of in vivo hippocampal-prefrontal cortex long-term potentiation. *Neuroscience*. **94**(4): p. 1019-27.
409. Jay, T.M. (2003). Dopamine: a potential substrate for synaptic plasticity and memory mechanisms. *Prog Neurobiol*. **69**(6): p. 375-90.
410. Hnasko, T.S., et al. (2010). Vesicular glutamate transport promotes dopamine storage and glutamate corelease in vivo. *Neuron*. **65**(5): p. 643-656.
411. Sulzer, D. and S. Rayport (2000). Dale's principle and glutamate corelease from ventral midbrain dopamine neurons. *Amino Acids*. **19**(1): p. 45-52.
412. Trudeau, L. (2004). Glutamate co-transmission as an emerging concept in monoamine neuron function. *Journal of psychiatry & neuroscience: JPN*. **29**(4): p. 296.
413. Tsai, H., et al. (2009). Phasic firing in dopaminergic neurons is sufficient for behavioral conditioning. *Science*. **324**(5930): p. 1080-1084.
414. Berger, B., et al. (1976). Dopaminergic innervation of the rat prefrontal cortex: a fluorescence histochemical study. *Brain Res*. **106**(1): p. 133-45.
415. Conde, F., et al. (1990). Afferent connections of the medial frontal cortex of the rat. A study using retrograde transport of fluorescent dyes. I. Thalamic afferents. *Brain Res Bull*. **24**(3): p. 341-54.
416. Herkenham, M. (1980). Laminar organization of thalamic projections to the rat neocortex. *Science*. **207**(4430): p. 532-5.
417. Krettek, J.E. and J.L. Price (1977). Projections from the amygdaloid complex to the cerebral cortex and thalamus in the rat and cat. *J Comp Neurol*. **172**(4): p. 687-722.
418. Krettek, J.E. and J.L. Price (1977). The cortical projections of the mediodorsal nucleus and adjacent thalamic nuclei in the rat. *J Comp Neurol*. **171**(2): p. 157-91.
419. Penit-Soria, J., E. Audinat, and F. Crepel (1987). Excitation of rat prefrontal cortical neurons by dopamine: an in vitro electrophysiological study. *Brain Res*. **425**(2): p. 263-74.
420. Ray, J.P. and J.L. Price (1992). The organization of the thalamocortical connections of the mediodorsal thalamic nucleus in the rat, related to the ventral forebrain-prefrontal cortex topography. *J Comp Neurol*. **323**(2): p. 167-97.
421. Slopsema, J.S., J. van der Gugten, and J.P. de Bruin (1982). Regional concentrations of noradrenaline and dopamine in the frontal cortex of the rat: dopaminergic innervation of the prefrontal subareas and lateralization of prefrontal dopamine. *Brain Res*. **250**(1): p. 197-200.

422. Van Eden, C.G., et al. (1987). Immunocytochemical localization of dopamine in the prefrontal cortex of the rat at the light and electron microscopical level. *Neuroscience*. **22**(3): p. 849-62.
423. Carr, D.B. and S.R. Sesack (1996). Hippocampal afferents to the rat prefrontal cortex: synaptic targets and relation to dopamine terminals. *J Comp Neurol*. **369**(1): p. 1-15.
424. Goldman-Rakic, P.S., et al. (1989). Dopamine synaptic complex with pyramidal neurons in primate cerebral cortex. *Proc Natl Acad Sci U S A*. **86**(22): p. 9015-9.
425. Kuroda, M., et al. (1996). The convergence of axon terminals from the mediodorsal thalamic nucleus and ventral tegmental area on pyramidal cells in layer V of the rat prelimbic cortex. *Eur J Neurosci*. **8**(7): p. 1340-9.
426. Kuroda, M., et al. (1995). Thalamocortical synapses between axons from the mediodorsal thalamic nucleus and pyramidal cells in the prelimbic cortex of the rat. *J Comp Neurol*. **356**(1): p. 143-51.
427. Smiley, J.F. and P.S. Goldman-Rakic (1993). Heterogeneous targets of dopamine synapses in monkey prefrontal cortex demonstrated by serial section electron microscopy: a laminar analysis using the silver-enhanced diaminobenzidine sulfide (SEDS) immunolabeling technique. *Cereb Cortex*. **3**(3): p. 223-38.
428. Smiley, J.F., et al. (1994). D1 dopamine receptor immunoreactivity in human and monkey cerebral cortex: predominant and extrasynaptic localization in dendritic spines. *Proc Natl Acad Sci U S A*. **91**(12): p. 5720-4.
429. Wang, Z., X.Q. Feng, and P. Zheng (2002). Activation of presynaptic D1 dopamine receptors by dopamine increases the frequency of spontaneous excitatory postsynaptic currents through protein kinase A and protein kinase C in pyramidal cells of rat prelimbic cortex. *Neuroscience*. **112**(3): p. 499-508.
430. Cepeda, C., et al. (1999). Electrophysiological and morphological analyses of cortical neurons obtained from children with catastrophic epilepsy: dopamine receptor modulation of glutamatergic responses. *Dev Neurosci*. **21**(3-5): p. 223-35.
431. Cepeda, C., et al. (1992). Differential modulation by dopamine of responses evoked by excitatory amino acids in human cortex. *Synapse*. **11**(4): p. 330-41.
432. Seamans, J.K., et al. (2001). Dopamine D1/D5 receptor modulation of excitatory synaptic inputs to layer V prefrontal cortex neurons. *Proc Natl Acad Sci U S A*. **98**(1): p. 301-6.
433. Zheng, P., et al. (1999). Opposite modulation of cortical N-methyl-D-aspartate receptor-mediated responses by low and high concentrations of dopamine. *Neuroscience*. **91**(2): p. 527-35.
434. Gonzalez-Islas, C. and J.J. Hablitz (2003). Dopamine enhances EPSCs in layer II-III pyramidal neurons in rat prefrontal cortex. *J Neurosci*. **23**(3): p. 867-75.
435. Wang, J.Y. and P. O'Donnell (2001). D1 Dopamine Receptors Potentiate NMDA-mediated Excitability Increase in Layer V Prefrontal Cortical Pyramidal Neurons. *Cerebral Cortex*. **11**(5): p. 452-462.
436. Chen, L. and C.R. Yang (2002). Interaction of dopamine D1 and NMDA receptors mediates acute clozapine potentiation of glutamate EPSPs in rat prefrontal cortex. *Journal of Neurophysiology*. **87**(5): p. 2324-2336.

437. Paspalas, C.D. and P.S. Goldman-Rakic (2005). Presynaptic D1 dopamine receptors in primate prefrontal cortex: target-specific expression in the glutamatergic synapse. *J Neurosci*. **25**(5): p. 1260-7.
438. Abekawa, T., et al. (2000). D1 dopamine receptor activation reduces extracellular glutamate and GABA concentrations in the medial prefrontal cortex. *Brain Res*. **867**(1-2): p. 250-4.
439. Gao, W.J., L.S. Krimer, and P.S. Goldman-Rakic (2001). Presynaptic regulation of recurrent excitation by D1 receptors in prefrontal circuits. *Proc Natl Acad Sci U S A*. **98**(1): p. 295-300.
440. Brozoski, T.J., et al. (1979). Cognitive deficit caused by regional depletion of dopamine in prefrontal cortex of rhesus monkey. *Science*. **205**(4409): p. 929-932.
441. Sawaguchi, T. and P.S. Goldman-Rakic (1994). The role of D1-dopamine receptor in working memory: local injections of dopamine antagonists into the prefrontal cortex of rhesus monkeys performing an oculomotor delayed-response task. *J Neurophysiol*. **71**(2): p. 515-28.
442. Seamans, J.K., S.B. Floresco, and A.G. Phillips (1998). D1 receptor modulation of hippocampal-prefrontal cortical circuits integrating spatial memory with executive functions in the rat. *J Neurosci*. **18**(4): p. 1613-21.
443. Floresco, S.B. and A.G. Phillips (2001). Delay-dependent modulation of memory retrieval by infusion of a dopamine D1 agonist into the rat medial prefrontal cortex. *Behav Neurosci*. **115**(4): p. 934-9.
444. Murphy, B.L., et al. (1996). Increased dopamine turnover in the prefrontal cortex impairs spatial working memory performance in rats and monkeys. *Proc Natl Acad Sci U S A*. **93**(3): p. 1325-9.
445. Zahrt, J., et al. (1997). Supranormal stimulation of D1 dopamine receptors in the rodent prefrontal cortex impairs spatial working memory performance. *J Neurosci*. **17**(21): p. 8528-35.
446. Arnsten, A.F. (1997). Catecholamine regulation of the prefrontal cortex. *Journal of psychopharmacology*. **11**(2): p. 151-162.
447. Cools, R. and M. D'Esposito (2011). Inverted-U–shaped dopamine actions on human working memory and cognitive control. *Biological psychiatry*. **69**(12): p. e113-e125.
448. Granon, S., et al. (2000). Enhanced and impaired attentional performance after infusion of D1 dopaminergic receptor agents into rat prefrontal cortex. *J Neurosci*. **20**(3): p. 1208-15.
449. Lidow, M.S., P.O. Koh, and A.F. Arnsten (2003). D1 dopamine receptors in the mouse prefrontal cortex: Immunocytochemical and cognitive neuropharmacological analyses. *Synapse*. **47**(2): p. 101-8.
450. Robbins, T.W. (2000). Chemical neuromodulation of frontal-executive functions in humans and other animals. *Exp Brain Res*. **133**(1): p. 130-8.
451. Robbins, T.W. and A.F. Arnsten (2009). The neuropsychopharmacology of fronto-executive function: monoaminergic modulation. *Annu Rev Neurosci*. **32**: p. 267-87.
452. Seamans, J.K. and C.R. Yang (2004). The principal features and mechanisms of dopamine modulation in the prefrontal cortex. *Prog Neurobiol*. **74**(1): p. 1-58.

453. Vijayraghavan, S., et al. (2007). Inverted-U dopamine D1 receptor actions on prefrontal neurons engaged in working memory. *Nature neuroscience*. **10**(3): p. 376-384.
454. Rhodes, J.S., S.C. Gammie, and T. Garland (2005). Neurobiology of Mice Selected for High Voluntary Wheel-running Activity. *Integrative and Comparative Biology*. **45**(3): p. 438-455.
455. Goldman-Rakic, P.S. (1997). The cortical dopamine system: role in memory and cognition. *Advances in pharmacology*. **42**: p. 707-711.
456. Puig, M.V., E.G. Antzoulatos, and E.K. Miller (2014). Prefrontal dopamine in associative learning and memory. *Neuroscience*. **282**: p. 217-29.
457. Braver, T.S. and J.D. Cohen (2000). On the control of control: The role of dopamine in regulating prefrontal function and working memory. *Control of cognitive processes: Attention and performance XVIII*. p. 713-737.
458. Robbins, T.W. (2005). Chemistry of the mind: neurochemical modulation of prefrontal cortical function. *Journal of Comparative Neurology*. **493**(1): p. 140-146.
459. Simon, H., B. Scatton, and M.L. Moal (1980). Dopaminergic A10 neurones are involved in cognitive functions. *Nature*. **286**(5769): p. 150-1.
460. Grace, A.A., et al. (2007). Regulation of firing of dopaminergic neurons and control of goal-directed behaviors. *Trends Neurosci*. **30**(5): p. 220-7.
461. Floresco, S.B. (2013). Prefrontal dopamine and behavioral flexibility: shifting from an "inverted-U" toward a family of functions. *Frontiers in neuroscience*. **7**: p. 62.
462. Goschke, T. and A. Bolte (2014). Emotional modulation of control dilemmas: the role of positive affect, reward, and dopamine in cognitive stability and flexibility. *Neuropsychologia*. **62**: p. 403-23.
463. Wise, R.A. (2004). Dopamine, learning and motivation. *Nature reviews neuroscience*. **5**(6): p. 483-494.
464. Bazyan, A.S. (2016). [Motivation and Emotional States: Structural Systemic, Neurochemical, Molecular and Cellular Mechanisms]. *Usp Fiziol Nauk*. **47**(1): p. 15-33.
465. Puglisi-Allegra, S. and R. Ventura (2012). Prefrontal/accumbal catecholamine system processes emotionally driven attribution of motivational salience. *Rev Neurosci*. **23**(5-6): p. 509-26.
466. Puglisi-Allegra, S. and R. Ventura (2012). Prefrontal/accumbal catecholamine system processes high motivational salience. *Front Behav Neurosci*. **6**: p. 31.
467. Diamond, A., et al. (2004). Genetic and neurochemical modulation of prefrontal cognitive functions in children. *American Journal of Psychiatry*. **161**(1): p. 125-132.
468. Bassett, D.S., et al. (2008). Hierarchical organization of human cortical networks in health and schizophrenia. *J Neurosci*. **28**(37): p. 9239-48.
469. Egan, M.F. and D.R. Weinberger (1997). Neurobiology of schizophrenia. *Current opinion in neurobiology*. **7**(5): p. 701-707.
470. Laviolette, S.R. (2007). Dopamine modulation of emotional processing in cortical and subcortical neural circuits: evidence for a final common pathway in schizophrenia? *Schizophr Bull*. **33**(4): p. 971-81.
471. Sigurdsson, T. (2016). Neural circuit dysfunction in schizophrenia: Insights from animal models. *Neuroscience*. **321**: p. 42-65.

472. Yang, C.R., J.K. Seamans, and N. Gorelova (1999). Developing a neuronal model for the pathophysiology of schizophrenia based on the nature of electrophysiological actions of dopamine in the prefrontal cortex. *Neuropsychopharmacology*. **21**(2): p. 161-194.
473. Castellanos, F.X. (1997). Toward a Pathophysiology of Attention-Deficit/Hyperactivint Disorder. *Clinical Pediatrics*. **36**(7): p. 381-393.
474. Durston, S. (2003). A review of the biological bases of ADHD: What have we learned from imaging studies? *Mental Retardation and Developmental Disabilities Research Reviews*. **9**(3): p. 184-195.
475. Levy, F. (1991). The Dopamine Theory of Attention Deficit Hyperactivity Disorder (ADHD). *Australian and New Zealand Journal of Psychiatry*. **25**(2): p. 277-283.
476. Russell, V., et al. (1995). Altered dopaminergic function in the prefrontal cortex, nucleus accumbens and caudate-putamen of an animal model of attention-deficit hyperactivity disorder — the spontaneously hypertensive rat. *Brain Research*. **676**(2): p. 343-351.
477. Phillipson, O.T. (1979). Afferent projections to the ventral tegmental area of Tsai and interfascicular nucleus: a horseradish peroxidase study in the rat. *J Comp Neurol*. **187**(1): p. 117-43.
478. Simon, H., et al. (1979). Anatomical relationships between the ventral mesencephalic tegmentum--a 10 region and the locus coeruleus as demonstrated by anterograde and retrograde tracing techniques. *J Neural Transm*. **44**(1-2): p. 77-86.
479. Geisler, S. and D.S. Zahm (2005). Afferents of the ventral tegmental area in the rat-anatomical substratum for integrative functions. *J Comp Neurol*. **490**(3): p. 270-94.
480. Liprando, L.A., et al. (2004). Ultrastructural interactions between terminals expressing the norepinephrine transporter and dopamine neurons in the rat and monkey ventral tegmental area. *Synapse*. **52**(4): p. 233-44.
481. Chandler, D.J., C.S. Lamperski, and B.D. Waterhouse (2013). Identification and distribution of projections from monoaminergic and cholinergic nuclei to functionally differentiated subregions of prefrontal cortex. *Brain Res*. **1522**: p. 38-58.
482. Mejias-Aponte, C.A., C. Drouin, and G. Aston-Jones (2009). Adrenergic and noradrenergic innervation of the midbrain ventral tegmental area and retrorubral field: prominent inputs from medullary homeostatic centers. *J Neurosci*. **29**(11): p. 3613-26.
483. Jones, L.S., L.L. Gauger, and J.N. Davis (1985). Anatomy of brain alpha 1-adrenergic receptors: in vitro autoradiography with [125I]-heat. *J Comp Neurol*. **231**(2): p. 190-208.
484. Lee, A., et al. (1998). Localization of alpha2C-adrenergic receptor immunoreactivity in catecholaminergic neurons in the rat central nervous system. *Neuroscience*. **84**(4): p. 1085-96.
485. Rosin, D.L., et al. (1993). Immunohistochemical localization of alpha 2A-adrenergic receptors in catecholaminergic and other brainstem neurons in the rat. *Neuroscience*. **56**(1): p. 139-55.

486. Rosin, D.L., et al. (1996). Distribution of alpha 2C-adrenergic receptor-like immunoreactivity in the rat central nervous system. *J Comp Neurol*. **372**(1): p. 135-65.
487. Talley, E.M., et al. (1996). Distribution of alpha 2A-adrenergic receptor-like immunoreactivity in the rat central nervous system. *J Comp Neurol*. **372**(1): p. 111-34.
488. Baumann, P.A. and W.P. Koella (1980). Feedback control of noradrenaline release as a function of noradrenaline concentration in the synaptic cleft in cortical slices of the rat. *Brain Res*. **189**(2): p. 437-48.
489. Curet, O., T. Dennis, and B. Scatton (1987). Evidence for the involvement of presynaptic alpha-2 adrenoceptors in the regulation of norepinephrine metabolism in the rat brain. *J Pharmacol Exp Ther*. **240**(1): p. 327-36.
490. Dennis, T., et al. (1987). Presynaptic alpha-2 adrenoceptors play a major role in the effects of idazoxan on cortical noradrenaline release (as measured by in vivo dialysis) in the rat. *J Pharmacol Exp Ther*. **241**(2): p. 642-9.
491. Raiteri, M., G. Maura, and P. Versace (1983). Functional evidence for two stereochemically different alpha-2 adrenoceptors regulating central norepinephrine and serotonin release. *J Pharmacol Exp Ther*. **224**(3): p. 679-84.
492. Isingrini, E., et al. (2016). Resilience to chronic stress is mediated by noradrenergic regulation of dopamine neurons. *Nat Neurosci*. **19**(4): p. 560-3.
493. Grenhoff, J. and T.H. Svensson (1993). Prazosin modulates the firing pattern of dopamine neurons in rat ventral tegmental area. *Eur J Pharmacol*. **233**(1): p. 79-84.
494. Guiard, B.P., et al. (2008). Functional interactions between dopamine, serotonin and norepinephrine neurons: an in-vivo electrophysiological study in rats with monoaminergic lesions. *Int J Neuropsychopharmacol*. **11**(5): p. 625-39.
495. Lategan, A.J., M.R. Marien, and F.C. Colpaert (1990). Effects of locus coeruleus lesions on the release of endogenous dopamine in the rat nucleus accumbens and caudate nucleus as determined by intracerebral microdialysis. *Brain Res*. **523**(1): p. 134-8.
496. Guiard, B.P., M. El Mansari, and P. Blier (2008). Cross-talk between dopaminergic and noradrenergic systems in the rat ventral tegmental area, locus ceruleus, and dorsal hippocampus. *Mol Pharmacol*. **74**(5): p. 1463-75.
497. Katz, N.S., et al. (2010). Effects of acute and sustained administration of the catecholamine reuptake inhibitor nomifensine on the firing activity of monoaminergic neurons. *J Psychopharmacol*. **24**(8): p. 1223-35.
498. Reith, M.E., M.Y. Li, and Q.S. Yan (1997). Extracellular dopamine, norepinephrine, and serotonin in the ventral tegmental area and nucleus accumbens of freely moving rats during intracerebral dialysis following systemic administration of cocaine and other uptake blockers. *Psychopharmacology (Berl)*. **134**(3): p. 309-17.
499. Jones, C., D. Hoyer, and J. Palacios (1990). Adrenoceptor autoradiography. *The Pharmacology of Noradrenaline in the Central Nervous System*. p. 41-75.
500. Arencibia-Albite, F., et al. (2007). Noradrenergic modulation of the hyperpolarization-activated cation current (Ih) in dopamine neurons of the ventral tegmental area. *Neuroscience*. **149**(2): p. 303-14.

501. White, F.J. and R.Y. Wang (1984). Pharmacological characterization of dopamine autoreceptors in the rat ventral tegmental area: microiontophoretic studies. *J Pharmacol Exp Ther*. **231**(2): p. 275-80.
502. Aghajanian, G.K. and B.S. Bunney (1977). Dopamine"autoreceptors": pharmacological characterization by microiontophoretic single cell recording studies. *Naunyn Schmiedebergs Arch Pharmacol*. **297**(1): p. 1-7.
503. Aghajanian, G.K. and B.S. Bunney (1977). Pharmacological characterization of dopamine "autoreceptors" by microiontophoretic single-cell recording studies. *Adv Biochem Psychopharmacol*. **16**: p. 433-8.
504. Jiménez-Rivera, C.A., et al. (2012). Presynaptic inhibition of glutamate transmission by α2 receptors in the VTA. *European Journal of Neuroscience*. **35**(9): p. 1406-1415.
505. Grenhoff, J., R.A. North, and S.W. Johnson (1995). Alpha 1-adrenergic effects on dopamine neurons recorded intracellularly in the rat midbrain slice. *Eur J Neurosci*. **7**(8): p. 1707-13.
506. Collingridge, G.L., T.A. James, and N.K. MacLeod (1979). Neurochemical and electrophysiological evidence for a projection from the locus coeruleus to the substantia nigra [proceedings]. *J Physiol*. **290**(2): p. 44P.
507. Grenhoff, J., et al. (1993). Noradrenergic modulation of midbrain dopamine cell firing elicited by stimulation of the locus coeruleus in the rat. *J Neural Transm Gen Sect*. **93**(1): p. 11-25.
508. Grenhoff, J. and T.H. Svensson (1988). Clonidine regularizes substantia nigra dopamine cell firing. *Life Sci*. **42**(20): p. 2003-9.
509. Grenhoff, J. and T.H. Svensson (1989). Clonidine modulates dopamine cell firing in rat ventral tegmental area. *Eur J Pharmacol*. **165**(1): p. 11-8.
510. Garris, P.A., et al. (1994). Efflux of dopamine from the synaptic cleft in the nucleus accumbens of the rat brain. *The Journal of neuroscience*. **14**(10): p. 6084-6093.
511. Velasquez-Martinez, M.C., R. Vazquez-Torres, and C.A. Jimenez-Rivera (2012). Activation of alpha1-adrenoceptors enhances glutamate release onto ventral tegmental area dopamine cells. *Neuroscience*. **216**: p. 18-30.
512. Velasquez-Martinez, M.C., et al. (2015). Alpha-1 adrenoreceptors modulate GABA release onto ventral tegmental area dopamine neurons. *Neuropharmacology*. **88**: p. 110-21.
513. Overton, P.G. and D. Clark (1997). Burst firing in midbrain dopaminergic neurons. *Brain Res Brain Res Rev*. **25**(3): p. 312-34.
514. White, F.J. (1996). Synaptic regulation of mesocorticolimbic dopamine neurons. *Annu Rev Neurosci*. **19**: p. 405-36.
515. Bayer, V.E. and V.M. Pickel (1990). Ultrastructural localization of tyrosine hydroxylase in the rat ventral tegmental area: relationship between immunolabeling density and neuronal associations. *J Neurosci*. **10**(9): p. 2996-3013.
516. Tan, K.R., et al. (2012). GABA neurons of the VTA drive conditioned place aversion. *Neuron*. **73**(6): p. 1173-83.
517. Gao, D.M., et al. (1990). Intensity-dependent nociceptive responses from presumed dopaminergic neurons of the substantia nigra, pars compacta in the rat and their modification by lateral habenula inputs. *Brain Res*. **529**(1-2): p. 315-9.

518. Luo, A.H., F.E. Georges, and G.S. Aston-Jones (2008). Novel neurons in ventral tegmental area fire selectively during the active phase of the diurnal cycle. *Eur J Neurosci*. **27**(2): p. 408-22.
519. Mileykovskiy, B. and M. Morales (2011). Duration of inhibition of ventral tegmental area dopamine neurons encodes a level of conditioned fear. *J Neurosci*. **31**(20): p. 7471-6.
520. Ungless, M.A., P.J. Magill, and J.P. Bolam (2004). Uniform inhibition of dopamine neurons in the ventral tegmental area by aversive stimuli. *Science*. **303**(5666): p. 2040-2.
521. Aston-Jones, G. and F.E. Bloom (1981). Norepinephrine-containing locus coeruleus neurons in behaving rats exhibit pronounced responses to non-noxious environmental stimuli. *J Neurosci*. **1**(8): p. 887-900.
522. Fiorillo, C.D. (2013). Two dimensions of value: dopamine neurons represent reward but not aversiveness. *Science*. **341**(6145): p. 546-9.
523. Pozzi, L., et al. (1994). Evidence that extracellular concentrations of dopamine are regulated by noradrenergic neurons in the frontal cortex of rats. *J Neurochem*. **63**(1): p. 195-200.
524. Herve, D., et al. (1982). Reduction of dopamine utilization in the prefrontal cortex but not in the nucleus accumbens after selective destruction of noradrenergic fibers innervating the ventral tegmental area in the rat. *Brain Res*. **237**(2): p. 510-6.
525. Kawahara, H., Y. Kawahara, and B.H. Westerink (2001). The noradrenaline-dopamine interaction in the rat medial prefrontal cortex studied by multi-probe microdialysis. *Eur J Pharmacol*. **418**(3): p. 177-86.
526. Berger, B., et al. (1974). Histochemical confirmation for dopaminergic innervation of the rat cerebral cortex after destruction of the noradrenergic ascending pathways. *Brain Res*. **81**(2): p. 332-7.
527. Thierry, A.M., et al. (1973). Dopaminergic terminals in the rat cortex. *Science*. **182**(4111): p. 499-501.
528. Gresch, P.J., et al. (1995). Local influence of endogenous norepinephrine on extracellular dopamine in rat medial prefrontal cortex. *J Neurochem*. **65**(1): p. 111-6.
529. Gobert, A., et al. (1998). Simultaneous quantification of serotonin, dopamine and noradrenaline levels in single frontal cortex dialysates of freely-moving rats reveals a complex pattern of reciprocal auto- and heteroreceptor-mediated control of release. *Neuroscience*. **84**(2): p. 413-29.
530. Gobert, A., et al. (1997). Alpha2-adrenergic receptor blockade markedly potentiates duloxetine- and fluoxetine-induced increases in noradrenaline, dopamine, and serotonin levels in the frontal cortex of freely moving rats. *J Neurochem*. **69**(6): p. 2616-9.
531. Yamamoto, B.K. and S. Novotney (1998). Regulation of extracellular dopamine by the norepinephrine transporter. *J Neurochem*. **71**(1): p. 274-80.
532. Carter, C.J. and C.J. Pycock (1980). Behavioural and biochemical effects of dopamine and noradrenaline depletion within the medial prefrontal cortex of the rat. *Brain Res*. **192**(1): p. 163-76.

533. Tassin, J.P., et al. (1979). Collateral sprouting and reduced activity of the rat mesocortical dopaminergic neurons after selective destruction of the ascending noradrenergic bundles. *Neuroscience*. **4**(11): p. 1569-82.
534. Rossetti, Z.L., et al. (1989). Brain dialysis provides evidence for D2-dopamine receptors modulating noradrenaline release in the rat frontal cortex. *Eur J Pharmacol*. **163**(2-3): p. 393-5.
535. El Mansari, M., et al. (2010). Relevance of norepinephrine-dopamine interactions in the treatment of major depressive disorder. *CNS Neurosci Ther*. **16**(3): p. e1-17.
536. Arnsten, A.F. (2009). Toward a new understanding of attention-deficit hyperactivity disorder pathophysiology: an important role for prefrontal cortex dysfunction. *CNS Drugs*. **23 Suppl 1**: p. 33-41.
537. Mesholam-Gately, R.I., et al. (2009). Neurocognition in first-episode schizophrenia: a meta-analytic review. *Neuropsychology*. **23**(3): p. 315-36.
538. Adler, L.E., M.C. Waldo, and R. Freedman (1985). Neurophysiologic studies of sensory gating in schizophrenia: comparison of auditory and visual responses. *Biol Psychiatry*. **20**(12): p. 1284-96.
539. Boutros, N.N., et al. (1999). Comparison of four components of sensory gating in schizophrenia and normal subjects: a preliminary report. *Psychiatry Res*. **88**(2): p. 119-30.
540. Freedman, R., et al. (1983). Neurophysiological evidence for a defect in inhibitory pathways in schizophrenia: comparison of medicated and drug-free patients. *Biol Psychiatry*. **18**(5): p. 537-51.
541. Venables, P.H. (1964). Input Dysfunction in Schizophrenia. *Prog Exp Pers Res*. **72**: p. 1-47.
542. Anonymous. (1985), Schizophrenia-a Mother`s Agony Over Her Son`s Pain, *Chicago Tribune,* 5: pp. 1-3
543. Graham, F.K. (1975). Presidential Address, 1974. The more or less startling effects of weak prestimulation. *Psychophysiology*. **12**(3): p. 238-48.
544. Hoffman, H.S. and J.L. Searle (1965). Acoustic Variables in the Modification of Startle Reaction in the Rat. *J Comp Physiol Psychol*. **60**: p. 53-8.
545. Ison, J.R. and G.R. Hammond (1971). Modification of the startle reflex in the rat by changes in the auditory and visual environments. *J Comp Physiol Psychol*. **75**(3): p. 435-52.
546. Pinckney, L.A. (1976). Inhibition of the startle reflex in the rat by prior tactile stimulation. *Animal Learning & Behavior*. **4**(4): p. 467-472.
547. Buckland, G., et al. (1969). Inhibition of startle response to acoustic stimulation produced by visual prestimulation. *J Comp Physiol Psychol*. **67**(4): p. 493-6.
548. Swerdlow, N.R., et al. (1994). Assessing the validity of an animal model of deficient sensorimotor gating in schizophrenic patients. *Arch Gen Psychiatry*. **51**(2): p. 139-54.
549. Eccles, J.C. (1969). The inhibitory pathways of the central nervous system (Vol. 9): Thomas.
550. Freedman, R., et al. (1987). Neurobiological studies of sensory gating in schizophrenia. *Schizophr Bull*. **13**(4): p. 669-78.

551. Breier, M.R., et al. (2010). Sensory and sensorimotor gating-disruptive effects of apomorphine in Sprague Dawley and Long Evans rats. *Behav Brain Res*. **208**(2): p. 560-5.
552. Brenner, C.A., et al. (2004). P50 and acoustic startle gating are not related in healthy participants. *Psychophysiology*. **41**(5): p. 702-8.
553. Nagamoto, H.T., et al. (1989). Sensory gating in schizophrenics and normal controls: effects of changing stimulation interval. *Biol Psychiatry*. **25**(5): p. 549-61.
554. Swerdlow, N.R., et al. (2006). Convergence and divergence in the neurochemical regulation of prepulse inhibition of startle and N40 suppression in rats. *Neuropsychopharmacology*. **31**(3): p. 506-15.
555. Fuster, J.M. and R.F. Docter (1962). Variations of optic evoked potentials as a function of reticular activity in rabbits with chronically implanted electrodes. *J Neurophysiol*. **25**: p. 324-36.
556. Lindsley, D.F. and W.R. Adey (1961). Availability of peripheral input to the midbrain reticular formation. *Exp Neurol*. **4**: p. 358-76.
557. Schwartz, M. and C. Shagass (1963). Reticular modification of somatosensory cortical recovery function. *Electroencephalogr Clin Neurophysiol*. **15**: p. 265-71.
558. Ison, J.R., D.W. McAdam, and G.R. Hammond (1973). Latency and amplitude changes in the acoustic startle reflex of the rat produced by variation in auditory prestimulation. *Physiol Behav*. **10**(6): p. 1035-9.
559. Szabo, I. (1965). Analysis of the muscular action potentials accompanying the acoustic startle reaction. *Acta physiol. Acad. sci. hung*. **27**: p. 167-178.
560. Pilz, P.K., M. Caeser, and J. Ostwald (1988). Comparative threshold studies of the acoustic pinna, jaw and startle reflex in the rat. *Physiol Behav*. **43**(4): p. 411-5.
561. Caeser, M., J. Ostwald, and P.K. Pilz (1989). Startle responses measured in muscles innervated by facial and trigeminal nerves show common modulation. *Behavioral neuroscience*. **103**(5): p. 1075.
562. Davis, M. (1980). Neurochemical modulation of sensory-motor reactivity: acoustic and tactile startle reflexes. *Neurosci Biobehav Rev*. **4**(2): p. 241-63.
563. Davis, M., et al. (1982). A primary acoustic startle circuit: lesion and stimulation studies. *The journal of neuroscience*. **2**(6): p. 791-805.
564. Leitner, D.S., A.S. Powers, and H.S. Hoffman (1980). The neural substrate of the startle response. *Physiol Behav*. **25**(2): p. 291-7.
565. Carlson, S. and J.F. Willott (1998). Caudal pontine reticular formation of C57BL/6J mice: responses to startle stimuli, inhibition by tones, and plasticity. *J Neurophysiol*. **79**(5): p. 2603-14.
566. Lingenhohl, K. and E. Friauf (1994). Giant neurons in the rat reticular formation: a sensorimotor interface in the elementary acoustic startle circuit? *J Neurosci*. **14**(3 Pt 1): p. 1176-94.
567. Wu, M.F., S.S. Suzuki, and J.M. Siegel (1988). Anatomical distribution and response patterns of reticular neurons active in relation to acoustic startle. *Brain Res*. **457**(2): p. 399-406.
568. Fendt, M., L. Li, and J.S. Yeomans (2001). Brain stem circuits mediating prepulse inhibition of the startle reflex. *Psychopharmacology (Berl)*. **156**(2-3): p. 216-24.
569. Koch, M. (1999). The neurobiology of startle. *Prog Neurobiol*. **59**(2): p. 107-28.

570. Swerdlow, N.R., et al. (1992). The neural substrates of sensorimotor gating of the startle reflex: a review of recent findings and their implications. *J Psychopharmacol*. **6**(2): p. 176-90.
571. Swerdlow, N.R., M.A. Geyer, and D.L. Braff (2001). Neural circuit regulation of prepulse inhibition of startle in the rat: current knowledge and future challenges. *Psychopharmacology (Berl)*. **156**(2-3): p. 194-215.
572. Koch, M., M. Kungel, and H. Herbert (1993). Cholinergic neurons in the pedunculopontine tegmental nucleus are involved in the mediation of prepulse inhibition of the acoustic startle response in the rat. *Exp Brain Res*. **97**(1): p. 71-82.
573. Koch, M., M. Fendt, and B.D. Kretschmer (2000). Role of the substantia nigra pars reticulata in sensorimotor gating, measured by prepulse inhibition of startle in rats. *Behav Brain Res*. **117**(1-2): p. 153-62.
574. Swerdlow, N.R., D. Braff, and M. Geyer (2000). Animal models of deficient sensorimotor gating: what we know, what we think we know, and what we hope to know soon. *Behavioural pharmacology*. **11**(3/4): p. 185-204.
575. Swerdlow, N.R. and M.A. Geyer (1998). Using an animal model of deficient sensorimotor gating to study the pathophysiology and new treatments of schizophrenia. *Schizophr Bull*. **24**(2): p. 285-301.
576. Arime, Y., et al. (2012). Cortico-subcortical neuromodulation involved in the amelioration of prepulse inhibition deficits in dopamine transporter knockout mice. *Neuropsychopharmacology*. **37**(11): p. 2522-30.
577. Mansbach, R.S., M.A. Geyer, and D.L. Braff (1988). Dopaminergic stimulation disrupts sensorimotor gating in the rat. *Psychopharmacology (Berl)*. **94**(4): p. 507-14.
578. Swerdlow, N.R., et al. (1986). Central dopamine hyperactivity in rats mimics abnormal acoustic startle response in schizophrenics. *Biol Psychiatry*. **21**(1): p. 23-33.
579. Rigdon, G.C. (1990). Differential effects of apomorphine on prepulse inhibition of acoustic startle reflex in two rat strains. *Psychopharmacology (Berl)*. **102**(3): p. 419-21.
580. Swerdlow, N.R., et al. (2005). Reduced startle gating after D1 blockade: effects of concurrent D2 blockade. *Pharmacol Biochem Behav*. **82**(2): p. 293-9.
581. Stevens, K.E., L.L. Fuller, and G.M. Rose (1991). Dopaminergic and noradrenergic modulation of amphetamine-induced changes in auditory gating. *Brain Res*. **555**(1): p. 91-8.
582. Pouzet, B., M.P. Andersen, and S. Hogg (2005). Effects of acute treatment with antidepressant drugs on sensorimotor gating deficits in rats. *Psychopharmacology (Berl)*. **178**(1): p. 9-16.
583. Mansbach, R.S., D.L. Braff, and M.A. Geyer (1989). Prepulse inhibition of the acoustic startle response is disrupted by N-ethyl-3,4-methylenedioxyamphetamine (MDEA) in the rat. *Eur J Pharmacol*. **167**(1): p. 49-55.
584. Swerdlow, N.R., et al. (1995). Increased sensitivity to the sensorimotor gating-disruptive effects of apomorphine after lesions of medial prefrontal cortex or ventral hippocampus in adult rats. *Psychopharmacology (Berl)*. **122**(1): p. 27-34.

585. Csomor, P.A., et al. (2007). Haloperidol Differentially Modulates Prepulse Inhibition and P50 Suppression in Healthy Humans Stratified for Low and High Gating Levels. *Neuropsychopharmacology*. **33**(3): p. 497-512.
586. Oranje, B., et al. (2002). Modulating sensory gating in healthy volunteers: The effects of ketamine and haloperidol. *Biological Psychiatry*. **52**(9): p. 887-895.
587. Witten, L., et al. (2016). Comparing Pharmacological Modulation of Sensory Gating in Healthy Humans and Rats: The Effects of Reboxetine and Haloperidol. *Neuropsychopharmacology*. **41**(2): p. 638-45.
588. Adler, L.E., G. Rose, and R. Freedman (1986). Neurophysiological studies of sensory gating in rats: effects of amphetamine, phencyclidine, and haloperidol. *Biol Psychiatry*. **21**(8-9): p. 787-98.
589. Siegel, S.J., et al. (2005). Monoamine reuptake inhibition and nicotine receptor antagonism reduce amplitude and gating of auditory evoked potentials. *Neuroscience*. **133**(3): p. 729-38.
590. Ford, C.P. (2014). The role of D2-autoreceptors in regulating dopamine neuron activity and transmission. *Neuroscience*. **282C**: p. 13-22.
591. Yamashita, M., et al. (2006). Norepinephrine transporter blockade can normalize the prepulse inhibition deficits found in dopamine transporter knockout mice. *Neuropsychopharmacology*. **31**(10): p. 2132-9.
592. Swerdlow, N.R., et al. (1990). Amphetamine disruption of prepulse inhibition of acoustic startle is reversed by depletion of mesolimbic dopamine. *Psychopharmacology (Berl)*. **100**(3): p. 413-6.
593. Swerdlow, N.R., S.B. Caine, and M.A. Geyer (1992). Regionally selective effects of intracerebral dopamine infusion on sensorimotor gating of the startle reflex in rats. *Psychopharmacology (Berl)*. **108**(1-2): p. 189-95.
594. Humby, T., et al. (1996). Prepulses inhibit startle-induced reductions of extracellular dopamine in the nucleus accumbens of rat. *J Neurosci*. **16**(6): p. 2149-56.
595. Dissanayake, D.W., et al. (2008). Auditory gating in rat hippocampus and medial prefrontal cortex: effect of the cannabinoid agonist WIN55,212-2. *Neuropharmacology*. **55**(8): p. 1397-404.
596. Dissanayake, D.W., et al. (2009). Effects of phencyclidine on auditory gating in the rat hippocampus and the medial prefrontal cortex. *Brain Res*. **1298**: p. 153-60.
597. Mears, R.P., N.N. Boutros, and H.C. Cromwell (2009). Reduction of prelimbic inhibitory gating of auditory evoked potentials after fear conditioning. *Behav Neurosci*. **123**(2): p. 315-27.
598. Mears, R.P., A.C. Klein, and H.C. Cromwell (2006). Auditory inhibitory gating in medial prefrontal cortex: Single unit and local field potential analysis. *Neuroscience*. **141**(1): p. 47-65.
599. Japha, K. and M. Koch (1999). Picrotoxin in the medial prefrontal cortex impairs sensorimotor gating in rats: reversal by haloperidol. *Psychopharmacology (Berl)*. **144**(4): p. 347-54.
600. Lacroix, L., et al. (2000). The effects of ibotenic acid lesions of the medial and lateral prefrontal cortex on latent inhibition, prepulse inhibition and amphetamine-induced hyperlocomotion. *Neuroscience*. **97**(3): p. 459-68.

601. Yee, B.K. (2000). Cytotoxic lesion of the medial prefrontal cortex abolishes the partial reinforcement extinction effect, attenuates prepulse inhibition of the acoustic startle reflex and induces transient hyperlocomotion, while sparing spontaneous object recognition memory in the rat. *Neuroscience*. **95**(3): p. 675-89.
602. Koch, M. and M. Bubser (1994). Deficient sensorimotor gating after 6-hydroxydopamine lesion of the rat medial prefrontal cortex is reversed by haloperidol. *Eur J Neurosci*. **6**(12): p. 1837-45.
603. Bubser, M. and M. Koch (1994). Prepulse inhibition of the acoustic startle response of rats is reduced by 6-hydroxydopamine lesions of the medial prefrontal cortex. *Psychopharmacology (Berl)*. **113**(3-4): p. 487-92.
604. Ellenbroek, B.A., S. Budde, and A.R. Cools (1996). Prepulse inhibition and latent inhibition: the role of dopamine in the medial prefrontal cortex. *Neuroscience*. **75**(2): p. 535-42.
605. Shoemaker, J.M., et al. (2005). Prefrontal D1 and ventral hippocampal N-methyl-D-aspartate regulation of startle gating in rats. *Neuroscience*. **135**(2): p. 385-94.
606. Taber, M.T. and H.C. Fibiger (1995). Electrical stimulation of the prefrontal cortex increases dopamine release in the nucleus accumbens of the rat: modulation by metabotropic glutamate receptors. *The Journal of neuroscience*. **15**(5): p. 3896-3904.
607. Karreman, M. and B. Moghaddam (1996). The prefrontal cortex regulates the basal release of dopamine in the limbic striatum: an effect mediated by ventral tegmental area. *Journal of neurochemistry*. **66**(2): p. 589-598.
608. Overton, P., Z.-Y. Tong, and D. Clark (1996). A pharmacological analysis of the burst events induced in midbrain dopaminergic neurons by electrical stimulation of the prefrontal cortex in the rat. *Journal of neural transmission*. **103**(5): p. 523-540.
609. Westerink, B.H., et al. (1998). The pharmacology of mesocortical dopamine neurons: a dual-probe microdialysis study in the ventral tegmental area and prefrontal cortex of the rat brain. *Journal of Pharmacology and Experimental Therapeutics*. **285**(1): p. 143-154.
610. Jaskiw, G.E., D.R. Weinberger, and J.N. Crawley (1991). Microinjection of apomorphine into the prefrontal cortex of the rat reduces dopamine metabolite concentrations in microdialysate from the caudate nucleus. *Biological psychiatry*. **29**(7): p. 703-706.
611. Louilot, A., M. Le Moal, and H. Simon (1989). Opposite influences of dopaminergic pathways to the prefrontal cortex or the septum on the dopaminergic transmission in the nucleus accumbens. An in vivo voltammetric study. *Neuroscience*. **29**(1): p. 45-56.
612. Pycock, C.J., C.J. Carter, and R.W. Kerwin (1980). Effect of 6-hydroxydopamine lesions of the medial prefrontal cortex on neurotransmitter systems in subcortical sites in the rat. *J Neurochem*. **34**(1): p. 91-9.
613. Pycock, C.J., R.W. Kerwin, and C.J. Carter (1980). Effect of lesion of cortical dopamine terminals on subcortical dopamine receptors in rats. *Nature*. **286**(5768): p. 74-6.
614. Sesack, S.R. and V.M. Pickel (1992). Prefrontal cortical efferents in the rat synapse on unlabeled neuronal targets of catecholamine terminals in the nucleus accumbens

septi and on dopamine neurons in the ventral tegmental area. *J Comp Neurol*. **320**(2): p. 145-60.
615. Leonard, C.M. (1969). The prefrontal cortex of the rat. I. Cortical projection of the mediodorsal nucleus. II. Efferent connections. *Brain Res*. **12**(2): p. 321-43.
616. Beckstead, R.M. (1979). An autoradiographic examination of corticocortical and subcortical projections of the mediodorsal-projection (prefrontal) cortex in the rat. *J Comp Neurol*. **184**(1): p. 43-62.
617. Romo, R., et al. (1986). In vivo presynaptic control of dopamine release in the cat caudate nucleus--I. Opposite changes in neuronal activity and release evoked from thalamic motor nuclei. *Neuroscience*. **19**(4): p. 1067-79.
618. Youngren, K.D., D.A. Daly, and B. Moghaddam (1993). Distinct actions of endogenous excitatory amino acids on the outflow of dopamine in the nucleus accumbens. *J Pharmacol Exp Ther*. **264**(1): p. 289-93.
619. Wan, F.J., M.A. Geyer, and N.R. Swerdlow (1995). Presynaptic dopamine-glutamate interactions in the nucleus accumbens regulate sensorimotor gating. *Psychopharmacology (Berl)*. **120**(4): p. 433-41.
620. Sesack, S.R. and V.M. Pickel (1990). In the rat medial nucleus accumbens, hippocampal and catecholaminergic terminals converge on spiny neurons and are in apposition to each other. *Brain Res*. **527**(2): p. 266-79.
621. Murase, S., et al. (1993). Prefrontal cortex regulates burst firing and transmitter release in rat mesolimbic dopamine neurons studied in vivo. *Neuroscience letters*. **157**(1): p. 53-56.
622. Thierry, A.M., J.M. Deniau, and J. Feger (1979). Effects of stimulation of the frontal cortex on identified output VMT cells in the rat. *Neurosci Lett*. **15**(2-3): p. 102-7.
623. Liang, R.Z., et al. (1991). Effects of dopamine agonists on excitatory inputs to nucleus accumbens neurons from the amygdala: modulatory actions of cholecystokinin. *Brain Res*. **554**(1-2): p. 85-94.
624. Yang, C.R. and G.J. Mogenson (1984). Electrophysiological responses of neurones in the nucleus accumbens to hippocampal stimulation and the attenuation of the excitatory responses by the mesolimbic dopaminergic system. *Brain Res*. **324**(1): p. 69-84.
625. Yim, C.Y. and G.J. Mogenson (1982). Response of nucleus accumbens neurons to amygdala stimulation and its modification by dopamine. *Brain Res*. **239**(2): p. 401-15.
626. Yim, C.Y. and G.J. Mogenson (1986). Mesolimbic dopamine projection modulates amygdala-evoked EPSP in nucleus accumbens neurons: an in vivo study. *Brain Res*. **369**(1-2): p. 347-52.
627. Yim, C.Y. and G.J. Mogenson (1988). Neuromodulatory action of dopamine in the nucleus accumbens: an in vivo intracellular study. *Neuroscience*. **26**(2): p. 403-15.
628. Broersen, L.M., J. Feldon, and I. Weiner (1999). Dissociative effects of apomorphine infusions into the medial prefrontal cortex of rats on latent inhibition, prepulse inhibition and amphetamine-induced locomotion. *Neuroscience*. **94**(1): p. 39-46.

629. Lacroix, L., et al. (2000). Effects of local infusions of dopaminergic drugs into the medial prefrontal cortex of rats on latent inhibition, prepulse inhibition and amphetamine induced activity. *Behav Brain Res*. **107**(1-2): p. 111-21.
630. Grace, A.A. (2000). Gating of information flow within the limbic system and the pathophysiology of schizophrenia. *Brain Res Brain Res Rev*. **31**(2-3): p. 330-41.
631. Carter, C.J. and C.J. Pycock (1980). Behavioural and biochemical effects of dopamine and noradrenaline depletion within the medial prefrontal cortex of the rat. *Brain Research*. **192**(1): p. 163-176.
632. Wan, F.J. and N.R. Swerdlow (1993). Intra-accumbens infusion of quinpirole impairs sensorimotor gating of acoustic startle in rats. *Psychopharmacology (Berl)*. **113**(1): p. 103-9.
633. Wan, F.J., M.A. Geyer, and N.R. Swerdlow (1994). Accumbens D2 modulation of sensorimotor gating in rats: assessing anatomical localization. *Pharmacol Biochem Behav*. **49**(1): p. 155-63.
634. Yamada, S., M. Harano, and M. Tanaka (1998). Dopamine autoreceptors in rat nucleus accumbens modulate prepulse inhibition of acoustic startle. *Pharmacol Biochem Behav*. **60**(4): p. 803-8.
635. Paladini, C.A. and J.T. Williams (2004). Noradrenergic inhibition of midbrain dopamine neurons. *J Neurosci*. **24**(19): p. 4568-75.
636. Inyushin, M.U., et al. (2010). Alpha-2 noradrenergic receptor activation inhibits the hyperpolarization-activated cation current (Ih) in neurons of the ventral tegmental area. *Neuroscience*. **167**(2): p. 287-97.
637. Paxinos, G. and C. Watson (2007). The Rat Brain in Stereotaxic Coordinates, 6th edition. *Elsevier Inc*.
638. Aghajanian, G.K. and C.P. Vandermaelen (1982). Intracellular identification of central noradrenergic and serotonergic neurons by a new double labeling procedure. *J Neurosci*. **2**(12): p. 1786-92.
639. Aghajanian, G.K. (1982). Central noradrenergic neurons: a locus for the functional interplay between alpha-2 adrenoceptors and opiate receptors. *J Clin Psychiatry*. **43**(6 Pt 2): p. 20-4.
640. Belitski, A., et al. (2008). Low-Frequency Local Field Potentials and Spikes in Primary Visual Cortex Convey Independent Visual Information. *The Journal of Neuroscience*. **28**(22): p. 5696-5709.
641. Bartho, P., et al. (2004). Characterization of neocortical principal cells and interneurons by network interactions and extracellular features. *J Neurophysiol*. **92**(1): p. 600-8.
642. Connors, B.W. and M.J. Gutnick (1990). Intrinsic firing patterns of diverse neocortical neurons. *Trends Neurosci*. **13**(3): p. 99-104.
643. Andermann, M.L., et al. (2004). Neural correlates of vibrissa resonance; band-pass and somatotopic representation of high-frequency stimuli. *Neuron*. **42**(3): p. 451-63.
644. Baeg, E.H., et al. (2001). Fast spiking and regular spiking neural correlates of fear conditioning in the medial prefrontal cortex of the rat. *Cereb Cortex*. **11**(5): p. 441-51.

645. Gardner, R.J., S.W. Hughes, and M.W. Jones (2013). Differential spike timing and phase dynamics of reticular thalamic and prefrontal cortical neuronal populations during sleep spindles. *J Neurosci*. **33**(47): p. 18469-80.
646. Spanagel, R. and M. Shoaib (1994). Involvement of Mesolimbic Kappa-Opioid Systems in the Discriminative Stimulus Effects of Morphine. *Neuroscience*. **63**(3): p. 797-804.
647. Borowski, T.B. and L. Kokkinidis (1996). Contribution of ventral tegmental area dopamine neurons to expression of conditional fear: effects of electrical stimulation, excitotoxin lesions, and quinpirole infusion on potentiated startle in rats. *Behav Neurosci*. **110**(6): p. 1349-64.
648. Munro, L.J. and L. Kokkinidis (1997). Infusion of quinpirole and muscimol into the ventral tegmental area inhibits fear-potentiated startle: implications for the role of dopamine in fear expression. *Brain Res*. **746**(1-2): p. 231-8.
649. Myers, R.D. (1966). Injection of Solutions into Cerebral Tissue - Relation between Volume and Diffusion. *Physiology & Behavior*. **1**(2): p. 171-&.
650. Myers, R.D. (1974). Handbook of drug and chemical stimulation of the brain: behavioral, pharmacological, and physiological aspects: Van Nostrand Reinhold Co.
651. Routtenberg, A. (1972). Intracranial chemical injection and behavior: a critical review. *Behav Biol*. **7**(5): p. 601-41.
652. Peterson, S.L. (1998). Drug microinjection in discrete brain regions. *Kopf Carrier*. **50**: p. 1-6.
653. Light, G.A. and D.L. Braff (2001). Measuring P50 suppression and prepulse inhibition in a single recording session. *Am J Psychiatry*. **158**(12): p. 2066-8.
654. Detari, L., D.D. Rasmusson, and K. Semba (1997). Phasic relationship between the activity of basal forebrain neurons and cortical EEG in urethane-anesthetized rat. *Brain Res*. **759**(1): p. 112-21.
655. Erchova, I.A., M.A. Lebedev, and M.E. Diamond (2002). Somatosensory cortical neuronal population activity across states of anaesthesia. *Eur J Neurosci*. **15**(4): p. 744-52.
656. Robinson, T.E., R.C. Kramis, and C.H. Vanderwolf (1977). Two types of cerebral activation during active sleep: relations to behavior. *Brain Res*. **124**(3): p. 544-9.
657. Wolansky, T., et al. (2006). Hippocampal slow oscillation: a novel EEG state and its coordination with ongoing neocortical activity. *J Neurosci*. **26**(23): p. 6213-29.
658. Freeman, W.J., et al. (2000). Spatial spectral analysis of human electrocorticograms including the alpha and gamma bands. *Journal of Neuroscience Methods*. **95**(2): p. 111-121.
659. Miller, K.J., et al. (2009). Power-law scaling in the brain surface electric potential. *PLoS Comput Biol*. **5**(12): p. e1000609.
660. Milstein, J., et al. (2009). Neuronal shot noise and Brownian 1/f 2 behavior in the local field potential. *PloS one*. **4**(2): p. e4338.
661. Olpe, H.R., et al. (1980). Some electrophysiological and pharmacological properties of the cortical, noradrenergic projection of the locus coeruleus in the rat. *Brain Res*. **186**(1): p. 9-19.

662. Sato, H., K. Fox, and N.W. Daw (1989). Effect of electrical stimulation of locus coeruleus on the activity of neurons in the cat visual cortex. *J Neurophysiol*. **62**(4): p. 946-58.
663. Waterhouse, B.D., et al. (2000). Differential modulatory effects of norepinephrine on synaptically driven responses of layer V barrel field cortical neurons. *Brain Res*. **868**(1): p. 39-47.
664. Yi, F., et al. (2013). Signaling mechanism underlying (2A)-adrenergic suppression of excitatory synaptic transmission in the medial prefrontal cortex of rats. *European Journal of Neuroscience*. **38**(3): p. 2364-2373.
665. Nakamura, S. (1977). Some electrophysiological properties of neurones of rat locus coeruleus. *J Physiol*. **267**(3): p. 641-58.
666. Simson, P.E. and J.M. Weiss (1987). Alpha-2 receptor blockade increases responsiveness of locus coeruleus neurons to excitatory stimulation. *J Neurosci*. **7**(6): p. 1732-40.
667. Fries, P., et al. (2001). Modulation of oscillatory neuronal synchronization by selective visual attention. *Science*. **291**(5508): p. 1560-1563.
668. Jones, M.S. and D.S. Barth (1997). Sensory-evoked high-frequency (gamma-band) oscillating potentials in somatosensory cortex of the unanesthetized rat. *Brain Research*. **768**(1-2): p. 167-176.
669. Macdonald, K.D. and D.S. Barth (1995). High-Frequency (Gamma-Band) Oscillating-Potentials in Rat Somatosensory and Auditory-Cortex. *Brain Research*. **694**(1-2): p. 1-12.
670. Pfurtscheller, G. and A. Aranibar (1977). Event-related cortical desynchronization detected by power measurements of scalp EEG. *Electroencephalogr Clin Neurophysiol*. **42**(6): p. 817-26.
671. Tan, A.Y.Y., et al. (2014). Sensory stimulation shifts visual cortex from synchronous to asynchronous states. *Nature*. **509**(7499): p. 226-+.
672. Wiest, M.C. and M.A. Nicolelis (2003). Behavioral detection of tactile stimuli during 7-12 Hz cortical oscillations in awake rats. *Nat Neurosci*. **6**(9): p. 913-4.
673. Lakatos, P., et al. (2005). An oscillatory hierarchy controlling neuronal excitability and stimulus processing in the auditory cortex. *J Neurophysiol*. **94**(3): p. 1904-11.
674. Dinse, H.R., et al. (1997). Low-frequency oscillations of visual, auditory and somatosensory cortical neurons evoked by sensory stimulation. *Int J Psychophysiol*. **26**(1-3): p. 205-27.
675. Mason, P., et al. (2001). Nociceptive responsiveness during slow-wave sleep and waking in the rat. *Sleep*. **24**(1): p. 32-38.
676. McGinley, M.J., et al. (2015). Waking State: Rapid Variations Modulate Neural and Behavioral Responses. *Neuron*. **87**(6): p. 1143-61.
677. Katz, Y., M. Okun, and I. Lampl (2012). Trial-to-trial correlation between thalamic sensory response and global EEG activity. *European Journal of Neuroscience*. **35**(6): p. 826-837.
678. Petersen, C.C.H., et al. (2003). Interaction of sensory responses with spontaneous depolarization in layer 2/3 barrel cortex. *Proceedings of the National Academy of Sciences*. **100**(23): p. 13638-13643.

679. Sachdev, R.N.S., F.F. Ebner, and C.J. Wilson (2004). Effect of Subthreshold Up and Down States on the Whisker-Evoked Response in Somatosensory Cortex. *Journal of Neurophysiology*. **92**(6): p. 3511-3521.
680. Fries, P., D. Nikolic, and W. Singer (2007). The gamma cycle. *Trends in Neurosciences*. **30**(7): p. 309-316.
681. Hasenstaub, A., et al. (2005). Inhibitory postsynaptic potentials carry synchronized frequency information in active cortical networks. *Neuron*. **47**(3): p. 423-435.
682. Mesulam, M.M. (1998). From sensation to cognition. *Brain*. **121 (Pt 6)**: p. 1013-52.
683. Aston-Jones, G. and J.D. Cohen (2005). An integrative theory of locus coeruleus-norepinephrine function: adaptive gain and optimal performance. *Annu Rev Neurosci*. **28**: p. 403-50.
684. Saper, C.B., T.E. Scammell, and J. Lu (2005). Hypothalamic regulation of sleep and circadian rhythms. *Nature*. **437**(7063): p. 1257-63.
685. Segal, D.S. and A.J. Mandell (1970). Behavioral activation of rats during intraventricular infusion of norepinephrine. *Proc Natl Acad Sci U S A*. **66**(2): p. 289-93.
686. Elam, M., T.H. Svensson, and P. Thoren (1986). Locus coeruleus neurons and sympathetic nerves: activation by cutaneous sensory afferents. *Brain Res*. **366**(1-2): p. 254-61.
687. Hajos, M. and G. Engberg (1990). A role of excitatory amino acids in the activation of locus coeruleus neurons following cutaneous thermal stimuli. *Brain Res*. **521**(1-2): p. 325-8.
688. Wemer, J., A.N. Schoffelmeer, and A.H. Mulder (1981). Studies on the role of Na+, K+ and Cl- ion permeabilities in K+-induced release of 3H-noradrenaline from rat brain slices and synaptosomes and in its presynaptic alpha-adrenergic modulation. *Naunyn Schmiedebergs Arch Pharmacol*. **317**(2): p. 103-9.
689. Akhmetova, E.R., et al. (2000). [Participation of D1 dopamine and alpha2 adrenoreceptors in formation of the frequency spectrum of the cortical activity in rats]. *Eksp Klin Farmakol*. **63**(3): p. 7-10.
690. Bol, C.J., J.P. Vogelaar, and J.W. Mandema (1999). Anesthetic profile of dexmedetomidine identified by stimulus-response and continuous measurements in rats. *J Pharmacol Exp Ther*. **291**(1): p. 153-60.
691. Emilien, G. (1989). Effect of drugs acting on monoaminergic and cholinergic systems on the quantified EEG of rats. *Neuropsychobiology*. **21**(4): p. 205-15.
692. Emilien, G. (1990). Effects of clonidine, yohimbine and eserine on the quantified EEG of rats. *Arch Int Pharmacodyn Ther*. **304**: p. 105-24.
693. Fukuda, M., et al. (2013). Effects of the alpha(2)-adrenergic receptor agonist dexmedetomidine on neural, vascular and BOLD fMRI responses in the somatosensory cortex. *Eur J Neurosci*. **37**(1): p. 80-95.
694. Carlsson, A. (1959). The occurence, distribution and physiological role of catecholamines in the nervous system. *Pharmacological Reviews*. **11**(2): p. 490-493.

695. Lamour, Y., J.C. Willer, and G. Guilbaud (1983). Rat somatosensory (SmI) cortex: I. Characteristics of neuronal responses to noxious stimulation and comparison with responses to non-noxious stimulation. *Exp Brain Res*. **49**(1): p. 35-45.
696. Moore, C.I., S.B. Nelson, and M. Sur (1999). Dynamics of neuronal processing in rat somatosensory cortex. *Trends in neurosciences*. **22**(11): p. 513-520.
697. Fukuda, T., et al. (2006). Systemic clonidine activates neurons of the dorsal horn, but not the locus ceruleus (A6) or the A7 area, after a formalin test: the importance of the dorsal horn in the antinociceptive effects of clonidine. *J Anesth*. **20**(4): p. 279-83.
698. Ernsberger, P., et al. (1987). Clonidine binds to imidazole binding sites as well as alpha 2-adrenoceptors in the ventrolateral medulla. *Eur J Pharmacol*. **134**(1): p. 1-13.
699. Ennis, M. and G. Astonjones (1988). Activation of Locus Coeruleus from Nucleus Paragigantocellularis - a New Excitatory Amino-Acid Pathway in Brain. *Journal of Neuroscience*. **8**(10): p. 3644-3657.
700. Ruiz-Ortega, J.A., et al. (1995). The stimulatory effect of clonidine through imidazoline receptors on locus coeruleus noradrenergic neurones is mediated by excitatory amino acids and modulated by serotonin. *Naunyn Schmiedebergs Arch Pharmacol*. **352**(2): p. 121-6.
701. Fernández-Pastor, B. and J.J. Meana (2002). In vivo tonic modulation of the noradrenaline release in the rat cortex by locus coeruleus somatodendritic α2-adrenoceptors. *European Journal of Pharmacology*. **442**(3): p. 225-229.
702. Mateo, Y., J. Pineda, and J.J. Meana (1998). Somatodendritic alpha2-adrenoceptors in the locus coeruleus are involved in the in vivo modulation of cortical noradrenaline release by the antidepressant desipramine. *J Neurochem*. **71**(2): p. 790-8.
703. Mölle, M., et al. (2002). Grouping of Spindle Activity during Slow Oscillations in Human Non-Rapid Eye Movement Sleep. *The Journal of Neuroscience*. **22**(24): p. 10941-10947.
704. Aserinsky, E. and N. Kleitman (1953). Regularly occurring periods of eye motility, and concomitant phenomena, during sleep. *Science*. **118**(3062): p. 273-274.
705. Dement, W. and N. Kleitman (1957). The relation of eye movements during sleep to dream activity: an objective method for the study of dreaming. *Journal of experimental psychology*. **53**(5): p. 339.
706. Muzur, A., E.F. Pace-Schott, and J.A. Hobson (2002). The prefrontal cortex in sleep. *Trends in Cognitive Sciences*. **6**(11): p. 475-481.
707. Steriade, M., R.C. Dossi, and A. Nunez (1991). Network modulation of a slow intrinsic oscillation of cat thalamocortical neurons implicated in sleep delta waves: cortically induced synchronization and brainstem cholinergic suppression. *J Neurosci*. **11**(10): p. 3200-17.
708. Steriade, M. and R. McCarley (2005). Brain control of wakefulness and sleeping: Springer, New York.
709. Steriade, M., F. Amzica, and D. Contreras (1996). Synchronization of fast (30-40 Hz) spontaneous cortical rhythms during brain activation. *J Neurosci*. **16**(1): p. 392-417.

710. LaBerge, S. and L.D.P. Verified (1990). Lucid dreaming: Psychophysiological studies of consciousness during REM sleep.
711. Herweg, N.A., et al. (2016). Theta-Alpha Oscillations Bind the Hippocampus, Prefrontal Cortex, and Striatum during Recollection: Evidence from Simultaneous EEG-fMRI. *J Neurosci*. **36**(12): p. 3579-87.
712. von Stein, A. and J. Sarnthein (2000). Different frequencies for different scales of cortical integration: from local gamma to long range alpha/theta synchronization. *Int J Psychophysiol*. **38**(3): p. 301-13.
713. Zaehle, T., et al. (2011). Transcranial direct current stimulation of the prefrontal cortex modulates working memory performance: combined behavioural and electrophysiological evidence. *BMC Neuroscience*. **12**(1): p. 2.
714. Lagopoulos, J., et al. (2009). Increased theta and alpha EEG activity during nondirective meditation. *The Journal of Alternative and Complementary Medicine*. **15**(11): p. 1187-1192.
715. Nishida, M., et al. (2009). Prefrontal theta during REM sleep enhances emotional memory. *Cereb Cortex*. **19**: p. 1158-1166.
716. Nishida, M., et al. (2009). REM Sleep, Prefrontal Theta, and the Consolidation of Human Emotional Memory. *Cerebral Cortex*. **19**(5): p. 1158-1166.
717. Popa, D., et al. (2010). Coherent amygdalocortical theta promotes fear memory consolidation during paradoxical sleep. *Proc Natl Acad Sci U S A*. **107**(14): p. 6516-9.
718. Anderson, K.L., et al. (2010). Theta oscillations mediate interaction between prefrontal cortex and medial temporal lobe in human memory. *Cereb Cortex*. **20**(7): p. 1604-12.
719. Jensen, O. and C.D. Tesche (2002). Frontal theta activity in humans increases with memory load in a working memory task. *European Journal of Neuroscience*. **15**(8): p. 1395-1399.
720. Sarnthein, J., et al. (1998). Synchronization between prefrontal and posterior association cortex during human working memory. *Proc Natl Acad Sci U S A*. **95**(12): p. 7092-6.
721. Kaplan, R., et al. (2014). Medial prefrontal theta phase coupling during spatial memory retrieval. *Hippocampus*. **24**(6): p. 656-665.
722. Fujisawa, S. and G. Buzsaki (2011). A 4 Hz oscillation adaptively synchronizes prefrontal, VTA, and hippocampal activities. *Neuron*. **72**(1): p. 153-65.
723. Jones, M.W. and M.A. Wilson (2005). Theta rhythms coordinate hippocampal-prefrontal interactions in a spatial memory task. *PLoS Biol*. **3**(12): p. e402.
724. Benchenane, K., et al. (2010). Coherent Theta Oscillations and Reorganization of Spike Timing in the Hippocampal- Prefrontal Network upon Learning. *Neuron*. **66**(6): p. 921-936.
725. Jones, M.W. and M.A. Wilson (2005). Phase precession of medial prefrontal cortical activity relative to the hippocampal theta rhythm. *Hippocampus*. **15**(7): p. 867-73.
726. Aftanas, L.I. and S.A. Golocheikine (2001). Human anterior and frontal midline theta and lower alpha reflect emotionally positive state and internalized attention:

high-resolution EEG investigation of meditation. *Neuroscience Letters*. **310**(1): p. 57-60.
727. Karalis, N., et al. (2016). 4-Hz oscillations synchronize prefrontal-amygdala circuits during fear behavior. *Nat Neurosci*. **19**(4): p. 605-12.
728. Fell, J., et al. (2011). Medial temporal theta/alpha power enhancement precedes successful memory encoding: evidence based on intracranial EEG. *The Journal of Neuroscience*. **31**(14): p. 5392-5397.
729. Klimesch, W. (1997). EEG-alpha rhythms and memory processes. *International Journal of Psychophysiology*. **26**(1-3): p. 319-340.
730. Klimesch, W. (1999). EEG alpha and theta oscillations reflect cognitive and memory performance: a review and analysis. *Brain Research Reviews*. **29**(2-3): p. 169-195.
731. Klimesch, W., et al. (1997). Brain oscillations and human memory: EEG correlates in the upper alpha and theta band. *Neuroscience Letters*. **238**(1-2): p. 9-12.
732. Mizuhara, H., et al. (2004). A long-range cortical network emerging with theta oscillation in a mental task. *NeuroReport*. **15**(8): p. 1233-1238.
733. Buzsaki, G. and A. Draguhn (2004). Neuronal oscillations in cortical networks. *Science*. **304**(5679): p. 1926-9.
734. Kopell, N., et al. (2000). Gamma rhythms and beta rhythms have different synchronization properties. *Proc Natl Acad Sci U S A*. **97**(4): p. 1867-72.
735. Manita, S., et al. (2015). A Top-Down Cortical Circuit for Accurate Sensory Perception. *Neuron*. **86**(5): p. 1304-16.
736. Müller-Putz, G.R., et al. (2007). Event-related beta EEG-changes during passive and attempted foot movements in paraplegic patients. *Brain Research*. **1137**: p. 84-91.
737. Müller, G.R., et al. (2003). Event-related beta EEG changes during wrist movements induced by functional electrical stimulation of forearm muscles in man. *Neuroscience Letters*. **340**(2): p. 143-147.
738. Houdayer, E., et al. (2006). Relationship between event-related beta synchronization and afferent inputs: Analysis of finger movement and peripheral nerve stimulations. *Clinical Neurophysiology*. **117**(3): p. 628-636.
739. Pfurtscheller, G., et al. (2005). Beta rebound after different types of motor imagery in man. *Neuroscience letters*. **378**(3): p. 156-159.
740. Formaggio, E., et al. (2013). Modulation of event-related desynchronization in robot-assisted hand performance: brain oscillatory changes in active, passive and imagined movements. *Journal of neuroengineering and rehabilitation*. **10**(1): p. 1.
741. Donner, T.H. and M. Siegel (2011). A framework for local cortical oscillation patterns. *Trends in Cognitive Sciences*. **15**(5): p. 191-199.
742. Cannon, J., et al. (2014). Neurosystems: brain rhythms and cognitive processing. *European Journal of Neuroscience*. **39**(5): p. 705-719.
743. Roopun, A.K., et al. (2008). Temporal Interactions between Cortical Rhythms. *Front Neurosci*. **2**(2): p. 145-54.
744. Roopun, A.K., et al. (2008). Period concatenation underlies interactions between gamma and beta rhythms in neocortex. *Front Cell Neurosci*. **2**: p. 1.

745. Huang, H.P., et al. (2007). Long latency of evoked quantal transmitter release from somata of locus coeruleus neurons in rat pontine slices. *Proc Natl Acad Sci U S A*. **104**(4): p. 1401-6.
746. Mateo, Y. and J.J. Meana (1999). Determination of the somatodendritic α2-adrenoceptor subtype located in rat locus coeruleus that modulates cortical noradrenaline release in vivo. *European Journal of Pharmacology*. **379**(1): p. 53-57.
747. Mateo, Y., J. Pineda, and J.J. Meana (1998). Somatodendritic α2-Adrenoceptors in the Locus Coeruleus Are Involved in the In Vivo Modulation of Cortical Noradrenaline Release by the Antidepressant Desipramine. *Journal of Neurochemistry*. **71**(2): p. 790-798.
748. Ramirez, O.A. and R.Y. Wang (1986). Electrophysiological evidence for locus coeruleus norepinephrine autoreceptor subsensitivity following subchronic administration of D-amphetamine. *Brain Res*. **385**(2): p. 415-9.
749. Chandler, D.J. (2016). Evidence for a specialized role of the locus coeruleus noradrenergic system in cortical circuitries and behavioral operations. *Brain Res*. **1641**(Pt B): p. 197-206.
750. Jasmin, L., et al. (2004). Rostral agranular insular cortex and pain areas of the central nervous system: a tract-tracing study in the rat. *J Comp Neurol*. **468**(3): p. 425-40.
751. Ji, G. and V. Neugebauer (2011). Pain-related deactivation of medial prefrontal cortical neurons involves mGluR1 and GABA(A) receptors. *J Neurophysiol*. **106**(5): p. 2642-52.
752. Nakamura, H., Y. Katayama, and Y. Kawakami (2010). Hippocampal CA1/subiculum-prefrontal cortical pathways induce plastic changes of nociceptive responses in cingulate and prelimbic areas. *BMC Neurosci*. **11**: p. 100.
753. Aston-Jones, G., S.L. Foote, and M. Segal (1985). Impulse conduction properties of noradrenergic locus coeruleus axons projecting to monkey cerebrocortex. *Neuroscience*. **15**(3): p. 765-77.
754. Aston-Jones, G., M. Segal, and F.E. Bloom (1980). Brain aminergic axons exhibit marked variability in conduction velocity. *Brain Res*. **195**(1): p. 215-22.
755. Devilbiss, D.M. and B.D. Waterhouse (2011). Phasic and Tonic Patterns of Locus Coeruleus Output Differentially Modulate Sensory Network Function in the Awake Rat. *Journal of Neurophysiology*. **105**(1): p. 69-87.
756. Grace, A.A. and B.S. Bunney (1983). Intracellular and extracellular electrophysiology of nigral dopaminergic neurons--3. Evidence for electrotonic coupling. *Neuroscience*. **10**(2): p. 333-48.
757. Grace, A.A. and B.S. Bunney (1983). Intracellular and extracellular electrophysiology of nigral dopaminergic neurons--2. Action potential generating mechanisms and morphological correlates. *Neuroscience*. **10**(2): p. 317-31.
758. Korotkova, T.M., et al. (2004). Functional diversity of ventral midbrain dopamine and GABAergic neurons. *Mol Neurobiol*. **29**(3): p. 243-59.
759. Margolis, E.B., et al. (2006). The ventral tegmental area revisited: is there an electrophysiological marker for dopaminergic neurons? *J Physiol*. **577**(Pt 3): p. 907-24.

760. Pupe, S. and A. Wallen-Mackenzie (2015). Cre-driven optogenetics in the heterogeneous genetic panorama of the VTA. *Trends Neurosci*. **38**(6): p. 375-86.
761. Roeper, J. (2013). Dissecting the diversity of midbrain dopamine neurons. *Trends in Neurosciences*. **36**(6): p. 336-342.
762. Ungless, M.A. and A.A. Grace (2012). Are you or aren't you? Challenges associated with physiologically identifying dopamine neurons. *Trends Neurosci*. **35**(7): p. 422-30.
763. Sanchez-Catalan, M.J., et al. (2014). The Antero-Posterior Heterogeneity of the Ventral Tegmental Area. *Neuroscience*. **282**: p. 198-216.
764. Steinberg, E.E. and P.H. Janak (2013). Establishing causality for dopamine in neural function and behavior with optogenetics. *Brain Res*. **1511**: p. 46-64.
765. Cohen, J.Y., et al. (2012). Neuron-type-specific signals for reward and punishment in the ventral tegmental area. *Nature*. **482**(7383): p. 85-U109.
766. Lammel, S., et al. (2015). Diversity of transgenic mouse models for selective targeting of midbrain dopamine neurons. *Neuron*. **85**(2): p. 429-38.
767. Feenstra, M.G., et al. (2001). Dopamine and noradrenaline efflux in the rat prefrontal cortex after classical aversive conditioning to an auditory cue. *Eur J Neurosci*. **13**(5): p. 1051-4.
768. Lorden, J.F., et al. (1980). Forebrain norepinephrine and the selective processing of information. *Brain Res*. **190**(2): p. 569-73.
769. Mason, S.T. and S.D. Iversen (1979). Theories of the dorsal bundle extinction effect. *Brain Res*. **180**(1): p. 107-37.
770. Roberts, D.C., M.T. Price, and H.C. Fibiger (1976). The dorsal tegmental noradrenergic projection: An analysis of its role in maze learning. *Journal of Comparative and Physiological Psychology*. **90**(4): p. 363-372.
771. Levy, F. (2009). Dopamine vs noradrenaline: inverted-U effects and ADHD theories. *Aust N Z J Psychiatry*. **43**(2): p. 101-8.
772. Morton, N., et al. (1995). The effect of apomorphine and L-dopa challenge on prepulse inhibition in patients with parkinsons disease. *Schizophrenia Research*. **15**(1): p. 181-182.
773. Perriol, M.-P., et al. (2005). Disturbance of sensory filtering in dementia with Lewy bodies: comparison with Parkinson's disease dementia and Alzheimer's disease. *Journal of Neurology, Neurosurgery & Psychiatry*. **76**(1): p. 106-108.
774. Kaji, R., et al. (2005). Abnormal sensory gating in basal ganglia disorders. *Journal of Neurology*. **252**(4): p. iv13-iv16.
775. Abbruzzese, G. and A. Berardelli (2003). Sensorimotor integration in movement disorders. *Movement Disorders*. **18**(3): p. 231-240.
776. Baker, N.J., et al. (1990). Sensory gating deficits in psychiatric impatients: Relation to catecholamine metabolites in different diagnostic groups. *Biological Psychiatry*. **27**(5): p. 519-528.
777. Wang, Y., et al. (2009). A follow-up study on features of sensory gating P50 in treatment-resistant depression patients. *Chinese Medical Journal (English Edition)*. **122**(24): p. 2956.

778. Perry, W., A. Minassian, and D. Feifel (2004). Prepulse inhibition in patients with non-psychotic major depressive disorder. *Journal of Affective Disorders*. **81**(2): p. 179-184.
779. Adler, L.E., et al. (1982). Neurophysiological evidence for a defect in neuronal mechanisms involved in sensory gating in schizophrenia. *Biol Psychiatry*. **17**(6): p. 639-54.
780. Judd, L.L., et al. (1992). Sensory gating deficits in schizophrenia: new results. *Am J Psychiatry*. **149**(4): p. 488-93.
781. Braff, D., et al. (1978). Prestimulus effects on human startle reflex in normals and schizophrenics. *Psychophysiology*. **15**(4): p. 339-43.
782. Gulledge, A.T. and D.B. Jaffe (1998). Dopamine decreases the excitability of layer V pyramidal cells in the rat prefrontal cortex. *J Neurosci*. **18**(21): p. 9139-51.
783. Ellenbroek, B.A., et al. (1999). Sensory Gating in Rats: Lack of Correlation Between Auditory Evoked Potential Gating and Prepulse Inhibition. *Schizophrenia Bulletin*. **25**(4): p. 777-788.
784. Nicholas, A.P., V. Pieribone, and T. Hokfelt (1993). Distributions of mRNAs for alpha-2 adrenergic receptor subtypes in rat brain: an in situ hybridization study. *J Comp Neurol*. **328**(4): p. 575-94.
785. Unnerstall, J.R., T.A. Kopajtic, and M.J. Kuhar (1984). Distribution of alpha 2 agonist binding sites in the rat and human central nervous system: analysis of some functional, anatomic correlates of the pharmacologic effects of clonidine and related adrenergic agents. *Brain Res*. **319**(1): p. 69-101.
786. Syková, E. and C. Nicholson (2008). Diffusion in brain extracellular space. *Physiological reviews*. **88**(4): p. 1277-1340.
787. Nicholson, C. and L. Tao (1993). Hindered diffusion of high molecular weight compounds in brain extracellular microenvironment measured with integrative optical imaging. *Biophysical Journal*. **65**(6): p. 2277.
788. Nicholson, C., et al. (2000). Diffusion of molecules in brain extracellular space: theory and experiment. *Progress in brain research*. **125**: p. 129-154.
789. Lalley, P.M. (1999). Microiontophoresis and Pressure Ejection, in *Modern Techniques in Neuroscience Research*, U. Windhorst and H. Johansson, Editors. Springer Berlin Heidelberg: Berlin, Heidelberg. p. 193-212.
790. Pikal, M.J. and S. Shah (1990). Transport Mechanisms in Iontophoresis. III. An Experimental Study of the Contributions of Electroosmotic Flow and Permeability Change in Transport of Low and High Molecular Weight Solutes. *Pharmaceutical Research*. **7**(3): p. 222-229.
791. Abla, N., et al. (2005). Effect of Charge and Molecular Weight on Transdermal Peptide Delivery by Iontophoresis. *Pharmaceutical Research*. **22**(12): p. 2069-2078.
792. Hudson, A.J. (2000). Pain perception and response: central nervous system mechanisms. *Can J Neurol Sci*. **27**(1): p. 2-16.
793. Ossipov, M.H., G.O. Dussor, and F. Porreca (2010). Central modulation of pain. *J Clin Invest*. **120**(11): p. 3779-87.
794. Baron, R. (2000). Peripheral neuropathic pain: from mechanisms to symptoms. *The Clinical journal of pain*. **16**(2): p. S12-S20.

795. Bodnar, R.J., et al. (1978). Elevations in Nociceptive Thresholds Following Locus Coeruleus Lesions. *Brain Research Bulletin*. **3**(2): p. 125-130.
796. Kuner, R. (2010). Central mechanisms of pathological pain. *Nature medicine*. **16**(11): p. 1258-1266.
797. Ohnami, S., et al. (2012). Effects of milnacipran, a 5-HT and noradrenaline reuptake inhibitor, on C-fibre-evoked field potentials in spinal long-term potentiation and neuropathic pain. *British journal of pharmacology*. **167**(3): p. 537-547.
798. Raja, S.N. (1997). Peripheral modulatory effects of catecholamines in inflammatory and neuropathic pain. *Advances in Pharmacology*. **42**: p. 567-571.

7. Supplemental Material

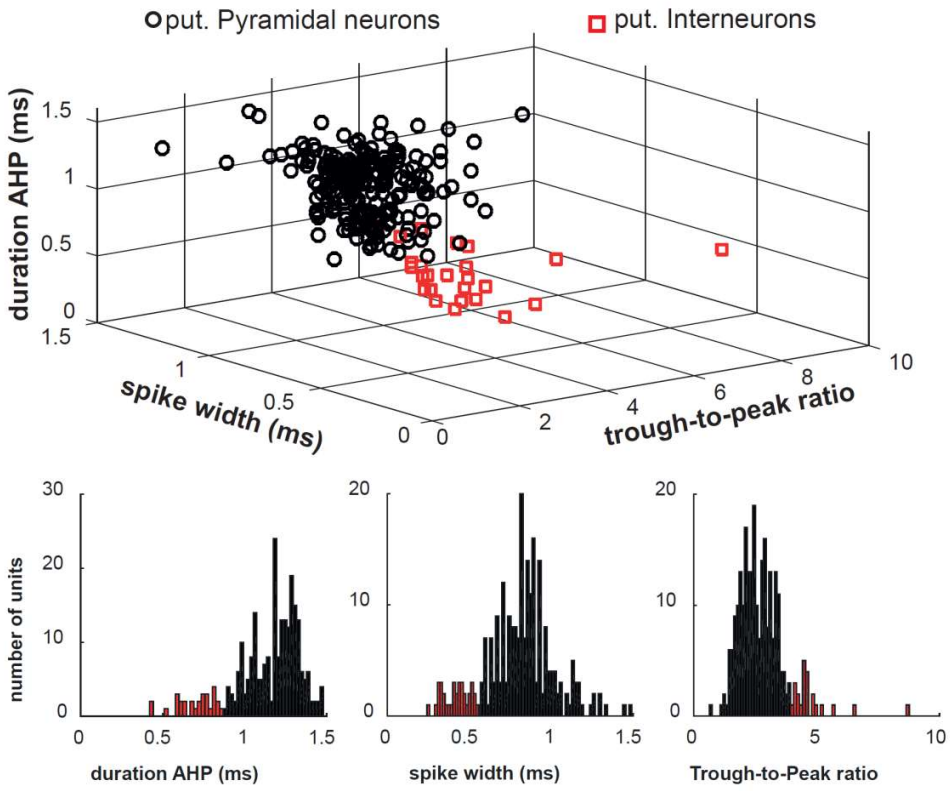

Supplementary Figure 7.1: Distribution of duration of AHP, spike width and trough-to-peak-ratio of recorded single units in the cortical regions revealed a population of putative (put.) interneurons (red) and a population of putative pyramidal neurons (black).

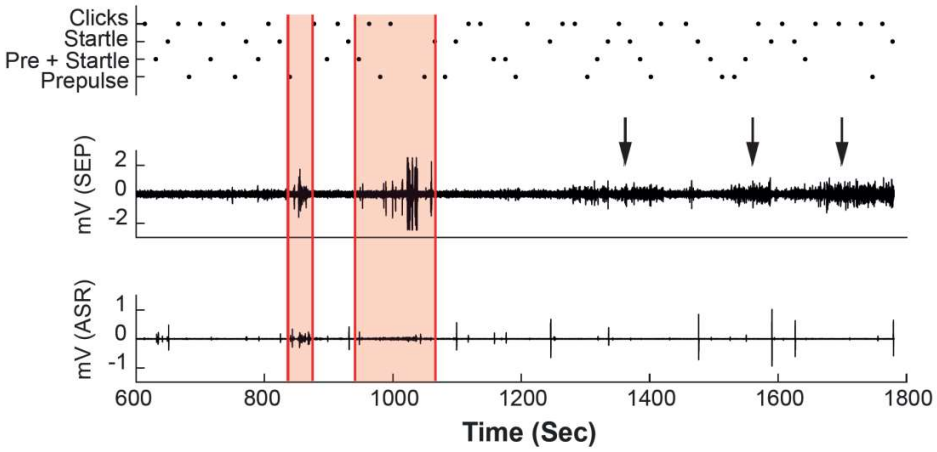

Supplementary Figure 7.2: Representative example of artifact removal in a fraction of continuously recorded data from one session. Illustrated are triggers to auditory stimulation using clicks, Startle stimulus only (Startle), Startle stimulus preceded by prepulse (Pre + Startle) and prepulse stimulus only (top row). The local field potential recorded from mPFC is shown in the medial row above the signal induced by movements of the animal recorded from the piezoelectric sensors under the floor (bottom row). Red shaded area indicates period of removed data because of high amplitude artifacts due to excessive movements easily distinguishable from sequentially increased amplitude of the neuronal signal due to change of cortical state activity to low frequency oscillations (arrows).

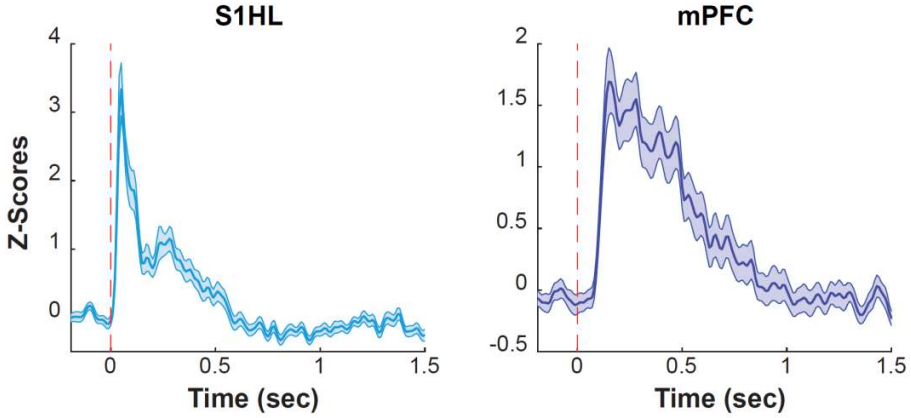

Supplementary Figure 7.3: Somatosensory stimulation induces single unit responses under urethane anesthesia. Illustrated are the PSTHs averaged over 25 repetitions during 1.5 sec after stimulus-presentation (red dashed line at 0 sec). PSTHs of population single unit response in S1HL consist of a short latency response component followed by a late response component. In mPFC the response profile resembles the SEP profile. Binwidth 10ms, Mean ± SE.

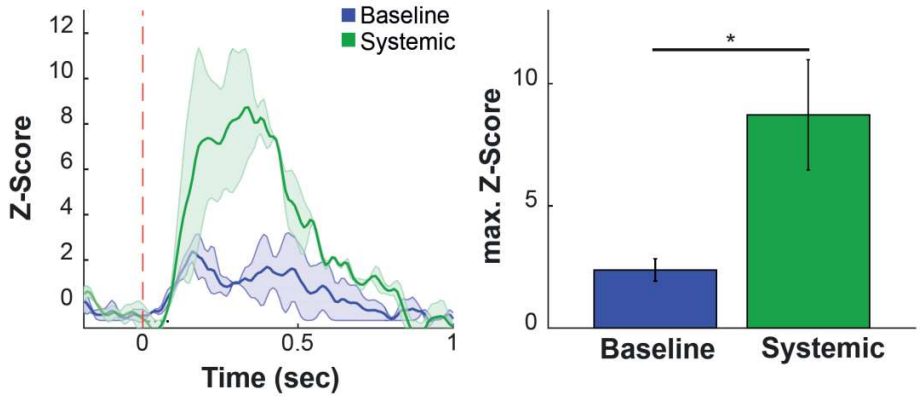

Supplementary Figure 7.4: Two exceptional single units out of mPFC group 2 increased sensory-evoked excitation under condition of systemic clonidine while, commonly, the responses of all neurons in both cortical regions were decreased under drug condition. Average PSTH of responses to sensory stimulation under baseline and drug condition are shown (left). The Stimulation was applied at time 0. Bin size = 10ms. Maximum amplitude of the response profile (right) illustrates the increase of excitation under systemic clonidine condition. Mean ± SE, * $p < 0.05$.

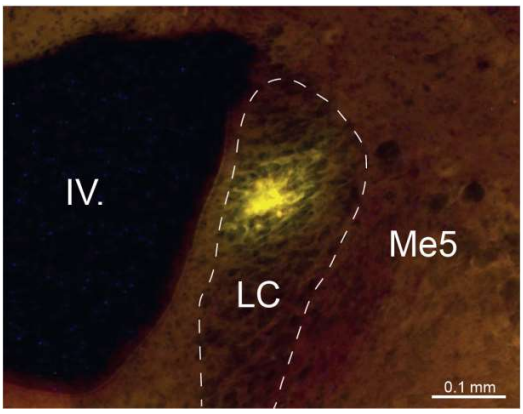

Supplementary Figure 7.5: Color photomicrograph of a coronal section through the LC region around the infusion site of iontophoretically applied apraclonidine labelled with rhodamine (yellow; 50 mg/ml, +50 to +90 nA, 20 min). Dashed line delimits LC nucleus. IV. = IV. ventricle; Me5 = mesencephalic trigeminal nucleus. Note, the diffusion width of the injected compound amounts to ~100 – 150 µm.

Supplementary Table 7.1: Average power source density during 4 sec prestimulus interval for each analyzed frequency band in S1HL and mPFC during baseline condition. Mean ± SE.

Frequency bands	S1HL	mPFC
pre SLO	0.1125 ± 0.0116 dB	0.1226 ± 0.0138 dB
pre Delta	0.1969 ± 0.0177 dB	0.1961 ± 0.0181 dB
pre Theta	0.0616 ± 0.0050 dB	0.0467 ± 0.0023 dB
pre Alpha	0.0231 ± 0.0019 dB	0.0184 ± 0.0006 dB
pre Sigma	0.0171 ± 0.0015 dB	0.0141 ± 0.0006 dB
pre Beta	0.0125 ± 0.0011 dB	0.0104 ± 0.0004 dB
pre Gamma	0.0060 ± 0.0005 dB	0.0051 ± 0.0002 dB

Supplementary Table 7.2: Average baseline change of BLP during 4 sec prestimulus interval following local and systemic clonidine administration for each analyzed frequency band in S1HL and mPFC. Mean ± SE.

	S1HL		mPFC	
	% Change systemic	% Change local	% Change systemic	% Change local
pre SLO	3.41 ± 12.91	11.71 ± 23.62	-23.48 ± 9.25	13.94 ± 12.52
pre Delta	4.08 ± 9.64	21.17 ± 30.61	-14.08 ± 7.92	2.37 ± 8.06
pre Theta	49.43 ± 15.34	8.76 ± 7.99	21.52 ± 7.07	-5.59 ± 3.92
pre Alpha	90.08 ± 15.82	21.79 ± 10.28	12.69 ± 4.69	3.85 ± 3.16
pre Sigma	112.81 ± 19.33	40.45 ± 13.27	-7.02 ± 4.78	0.88 ± 3.17
pre Beta	63.35 ± 10.65	32.07 ± 9.84	-10.05 ± 3.79	-0.35 ± 3.00
pre Gamma	6.60 ± 3.13	7.45 ± 2.06	-2.57 ± 1.87	5.44 ± 1.80

Supplementary Table 7.3: Average baseline change of firing rate in populations of cortical neurons dependent on the direction of spontaneous activity modulation following local and systemic clonidine administration. Mean ± SE.

Direction of modulation	S1HL		mPFC	
	% Change systemic	% Change local	% Change systemic	% Change local
increase	+212.64 ± 73.56	+288.77 ± 96.26	+112.77 ± 46.91	+87.77 ± 29.42
decrease	-66.32 ± 20.47	-37.35 ± 18.06	-68.48 ± 6.63	-48.27 ± 16.21
unchanged	+22.48 ± 15.96	+19.64 ± 17.39	-21.54 ± 7.24	+10.54 ± 6.4

Supplementary Table 7.4: Average maximum firing amplitudes of unit activity in LC, S1HL and mPFC in response to electrical foot-shock (FS) stimulation using single pulse (SP) or train (TR) stimulation with 5 mA stimulation current. Mean ± SE.

	SP	TR
LC-MUA (norm. spikes/sec)	6.68 ± 0.78	8.62 ± 1.99
S1HL-SUA (Z-Scores)	21.69 ± 2.92	21.69 ± 2.71
mPFC-SUA (Z-Scores)	4.56 ± 0.74	8.95 ± 1.30

Supplementary Table 7.5: Average maximum firing amplitudes (spikes/sec) of units in LC, S1HL and mPFC in response to TR stimulation using increasing stimulation currents from 1 mA to 5 mA, Mean ± SE.

	LC-MUA	S1HL-SUA	mPFC-SUA
1 mA	60.92 ± 9.53	47.54 ± 5.59	13.33 ± 1.24
2 mA	81.13 ± 12.05	31.67 ± 3.62	15.74 ± 1.69
3 mA	89.07 ± 12.45	34.40 ± 4.57	16.46 ± 1.83
4 mA	95.97 ± 12.93	30.96 ± 4.03	17.89 ± 1.87
5 mA	95.37 ± 12.01	34.31 ± 3.10	20.53 ± 2.06

Supplementary Table 7.6: Summary of stimulus-induced BLP change in S1HL dependent on TCA+ and TCA- cases in mPFC. Given is the average BLP change for each analyzed frequency band in addition to statistical evaluation of the change using one-sample t-test against 0. Mean ± SE.

	TCA+		TCA-	
	post BLP change	one-sample t-test	post BLP change	one-sample t-test
Delta	-30.34 ± 6.98 %	$t(6) = -4.35$, $p < 0.01$	-9.69 ± 7.24 %	$t(8) = -1.34$, p = n.s.
Theta	-20.74 ± 6.94 %	$t(6) = -2.99$, $p < 0.05$	4.69 ± 3.16 %	$t(8) = 1.49$, p = n.s.
Alpha	-17.85 ± 4.43 %	$t(6) = -4.03$, $p < 0.01$	6.50 ± 3.12 %	$t(8) = 2.08$, p = n.s.
Sigma	5.36 ± 6.01 %	$t(6) = 0.89$, p = n.s.	23.05 ± 6.36 %	$t(8) = 3.62$, $p < 0.01$
Beta	32.09 ± 11.26 %	$t(6) = 2.85$, $p < 0.05$	44.79 ± 11.89 %	$t(8) = 3.77$, $p < 0.01$
Gamma	77.32 ± 20.07 %	$t(6) = 3.85$, $p < 0.01$	52.51 ± 11.80 %	$t(8) = 4.45$, $p < 0.01$

Supplementary Table 7.7: Comparison of stimulus-induced change in BLP between S1HL and mPFC in TCA+ cases only. Given are the average change in BLP for each analyzed frequency band in S1HL and mPFC in addition to statistical evaluation of the difference between cortical regions. Mean ± SE.

	S1HL	mPFC	One-Way ANOVA
Delta	-22.47 ± 4.56 %	-36.19 ± 2.93 %	$F(1, 38) = 6.12$, $p < 0.05$
Theta	-10.93 ± 5.06 %	-23.25 ± 3.55 %	$F(1, 38) = 3.82$, p = n.s.
Alpha	-3.41 ± 4.57 %	-11.46 ± 2.08 %	$F(1, 38) = 2.39$, p = n.s.
Sigma	16.69 ± 4.83 %	0.25 ± 2.91 %	$F(1, 38) = 8.05$, $p < 0.01$
Beta	38.84 ± 7.56 %	13.74 ± 2.66 %	$F(1, 38) = 9.03$, $p < 0.01$
Gamma	65.56 ± 7.91 %	40.27 ± 5.37 %	$F(1, 38) = 6.70$, $p < 0.05$

Supplementary Table 7.8: Effect of clonidine injection on average stimulus-induced change of BLP in TCA- cases in mPFC. Listed is BLP change under baseline and corresponding drug condition for either manipulation in each frequency band individually. Mean ± SE. Statistical evaluation of difference between baseline and drug condition is additionally provided.

	Baseline (Systemic) (% Change)	Systemic (% Change)	One-way ANOVA
Delta	1.09 ± 4.48	-9.14 ± 4.78	F(1, 23) = 2.44, p = n.s.
Theta	2.70 ± 2.40	-12.85 ± 7.40	F(1, 23) = 3.99, p = n.s.
Alpha	0.05 ± 1.85	1.21 ± 3.23	F(1, 23) = 0.10, p = n.s.
Sigma	0.95 ± 3.24	15.43 ± 4.24	F(1, 23) = 7.37, p < 0.05
Beta	2.74 ± 3.18	15.39 ± 3.51	F(1, 23) = 7.13, p < 0.05
Gamma	4.78 ± 2.48	14.88 ± 3.15	F(1, 23) = 6.33, p < 0.05
	Baseline (Local) (% Change)	Local (% Change)	One-way ANOVA
Delta	-5.78 ± 3.67	-11.67 ± 7.69	F(1, 19) = 0.45, p = n.s.
Theta	-0.01 ± 4.15	-6.08 ± 4.76	F(1, 19) = 0.92, p = n.s.
Alpha	-0.85 ± 4.33	-2.29 ± 5.16	F(1, 19) = 0.05, p = n.s.
Sigma	-3.10 ± 2.38	8.53 ± 4.77	F(1, 19) = 4.76, p < 0.05
Beta	0.79 ± 2.29	14.25 ± 3.96	F(1, 19) = 8.64, p < 0.01
Gamma	2.99 ± 2.08	13.81 ± 4.75	F(1, 19) = 4.36, p = 0.05

Supplementary Table 7.9: Clonidine-induced cortical state activation in initially TCA- cases in mPFC. Change in poststimulus BLP under baseline and drug condition for each frequency band was tested against 0 (one-sample t-test). Note a significantly increased power in high frequency range after either pharmacological manipulation.

	Baseline (Systemic)	Systemic
Delta	$t(11) = 0.24$, p = n.s.	$t(11) = -1.91$, p = n.s.
Theta	$t(11) = 1.12$, p = n.s.	$t(11) = -1.74$, p = n.s.
Alpha	$t(11) = 0.03$, p = n.s.	$t(11) = 0.37$, p = n.s.
Sigma	$t(11) = 0.29$, p = n.s.	$t(11) = 3.64$, $p < 0.01$
Beta	$t(11) = 0.86$, p = n.s.	$t(11) = 4.39$, $p < 0.01$
Gamma	$t(11) = 1.93$, p = n.s.	$t(11) = 4.72$, $p < 0.001$
	Baseline (Local)	Local
Delta	$t(9) = -1.57$, p = n.s.	$t(9) = -1.46$, p = n.s.
Theta	$t(9) = -0.00$, p = n.s.	$t(9) = -1.28$, p = n.s.
Alpha	$t(9) = -0.20$, p = n.s.	$t(9) = -0.44$, p = n.s.
Sigma	$t(9) = -1.30$, p = n.s.	$t(9) = 1.79$, p = n.s.
Beta	$t(9) = 0.34$, p = n.s.	$t(9) = 3.60$, $p < 0.01$
Gamma	$t(9) = 1.44$, p = n.s.	$t(9) = 2.91$, $p < 0.05$

Supplementary Table 7.10: Comparison of SEP characteristics in S1HL between baseline and clonidine condition after either pharmacological manipulation. Note identical values under baseline conditions due to combined average of baseline before local and baseline before systemic injection. Mean ± SE.

	Baseline	Systemic	Statistics
Max. Amplitude early (mV)	-0.55 ± 0.07	-0.55 ± 0.10	$F(1, 34) = 0.00$, p = n.s.
Max. Amplitude late (mV)	-0.31 ± 0.04	-0.26 ± 0.04	$F(1, 32) = 1.59$, p = n.s.
Integral entire profile (mV * sec)	-0.02 ± 0.00	-0.02 ± 0.01	$F(1, 34) = 0.37$, p = n.s.
Integral late (mV * sec)	-0.04 ± 0.02	-0.06 ± 0.00	$F(1, 32) = 1.41$, p = n.s.
	Baseline	Local	Statistics
Max. Amplitude early (mV)	-0.55 ± 0.07	-0.51 ± 0.07	$F(1, 33) = 0.31$, p = n.s.
Max. Amplitude late (mV)	-0.31 ± 0.04	-0.23 ± 0.04	$F(1, 32) = 4.02$, $p = 0.05$
Integral entire profile (mV * sec)	-0.02 ± 0.00	-0.02 ± 0.00	$F(1, 33) = 1.22$, p = n.s.
Integral late (mV * sec)	-0.04 ± 0.02	-0.05 ± 0.02	$F(1, 32) = 0.09$, p = n.s.

Supplementary Table 7.11: Comparison of SEP characteristics in mPFC TCA+ cases between baseline and clonidine condition after either pharmacological manipulation. Note identical values under baseline conditions due to combined average of baseline before local and baseline before systemic injection. Mean ± SE.

	Baseline	Systemic	Statistics
Max. Amplitude (mV)	-0.29 ± 0.04	-0.19 ± 0.03	$F(1, 24) = 1.60$, p = n.s.
Integral (mV * sec)	-0.08 ± 0.01	-0.03 ± 0.01	$F(1, 24) = 5.92$, $p < 0.05$
	Baseline	Local	Statistics
Max. Amplitude (mV)	-0.29 ± 0.04	-0.25 ± 0.05	$F(1, 28) = 0.00$, p = n.s.
Integral (mV * sec)	-0.08 ± 0.01	-0.06 ± 0.02	$F(1, 28) = 0.32$, p = n.s.

Supplementary Table 7.12: Comparison of SEP characteristics in mPFC TCA- cases between baseline and clonidine condition after either pharmacological manipulation. Note identical values under baseline conditions due to combined average of baseline before local and baseline before systemic injection. Mean ± SE.

	Baseline	Systemic	Statistics
Max. Amplitude (mV)	-0.26 ± 0.05	-0.21 ± 0.04	$F(1, 20) = 0.16$, p = n.s.
Integral (mV * sec)	-0.05 ± 0.01	-0.05 ± 0.01	$F(1, 20) = 0.54$, p = n.s.
	Baseline	Local	Statistics
Max. Amplitude (mV)	-0.26 ± 0.05	-0.14 ± 0.02	$F(1, 17) = 2.44$, p = n.s.
Integral (mV * sec)	-0.05 ± 0.01	-0.02 ± 0.01	$F(1, 17) = 3.97$, p = n.s.

Supplementary Table 7.13: Average maximum firing amplitudes (spikes/sec) of neurons recorded in the ventral midbrain in response to electrical FS stimulation using increasing stimulation currents from 1 mA to 5 mA. Mean ± SE.

	Ventral midbrain population SUA (max. Spikes/Sec)
1 mA	23.45 ± 1.39
2 mA	25.12 ± 1.72
3 mA	27.45 ± 1.87
4 mA	28.61 ± 1.90
5 mA	30.55 ± 2.00

Supplementary Table 7.14: Comparison of explored parameters during sensory gating after non-effective ventral midbrain infusion of D_2-receptor agonist quinpirole. Given are average percentages of PPI and ASG in addition to respective absolute amplitudes of SEPs and ASR in response to different stimulus parameters during control and drug condition and statistical comparison between those conditions. Mean ± SE.

	Saline	Quinpirole	ANOVA
PPI ASR (%)	65.41 ± 3.65	64.68 ± 2.48	F(1, 43) = 0.03, p = n.s.
Gated ASR (mV)	-0.15 ± 0.04	-0.17 ± 0.03	F(1, 43) = 0.15, p = n.s.
Non-gated ASR (mV)	-0.41 ± 0.08	-0.44 ± 0.08	F(1, 43) = 0.07, p = n.s.
PPI SEP (%)	52.57 ± 11.48	55.38 ± 9.22	F(1, 41) = 0.04, p = n.s.
Gated SEP (mV)	-0.05 ± 0.02	-0.06 ± 0.01	F(1, 41) = 0.18, p = n.s.
Non-gated SEP (mV)	-0.11 ± 0.02	-0.12 ± 0.01	F(1, 41) = 0.03, p = n.s.
ASG (%)	52.38 ± 9.00	61.07 ± 7.44	F(1,27) = 0.55, p = n.s.
Gated ASG (mV)	-0.02 ± 0.01	-0.02 ± 0.01	F(1, 27) = 0.01, p = n.s.
Non-gated ASG (mV)	-0.05 ± 0.01	-0.06 ± 0.01	F(1, 27) = 1.28, p = n.s.

Acknowledgements

First of all, I especially thank Prof. Dr. Nikos Logothetis and Dr. Oxana Eschenko for giving me the opportunity, outstanding support and advice which enabled me to perform this work.

Moreover, I would like to thank the Team of the Graduate Training Center of Neuroscience for support, advice and excellent education.

Furthermore, without the patient help of Aude Marzo and Ricardo Melo Neves, I would never have been able to electrophysiologically find the midget nucleus locus coeruleus in the rat brain. Thank you both also for mental and physical support during the sometimes unbearable long experiments and for being good friends.

I would also thank the members of the mechanical and technical workshops in the institute for their help in building experimental devices, creative ideas and patient explanations regarding electrical engineering. My special thanks goes to Oliver Holder, Theodor Steffen, Axel Öltermann and Matthias Arndt.

Further, I would like to thank all friends and colleagues within and outside of the lab who were always there for advice, fruitful discussions, motivating speeches and pleasant distractions. Thank you for being such good friends without expecting anything back.

Special thanks goes to my mother who always believes in her kids, no matter what they aim for. Thank you for teaching me to be modest and to never give up.

Last but not least, I sincerely thank Chris for always being there for me, regardless of the circumstances. You critically make me think to find the right decisions, you motivate me to constantly learn new things but most of all, I thank you for making me laugh.
I love you!